# Molecular, Morphological, and Kinetic Diagnosis of Human Preimplantation Embryo Viability

**By Sarah Louise Drury**

**0866001**

**A thesis submitted in partial fulfilment of the requirements for the degree of Doctor of Philosophy in Medicine**

**Warwick Medical School**

**University of Warwick**

**December 2016**

# Contents

## 3 Chapter Three

## Research Material

## Abbreviations

All abbreviations, in addition to being noted at the first instance in the main text of this thesis, are listed below, in alphabetical order.

**0PN** Zero pronuclei (failed fertilisation oocyte)

**AH** Assisted hatching

**ANOVA** analysis of variance

**ART** Assisted reproductive treatment

**AV axis** antero-posterior axis

**AVI** Audio Video Interleave

**BFC** Bath Fertility Centre

**BMI** Body mass index

**BSA** Bovine serum albumin

**CCD** Charge-coupled device

**cDNA** Complementary deoxyribonucleic acid

***C.elegans*** *Caenorhabditis elegans*

**$CO_2$** Carbon dioxide

**CRM** Centre for Reproductive Medicine

**CSRI** Clinical Sciences Research Institute

**csv** comma separated value

**CY2** Cyanine dye 2

**DAPI** 4',6-diamidino-2-phenylindole

**DMEM** Dulbecco's Modified Eagle Medium

**DNA** Deoxyribonucleic acid

**DNase** Deoxyribonuclease

**DV axis** Dorso-ventral axis

**EDTA** ethylene-diamine-tetraacetic acid

**EHS** Engelbeth-Holm-Swarm mouse sarcoma

**F-actin** Filamentous actin

**FITC** Fluorescein isothiocyanate

**FSH** Follicle-Stimulating Hormone

**GIF** Graphics interchange format

**GnRH** Gonadotropin-releasing hormone

**GV** Germinal vesicle

**hCG** Human chorionic gonadotropin

**HEPES** 4-(2-hydroxyethyl)-1-piperazineethanesulfonic acid

**HFEA** Human Fertilisation and Embryology Authority

**ICSI** Intracytoplasmic Sperm Injection

**ICM** Inner cell mass

**IgG** Immunoglobulin G

**ISM1** Culture medium suitable for zygotes (day 1) to 4 cell embryos (day 2)

**ISO** International Organisation for Standardisation

**IVF** *In vitro* fertilisation

**IVM** *In vitro* maturation

**k-Da** Kilo Dalton

**LFC** Leicester Fertility Centre

**LH** Lutenising hormone

**$LN_2$** Liquid Nitrogen

**LR axis** Left-right axis

**LREC** Coventry Research Ethics Committee

**MCL-1** myeloid cell leukaemia 1

**MPN** Multipronucleate

**mRNA** messenger ribonucleic acid

**MT form** Men's consent to treatment and storage form

**MtDNA** Mitochondrial DNA

**$NaHCO_3$** Sodium bicarbonate

**NICE** National Institute for Health and Care Excellence

**OB-$R_L$** Long form of the leptin receptor

**OHSS** Ovarian hyperstimulation syndrome

**PB** Polar body

**PBS** Phosphate buffered saline

**PCO** Polycystic ovaries

**PGD** Preimplantation Genetic Diagnosis

**PGS** Preimplantation Genetic Screening

**PN** Pronuclei

**pSTAT3** Phosphorylated Signal Transducer and Activator of Transcription 3

**PVP** Polyvinylpyrrolidone

**PVS** Perivitelline space

**PCR** Polymerase chain reaction

**qRT-PCR** Quantitative real time polymerase chain reaction

**R&D** Research and Development

**RGB** Red Green Blue

**RNA** Ribonucleic acid

**RNase** Ribonuclease

**RT** Reverse transcription

**sET** Single embryo transfer

**SH2 domain** Src Homology 2 domain

**STAT3** Signal Transducer and Activator of Transcription 3

**TE** Trophectoderm

**TIFF** Tagged image file format

**UHCW** University Hospitals Coventry and Warwickshire NHS Trust

**UV** Ultraviolet

**WHO** World Health Organisation

**WMS** Warwick Medical School

**WT form** Women's consent to treatment and storage form

**ZP** *Zona pellucida*

# List of Tables

## List of Figures

### Chapter One



### Chapter Two

on the left hand side of the image. Distinct actin borders are seen around each cell, intact nuclei, and small individual fragments, but not around the disorganised chromatin of the fragmenting nuclei

***Figure 4.2*** Confocal images showing actin distribution in the cells of (a) 2-cell frozen-thawed embryo (b) 3-cell frozen-thawed embryo. The cytoplasmic actin distribution is non-uniform, and the blastomeres lack a distinct actin border

***Figure 4.3*** Confocal images showing (a) a day 3 frozen-thawed morphologically normal appearing embryo with chromosomes apparently well aligned in metaphase, (b) a day 3 frozen-thawed embryo with some multi-nucleated cell,s (c) a day 2 frozen-thawed embryo , (d) a day 2 frozen-thawed embryo, (e) a day 2 frozen-thawed embryo (f) a day 2 frozen-thawed embryo

***Figure 4.4*** Confocal images showing actin distribution in a compacting day 4 fresh embryo. There are distinct actin borders at the junctions between cells. The differences in image intensity are due to the focal z-plane

***Figure 4.5*** Confocal images showing actin borders around individual cells of the trophectoderm and inner cell mass of (a) a day 6 fresh early blastocyst (b) a day 6 fresh 1CC grade blastocyst, and (c) a day 6 fresh hatching blastocyst

***Figure 4.6*** Distribution of leptin at the periphery versus the centre, and beneath the polar body versus opposite the polar body in

unfertilised mature oocytes. There is a distinct pattern of leptin distribution between the periphery and centre of the 0PNs, but no discernible difference between the region under the polar body versus the area directly opposite the polar body

***Figure 4.7*** Intracellular leptin distribution in cleavage stage embryos. There is evidence of higher leptin levels at the edge of each cell in comparison to the perinuclear region

***Figure 4.8*** Confocal images showing examples of the distribution of leptin (green) in (a) day 6 fresh 2BB (b) day 7 fresh 4CC (c) day 7 fresh 2CC blastocysts

***Figure 4.9*** The distribution of leptin in the inner cell mass relative to the trophectoderm in blastocysts of varying degrees of expansion and quality. Whilst there was a trend towards higher levels of leptin in the TE compared to the ICM, there were no significant differences and no correlation between leptin distribution and the stage of development

***Figure 4.10*** Distribution of STAT3 at the periphery versus the centre, and beneath the polar body as compared to opposite the polar body in unfertilised mature oocytes (a) (b). There appeared to be more STAT3 at the periphery compared to the centre of the 0PNs (c), however these differences were insignificant. There was no discernible difference between the region under the polar body and the area directly opposite the polar body

***Figure 4.11*** Cleavage stage embryos fluorescently labelled to identify the distribution of STAT3 between individual cells (a) day seven fresh 5 cell (b) day seven fresh 5 cell

***Figure 4.12*** Confocal images of blastocysts of varying degrees of expansion and quality fluorescently labelled for STAT3 (green). There was a trend for higher levels of STAT3 in the ICM compared to the TE, although the differences were not significant, and there was no apparent relationship between STAT3 distribution and the stage of development

***Figure 4.13*** The distribution of leptin in the inner cell mass relative to the trophectoderm in blastocysts of varying degrees of expansion and quality. Whilst there was a trend towards higher levels of leptin in the TE compared to the ICM, there were no significant differences and no correlation between leptin distribution and the stage of development

***Figure 4.14*** The distribution of pSTAT3 at (a) the periphery and centre of 0PNs, beneath the polar body versus opposite the polar body and (b) at the periphery and perinuclear regions of individual blastomeres. There was no discernible pattern of distribution, and the levels were generally similar at all measured points

***Figure 4.15*** Confocal images of (a) day 7 fresh 2DC blastocyst (b) day 6 fresh 1CC blastocyst (c) day 6 fresh 1CC blastocyst, fluorescently labelled for pSTAT3

***Figure 4.16*** The distribution of pSTAT3 in the inner cell mass relative to the trophectoderm in blastocysts of varying degrees of expansion and quality. Whilst there was a trend towards higher levels of pSTAT3 in the ICM compared to the TE, there were no significant differences and no correlation between leptin distribution and the stage of development

***Figure 4.17*** Confocal images of (a) cleavage stage and (b) blastocyst stained with secondary antibody only, and mounted in DAPI media

***Figure 4.18*** (a) blastocyst labelled with OCT-4 antibodies and (b) cleavage stage embryo labelled to detect JC-1

***Figure 4.19*** Bar graph showing the relative fluorescence intensities of pSTAT3 staining in ICM, TE and free cells (FC). The ICM and FC have similar fluorescent staining profiles

***Figure 4.20*** (a) confocal images showing fluorescently labelled blastocysts with free cells in the blastocoelic cavity and (b) time lapse images showing the free cells originating from the ICM of live blastocysts. White arrows indicate location of free cells

***Figure 4.21*** Confocal images of fluorescently labelled blastocysts at varying degrees of expansion and quality showing cells extruded into the perivitelline space, or in one example, into the blastocoelic cavity. White arrows indicate location of excluded cells

***Figure 4.22*** (a) the number of cells in the ICM and the TE. Approximately one fifth of cells in the blastocyst were allocated to

(b) 20 minutes and (c) 30 minutes, and labelled with FITC-conjugated anti-pSTAT3 antibody

***Figure 5.4*** Confocal images of frozen-thawed human blastocysts cultured with 20ng/ml human recombinant leptin protein for 24 hours, stained with FITC-conjugated anti-pSTAT3 antibody

***Figure 5.5*** Mean relative intensity values for pSTAT3 fluorescence in the nuclei (N) and cytoplasm (C) of the ICM in human blastocysts

***Figure 5.6*** Mean relative intensity values for pSTAT3 fluorescence in the nuclei (N) and cytoplasm (C) of the TE of human blastocysts

***Figure 5.7*** Cell numbers in the ICM versus the TE in blastocysts exposed to human recombinant leptin protein compared to blastocysts that were not exposed

***Figure 5.8*** Comparison of the amount of $LEPR_L$ mRNA in frozen-thawed pronucleates, cleavage stage embryos, and blastocysts

***Figure 5.9*** Comparison of the level of SUMO mRNA in frozen-thawed metaphase II oocytes, pronucleates, cleavage stage embryos, and blastocysts

**Chapter Six**

***Figure 6.1*** Comparison of the developmental stages at which fresh and frozen-thawed embryos arrested during culture in the Embryoscope time lapse incubator

***Figure 6.2*** Mean cleavage completion times in all fresh embryos. Error bars represent standard error of the mean

***Figure 6.3*** Mean cleavage completion times in all frozen embryos. Error bars represent standard error of the mean

***Figure 6.4*** Mean cleavage completion time in all frozen versus fresh embryos. Error bars represent standard error of the mean.

***Figure 6.5*** Mean cleavage completion times in all frozen IVF versus ICSI embryos. Error bars represent standard error of the mean

***Figure 6.6*** Mean time spent at each developmental stage in all fresh embryos. Error bars represent the standard error of the mean (a vs b; $p = 0.02$; independent groups t-test)

***Figure 6.7*** Mean time spent at each stage of development in all frozen embryos. Error bars represent the standard error of the mean (a vs b; $p = 0.02$; independent groups t-test)

***Figure 6.8*** Absolute cleavage timings at each developmental stage in frozen versus fresh embryos. Error bars represent the standard error of the mean. There were no significant differences in the mean time

***Figure 7.3*** Edge detection in confocal images of human preimplantation blastocysts at various stages of development

***Figure 7.4*** Circle detection, growth and colour coding of oocytes (a), (b) and the individual blastomeres of an embryo (c)

***Figure 7.5*** Three-dimensional plotting and rendering of segmented images of oocytes (a), (b), blastomeres of an embryo (c), (d) and the nuclei in a blastocyst (e)

***Figure 7.6*** Cell volumes versus nuclear volumes in cleavage stage embryos. The embryos were fluorescently labelled with actin (green), anti-STAT3 or anti-leptin antibodies, and DAPI (blue)

***Figure 7.7*** Nuclear volumes in the ICM versus the TE of fresh blastocysts. ICM nuclei are genrally smaller than TE cells in all blastocysts analysed

## Acknowledgments

I would like to extend my thanks to my supervisor Professor Geraldine Hartshorne, without whom I would not have had the opportunity to undertake this research. Thankyou for keeping the faith!

Thanks also to Dr Silvester Czanner and Anna Mölder for their expert advice and the development of computer programmes.

To my colleagues at CRM, Coventry for supporting me in my endeavour and helping me collect research material.

But mainly, I dedicate this thesis to my family.

To my wonderful parents, Annie and Bob, thankyou for your unwavering love and support over the years. I could not have done this without you.

My lovely brothers Stuart and Russell, for always being there for me.

And to Leroy, my partner, for being my cheerleader.

## Publications


1. S.L. Drury, J. Rai, P. Kachhwaha, D. Darrell, & G.M. Hartshorne (2010) An interesting case of tripronucleate cleavage observed during live cell time-lapse imaging. *Human Fertility* **13** (2) 8.

2. Lishman S (2012) A History of Pathology in 50 objects, Image 9 (IVF) S Drury and G Hartshorne p16.

3. Rafferty K, Drury S, Hartshorne G and Czanner S (2013) Use of Concave Corners in the Segmentation of Embryological Datasets. International Journal of Biometrics and Bioinformatics 1 1-8.

4. Drury SL, Taylor D, Gadd SC and Hartshorne GM (2013) Leptin stimulates activation of STAT3 in human blastocysts. Human Reproduction 28 (5) S1 i25.

5. Mölder A, Drury S, Costen N, Hartshorne G and Czanner S (2015) Semiautomated Analysis of Embryoscope Images: Using Localised Variance of Image Intensity to Detect Embryo Developmental Stages. Cytometry Part A 87A 119-128

6. Anna Mölder, Sarah Drury, Nicholas Costen, Geraldine Hartshorne, and Silvester Czanner (2016) Three Dimensional Visualisation of Microscope Imaging to Improve Understanding of Human Embryo Development. ©Springer International Publishing Switzerland L. Linsen *et al* (eds) *Visualisation in Medicine and Life Sciences III,* Mathematics and Visualisation.

## Summary

## Summary

There have been phenomenal advances in the field of reproductive medicine and success rates following *in vitro* fertilisation have improved dramatically in recent years.

The aim of this project was to improve our understanding of human preimplantation embryo development by identifying potential markers of viability that may aid us in selecting the best embryo for uterine transfer in the clinical embryology laboratory.

Investigations into the distribution of cytoskeletal F-actin in human embryos demonstrated that a highly organised actin cortex is important for embryo cleavage and continued development to the blastocyst stage. Whilst they are polarised in the mouse from the oocyte to the blastocyst, the regulatory proteins leptin and STAT3 are co-localised only at the oocyte stage in humans, and are distributed within different cytoplasmic domains in human cleavage stage embryos and blastocysts. Whether polarity in humans is predetermined in the oocyte remains elusive, but none of the evidence generated in this thesis supports this idea.

Leptin transiently activates STAT3 via the long form of the leptin receptor, and most significantly in the ICM of human day 6 blastocysts. Morphological features of blastocysts that can be visualised microscopically, such as a double ICM and cytoplasmic projections connecting the ICM to the TE, provide clues to their viability and may help us to choose the most suitable embryo from a cohort when deciding which to transfer. Nuclear volumes may in future contribute to this selection.

Using time lapse technology to study cleavage patterns is now a routine occurrence in the clinical embryology laboratory. The results in this thesis show that distinctive patterns of divisions and the site at which blastocysts hatch can provide us with more information than a snap-shot morphological evaluation.

Finally, contributing to the development of modelling software and predictive algorithms for the study of human embryos, particularly in time lapse imaging, means that our understanding of this fascinating area of medicine will continue to progress.

# Chapter One

# General Introduction

# Chapter One

# General Introduction

## *1.1 Infertility*

Infertility, defined as the inability to conceive after regular unprotected intercourse for a period of twelve months or more (De Melo-Martin 2002; WHO), affects around one in seven UK couples, a situation that has remained largely unchanged since the first investigations began during the 19th century (Evers 2002). While the prevalence of the condition has not significantly altered since statistics were first published around 30 years ago (Hull *et al* 1985), the number of people seeking help for fertility problems has increased (NICE 2013). Primary infertility describes a delay in conception with no previous pregnancies, whilst secondary infertility means successful conception has previously occurred, regardless of whether the pregnancy resulted in a live birth (Taylor 2003). Primary and secondary infertility may relate to individuals or to a couple. The aetiology of infertility varies greatly, with the National Institute for Health and Care Excellence (NICE) estimating male factors at 30% combined female factors at 45%, and unexplained factors at 25% (NICE, 2014). However, published research data estimates male factor infertility at 17%, female factors at 49-72%, and unexplained infertility at 12-32% (Haxton and Black 1987; Kuivasaari-Pirinen *et al* 2012). These discrepancies are likely to be due to the specific patient populations included in clinical research, which are frequently conducted at fertility centres and therefore may show population bias. The underlying cause of infertility reportedly has no influence on first trimester

pregnancy loss after intracytoplasmic sperm injection (ICSI) (Bahceci and Ulug 2005), although female factors specifically contribute to a higher risk of preterm birth, and male factors to an increased chance of neonatal intensive care admission (Kuivasaari-Pirinen *et al* 2012).

### *1.2 Assisted reproductive treatment*

There have been marked improvements in success rates during recent years. Reasons for this may include the introduction of ICSI into routine clinical practice (Palermo *et al* 1992), and the current trend towards extended culture of embryos to the blastocyst stage of development (5-6 days after fertilisation) in specially formulated sequential media (Gardner and Lane 1998). *In vitro* fertilisation (IVF) treatment has expanded at a phenomenal rate since the birth of Louise Brown in 1978 (Steptoe and Edwards 1978; Wang and Sauer 2006). However, human assisted reproductive treatment (ART) is still relatively inefficient; with live birth rates approximating 32% in women <35 years to 2% in women aged ≥45 years, according to the most recently published data from the HFEA. The ultimate aim for clinical embryologists is to identify the single most viable embryo from an available cohort, with a view to achieving a healthy singleton pregnancy and live birth for every patient (Montag *et al* 2013).

There are two predominant modalities of ART utilised in clinical embryology laboratories, namely standard IVF and ICSI. IVF has been successfully used in humans since the 1970s (De Kretzer *et al* 1973; Steptoe and Edwards 1976; Steptoe and Edwards 1978), whilst ICSI, a treatment specifically aimed at treating male infertility due to low sperm numbers or quality, was introduced into clinical practice

in the early 1990s (Palermo *et al* 1992). In the UK, 224,196 babies were born as a result of ART between 1991 and 2012, and in 2011 2.2% of all UK newborns were conceived following ART (HFEA 2012). It is estimated that at least 5 million babies have been born worldwide as a result of ART to date (Kamel 2013).

### *1.3 Oocyte maturity*

In order for an oocyte to achieve the ability to become fertilised, it must first reach maturity. The dormant oocyte, suspended at prophase of the first meiotic division during foetal life, proceeds to metaphase I and completes anaphase and telophase, entering metaphase II just prior to ovulation (Cha and Chian 1998). The prophase I oocyte is characterised by the presence of a large nucleus, the germinal vesicle (GV), located eccentrically in the ooplasm, whilst the metaphase I stage oocyte is identifiable by the lack of both a visible GV and a visible polar body (PB). Metaphase II oocytes have a visible PB in the perivitelline space (PVS), a result of extrusion of half of the maternal genetic material at the first meiotic division. At this stage, homologous chromosomes are paired (Mandelbaum 2000). This entire process is initiated and controlled during clinical ART procedures by manipulating the menstrual cycle and inducing oocyte maturation using hormonal medication, as detailed in section 2.3 of this thesis. Oocyte maturity is normally assessed using light microscopy following the removal of the surrounding cumulus cell complexes using digestive enzymes prior to ICSI, as described in section 2.3, or after co-incubation with spermatozoa, as described in section 2.4.

Whilst the aim of a controlled ovarian stimulation regime is to induce oocyte maturation prior to follicular aspiration, *in vitro* oocyte maturation (IVM) is an

alternative method, most commonly employed when a minimal stimulation ART protocol is favoured, such as for oncology patients or women with pre-diagnosed polycystic ovaries who are at increased risk of ovarian hyperstimulation syndrome (OHSS) (Chang *et al* 2014). Since the first report of a live birth following IVM (Cha *et al* 1991) there has been variable success with *in vitro* matured human oocytes (Roesner *et al* 2012).

Previously published data identified a link between exposure of mouse oocytes to high concentrations of Follicle-Stimulating Hormone (FSH) during IVM, and an increase in chromosomal abnormalities (Roberts *et al* 2005). A comparison of the developmental potential of *in vitro* versus *in vivo* matured mouse oocytes determined that fertilisation rate, synchronous cleavage, and blastocyst development were adversely affected by *in vitro* oocyte maturation, and that abnormalities in cellular symmetry and nuclear morphology were also apparent (Sanfins *et al* 2015). Furthermore, the developmental incompetence of human oocytes matured *in vitro* is thought to relate to dysfunctional gene transcription or modification of genes post-transcription, which may disrupt normal gene utilisation, thus affecting the development of embryos derived from these oocytes (Jones *et al* 2008). This may also contribute to the low efficacy of human *in vitro* fertilisation, since some oocytes aspirated from the ovary during clinical IVF cycles will undergo final maturation spontaneously *in vitro* from MI to MII, in the time period between collection and insemination.

## *1.4 Human fertilisation and preimplantation embryo development*

Standard IVF usually involves the co-incubation of oocytes and spermatozoa for a period of 16-18 hours, although reduced gamete incubation times of ~2 hours may improve the number of top quality embryos available, the clinical pregnancy rate, and the implantation rate in women ≤30 years (Li *et al* 2016). Prior to ICSI, cumulus cells surrounding the oocyte are enzymatically digested and mechanically removed in order to ascertain the maturity of the oocyte. A single spermatozoon is immobilised and injected into the ooplasm of mature oocytes in an area away from the first extruded PB, to minimise the chance of damaging the meiotic spindle, which is purported to reside in the same hemisphere as the first PB (Hardarson *et al* 2000; Woodward *et al* 2008). Interestingly, despite injecting oocytes with the PB at the 12 o'clock position, approximately 10% of metaphase spindles may contain decondensed sperm heads (Flaherty *et al* 1998), suggesting that the position of the spindle does not always correspond with the location of the first PB. Visualising the meiotic spindle in oocytes using polarised light microscopy prior to injection resulted in significantly higher normal fertilisation rates, percentage of early cleaving embryos, and implantation rates when compared to oocytes that were injected without prior spindle visualisation (Madaschi *et al* 2008).

Fertilisation is defined as the combining of male and female chromosomes following penetration of the oocyte by the spermatozoa, resulting in the formation of a zygote (Plachot 2000). Normal fertilisation is evidenced by the appearance of two extruded PB in the PVS, and two centrally located abutting pronuclei (PN) in the

ooplasm 16-18 hours post-insemination (Nagy *et al* 1994). Abnormal multipronucleate (MPN) fertilisation occurs in approximately 7% of zygotes derived from standard IVF (Englert *et al* 1986) and approximately 4% of zygotes resulting from ICSI (Grossman *et al* 1998), and is characterised by the presence of three or more PNs in the ooplasm of oocytes 16-18 hours post-insemination. MPN formation following IVF is thought to occur most commonly due to polyspermy (diandric) (Englert *et al* 1986) and following ICSI due to retention of the second PB (digynic) (Grossman *et al* 1998). Stimulation regimes <10 days have been found to increase the incidence of tripronucleate fertilisation after ICSI, and a higher rate of MPN formation within a cohort of zygotes is a significant predictor of reduced implantation following transfer of an embryo originating from a normally fertilised zygote (Rosen *et al* 2006). The majority of triploid conceptuses spontaneously abort early in pregnancy, and account for ~10% of all miscarriages (Hassold *et al* 1980), however it is possible for triploid embryos to develop to term, giving rise to babies with severe disabilities which are incompatible with life (Sherard *et al* 1986). Examples of normally and abnormally fertilised zygotes are shown in figure 1.1.

***(a)***

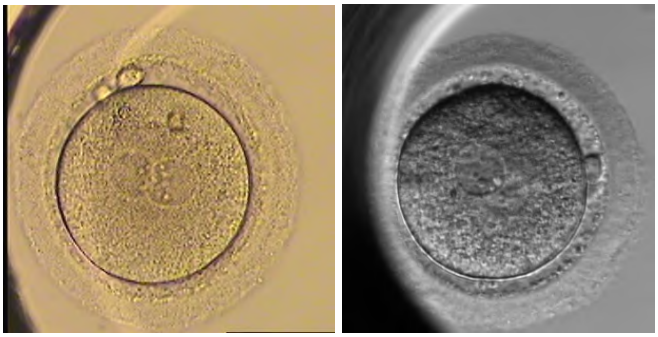

***(b)***

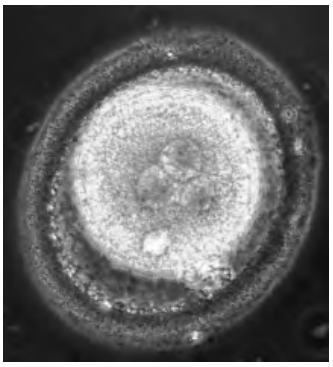

***Figure 1.1: (a) normally fertilised oocytes with two pronuclei and two extruded polar bodies (b) abnormally fertilised oocyte with three pronuclei and one extruded polar body.***

The extrusion of the second polar body is thought to occur by 8 hours post-insemination for IVF oocytes and by 4 hours post-injection for ICSI oocytes (Nagy *et al* 1998). The apposition of the male and female PNs in the centre of the ooplasm precedes the assembly of the parent chromosomes on the mitotic spindle of the zygote prior to the first cleavage division (Plachot 2000).

The morphology of the PN has been suggested as a predictor of embryo quality, and successful pregnancies have been achieved following the transfer of day 1 zygotes (Scott and Smith 1998). Likewise, superior morphology PN are reportedly

significantly more likely to develop into good quality blastocysts (Scott *et al* 2000). The fusion and disappearance of the pronuclei following breakdown of the nuclear membranes approximately 6 hours after they first appear in the ooplasm is termed syngamy (Papale *et al* 2012).

Cleavage of the zygote into two distinct blastomeres 25-27 hours post insemination or injection is associated with a significantly higher proportion of good quality embryos, significantly higher blastocyst development rate, and increased pregnancy, implantation and live birth rates (Lundin *et al* 2001; Van Montfoort *et al* 2004). Indeed, this method of predicting which embryo has the highest implantation potential is hailed as superior to pronuclear scoring (Brezinova *et al* 2009). Several studies have confirmed early cleavage as a predictor of embryo viability leading to an improvement in pregnancy rates (Shoukir *et al* 1997; Sakkas *et al* 1998; Sakkas *et al* 2001; Lundin *et al* 2001; Lee *et al* 2012), and early cleavage assessments can be performed in the laboratory rapidly with a simple microscopic evaluation causing minimal disruption to the embryo culture system. Therefore, early cleavage checks are considered a highly valuable inclusion into routine embryo morphology scoring procedures.

The expected timeline of human preimplantation embryo development following fertilisation has been established over many years via observations in research and clinical laboratories (Niakan *et al* 2012). Embryos may begin to divide into two cells as early as 24 hours post-insemination (Van Montfoort *et al* 2004), with normally developing embryos cleaving to four cells by the morning of day 2, and eight cells by

the morning of day 3 (Alpha Scientists in Reproductive Medicine and ASHRE Special Interest Group in Embryology 2011), as shown in figure 1.2.


***Figure 1.2: Cleavage stage embryos (a) 2-cells (b) 4-cells (c) 8-cells***

Evaluation of cleavage stage embryo quality takes into consideration the symmetry of each blastomere and the degree of fragmentation within the confines of the *zona pellucida* (ZP) (Hardarson *et al* 2001), as described in section 2.7. Poorer quality cleavage stage embryos are associated with the subsequent development of a significantly higher percentage of poor quality and chromosomally abnormal blastocysts (Hardarson *et al* 2003). Compaction of distinct blastomeres into a cohesive mass of cells, the so-called morula, is expected to begin on day 4 post-insemination (Prados *et al* 2012), as shown in figure 1.3.

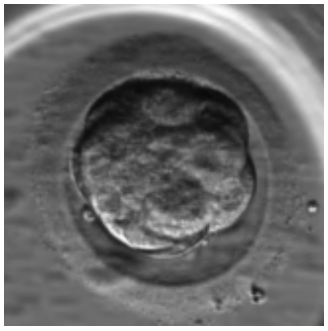

***Figure 1.3: Compacting embryo (morula)***

The next phase of preimplantation embryo development, namely cavitation and expansion of the blastocoel, should occur by day 5 post-insemination, as described in section 2.7. The formation of a blastocyst, the final stage of preimplantation embryo development and differentiation, will only occur following the activation of the embryonic genome, itself a pre-requisite for implantation (Dey *et al* 2004). Figure 1.4 shows examples of a cavitating embryo, an early blastocyst, and a fully expanded hatching blastocyst.

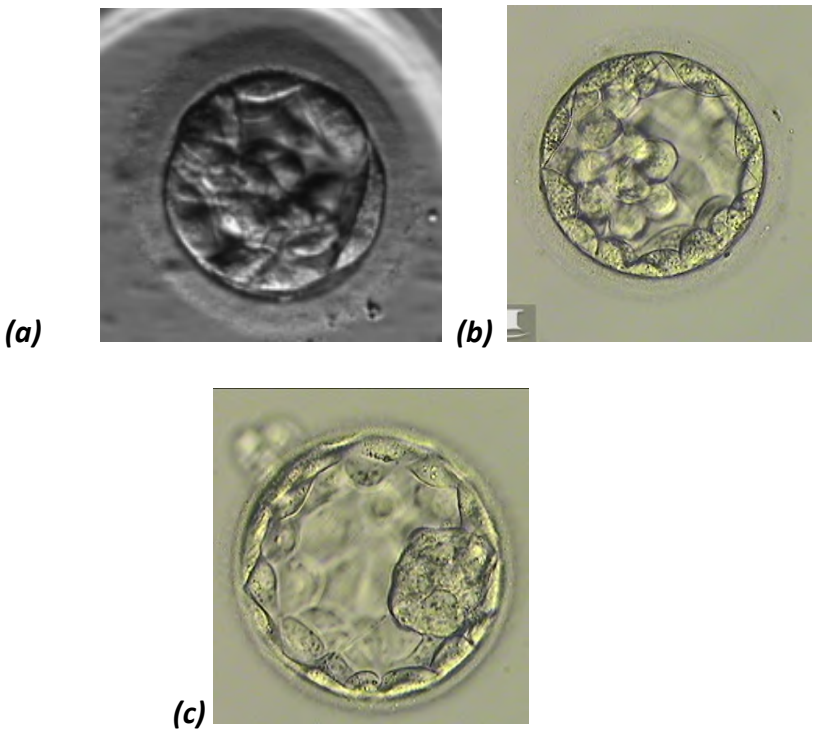


***Figure 1.4: (a) cavitating embryo (b) early blastocyst (c) fully expanded hatching blastocyst***

Blastocyst culture is used as an additional selection tool at a time when the uterus is at its most receptive to implantation. The blastocyst stage is considered to be the time at which the embryo and the endometrium are most physiologically synchronised (Maheshwari *et al* 2016). Extended culture to the blastocyst stage (day 5-6 post insemination) is becoming more commonplace clinically, and is associated with an increase in pregnancy and implantation rates (Gardner *et al* 1998), but only when laboratory culture conditions are optimised. It is thought that the prolonged culture period allows the selection of the most developmentally competent embryos for transfer (Schwarzler *et al* 2004) since many embryos will not survive the transition to a blastocyst, and will therefore be removed from the

pool available for transfer. Additionally, there is a window of implantation in humans that opens six days after ovulation, and remains open for a maximum of four days (Wilcox et al 1999).

Current blastocyst grading systems examine the morphological appearance of the cells of the trophectoderm (TE) and inner cell mass (ICM), along with the extent of expansion of the fluid-filled cavity known as a blastocoel (Gardner *et al* 2000). Desirable features include a TE made up of many tightly-packed cells, a distinct peripherally located ICM, and a fully expanded blastocoelic cavity (Van den Abbeel *et al* 2013). There are many studies of blastocyst culture, with diverse outcomes; however, meta-analysis of clinical trials indicates an advantage of blastocyst culture in terms of pregnancy rate. For example, a study by Kalu *et al* observed that transfer of a single day 5 blastocyst yielded pregnancy rates of 59.0% in women aged ≤37 years, whilst transfer of two blastocysts in the same group resulted in pregnancy rates of 60.7%. The multiple birth rates in each group were 2.3% and 47.6% respectively (Kalu *et al* 2008). In the same study, women between the ages of 38-43 years having a single blastocyst transferred achieved a live birth rate of 29.4%, whilst those who had two blastocysts transferred had an overall live birth rate of 44.3% (Kalu *et al* 2008), indicating that while present selection methods are certainly a valuable tool in identifying the most viable embryo for transfer, there is a definite need for improvement if we are to reduce the incidence of multiple pregnancies by moving towards single embryo transfer, without affecting the success rates of IVF. This ideal may be realised with more informed morphological evaluation of blastocysts with regard to ICM and TE appearance. The shape and size

of the ICM in expanded day 5 blastocysts has been positively correlated with implantation rates, with slightly oval larger ICMs being more likely to implant than rounder and elongated smaller ICMs. Interestingly, blastocysts that fully expanded on day 6 post-insemination generally had smaller, more elongated ICMs (Richter *et al* 2001). Similarly, a blastocyst diameter of >190μm on day 5 was associated with an increase in clinical pregnancy rates, whilst smaller blastocysts and those expanding on day 6 were predictors of reduced clinical pregnancy (Shapiro *et al* 2008). Additionally, higher cell numbers in the ICM and TE of frozen-thawed blastocysts have been related to superior morphological quality (Matsuura *et al* 2010). In contrast to the findings of Richter *et al* (2001), the cell number of the TE combined with the quality of the cells has been recently shown to be a significant predictor of pregnancies that progress to live birth, however the shape and size of the ICM was not found to be related to pregnancy and implantation rates (Ebner *et al* 2016). Interestingly, whilst superior ICM and TE morphology have been confirmed to be strongly indicative of viability, the expansion and hatching stage of blastocysts has been previously identified as the most significant predictor of live birth (Van den Abbeel *et al* 2013).

Complete hatching of the blastocyst from the ZP is a prerequisite for implantation (Ren *et al* 2013). Since it is not feasible, from either a practical or ethical point of view, to study the process of human preimplantation embryo hatching *in vivo*, research is restricted to animal models and *in vitro* studies. In humans, progressive expansion and an accumulation of fluid in the blastocoelic cavity leads to a 2- to 3-fold increase in volume, an increase in internal hydrostatic pressure, and thinning of

the ZP (Sathananthan *et al* 2003), following which the blastocyst herniates through one or more breaks in the ZP. It is hypothesised that "zona breaker" cells, distinct plump TE cells with secretory vesicles and micronuclei that gather around the hatching site, may aid in this process by interacting with the ZP, suggesting that a chemical element exists in the process of hatching *in vitro* (Sathananthan *et al* 2003). Failure of the blastocyst to hatch may be due to hardening of the ZP or to suboptimal culture conditions (Sathananthan *et al* 2003). Hardening of the ZP in fertilised bovine oocytes *in vitro* is characterised by an increase in the stiffness of the ZP, with a concomitant increase in resistance to digestion by proteolytic enzymes (Papi *et al* 2010). Transfer of spontaneously hatched human blastocysts resulted in significantly higher live birth rates when compared to non-hatched blastocysts, with no increase in multiple gestation rates (Chimote *et al* 2013). Assisted hatching (AH) involves artificially creating breaks in the ZP using mechanical or chemical processes, to aid the escape of the blastocyst in preparation for implantation, prior to uterine transfer (Sallam *et al* 2003). Laser-assisted hatching of frozen-thawed human embryos resulted in significantly higher implantation and clinical pregnancy rates when compared to non-hatched embryos; however there was a simultaneous significant increase in multiple gestations (Balaban *et al* 2006). This concurs with an earlier study, in which one of the risk factors for a monozygotic pregnancy was AH (Abusheika *et al* 2000). The site at which the artificial opening is made in relation to the position of the ICM reportedly has no significant influence on clinical pregnancy, implantation, or live birth rate (Ren *et al* 2013), although complete hatching of the blastocyst may be significantly

more likely to occur when the ZP breach is nearer to the ICM (Miyata *et al* 2010). Murine blastocysts are thought to initiate hatching *in vitro* at the mural TE under the influence of proteolytic enzymes (Perona and Wassarman 1986). Studies of hamster blastocysts have shown that blastocyst hatching *in vivo* involves the uniform thinning and disappearance of the ZP, in contrast to those hatching *in vitro*, where focal lysis of the ZP occurred, followed by escape of the blastocyst, with a comparative time delay of ≥29 hours. The authors concluded that uterine contributions are likely to be a factor in hamster blastocyst hatching *in vivo*, and that the behaviour of *in vitro* cultured blastocysts was markedly different (Gonzales and Bavister 1995), a finding similar to that in early bovine studies, which seemed to suggest that factors controlling the digestion of the ZP *in vivo* differed from those *in vitro* (Wright *et al* 1976).

## *1.5 Implantation*

The ultimate evidence of embryo competence is implantation and development. In humans, implantation begins when the blastocyst assumes a fixed position, with the inner cell mass orientated towards the uterine epithelium (Bischof and Campana 1996). Hatched human blastocysts attach to and invade human endometrial stromal fibroblasts with the ICM apposed to the cell layer, indicating that attachment is mediated via the polar trophectoderm (Carver *et al* 2003). For successful implantation to occur, the endometrial lumen epithelium must acquire the transient receptivity required to accept a hatching blastocyst (Dey et al 2004), with the trophoblast invasion eliciting a decidual response. Implantation is initiated when the trophoblast cells of the hatched blastocyst attach to the luminal epithelium of the receptive endometrium, and stromal cells at the site of attachment proliferate and differentiate. This process is known as decidualisation, and is essential to promote development of the placenta and foetus (Abrahamsohn and Zorn 1993). Implantation is a fundamental event in the establishment of pregnancy, and would be impossible without the differentiation of the endometrium via oestrogen and progesterone into a receptive state. This is hypothesised to represent a natural selection process whereby the endometrium acts as a biosensor for developmentally incompetent embryos, rejecting those that have arrested and are therefore incapable of implanting (Teklenburg *et al* 2010). This idea appears to be supported by the findings that decreased levels of the decidual marker prolactin, in association with increased levels of implantation

promoter prokineticin-1, were observed in endometrial biopsies of women suffering from recurrent pregnancy loss. It seems that defective maternal-embryonic communication due to impaired decidualisation results in a disruption of the natural selection capacity of the endometrium, which may facilitate implantation of non-viable embryos, yet culminate in spontaneous abortion (Salker et al 2010). Embryos entering the undifferentiated uterus will not implant (Catalano *et al* 2005). In humans, this response is under cyclic maternal control and occurs spontaneously, thus if no embryo is available to implant, menstrual shedding results.

Whilst assisted reproductive technologies have vastly increased our understanding of human preimplantation embryo development, implantation remains the limiting factor in the achievement of a successful pregnancy in many cases (Fatemi and Popovic-Todorovic 2013). The failure to achieve a pregnancy following three cycles of IVF with embryos transferred may be considered a case of recurrent implantation failure (Margalioth *et al* 2006). The process of blastocyst attachment to the receptive endometrium is summarised in figure 1.5.

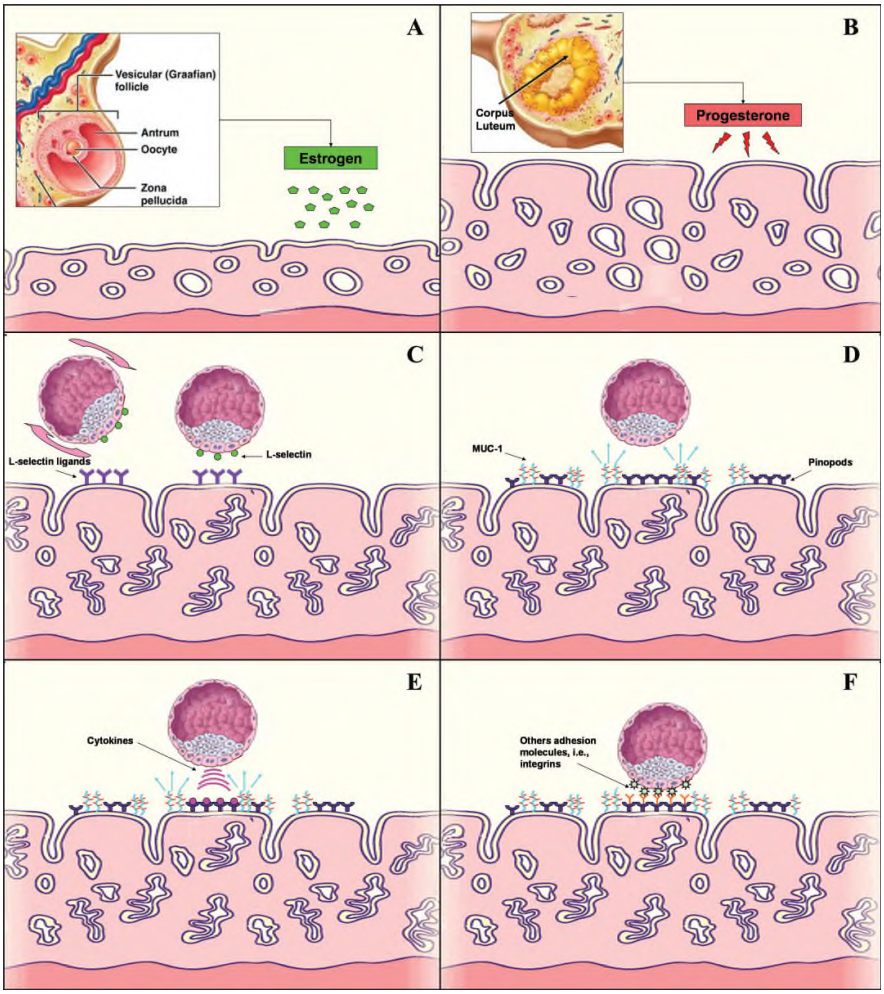


***Figure 1.5: Human embryo implantation in utero (A) Endometrium proliferates under estrogen enhancement. (B) Progesterone from luteinized follicles leads to endometrial differentiation. (C) The blastocyst enters the uterus through the ostia and rolls freely over the endometrium under signals by L-selectin. (D) Mucin-1(MUC-1) repels the blastocyst and prevents its adhesion to endometrial areas with poor chances of implantation. (E) Chemokines and cytokines attract the blastocyst to the optimal implantation spot. (F) Adhesion molecules (e.g. integrins and cadherins) firmly attach the blastocyst to the endometrial pinopods to ensure further successful implantation (Achache and Revel 2006)***

### *1.6 Implantation models*

*In vitro*, the initial stages of *in vivo* implantation can be modelled to assess interaction between the blastocyst and the uterus, which may involve culturing human blastocysts with substrate containing endometrial stromal cells, or on an extracellular matrix such as Matrigel, a commercially available gel containing similar structural proteins and growth factors to the endometrial matrix (Ghaffari Novin *et al* 2007). Early studies involving the co-culture of mouse embryos with Matrigel found that significantly higher numbers of blastocysts reached the hatching stage when cultured with Matrigel, as compared to culture with medium alone (Carnegie *et al* 1995). Similarly, in human studies, a significantly higher percentage of embryos developed into blastocysts and proceeded to hatch when cultured with Matrigel-supplemented medium, in comparison with those cultured in medium alone (Ghaffari Novin *et al* 2007).

### *1.7 Optimisation of the culture system*

Optimisation of the embryo culture system is crucial if human preimplantation embryo development is to be supported and maintained to the hatching blastocyst stage, in order to achieve the best possible clinical outcomes. Early culture media were based upon simple balanced salt solutions, supplemented with glucose and phosphate. However, with increasing understanding of human embryo nutritional and energy requirements, more complex media containing amino acids, EDTA, vitamins and antibiotics were developed (Mantikou *et al* 2013). The varying metabolic requirements of embryos at different developmental stages, namely pyruvate at the cleavage stage and glucose at the blastocyst stage, caused difficulty

with finding single media to support the development of competent blastocysts (Hardy *et al* 1989; Gardner 1998). Sequential media systems, which provided the developing embryo with tailored substrates according to the metabolic needs at a particular stage of development, were subsequently produced and introduced into clinical practice (Gardner and Lane 1998). The rationale behind the development of sequential media was the fact that, *in vivo*, the developing human preimplantation embryo experiences exposure to vastly differing secretory regions in the female reproductive tract (Schultz and Heyner 1993; Bavister 1995). Supplementation of culture medium with granulocyte-macrophage colony-stimulating factor (GM-CSF) resulted in a significant increase in the clinical pregnancy rate in women >35 years (Zhou *et al* 2016).

A systematic review of commercially available culture media discovered that very little high quality research has been conducted into the selection of media to use in the clinical embryology laboratory (Mantikou *et al* 2013), and the brand of media used is widely empirical, perhaps a historical decision, or based upon value for money (Bavister 1995). Additionally, despite fears regarding the health of children born following ART, neither the brand of culture medium used nor the duration of culture (3 versus 5 day post-insemination) has been shown to influence the birthweight of live born singletons (De Vos *et al* 2015).

Recently, single-step culture media systems, which support development from the zygote to the blastocyst, have emerged as an alternative for use in the clinical IVF laboratory. Benefits of using a single-step media system, particularly when the medium is used as intended without refreshing for the entire incubation time,

include minimal disruption of the embryos during the culture period, along with cost-saving and a decrease in the laboratory workload due to lower usage of consumables and eliminating the need to transfer embryos from one medium to another during the culture period. The blastulation rates using single-step media are comparable to those achieved using sequential media systems (Machtinger and Racowsky 2012). The principle behind single step medium is to “let the embryo choose”, that is to provide all nutrients and energy substrates in one medium, and allow the embryo to utilise as necessary, according to the requirements at each developmental stage (Biggers 2001). Studies have shown an increase in blastocyst development during single-step uninterrupted culture, and comparable implantation and pregnancy rates to embryos cultured in sequential media systems (Stout *et al* 2013). The use of single-step media as an adjunct to uninterrupted time lapse monitoring in the clinical embryology laboratory may aid in the reduction of stress experienced by the developing embryo.

### *1.8 Multiple pregnancy*

The inefficiency of IVF treatments in the early days prompted many clinics to adopt a multiple embryo transfer strategy (Martikainen *et al* 2001), resulting in a concomitant increase in multiple pregnancies. Initially, this was viewed by clinicians as necessary and by patients as an added bonus (Child *et al* 2004); however tolerance of the consequent high rate of multiple pregnancies has now waned due to increasing evidence about the adverse consequences associated with twin and higher order gestations (Gerris *et al* 1999). Multiple gestations remain the single most problematic outcome of *in vitro* fertilisation treatments, with associated medical, social, and financial consequences to consider (Templeton and Morris 1998; Chambers *et al* 2007). Twins are associated with a neonatal mortality rate seven-fold higher than singletons, along with a six-fold increase in the incidence of cerebral palsy (El-Toukhy *et al* 2006) whilst higher rates of miscarriage, pregnancy-induced hypertension and pre-eclampsia, ante-partum haemorrhage, gestational diabetes, operative delivery, maternal morbidity and prematurity, are additional maternal and perinatal complications commonly reported in multiple pregnancy (Kalu *et al* 2008). Furthermore, these problems are exacerbated with each additional foetus *in utero* (Min *et al* 2010). The increased financial burden and social consequences of multiple births on the healthcare system, the parents and existing children in the family must also be taken into consideration (Shenfield *et al* 2003). Interestingly, the risk of pre-term birth in women ≥35 years decreases in comparison with younger women following IVF treatment, in both singleton and

twin pregnancies (Xiong *et al* 2014). However, risk factors for monozygotic twin pregnancies following ART include female age at treatment ≥35 years (Abusheika *et al* 2000) and prolonged *in vitro* culture of embryos (Vaughan *et al* 2016).

The incidence of monozygotic twin pregnancies following IVF treatment is significantly higher than that reported in natural conceptions, the incidence being around 0.4% in natural conception (Abusheika *et al* 2000; Saito *et al* 2000). Whilst the underlying mechanism for monozygotic multiple gestations is clear, the splitting of a single preimplantation embryo, the speculative causes of this are varied. The incidence of monozygotic multiple gestations in ART has been previously reported at up to 8.9% (Abusheika *et al* 2000). One theory suggests that artificially breaching the ZP via chemical or mechanical means may impair the ability of the blastocyst to hatch normally, causing division of the ICM into two (Cohen *et al* 1990). Indeed, those patients requiring preimplantation genetic diagnosis (PGD) were deemed at higher risk of monozygotic twinning, even higher than those specifically opting for AH (Vaughan *et al* 2016). The occurrence of monozygotic multiple pregnancy after ICSI is increased substantially in comparison to IVF (7.2%-8.9% versus 0.9%-1.5% respectively), which may be related to the breach of the ZP at the time of microinjection (Abusheika *et al* 2000; Saito *et al* 2000). A quadruplet pregnancy after transfer of a single day 4 embryo which had been biopsied on day 3, and a triplet pregnancy following transfer of a single day 5 blastocyst have been reported (Saravelos *et al* 2016), providing further evidence of an association between monozygotic higher order pregnancies, ZP manipulation and prolonged *in vitro*

culture. Both of the pregnancies reported were selectively reduced, providing yet another reason to avoid multiple gestations wherever possible.

Studies in the mouse have demonstrated that double ICMs may form after IVF, which are capable of continuing to develop and form trophoblastic outgrowths. The incidence of double ICMs in the *in vitro* cultured blastocysts was greatly increased in comparison with the *in vivo* derived blastocysts (3.1% and 0.6% respectively), indicating that *in vitro* culture may predispose to monozygotic twinning via this mechanism (Chida 1990). A human monozygotic triplet pregnancy has been reported after transfer of a blastocyst with two inner cell masses (Meintjes *et al* 2001), suggesting that such blastocysts should be avoided if possible when selecting prior to uterine transfer. Perhaps the most curious finding in the investigation of monozygotic twin pregnancies has been the discovery of a clustering pattern, with an increase in such pregnancies during the last six months of the calendar year (Vaughan *et al* 2016). This is a remarkably under-researched area, and further studies into the potential causes of increased incidence of monozygotic twinning after ART are necessary, particularly if morphological clues exist that can be microscopically identified in the clinical IVF laboratory, thus aiding us in the selection of embryos prior to uterine transfer.

### *1.9 Single embryo transfer*

The introduction of the HFEA Multiple Births Minimisation Strategy in 2009 meant that clinics were required to find ways in which to reduce the incidence of multiple gestations whilst maintaining acceptable pregnancy rates. There has been a major shift towards single embryo transfer (sET) in the last 15 years or so, with a view to

reducing the incidence of multiple gestations (Gerris *et al* 1999; Gerris and Van Royen 2000; De Neubourg *et al* 2002; Hamberger and Hardarson 2003; Pandian *et al* 2005). In our clinic, sET is currently performed in ~80% of fresh treatment cycles, with a multiple pregnancy rate of ~4%, a figure comparable with previously published data (Martikainen *et al* 2001). Success rates have steadily increased, and it is now recommended that sET should always be the preferential option for women with a good prognosis for pregnancy, having two or more good quality embryos, aged 37 years or younger in the initial fresh cycle, and any subsequent frozen cycles (Min *et al* 2010). A significant increase in the clinical pregnancy rate and a significant decrease in the multiple pregnancy rate after day 5 blastocyst sET in good prognosis patients (four top quality embryos on day 3) has been previously reported (Khalaf *et al* 2008). Furthermore, the live birth rate after sET has recently been reported as 52%, with a multiple birth rate of 6% in women aged between 18-38 years (Bensdorp *et al* 2015)

### *1.10 Embryo cryopreservation*

The increase in elective sET has led to a simultaneous increase in the number of good quality supernumerary preimplantation embryos being cryopreserved for use in future treatment cycles (Stokes *et al* 2007), with pregnancy results comparable to those attained after fresh embryo transfer. Certainly, cumulative pregnancy rates in women aged 25-37 years who had a frozen blastocyst replaced if the corresponding fresh cycle was unsuccessful were higher than those achieved after transfer of two fresh blastocysts (Kalu *et al* 2008). Indeed, a significantly higher implantation and clinical pregnancy rate may be achieved after the transfer of good quality

blastocysts in frozen embryo transfer cycles in comparison to fresh cycles (Ozgur *et al* 2015), thought to be due to the physiologically more natural state of the uterus. Zygotes, embryos and blastocysts may be cryopreserved using controlled rate freezing or vitrification (Stokes *et al* 2007; Balaban *et al* 2008), which are discussed in more detail in the methods section of this thesis.

### *1.11 Improving human embryo selection*

Any method routinely applied in the clinical situation has to be non-detrimental to embryo development, and ideally non-invasive. However, such methods do not have high predictive value, ie, implantation of poor morphology embryos regularly occurs, while good morphology embryos frequently fail to implant. Whilst the aforementioned zygote, embryo and blastocyst morphology scoring are useful minimally-invasive selection tools, human embryo selection is inefficient and flawed. The continual need to improve the efficacy of human embryo selection means that advancements in methods used to identify viable embryos are necessary if the desired high pregnancy rates from single embryo transfers are to be achieved (Montag *et al* 2013). Many techniques have been proposed as tools to determine human embryo viability; however some of these are highly invasive, and others may require expensive specialised equipment.

Extended culture of embryos to the blastocyst stage is hypothesised to improve pregnancy rates partly due to a mechanism of natural selection whereby those embryos with abnormal constitution, such as aberrant chromosome complement or delayed cleavage, arrest in their development and are not transferred (Magli *et al* 1998; Rubio *et al* 2007). However, some studies have suggested that singletons

born after blastocyst transfer on day 5 post-insemination have significantly higher birthweights than those born following embryo transfer on day 2 post-insemination (Makinen *et al* 2012), and on day 3 post-insemination (Zhu *et al* 2014).

There was early speculation that euploid cells were preferentially allocated to the ICM, which will become the embryo proper, and aneuploid cells were allocated to the TE, which gives rise to the placenta and extraembryonic membranes (Hardy *et al* 1989). However, several researchers have since found that the proportion of aneuploid cells in the ICM was similar to the proportion in the blastocyst as a whole (Evsikov and Verlinsky 1998; Liu *et al* 2012; Capalbo *et al* 2013) so the mechanism of cellular control, selection and allocation within the blastocyst remains uncertain. In particular, embryos can have a range of different chromosomal abnormalities, including consistent aneuploidy in every cell, or partial aneuploidy where only certain cell lines are affected (Rubio *et al* 2007). It has been shown that aneuploid embryos are around 25% more likely to arrest between day 3 and days 5-6 (59%) than euploid embryos (34%), and although chromosomally abnormal embryos are capable of developing to the blastocyst stage, the likelihood of implantation failure thereafter is increased (Magli *et al* 2000). Certain classifications of chromosome abnormalities are not conducive to the continuing development of pre-implantation embryos, such as autosomal monosomies, haploidy and polyploidy (Munne *et al* 2003). Conversely, some abnormal embryos can progress to blastocyst and implant, although analysis of embryos undergoing biopsy and preimplantation genetic diagnosis (PGD), demonstrates that those embryos exhibiting two chromosomally abnormal cells are more likely to arrest prior to blastocyst formation than those

with one aneuploid and one euploid cell (Rubio *et al* 2007). Bearing in mind that implantation of chromosomally compromised embryos can result in either spontaneous abortion or the birth of genetically abnormal babies, it is imperative that developmentally competent, chromosomally normal embryos are selected prior to uterine transfer (Campbell *et al* 2013). However, a further unusual property of embryos is the ability to 'self-correct' by jettisoning abnormally developing cells (Bazrgar *et al* 2013), which may be via apoptosis in cells destined to the foetal lineage, and proliferative defects in those destined for the placental lineage, thus progressively eliminating aneuploid cells in the blastocyst (Bolton *et al* 2016). This phenomenon is not well understood but may result in rescue of otherwise abnormal embryos resulting in birth of normal offspring.

Preimplantation genetic diagnosis (PGD) and screening (PGS) are routinely used in clinical embryology in order to identify chromosomal and genetic disorders which may result in implantation failure and foetal loss (Sermon *et al* 2004). Aneuploidy is the most commonly occurring chromosomal anomaly in human embryos, accounting for the majority of spontaneous abortions and congenital birth defects (Hassold *et al* 2007). The incidence of aneuploidy in meiotically mature human oocytes following controlled ovarian stimulation has been estimated at between ~8% and ~49% (Van Blerkom and Henry 1988; Gianaroli *et al* 2010) rising to between ~52% and ~57% (Kuliev *et al* 2003; Gianaroli *et al* 2010) in women of advanced maternal age.

Several techniques are available in order to the obtain material necessary for genetic testing of human oocytes and preimplantation embryos (Sermon *et al* 2004).

PB biopsy may be performed in order to ascertain the maternal genotype of the oocyte (Verlinsky *et al* 1992; Strom *et al* 1998), whilst biopsy of one or more blastomeres from the cleavage stage embryo is a widely utilised technique (Sermon *et al* 2004). Recent advances in successful culture of embryos to the blastocyst stage have led to the implementation of TE biopsy as an alternative to cleavage stage biopsy (Mir *et al* 2016). Both cleavage stage and TE biopsy generate results representative of the genetic complement of the whole embryo, the main difference being that biopsied blastocysts must be cryopreserved and transferred in a later cycle in order to wait for the results of the analysis (Mir *et al* 2016), which may have an impact on the clinical outcome.

It has been previously reported that removal of one or two blastomeres from human embryos at day 3 post-fertilisation has no significant adverse effects on viability, metabolism, or blastocyst development (Hardy *et al* 1990). Likewise, removal of two cells from a day 3 embryo containing ≥7 cells does not reduce the pregnancy or implantation rate following day 3 or day 4 embryo transfer (Van de Velde *et al* 2000). However, a different study has shown a significant influence on blastocyst formation rate and quality when comparing the removal of one versus two blastomeres from day 3 embryos (Goossens *et al* 2008), and blastocyst formation and live birth rates after 1-cell biopsy were significantly better in comparison to those after 2-cell biopsy (De Vos *et al* 2009). Additionally, mouse blastocyst inner cell mass formation arising from biopsied 2-cell embryos was significantly impaired in comparison with non-biopsied controls (Nijs and Van Steirteghem 1987), suggesting that removal of blastomeres at early developmental

stages substantially reduces cellular mass, and may disrupt polarised allocation of cells in the blastocyst. Moreover, mice derived from embryos that had been biopsied were of a lower birthweight than those from non-biopsied embryos, possibly as a result of steroid metabolism dysfunction during pregnancy (Sugawara *et al* 2012).

Other advanced methods of predicting human embryo viability are non-invasive, and include time-lapse imaging, which is discussed in greater detail later in this chapter. Whilst time lapse imaging has become routinely utilised in some clinical embryology laboratories in recent years, other techniques were initially employed when searching for suitably accurate methods with minimal manipulation and disruption to the developing embryo. One such method is the measurement of pyruvate and glucose in the culture medium surrounding developing human preimplantation embryos as a predictor of viability, since a higher utilisation of these energy substrates from fertilisation to blastocyst may indicate optimal development *in vitro* (Hardy *et al* 1989). Other non-invasive techniques to predict human embryo viability include analysis of the follicular fluid, cumulus cells, and spent culture media (Montag *et al* 2013), although these methods are not easily implemented in a clinical setting, and require time and expertise for execution.

### *1.12 Time lapse imaging*

Time lapse cinematography has been used to investigate the dynamics of embryo development for more than five decades (Bavister 1995). For many years, visual markers of embryo growth and morphology were assessed at 24-hourly intervals including embryo cleavage rate, cell number, cell shape, cell surface contact, degree

of fragmentation (Prados *et al* 2012), and blastocyst expansion status, ICM location and appearance, and TE morphology (Hardarson *et al* 2012). These were the predominant methods of identifying potentially viable embryos in the clinical embryology laboratory. The introduction of live cell imaging to improve selection criteria, using techniques based upon precise timings of more complex markers such as the appearance and disappearance of pronuclei, and early cell division, have provided a much more comprehensive view of embryo development, and offered further insight into the prediction of preimplantation embryo viability (Lemmen *et al* 2008; Azarello *et al* 2012; Montag *et al* 2013), without compromising the developmental capability of the embryos being monitored (Lemmen *et al* 2008; Nakahara *et al* 2010). An assessment of 102 zygotes using a novel time lapse imaging system, determined that there was no detrimental effect of imaging embryos every five minutes from day one (zygote) until day two (cleavage stage) with regard to early cleavage and embryo quality (Lemmen *et al* 2008). Similarly, no significant differences in fertilisation rate or percentage of top quality embryos was observed after culture in a time lapse incubator capturing images at 15 minute intervals, in comparison with a conventional incubator without regular image capture (Nakahara *et al* 2010).

With the widespread introduction of advanced time lapse technology into routine clinical practice during the past five years or so (Armstrong *et al* 2014), previously unreported phenomena surrounding the development of human preimplantation embryos are emerging. Atypical embryo behaviour, which would ordinarily be missed using traditional “snap-shot” morphological assessment, has increased our

understanding of aberrant developmental events and their relationship to embryo viability, allowing de-selection of such embryos for uterine transfer. Additionally, the embryos may remain undisturbed for the entire culture period, thus minimising embryo stress (Meseguer *et al* 2012; Montag *et al* 2013).

The seminal paper on advanced time lapse imaging evidence correlated live cell time lapse images with molecular profiles of human embryos, indicating that development of embryos to the blastocyst stage *in vitro* can be predicted two days post-insemination using information on cell division patterns (Wong *et al* 2010). Additionally, analysis of the gene expression profiles of cultured embryos at various stages points to evidence of maternally-derived transcripts that determine developmental success or failure prior to embryonic gene activation, suggesting that some aspects of human embryo fate are established early in development as a result of determinants inherited from the oocyte (Wong *et al* 2010).

Since the publication of the Wong *et al* study, several groups have described using a plethora of spatio-temporal features of human preimplantation embryo development to identify which embryos are likely to result in a pregnancy, and which embryos are not (Chen *et al* 2013). One study reported that live birth rates were significantly associated with pronuclear breakdown later than 20h45min post-injection (Azarello *et al* 2012). Euploid embryos reportedly display a unique division pattern until the 4-cell stage, and analysis of fragmentation in conjunction with these parameters may indicate chromosomally normal embryos, to aid in selection and potentially avoid miscarriage (Chavez *et al* 2012). Atypical embryo phenotypes have been identified as prevalent in human preimplantation embryos, and which

relate to significantly reduced development potential (Athayde Wirka *et al* 2012). Abnormal syngamy, whereby pronuclei movement within the cytoplasm of the fertilised oocyte is disordered prior to disappearance, has been observed in 25.1% of zygotes, whilst oolemma ruffling and the appearance of pseudo furrows, as well as the timing of the first complete cell division were noted in 31% of zygotes. Direct cleavage of the zygote or one of the daughter cell into more than two cells has been observed in 17%-18%, and disordered cleavage behaviours in 15% of embryos assessed (Athayde Wirka *et al* 2012; Hlinka *et al* 2012). Elsewhere, directly cleaving embryos have been reported as having a significantly reduced chance of implanting (Rubio *et al* 2012), however, such cleavage anomalies do not necessarily preclude successful outcomes (Stecher *et al* 2014), and so caution is advised when deciding whether to discard or transfer embryo based upon these observations. Early cleavage timings appear to be predictive of blastocyst formation (Milewski *et al* 2015) and implantation potential (Dal Canto *et al* 2012; Chamayou *et al* 2013). A rather interesting finding was that embryos that had one blastomere removed for PGD began compaction, cavitation and blastocoelic expansion significantly later than their non-biopsied counterparts (Kirekegaard *et al* 2012).

The use of time lapse in the clinical embryology laboratory is a useful tool for selecting (or de-selecting) embryos prior to transfer, however the technology is still relatively new and further studies into the usefulness of time lapse monitoring for the selection of embryos are needed (Kirkegaard *et al* 2015). Additionally, the equipment is expensive, and non-automated systems require a great deal of time dedicated to annotating the images. Semi-automated systems using darkfield

microscopy may make on-screen morphology scoring difficult, and lead to disturbance of the embryos if their quality is to be assessed using a standard brightfield microscope, thus causing a reduction in the benefits of uninterrupted embryo culture.

### *1.13 Embryo polarity*

In animal species such as insects, fish, reptiles and birds, the spatial arrangement of the oocyte and the preimplantation embryo is known to be important for its developmental potential (Ajduk and Zernicka-Goetz 2015). Polarised development from the fertilised egg to the implanting embryo gives rise to the eventual axes of the organism, a fundamental requirement for normal function. However, the mechanisms involved in the establishment and maintenance of polarity before and at implantation are the subject of continuing debate and are known to vary among species (Edwards and Beard 1997). In most species the polarity of the whole organism can be traced back to the polarity of the egg; however mammals were thought to be the exception to this rule, with the axes of the embryo developing only post-implantation (Weber *et al* 1999). Conversely, some evidence suggests that establishment of axes during normal murine development can indeed be traced back to the preimplantation embryo (Weber *et al* 1999). However, in contrast to model mammalian species, human embryos do not necessarily follow this pattern and are more variable in appearance, which requires examination in terms of axis development. Whether the body plan of the human adult relates to the polarity of the early preimplantation embryo is yet to be determined.

The polar axes in the human are shown diagrammatically in figure 1.6.

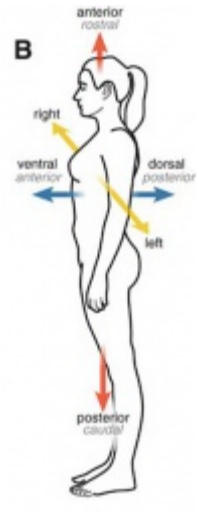


***Figure 1.6: The polar axes in the human (Hill 2016)***

Oocyte polarity in non-mammalian species is well-documented, as demonstrated by pigment distribution in *Xenopus laevis* and by shape in *Drosophila* and *C. elegans.* (Ajduk and Zernicka-Goetz 2015).

In mammals, oocyte polarity is less obvious, but may be implied by the location of the first polar body marking the animal pole and the non-random site of the second polar body, extruded after fertilisation, indicating the position of the embryonic pole (Gardner 1997). Embryonic differentiation and the formation of AV, dorso-ventral (DV) and left-right (LR) embryonic axes are fundamental to life, and are regulated by polarised ooplasmic determinants giving rise to an animal pole and a vegetal pole. The position of the animal pole, containing nuclear material and indicated by the first polar body, is positioned diametrically opposite the yolk-containing vegetal pole in the oocyte, establishing the first embryonic axis (Edwards and Beard 1997). It is hypothesised that rotation of pronuclei within the cytoplasm

of fertilised oocytes in order to direct their axis towards the second polar body in a standardised orientation may prepare the zygote for normal development (Edwards and Beard 1997). Indeed, the orientation of the pronuclear axis relative to the first polar body is significantly correlated with embryo morphology, where a greater deviation is related to decreasing embryo quality, possibly due to a higher degree of cytoplasmic turbulence and subsequent disturbance in the achievement of axes polarity and consequent disruption of normal division (Garello *et al* 1999), suggesting that oocyte polarity influences embryonic developmental competence. Zygotes with eccentric pronuclei have a significantly increased chance of developing irregularly shaped blastomeres than those with centrally placed pronuclei (Garello *et al* 1999).

Following the first cleavage division along the meridian of the pronuclear axis, the first dividing blastomere of the newly formed 2-cell will form a cleavage furrow along the meridian axis prior to division into daughter cells which pass through the embryonic and vegetal poles. The second-cleaving blastomere then rotates and divides transversely, resulting in the classical “crosswise” 4-cell arrangement observed in normally cleaving embryos (Edwards and Beard 1997), thus providing evidence that cleavage planes are regulated rather than random, and reiterating the concept of oocyte polarity.

Examples of tetrahedral and non-tetrahedral cleavage patterns are shown in figure 1.7.

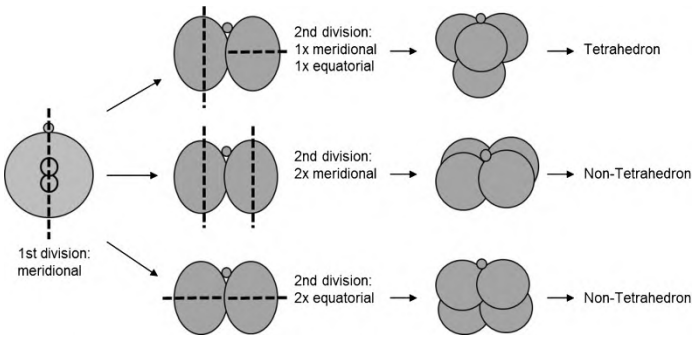


***Figure 1.7: Tetrahedral and non-tetrahedral cleavage patterns (Cauffman et al 2014)***

Disruption of normal cleavage may lead to interruption of formation of axes, and thus embryonic developmental delay or lethality. During cleavage, cell division may be symmetrical or asymmetrical, giving rise to inside and outside cell populations that differentiate into the inner cell mass and the trophectoderm in the blastocyst (Bischoff *et al* 2008), although it is hypothesised that cells of the ICM can differentiate into TE cells (Pierce *et al* 1988). Evidence of polarity in mammalian species becomes obvious at the light microscopy level only at the blastocyst stage (day 5/6 post-insemination), with the development of the peripherally placed ICM within the blastocoelic cavity (Edwards and Beard 1997), although polarity is evident using scanning electron microscopy at the compaction stage (day 4 post-insemination) (Nikas *et al* 1996).

Tracking individual blastomeres throughout cleavage and development to the blastocyst stage provides a direct method of detecting developmental regulation within the embryo, and previous studies have indicated that cellular allocation is a non-random event, and that the frequency of symmetric/asymmetric divisions of a

blastomere correlates with its origin in relation to the AV axis of the zygote (Bischoff *et al* 2008). Furthermore, symmetrically dividing cells contribute more frequently to the cells of the trophectoderm (outside cells), whilst asymmetrically dividing cells are more likely to contribute to the cells of the inner cell mass (inside cells), and that the positioning of the cavity, and thus the orientation of the embryonic-abembryonic axis, is influenced by the pattern of earlier cell divisions (Bischoff *et al* 2008). The transcription factor Oct-4, a product of the *OTF3* gene, is expressed at a level 31-times higher in the ICM in comparison to the TE cells of human blastocysts, suggesting that Oct-4 may play a role in maintenance of cellular totipotency (Hansis *et al* 2000), and the expression of Oct-4 by blastomeres of the cleavage stage human embryo may predict whether they will develop into ICM or TE cells at the blastocyst stage (Hansis *et al* 2001). These findings confirm those previously reported in murine studies (Palmieri *et al* 1994). Also In the mouse, heterogeneous expression of Oct-4 transcription targets in the 4-cell embryo creates bias towards cell fate into ICM or TE cells (Goolam *et al* 2016), which is in agreement with previously published data showing that slower rates of nuclear export and import kinetics of Oct-4 in individual blastomeres of the cleavage stage mouse embryo predict preferential differentiation into cells of the ICM (Plachta *et al* 2011).

Certain polarised molecular markers have been identified in mice and other species, but very little research has studied polarity in human embryos. Moreover, human embryos are more variable morphologically than those of other animals, on average having lower implantation potential, and there are no reliable routine markers of

quality to select the best embryos during clinical infertility treatments. Disorganised development of polarity may at least partially explain delayed embryo growth, poor embryo morphology and low fertility in women.

It is thought that chromatin becomes polarised in newly fertilised oocytes, with that in both the paternal and maternal pronuclei rotating to face each other internally within the ooplasm, becoming highly condensed during pronuclear apposition, with the male pronucleus seemingly influencing the formation of the polar axes (Van Blerkom *et al* 1995). Ooplasmic rotation, as observed following intracytoplasmic sperm injection, and prior to second polar body extrusion (Payne *et al* 1997), may account for the polarisation of the apposed pronuclei in line with the second polar body, with the axis orientated through the centre of the pronuclei in preparation for the first cleavage division. Some pronuclei, however, appear to become arranged at right angles to the second polar body (Edwards and Beard 1997).

With the evidence of polarity in oocytes and embryos, and the potential effects of this on subsequent development, it follows that assessment of polarised characteristics and markers may provide an additional measure of embryonic developmental viability and enable the selection of the embryo most likely to result in pregnancy and live birth. The identification of suitable markers to delineate polarised regions in oocytes and embryos will aid in the process of determining which molecules are restricted to the embryonic and vegetal hemispheres (Fulka Jr *et al* 1998), which in turn will increase the understanding of the influence of polarity on future development and enable clinically relevant tools to be developed for use in laboratory procedures.

Evidence of embryo polarity is suggested by the spatial arrangements of organelles such as mitochondria (Van Blerkom *et al* 2000), the regulatory proteins leptin and STAT3 (Antczak and Van Blerkom 1997), cell surface structures such as microvilli (Nikas *et al* 1996), and the cytoskeletal protein actin (Wedlich-Soldner and Li 2004) in developing embryos. For example, the cytoskeletal protein actin undergoes rearrangements during embryonic development, resulting in polarised morphogenesis (Hall and Nobes 2000), and the putative animal pole is characterised by increased concentrations of cytoplasmic organelles such as mitochondria (Calarco 1995). Mitochondria are essential for embryonic development, and may be disproportionately inherited by blastomeres during development as a result of asymmetrical cleavage (Van Blerkom *et al* 2000). Those blastomeres with mitochondrial deficiencies as a result of unequal inheritance subsequently arrest and lyse, and are shown to have a reduced ATP content, suggesting that diminished ATP generation can adversely affect developmental competence. Indeed, it is suggested that the number of blastomeres affected by disproportionate mitochondrial inheritance may be an indicator of developmental potential (Van Blerkom *et al* 2000), and may also be important in mtDNA inheritance. Mitochondria-related activity, such as ATP production, may be influenced by the magnitude of the inner mitochondrial membrane potential, which has a heterogeneous distribution within cells of the preimplantation embryo (Van Blerkom *et al* 2002). Mitochondrial membrane potential may be quantified in cells using the cationic lipophilic carbocyanine-based dye JC-1, which accumulates within the mitochondrial matrix and emits a green (low-polarised) or red (high-polarised)

fluorescence reflecting the formation of J-aggregates, resulting from a unique chemical reaction (Van Blerkom *et al* 2002). It is hypothesised that the shift from uniform distribution of J-aggregate fluorescence throughout the cytoplasm of the germinal vesicle stage oocyte, to an accumulation of J-aggregate fluorescence specifically in the animal hemisphere of the MII stage oocyte, may signal an early regulatory event in the activation of the embryonic genome. Furthermore, a role for domains of high-polarised mitochondria in the $Ca^{2+}$dependant activation of oocytes may have downstream effects on developmental competence in morphologically normal preimplantation embryos that arrest prior to blastocyst formation or fail to implant after uterine transfer. It is possible that there is a link between the distribution of high-polarised mitochondria within the blastocyst and the generation of polar and apolar cells which form the diverse cell populations of the trophectoderm and the ICM respectively (Van Blerkom *et al* 2002). The distribution of mitochondria is associated with cytoplasmic microtubular organisation, which in turn is associated with cell function, ie blastomeres deficient in mitochondria are also deficient in microtubules (Van Blerkom *et al* 2000). In cases where indicators of competence are apparent at the pronuclear stage, such as pronuclear alignment and the presence of a cytoplasmic halo, unequal distribution of mitochondria may still occur between blastomeres, thus these authors considered that the degree of disproportionate mitochondrial distribution, rather than its presence, was most relevant to developmental potential (Van Blerkom *et al* 2000). Assessments of mitochondrial organisation may perhaps be useful for predicting which embryos are most likely to arrest. Analysis of spent culture medium for the detection of mtDNA,

implied that a high mtDNA to genomic DNA (gDNA) ratio was positively correlated with improved blastocyst formation and implantation potential (Stigliani *et al* 2014), which may provide a non-invasive method of predicting embryo viability in the clinical embryology laboratory.

## *1.14 Molecular markers associated with preimplantation embryo development*

### 1.14.1 Actin

Actin is an omnipresent structural protein with particular roles in the control of embryo cleavage and compaction (Danilchik and Brown 2008), and has a key function in maintenance of cell shape and structure, cytokenesis, cell motility, and in the establishment of cell-cell interactions (Small *et al* 1999). The human preimplantation embryo comprises large cells, which approximately halve in volume with each normal cell division at least until the 8-cell stage. The actin cytoskeleton undergoes dynamic rearrangements during embryonic development, resulting in polarised morphogenesis as a response to early signalling events in the establishment of cell polarity (Hall and Nobes 2000). Fragments present in poor quality embryos are also reportedly surrounded by a regular intact actin cortex. Furthermore, the actin cytoskeleton is of uniform distribution and thickness in all blastomeres of an embryo apart from those which have begun to degenerate, when a total disorganisation of the protein framework is noted. This is also observed in embryos that have failed to survive thawing after cryopreservation, ie those exhibiting no intact blastomeres upon thawing (Levy *et al* 1998). During the blastocyst hatching process immediately preceding implantation, trophectoderm cells protrude through a hole in the ZP. In some species such as mouse, hatching

requires contraction and expansion of the embryo (Perona and Wassarman 1986). Similar expansion and collapse has been observed in human embryos, but does not appear to be mandatory for hatching (Ebner *et al* 2007). Molecular induction of cell motility involves components of the actin cytoskeleton, and actin filaments play a part in mammalian cell movement (Mitchison and Cramer 1996), with trophectoderm motility during blastocyst hatching thought to be promoted by the action of actin filaments (Niimura and Wakasa 2001). This appears to be confirmed by the findings that the hatching rate of mouse blastocysts was significantly reduced in those incubated with the actin polymerisation inhibitor H-89 (Suzuki and Niimura 2010). This research suggests that actin is involved in both maintenance of cell structure and in physiological dynamic processes. Thus by investigating the distribution of this cytoskeletal protein in human embryos, not only are we able to study the spatial distribution of protein within the embryo, but we may also gain insight into aspects of developmental capacity and implantation potential.

### 1.14.2 STAT3, pSTAT3 and leptin

Signal transducers and activators of transcription (STATs) are a family of cytoplasmic proteins which remain latent until activated by specific binding of polypeptides to receptors on the cell surface (Duncan et al 1997). Six STAT proteins (STAT1 –STAT6) have thus far been identified (Takeda et al 1997). The structure of STAT3 is similar to other STAT proteins, having a conserved amino-terminus, a DNA-binding domain, an SH2 domain, and a carboxy-terminal transactivation domain (Levy and Lee 2002). The structure of STAT3 is shown in figure 1.8.

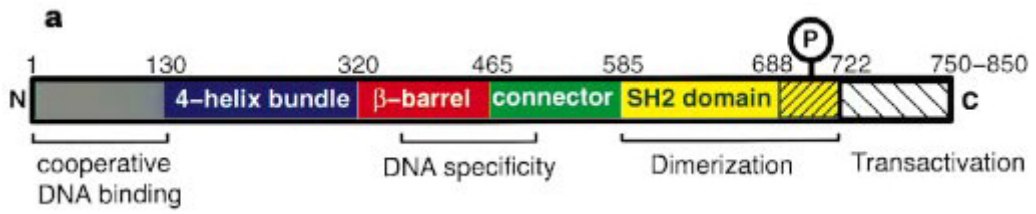


***Figure 1.8: Structure of STAT3β protein (Becker et al 1998)***

STAT3 is expressed by developing human and mouse embryos (Antczak and Van Blerkom 1997), and is thought to be localised exclusively to the region of the oocyte at which the first polar body is extruded, the presumed animal pole (Antczak and Van Blerkom 1997). The distribution of STAT3 may remain polarised throughout embryo cleavage, where it is differentially distributed between the daughter cells of early embryos and the ICM and TE of the blastocyst (Antczak and Van Blerkom 1997). STAT3 is implicated in the process of successful apposition, adhesion and penetration of the luminal epithelium by the trophoblast of the hatched mouse blastocyst (Nakamura *et al* 1997), in agreement with findings which have implicated STAT3 in embryo attachment, invasion and decidualisation via interaction with the progesterone receptor in mice (Lee *et al* 2013). It has also been suggested that STAT3 is critical for implantation since decidualisation of the luminal epithelium, essential for attachment of the blastocyst, does not occur in STAT3-deleted mice (Sun *et al* 2013). Furthermore, dysregulation of the LIF-STAT3 pathway due to high levels of circulating oestrogen in diabetic mice leads to impairment of implantation (Wang *et al* 2015), and STAT3, in association with myeloid cell leukaemia 1 (MCL-1), is regulated by oestrogen and progesterone during the implantation window in mice (Renjini *et al* 2014). Additionally, STAT3 regulates the OCT4-NANOG circuit in the maintenance of ICM cell pluripotency (Do *et al* 2013).

Cytoplasmic STAT molecules remain in a dormant state until they are activated via the Jak-STAT pathway, when a single tyrosine residue is phosphorylated, forming dimers, and results in translocation of STAT3 to the nucleus from the cytoplasm (Teng *et al* 2004). Here, they have the ability to transcribe target genes (Duncan *et al* 1997).

The Jak-STAT signalling pathway is summarised in figure 1.9.

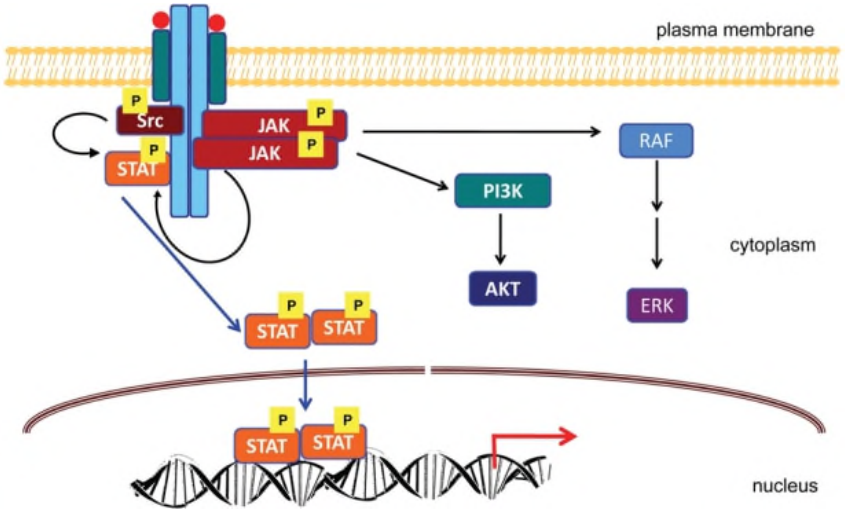


***Figure 1.9: The Jak-STAT signalling pathway (Jatiani et al 2010)***

Activation of STAT3 (pSTAT3) in mouse endometrium occurs only during the implantation window, four days post-fertilisation, which suggests that pSTAT3 has a role in the preparation of uterine receptivity in readiness for implantation (Cheng *et al* 2001). Furthermore, inhibition of STAT3 activation in murine endometrium has been found to reduce implantation significantly (Catalano *et al* 2005). Analysis of endometrial biopsies collected 6-10 days after the luteinising hormone (LH) surge from women presenting with unexplained infertility, found a significant reduction in

pSTAT3 staining in the uterine glandular epithelium, compared to fertile age-matched controls (Dimitriadis *et al* 2007). Detection of pSTAT3 during decidualisation in mice also suggests that it is involved in the establishment and maintenance of early pregnancy (Teng *et al* 2004). STAT3, in both latent and active forms, has been investigated extensively in humans in the pathology of cancers, particularly breast (Banerjee and Resat 2016), but it has not been investigated in human embryonic implantation in any great detail.

The putative role of leptin in reproductive processes is controversial and the published data are contradictory (Herrid *et al* 2014). Leptin, the protein product of the obese gene, is a 16kDa non-glycosylated regulatory peptide hormone synthesised by several cell types, including adipose tissue (Zhang *et al* 1994) and human placenta (Senaris *et al* 1997), is expressed by human follicular granulosa and cumulus oophorus cells (Cioffi *et al* 1997), and is present in the human endometrium and the blastocyst (Cervero *et al* 2005). The structure of leptin is shown in figure 1.10.

***Figure 1.10: Structure of a leptin molecule (Farooqi and O'Rahilly 2005)***

Leptin is associated with the activation of STAT3 (Takeda *et al* 1997), via the long form of the leptin receptor, OB-$R_L$, belonging to the class I cytokine receptor superfamily (Tartaglia *et al* 1995). Leptin receptor is found in the human pre-

implantation embryo and in the endometrium (Cervero *et al* 2005). The detection of leptin receptor in mature murine oocytes and the ability of exogenous recombinant leptin protein to phosphorylate STAT3 in these oocytes suggest that STAT3 has a pivotal role in preimplantation mouse embryo development (Matsuoka *et al* 1999). Whilst both the long and truncated forms of leptin receptor mRNA and protein are highly expressed in human endometrium, leptin mRNA and protein are not (Kitawaki *et al* 2000). It is hypothesised that leptin may play a specific role in acceptance of the blastocyst and support of early pregnancy (Kitawaki *et al* 2000). Like STAT3, the distribution of leptin may remain polarised throughout embryo cleavage, where it is differentially distributed between daughter cells of early embryos and the ICM and TE of the blastocyst (Antczak and Van Blerkom 1997). This differential distribution apparently originates with the specific planes of cell division through the polarised leptin/STAT3 domains during each cleavage round, and since the relative localisation of regulatory molecules within the oocyte may influence subsequent embryo development, this could represent a significant molecular process in the generation of specialised cells with diverse developmental potential within the preimplantation embryo (Antzcak and Van Blerkom 1997). Significantly higher numbers of mouse two-cell embryos developed into expanded and hatching blastocysts with the addition of 10ng/ml human recombinant leptin into the culture system, whilst the addition of 100ng/ml appeared to have an inhibitory effect on embryo development (Herrid *et al* 2006), and whilst leptin mRNA was absent in mouse cleavage stage embryos, long and short leptin receptors were present,

suggesting that leptin influences preimplantation embryo development via a paracrine signalling system (Herrid *et al* 2006).

### *1.15 Image acquisition using fluorescence microscopy*

High-resolution confocal imaging of fluorescently-labelled internal cell structures enables the acquisition of high quality, 3-dimensional images of high volume specimens (Liu and Chiang 2002). A confocal microscope samples diffraction-limited regions of fluorescently labelled specimens in a point-by-point fashion to build a stacked image, without the degradation of the image by the fluorescence of out-of-focus structures. This offers an advantage over conventional epifluorescent microscopy when studying an increasing number of closely packed cells in a constant overall embryonic volume (Levy *et al* 1998). The result is an image of considerably greater resolution, particularly with regard to the spatial distribution of specific macromolecules within multi-cellular structures such as embryos (Paddock 1994). However, photobleaching of illuminated, fluorescently labelled molecules may occur during image collection, particularly if repeated scanning is required over time, such as during optical slicing in confocal microscopy, resulting in decreased image quality, and impaired resolution of spatially orientated molecules. This usually occurs in excited molecules that undergo permanent structural changes following reaction with another species such as oxygen or dye molecules (Bernas *et al* 2004).

### *1.16 Medical imaging and visualisation*

The assessment of embryo morphology may be more accurately achieved using medical imaging techniques such as segmentation alongside conventional grading systems. Segmentation is a method utilised for the visualisation of 3-dimensional images of various tissues including brain, cardiac and tumour tissues as well as embryos, and allows images to be partitioned into regions to enable the extraction of specific features and obtain informative measurements (Rogowska 2000). One such application of medical imaging assessed the thickness of the ZP of human embryos, and involved edge mapping of the externa and interna membranes with an automated active contour model (snake segmentation) to distinguish the boundaries, and allow the exact measurements to be obtained. The ZP thickness variation was then retrospectively compared with pregnancy results in order to identify a correlation, and provides evidence for utilising this technique to provide additional selection criteria for embryos prior to uterine transfer (Morales *et al* 2008).

There are several different classifications of segmentation techniques depending upon their intended application including but not limited to, manual, automatic and semi-automatic, pixel-based and region-based, manual delineation, and classical (Rogowska 2000). Edge-based segmentation identifies distinct boundaries between regions with different characteristics, and this technique is suitable for imaging embryos since they contain several membranes enclosing various cell structures , for example the ZP surrounding the cytoplasm of zygotes, individual blastomere

membranes in cleavage stage embryos, and the cells of the inner cell mass and trophectoderm of blastocysts. Definition of boundaries depends upon the local pixel intensity gradient, with images created according to both the magnitude and direction of the gradient, and by calculation of the summation of localised pixel intensities (Rogowska 2000). Semiautomatic edge linking, where the operator manually draws the edge when the automatic tracing becomes ambiguous, circumvents the problem of incomplete enclosure of the cell often seen with segmentation. Multimodal or multispectral techniques incorporate data from a series of images during which the intensity gradients alter but the anatomical structure remains constant, such as those acquired in embryo time-lapse recordings. These allow the incorporation of data from a spectrum of features, providing an array of information for use in segmentation and imaging. The parametric analysis technique, where the pixel intensity for each region of interest is plotted against time, is commonly employed when analysing serial images procured over extended time periods. Parameters are selected according to the functional characteristics of the object in question (eg an individual blastomere), such as time of occurrence of minimum and maximum intensities, and an image calculated for each of the parameters, hence the term parametric imaging. Edge detection segmentation can be used to create 3-dimensional images, and combined with 3-dimensional rendering, allows for detailed analysis of image structures (Rogowska 2000).

Visualisation aims to develop tools that allow the “inside” of complex living systems to be observed and explored, and involves the use of computing environments,

graphics hardware and software that facilitate the interaction between humans, machines and data. Visualisation techniques enable the generation of realistic 3-dimensional images, development of automated methods for manipulation of multidimensional images and their associated parametric data, advancement of measurement tools for analysis of images, and the design and validation of models that improve the interpretation of diagnostic and clinical applications (Robb 2000). Virtual reality facilitates interactive visualisation, allowing the operator to control detailed computer-generated 3-dimensional images that mimic real-life situations, enabling manipulation of images in such a way that the operator may “enter” the visualisation and change their viewpoint as if the image were a real object (Robb 2000). This has huge implications in the development of tools for the purposes of teaching and demonstrating, as well as for diagnostic applications, and virtual procedures have been found to provide accurate, reproducible visualisations that are clinically useful and minimally invasive (Robb 2000). This suggests that the inclusion of virtual models in the routine clinical environment is a very real possibility, and may prove invaluable in the future of medical advancement. Visualisation in medicine may be characterised, according to the complexity of the resulting user interaction, as illustrative, investigative or imitative. Illustrative visualisation presents extracted data in the form of three-dimensional displays, whilst investigative visualisation is more focussed on explorative techniques such as multidimensional interpretations useful for clinical tools. Imitative visualisation refers to virtual reality systems, simulators and modelling (Solaiyappan 2000).

The use of computer software for the development of advanced image processing systems has led to an increase in the application of digital imaging to human medicine. Medical visualisation describes the generation of three-dimensional (3D) models using digital algorithms, based upon living specimens, to increase the understanding of biological structures and their functions (Klauschen *et al* 2009), and is a useful tool when attempting to understand the mechanisms of development and/or abberant behaviours. Therefore, development of semi-automated human embryo analysis tools may assist in generating high volumes of data to increase understanding of cell division patterns in relation to clinical outcomes, and may improve our ability to select the most viable embryos from a cohort from an early stage of development.

# Aims

# Aims

The overall aim of this project was to investigate possible molecular, morphological and kinetic markers of preimplantation human embryo viability, with a view to increasing our understanding of human embryo development and improving embryo selection methods in the clinical embryology laboratory.

Briefly, the main aims of this project were:

- To detect and confirm the distribution of the actin cytoskeleton in cleavage stage, compacting, and arrested human preimplantation embryos and blastocysts.
- To establish whether the regulatory proteins STAT3 and leptin are polarised within human oocytes and preimplantation embryos
- To determine the number of cells in the inner cell mass and the trophectoderm in human blastocysts during *in vitro* development, and to consider morphological characteristics of blastocysts and their relationship with quality and possible clinical outcomes.
- To investigate the occurrence of chromatin-containing fragments and micronuclei in human preimplantation embryos of all developmental stages
- To establish whether STAT3 activation may represent a mechanism by which the embryo and endometrium communicate at implantation in humans.
- To detect the presence of leptin receptor mRNA on human blastocysts in order to determine whether the leptin system plays a role in the activation of STAT3 in human pre-implantation embryos.

- To investigate the interaction between embryos and Ishikawa cells, as a model of the endometrial epithelium.
- To identify potential markers of embryo viability and predictors of embryo development by assessment of human preimplantation embryos using time lapse monitoring.
- To assess the potential effect of deliberately damaging the daughters of the first dividing cell at the third cleavage division (4-8 cells) with respect to ensuing cleavage patterns and blastocyst formation, to determine whether damage of specific blastomeres may impact on axis establishment and subsequent embryo development.
- To identify the initial site of blastocyst hatching from the ZP with respect to the position of the inner call mass, to establish whether there is any association between the site of hatching and pregnancy potential.
- To explore different options for computer-assisted image analysis of human embryos at different stages of development and using different image types.
- To apply the most effective semi automated computer-assisted options to investigate the nuclear to cell ratio in cleavage stage human preimplantation embryos, and the nuclear volumes of different cell lineages in blastocysts, using data derived from a semi-automated computer programme developed in collaboration with colleagues at the Warwick Digital Laboratory, and Manchester University School of Computing.

# Chapter Two

# Methods

# Chapter Two

# Methods

## *2.1 Introduction*

This chapter describes in detail all the methodologies employed during the preparation and execution of experiments carried out during the course of this project.

### *2.1.1 Governance*

This project received ethics approval (Coventry Research Ethics Committee, LREC 04/Q2802/26) and was licensed by the HFEA, project number R0155, for conduct at the University of Warwick Clinical Sciences Research Laboratories (CSRL), and the Centre for Reproductive Medicine (CRM), UHCW NHS Trust. Approval from the Research and Development Department at the Trust was also granted **(R&D GH04/0504)**.

The project title is 'Indicators of oocyte and embryo development' and the Person Responsible to the HFEA is Professor Geraldine Hartshorne, who was my supervisor on this project. The work was conducted according to standard operating procedures for the standardised processes involved. Where appropriate, documents were controlled under ISO 9001 at CRM.

### *2.2 Embryos*

Embryos were donated by patients undergoing *in vitro* fertilisation (IVF) treatment at the CRM, University Hospitals Coventry and Warwickshire NHS Trust, Bath Fertility Centre (BFC), Royal United Hospitals NHS Trust, and Leicester Fertility Centre (LFC), University Hospitals of Leicester NHS Trust. During this project, oocytes and embryos that were collected or created during the current treatment cycle but deemed unsuitable for uterine transfer or cryopreservation due to failed or abnormal fertilisation, retarded development, or poor morphological quality were used. Additionally, good quality embryos that were cryopreserved during previous IVF treatment cycles but were no longer required by the patients were also used. No patient was disadvantaged as a result of this research project.

### *2.3 Acquisition of fresh oocytes and embryos for research*

During the pre-treatment information session, patients were provided with a research pack including information about the project and a consent form, for them to consider. If the patients indicated a willingness to be approached about research projects in section 5.1 and 5.2 of the HFEA consent to treatment (MT and WT) forms, a discussion regarding specific project consent took place shortly before oocyte retrieval. This involved a short verbal explanation of the project and the type of material required, and an opportunity for the patients to ask questions prior to making a decision regarding consenting. Patients could consent to oocytes, fresh embryos and/or frozen embryos being included. Both male and female members of

the couple (or the gamete donor if appropriate) must have consented if embryos were to be used for research.

Patients were prepared for oocyte collection according to a standard protocol with clinical decisions regarding the appropriate ovarian stimulation regimen depending upon patient-specific factors. Usually, the pituitary GnRH agonist Buserelin (Sanofi, Paris, France) was administered until down-regulation of pituitary hormones was confirmed by a scan of the ovaries showing quiescence and an absence of follicles ≥10mm. This was followed by ovarian stimulation with gonadotrophin injections daily for up to two weeks. The most commonly used gonadotrophin preparation was Menopur (Ferring, Middlesex, UK). Growing follicles in the ovaries were tracked via ultrasound scanning until the leading follicle reached 14mm diameter. Oocyte collection was then scheduled with instructions given to self-administer 10,000 iu of human chorionic gonadotrophin (hCG) by subcutaneous injection (MerckSerono, Middlesex, UK) 36 hours prior to the planned oocyte collection time, to cause oocyte maturation *in vivo*.

For the oocyte collection procedure, patients received sedation with or without anaesthetic. Follicle contents were aspirated under ultrasound guidance using a 17 gauge x 31cm needle with 60cm fluorinated ethylene propylene tubing attached (Casmed, Epsom, Surrey). Oocytes, in their cumulus cell clusters, were identified in the aspirated fluid using light microscopy, and were collected into 250µl drops of pre-equilibrated HEPES-buffered sperm preparation medium (Origio) under sterile light paraffin oil (Origio). Oocytes were transferred into 100µl drops of pre-equilibrated IVF medium (Origio) under sterile paraffin oil upon completion of the

oocyte collection and incubated in an incubator at 5% $CO_2$ and 37°C. For standard IVF treatment, oocytes were inseminated approximately 4 hours after collection, with the addition of approximately 150,000 prepared sperm per ml to a maximum of two oocytes in 100µl drops of IVF medium (Origio) under oil. For intracytoplasmic sperm injection (ICSI) treatment, cumulus cells were removed from oocytes approximately 4 hours after collection using 100µl 80 U/ml Cumulase (Origio) enzymatic digestion and a 135µm denuding pipette (Hunter Scientific, Essex, UK). Approximately 2 µl of prepared sperm was added to a 5µl drop of polyvinylpyrrolidone (PVP) (Origio) to decrease the velocity of the sperm prior to immobilising. Oocytes were transferred to 5µl drops of sperm preparation medium (Origio) in a pre-prepared 50x9mm petri dish (Falcon, BD Biosciences) and each injected individually with one immobilised spermatozoa using a micromanipulator (Research Instruments, Cornwall, UK) with an IX51 inverted microscope (Olympus). After insemination or injection, oocytes were transferred to pre-equilibrated IVF medium (Origio) under oil, and incubated at 37°C in an atmosphere of 5% $CO_2$in air overnight.

### *2.4 Embryo culture*

Embryo culture dishes were prepared 24 hours prior to requirement to allow equilibration of the media in a 5% $CO_2$environment. The protocol used was the Origio sequential media culture system, capable of supporting embryo development from fertilisation on day 1 to the blastocyst stage on day 5 or 6.

Pronuclear formation was assessed 16-18 hours after insemination or injection (day 1), and normally fertilised embryos, identified by the presence of two pronuclei and

two polar bodies, were transferred to pre-equilibrated ISM1 medium (Origio) under oil at 37°C in 5% $CO_2$. Embryos were assessed the following day (day 2) to assess cleavage and morphology. Those embryos deemed suitable for extended culture to the blastocyst stage were transferred to BlastAssist medium (Origio) at approximately 4pm on day 2, whilst those of poorer quality or with a retarded developmental rate were either transferred to BlastAssist medium (Origio) at the same time, or remained in ISM1 medium (Origio) for one more day before transfer into BlastAssist medium (Origio), depending on the decisions made regarding the other embryos.

Fresh oocytes and embryos donated for research were collected from the embryology laboratory at any time from day one after oocyte collection (immature oocytes, unfertilised and multi-pronucleate) until day seven (arrested cleavage stage and poor quality blastocyst stage embryos), dependent upon the time at which they became no longer needed by the patient and therefore available for research. Oocytes and embryos donated to research were then transferred to a separate research incubator in the presence of a clinical embryologist who acted as a witness. A checklist for collecting fresh embryos for research was completed to ensure that all necessary procedures were followed.

### *2.5 Acquisition of frozen embryos for research*

Patients with cryopreserved embryos in storage were contacted approximately annually with a regular mailing to confirm their wishes with regard to the embryos. If they wished to donate them to research, they were provided with written information by letter regarding the project and were asked to complete the appropriate consent forms. If the patients (both partners of the couple) requested that they be donated for research, the frozen embryos were then transferred to the dedicated research embryo storage tank in the presence of a witness, and could be used at any time within the HFEA-authorised storage period. Availability of donated embryos was documented in an index card file. Patient consents were filed in the notes and cross-checked for expiry date and signatures. Identity was verified with at least three identifiers (e.g. name/date of birth/hospital number).

In all cases, to ensure auditable records of traceability complying with HFEA legislation, details of each embryo used for research purposes were recorded. Reversible anonymisation was performed by allocating each patient a unique code for research use. The completed anonymisation forms were filed together with copies of patient consent forms, whilst non-identifying relevant clinical and laboratory information was recorded on data sheets. Completion of detailed laboratory logbooks and index cards summarising the fate of each anonymised embryo ensured that a robust two-way audit trail was maintained.

### *2.6 Thawing embryos*

When required, research embryos were thawed according to CRM protocol depending upon the mode of cryopreservation. For embryos that were frozen using controlled rate freezing, which was the preferred method at the CRM until 2009 and also the method used by LFC, embryos were thawed using an adapted version of the Origio standard clinical protocol.

Two hours prior to thawing, embryo thawing media solutions 1-4 (Origio, Reigate, UK) were dispensed into non-toxic 5-well plates (Nunc, Thermo Scientific, Roskilde, Denmark) in 0.5ml aliquots, and equilibrated at room temperature. Embryos were removed from liquid nitrogen ($LN_2$) and the straw warmed for approximately 1 minute until the contents had liquefied. Embryos were removed from the straw into the centre of the 5-well plate. The 5-well plate was then placed on a heated stage at room temperature, and the stage turned on with a set temperature of 37°C, to gradually warm the embryos as they thawed. Embryos were placed in each of the four sequential thawing solutions for 5 minutes each. Following thawing, the embryos were transferred to 25µl drops of pre-equilibrated ISM1 or BlastAssist (Origio) culture media under paraffin oil and incubated at 37°C/5% $CO_2$until ready to use.

Some embryos had been originally cryopreserved using a vitrification technique. Vitrification was routinely used at the CRM from 2009. Vitrified embryos from CRM were warmed as follows, using the Origio standard protocol.

Thirty minutes prior to use, the vitrifcation warming medium was warmed to 37°C, whilst the dilution media and washing media were warmed to room temperature.

Embryos were removed from liquid nitrogen and the support immersed in the warming medium to allow the embryo to float off the tip. After exactly three minutes, embryos were transferred through two dilution media and two washing media steps, each for three minutes, before transfer to pre-equilibrated ISM1 or BlastAssist (Origio) media for a minimum of two hours prior to quality assessment. For those embryos originating from BFC, vitrified embryos were warmed according to the Irvine Scientific Vit Kit® (Irvine Scientific, Santa Ana, Ca) protocol.Heat-sealed straws containing embryos were removed from liquid nitrogen and swirled in a 37°C water bath for approximately 3 seconds, then wiped dry using a sterile tissue. Sharp sterile scissors were used to cut the straw just below the seal at the thicker end, and the metal jacket moved up the shaft to reveal the thinner end of the straw. A syringe with plunger withdrawn to the halfway position was attached to the cut end of the straw with a connector ensuring a secure seal, before the fine end was snipped just below the seal. The embryos were expelled as a small drop directly into a pre-dispensed 50µl drop of thawing solution by depressing the syringe and touching the tip of the straw on the media. After exactly one minute, the embryos were transferred to a 25µl drop of dilution solution, pipetted to rinse, and then left undisturbed for four minutes. During this time, two 25µl drops of washing solution were dispensed into the same dish. The embryos were transferred to the bottom of the first drop for four minutes, and then to the top of the final wash drop for four minutes undisturbed. Finally, the embryos were transferred to pre-equilibrated ISM1 or BlastAssist media (Origio) under oil for further culture.

### *2.7 Embryo grading*

All research embryos were assessed for quality based upon their cell number and appearance by light microscopy both at the time of collection or thawing and at the time of subsequent imaging, to detect changes in cell number or quality between collection or thawing and processing of the embryo. Each cleavage stage embryo was allocated a grade from 1 to 4 based upon the shape of the cells, symmetry of division, cell orientation, degree of fragmentation, appearance of membranes and ZP shape.

The criteria for the grading of cleavage stage embryos are summarised in table 2.1 (Balaban *et al* 2001).

| **Grade** | **Blastomeres** | **Fragmentation** |
|---|---|---|
| 1 | Equal size<br>Homogenous | <10% |
| 2 | Equal size<br>Homogenous | 10-20% |
| 3 | Equal/unequal size<br>Homogenous/non homogenous | 20-50% |
| 4 | Equal/unequal size<br>Homogenous/non homogenous | >50% |

***Table 2.1: Cleavage stage grading criteria***

Compacted/morula stage embryos were graded according to the criteria summarised in table 2.2 (Tao *et al* 2002).

| Score | Compacting cells | Morphology | Fragmentation |
|---|---|---|---|
| 1 | 100% | Full size, close to sphere with smooth profile | <5% |
| 2 | >75%<br><br>65-75% | Close to sphere with shallow indent<br><br>Close to sphere with smooth profile | <25% |
| 3 | 50-65% | Irregular with deep indentation | >50% |
| 4 | <50% | Irregular with small compact mass | >50% |

***Table 2.2: Compacted/morula stage grading criteria***

Blastocysts were graded using the criteria described by Gardner *et al* (1999), according to the extent of expansion of the blastocoel, and the quality and appearance of the inner cell mass and trophectoderm cells (Teranishi *et al* 2009). Blastocyst grading criteria are summarised in table 2.3 and table 2.4.

| **Size** | **Degree of expansion** |
|---|---|
| **1** | An early blastocyst with a blastocoel ≤ half the volume of the embryo |
| **2** | A blastocyst with a blastocoel ≥ half the volume of the embryo |
| **3** | A full blastocyst with a blastocoel completely filling the embryo |
| **4** | A fully expanded blastocyst with large blastocoel and thinning zona |
| **5** | A hatching blastocyst with the trophectoderm starting to herniate through the zona |
| **6** | A fully hatched blastocyst, in which the blastocyst has completely escaped through the zona |

***Table 2.3: Grading criteria for the degree of expansion and hatching status of the blastocyst***

| **Grade** | **Inner cell mass** |
|---|---|
| A | Tightly packed, many cells |
| B | Loosely grouped, several cells |
| C | Very few cells |
| **Grade** | **Trophectoderm** |
| A | Many cells forming a cohesive epithelium |
| B | Few cells forming a loose epithelium |
| C | Very few large cells |

***Table 2.4: Grading criteria for the inner cell mass and trophectoderm of the blastocyst***

The expected development rate during culture was also taken into account, as detailed in table 2.5.

| Day of culture | Stage of development |
|---|---|
| 2 | 4 cells |
| 3 | 8 cells |
| 4 | Compacting or cavitating |
| 5 | Early blastocyst to expanded blastocyst |
| 6 | Expanded blastocyst to hatching blastocyst |

***Table 2.5: Expected development rate of embryos at all stages from day 2 to day 6 post-insemination***

### *2.8 Sperm preparation for creation of research embryos*

For some experiments embryos were created *in vitro* for research by using intracytoplasmic sperm injection to attempt to fertilise oocytes available due to failed fertilisation or *in vitro* maturation. The women whose oocytes were used for this gave informed consent, while the sperm was from a donor who approved research use in this project.

Approximately 10-15% of oocytes display no evidence of fertilisation 16-18 hours following insemination (Kalantar *et al* 2007). In addition, 15-20% of oocytes (Reichman *et al* 2010) may be immature at collection at either prophase I (germinal vesicle) or metaphase I (no germinal vesicle and no polar body) but exhibit polar body extrusion (assessed to indicate metaphase II stage) after one day in culture. Such oocytes are considered to have matured *in vitro.* ICSI using previously frozen sperm from a consenting donor was used to create embryos from such oocytes for

use in experimental procedures. Prior to performing ICSI, sperm were prepared in order to isolate a population of viable spermatozoa free from debris and seminal plasma.

A heat-sealed straw containing semen in a 50:50 mixture with glycerol-based Sperm Freezing Medium (Origio) was removed from liquid nitrogen, and the sample date and number recorded. Following thawing at 37°C for approximately 10 minutes, sperm concentration was estimated by assessing a 10µl drop on a Makler counting chamber (Irvine Scientific, London, UK) to ensure sufficient motile sperm were available. A sample of sperm suitable for injection was prepared as follows:

A two layer density gradient was constructed by layering 1ml 55% SupraSperm® medium upon 1ml 80% SupraSperm® medium (Origio) in a non-toxic sterile conical tube (BD Biosciences, Oxford, UK). Immediately, 2ml of cryopreserved semen was added to the top of the column, and centrifuged at 1600rpm for 10 minutes. The seminal plasma and gradient media were removed using a glass pipette, and the pellet was re-suspended in 1ml sperm preparation medium (Origio) and centrifuged at 3000g for 5 minutes to wash.

If the concentration of motile sperm was insufficient for preparation using a discontinuous density gradient, the sample was prepared by centrifugation at 3000g for 5 minutes, plus washing the pellet twice in 1ml sperm preparation medium (Origio). For both preparation methods, the uppermost 0.5ml of media was removed after the second centrifugation step, and the preparation incubated at

37°C for approximately 30 minutes to allow motile spermatozoa to swim out of the pellet.

### *2.9 Intracytoplasmic sperm injection for creation of research embryos*

ICSI was performed as for clinical insemination, using an Olympus IX51 inverted microscope (Olympus) with integrated micromanipulator (Research Instruments) as described in section 2.3.

Individual sperm were selected for injection using high power magnification based upon their morphology and motility. Oocytes were held with the polar body at the 12 or 6 o'clock position to avoid injection at the purported spindle location. An immobilised sperm was positioned head first at the tip of the injection pipette prior to insertion of the pipette through the zona of the oocyte and into the ooplasm. Suction was applied until the oolemma was ruptured and cytoplasm was sucked into the pipette. The sperm was then deposited in the centre of the cytoplasm, taking care to avoid introducing excess medium into the oocyte, and the injection needle slowly removed to avoid damaging the oocyte or causing the sperm to exit, as shown in figure 2.1.

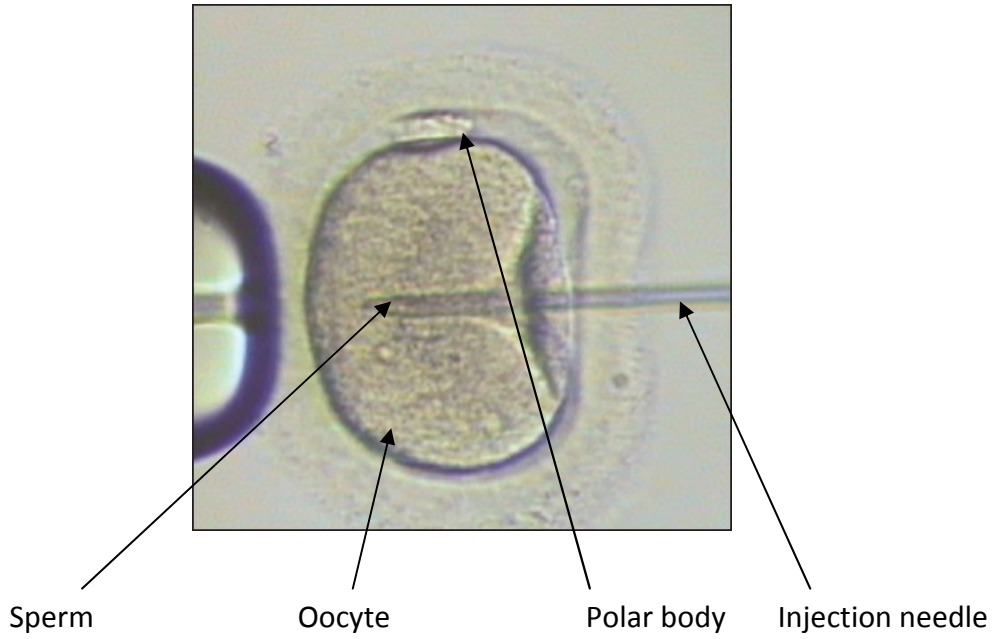


***Figure 2.1: Intracytoplasmic Sperm Injection (ICSI) technique (Merchant et al 2011)***

### *2.10 Microscopy*

Assessment of oocyte and embryo morphology and development during routine clinical IVF treatment employs the use of brightfield, phase contrast and Hoffmann optical microscopes, with UV exposure avoided by inclusion of neutral density filters.

#### *2.10.1 Research microscopy*

Brightfield and fluorescence live cell time lapse images and fixed cell images were acquired using an Olympus IX81 microscope with integrated Solent Scientific environmental chamber(Solent Scientific, Portsmouth, UK), high resolution digital CCD camera (Hamamatsu, Hertfordshire, UK), and CellM imaging system software (Olympus, Middlesex, UK).

Some live embryos were imaged using a Cryo Innovation PRIMO Vision compact continuous monitoring system (Parallabs, St Albans, UK), placed inside an Heraeus BB6220 incubator set to 37°C and 5% $CO_2$.

Additionally, live embryos were imaged using the Unisense FertiliTech Embryoscope™ time-lapse system, a fully integrated 5% $C0_2$/37°C incubator with Leica Hoffman modulation contrast optics and camera. Images were analysed using EmbryoViewer software (Unisense FertiliTech A/S, Denmark).

Fixed cell fluorescent images were captured using a Zeiss LSM 510 laser scanning confocal microscope and LSM5 software package version 4.0 (Zeiss, Hertfordshire, UK). In order to excite the AlexaFluor488, FITC and DAPI fluorophores, the microscope was configured prior to imaging by selecting the Enterprise and Argon lasers and the CY2 (488) and DAPI (364) filters.

### *2.11 Fluorescent labelling of embryos*

Labelling fixed human preimplantation embryos with fluorophores enables the visualisation and imaging of cellular, sub-cellular and microscopic structures in a three-dimensional arrangement. Specifically targeted fluorescent probes may be used to highlight proteins of interest in order to study the spatial organisation of cellular components, such as the cytoskeleton, and temporally expressed regulatory proteins, which may be polarised to specific regions of cells.

#### *2.11.1 Actin labelling*

50 embryos were labelled for the cytoskeletal protein F-actin using the fluorescent probe AlexaFluor® 488 phalloidin (Invitrogen, Paisley, UK). Embryo fixation in 1ml

3.7% formaldehyde/PBS for ≥1 hour at room temperature was followed by washing in PBS for 5 minutes at room temperature, permeabilisation in 0.1% Triton X-100/PBS (Sigma-Aldrich, St Louis, MO) for 5 minutes at room temperature, and a second PBS wash. Embryos were then incubated in 100µl IVF media (Origio) containing 5µl (1 unit) AlexaFluor® 488 for 20 minutes at room temperature protected from light, followed by a final wash in PBS for 5 minutes at room temperature. All washing steps and AlexaFluor® 488 incubations were performed in Nunc 5-well plates (Thermo Scientific). Following staining, the embryos were transferred to 10µl drops of IVF/ISM1 media (Origio) overlaid with mineral oil (Origio) and stored at 4°C wrapped in foil until imaged. Embryos were either imaged immediately or the next day.

### *2.11.2 STAT3, pSTAT3 and leptin labelling*

33 embryos were labelled for STAT3 using an affinity purified rabbit polyclonal antibody raised against mouse (C-20-R) as the primary antibody (Santa Cruz Biotechnology, Santa Cruz, Ca) and either anti-rabbit IgG FITC conjugate developed in goat (Sigma-Aldrich) or anti-mouse IgG Texas Red™ Sulfonyl Chloride conjugate developed in rabbit (Abcam, Cambridge, UK) as the secondary antibody.

47 Embryos were labelled for pSTAT3 using an affinity purified goat polyclonal antibody raised against human as the primary antibody (Santa Cruz Biotechnology) and anti-rabbit IgG FITC conjugate developed in goat (Sigma-Aldrich) as the secondary antibody.

41 embryos were labelled for leptin using an affinity purified rabbit polyclonal antibody raised against human (Ob Y-20) as the primary antibody (Santa Cruz

Biotechnology) and anti-rabbit IgG FITC conjugate developed in goat (Sigma-Aldrich) as the secondary antibody.

All embryos were fixed in 1ml 3.7% formaldehyde for ≥ 1 hour at room temperature, and either stored in Falcon 5ml round bottom tubes (BD Biosciences) in the fixative at 4°C until ready to label, or immediately removed from the fixative and transferred to PBS wash for 5 minutes at room temperature. Permeabilisation with 0.1% Triton X-100/PBS (Sigma-Aldrich) for 1 hour at room temperature, was followed by a second PBS wash (5 minutes, room temperature). Embryos were transferred to 1% BSA/PBS (Sigma-Aldrich) and incubated for 1 hour at 4°C, then transferred to fresh 1% BSA/PBS (Sigma-Aldrich) for a further incubation (≥1 hour, 4°C). Embryos were kept in this solution until ready for staining, or washed in PBS (5 minutes, room temperature) and stained immediately. For incubation with primary antibody, embryos were transferred to 4µg/ml anti-STAT3, anti-pSTAT3 or anti-leptin antibody in 100µl IVF medium under oil, and left overnight (≥ 8 hours) at 4°C wrapped in foil.

Following primary antibody incubation, embryos were washed in 1% BSA/PBS for 30 minutes at 4°C to prevent non-specific binding of the primary antibody with any remaining free protein, before incubation with FITC (Sigma-Aldrich) or Texas Red (Abcam) secondary antibody solution (both 1:100 dilution) for 2 hours at 4°C in foil wrap. A final wash in 1% BSA/PBS (Sigma-Aldrich) for 30 minutes at 4°C completed the staining procedure. Embryos were either imaged immediately or stored at 4°C in 1% BSA/PBS protected from light, until imaged. All washing steps, antibody incubations and storage were carried out in Nunc 5-well plates (Thermo Scientific).

Negative controls were performed by culturing the embryos overnight in 100µl IVF media under oil, omitting the primary antibody. All other conditions and subsequent steps were retained.

### *2.12 Confocal Imaging*

Prior to imaging, up to three embryos were transferred to 5µl Vectashield media containing 4',6-diamidino-2-phenylindole (DAPI) (Vector Laboratories, Burlingame, CA), diluted in a 1:4 ratio with PBS. DAPI mounting medium serves the dual purpose of preserving the fluorescence signal during imaging and labelling chromatin in the cell nuclei. Embryos were mounted in a 35mm gamma-irradiated collagen-coated plastic petri dish with a 14mm x 1.5mm glass well insert designed especially for high resolution microscopy (MatTek, Ashland, MA), as shown in figure 2.2.

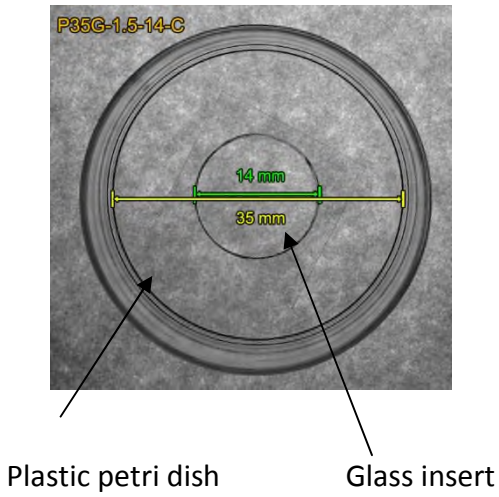


***Figure 2.2: Petri dish with glass well insert (MatTek)***

Embryos were covered with a round 13mm diameter, 1.5mm thickness coverslip (Scientific Laboratory Supplies) mounted on petroleum jelly columns to prevent the coverslip from squashing the embryo, and to enable the entire vertical axis (z-axis) of the embryo to be successfully imaged.

Images were obtained as both single plane and z-stack series with CY2/DAPI filters and Argon/Enterprise lasers (see figure 2.3), at a magnification x400 under oil immersion. Optical slices were taken at 1µm intervals through the z-axis and saved in Tagged Image File Format (TIFF) using the Zeiss LSM5 image browser software. Single track beam path and laser configuration produced images more rapidly as both tracks were simultaneously scanned, but since more than one fluorophore was present in each embryo, this resulted in bleed-through of target colours. Therefore, multiple track configurations were enabled to allow sequential scanning of channels, thus minimising cross-talk of fluorescence emissions and optimising image resolution. Images were analysed using LSM5 software and Image J.

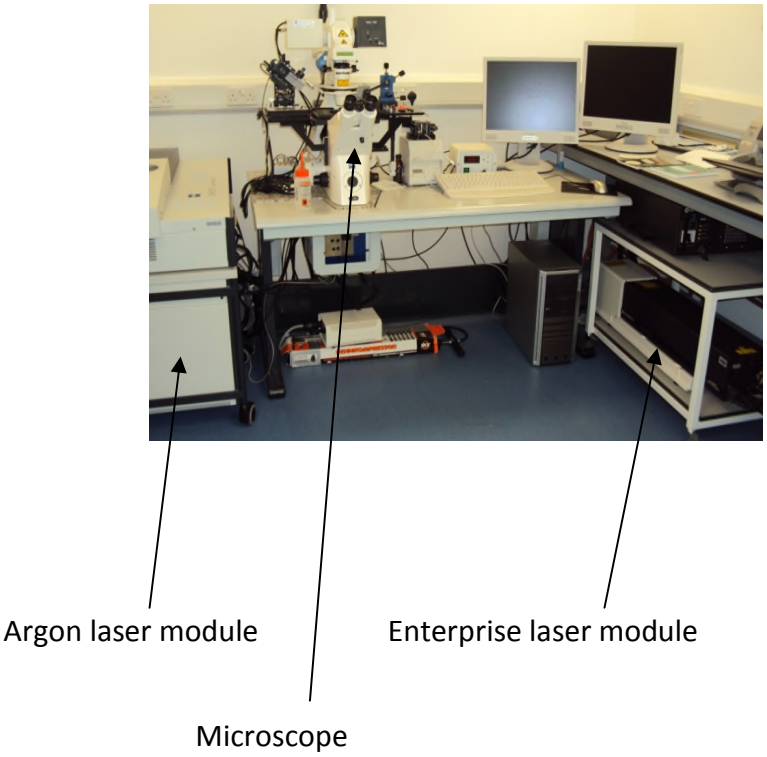


***Figure 2.3: Zeiss LSM510 confocal microscope and laser modules***

### *2.13 Image analysis*

The distribution of STAT3 and leptin in the embryos was determined by measuring the relative intensity of the fluorescent signal in the reconstructed confocal z-stacks using Image J.

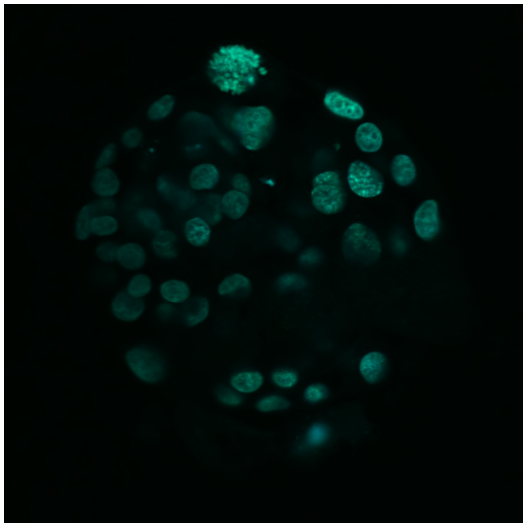

***Figure 2.4: A single plane confocal image of a blastocyst imported into Image J***

The Z-stacks could then be transformed into 3-dimensional GIF files, as shown in the static image in figure 2.5.

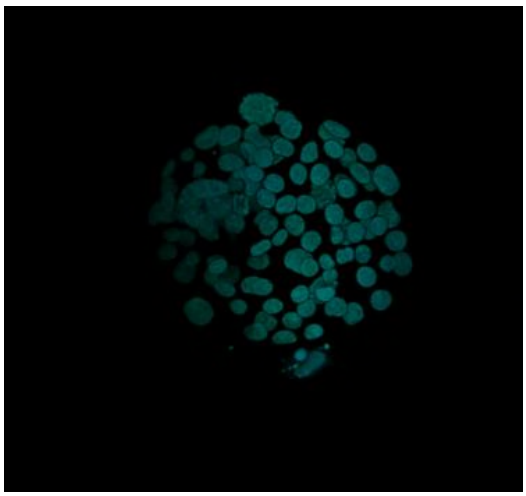

***Figure 2.5: 3D reconstruction of the entire confocal z-stack of the blastocyst seen in figure 2.4, imported into Image J***

A sampling technique was employed when comparing the fluorescence intensities at different areas within blastomeres, to investigate whether the target proteins were polarised intercellularly. Small areas around the cell periphery and centre were selected using the oval or elliptical selection tool as shown in figure 2.6, and the RGB pixel values of each selected area measured using the "Analyze" plugin. The average of each sampled area from around the periphery and the centre of each cell were calculated, and the values compared to determine whether differences in relative fluorescence intensity existed between different areas of the cells.

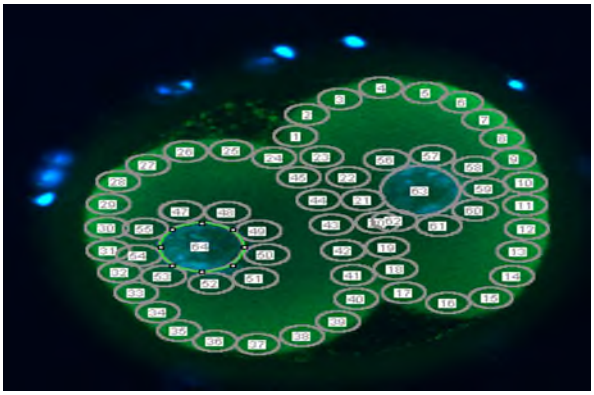

***Figure 2.6: Example of sampling technique used to measure relative fluorescence intensity in a 2-cell embryo***

When the average fluorescence intensity of the cell as a whole was required, to determine whether the target proteins were differentially distributed between the blastomeres of the embryo, RGB values of the whole cell were measured by selecting the entire cell area using the oval or elliptical selection tool, as shown in figure 2.7.

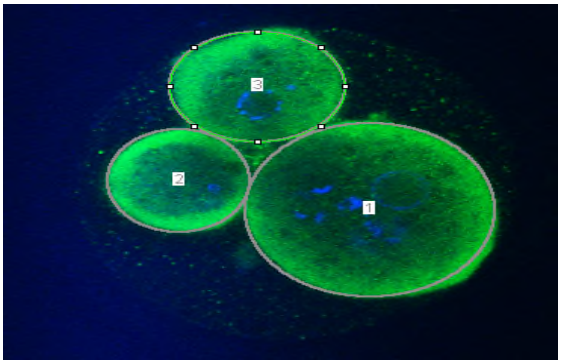


***Figure 2.7: Example of whole-cell selection technique used to measure relative fluorescence intensity in a 3-cell embryo***

High volumes of data were generated using the sampling technique (~150 measurements for a 0PN up to ~700 measurements for a 6-cell embryo), and although a much smaller data set was generated using the whole-cell method, the pixel values were comparable using either technique, as shown in figure 2.8.

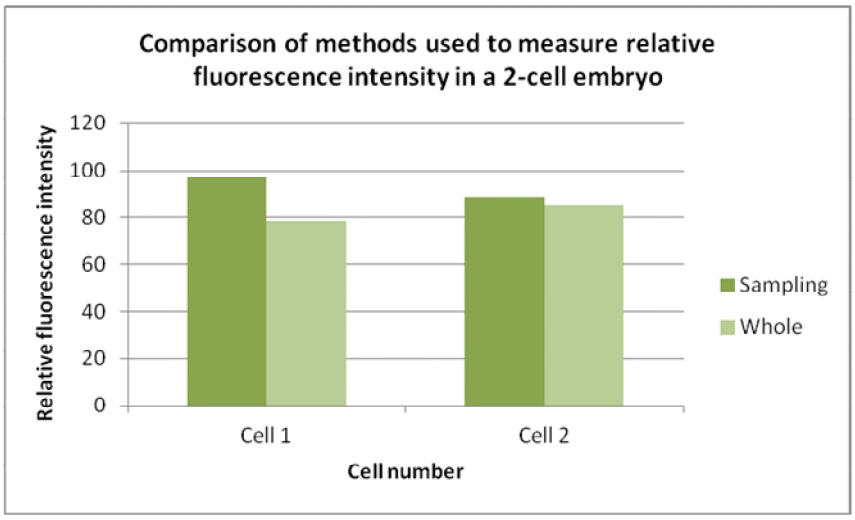


***Figure 2.8: Comparison of sampling technique and whole-cell technique used to measure relative fluorescence intensity in a 2-cell embryo***

In order to validate the relative fluorescence intensity measurement methods, the same technique was used to measure fluorescence intensity in embryos which had no primary antibody exposure, as described in section 2.11.2. Additionally, fluorescence intensity was measured in pre-labelled beads on three different occasions using the same confocal microscope settings, to demonstrate that there was minimal variation in the levels of fluorescence detected. These results are summarised graphically in figure 2.9 and 2.10.

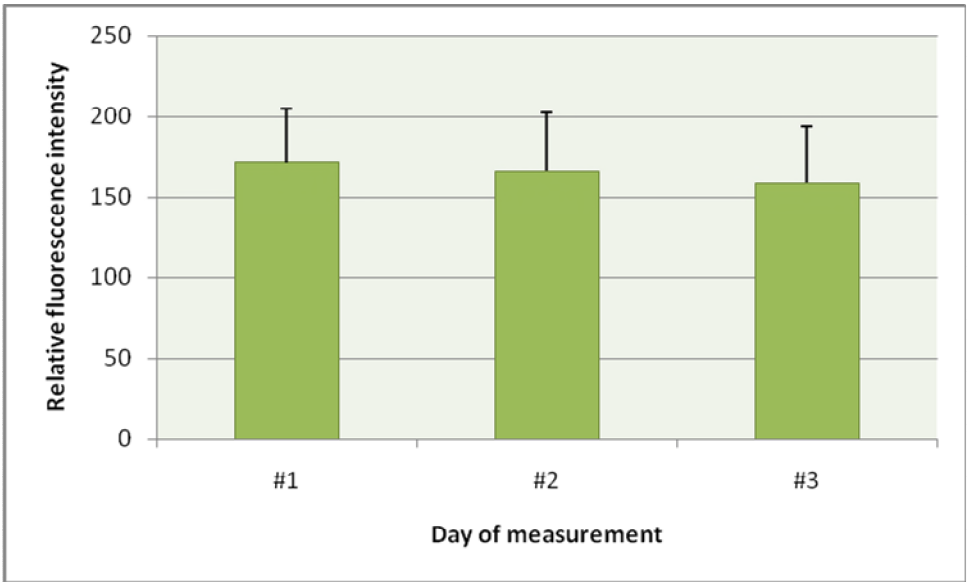


***Figure 2.9: Measurment of relative fluorescence intensity using Image J on three separate days, using pre-labelled beads and the same confocal settings as those used for all embryo analysis.***

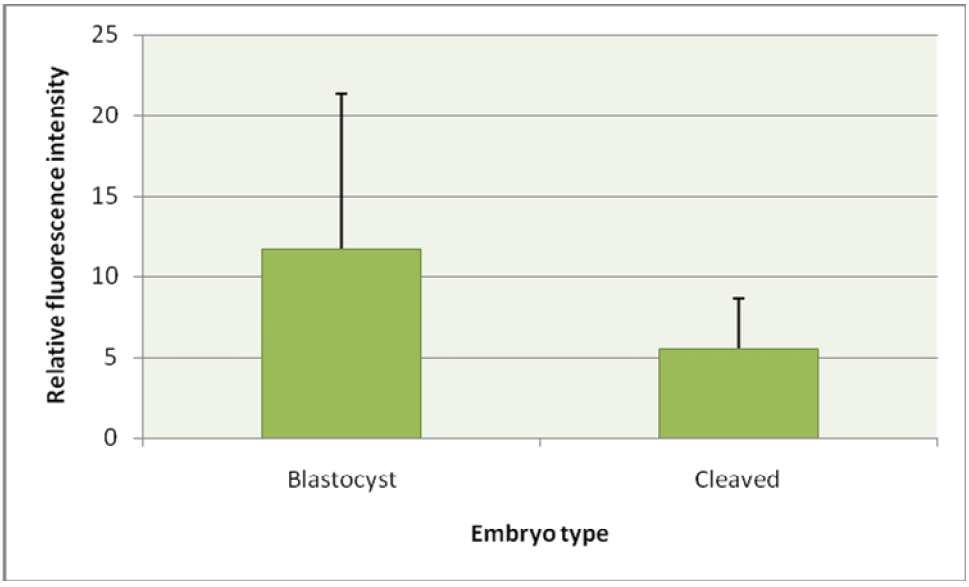


***Figure 2.10: Measurement of relative fluorescent intensity in a blastocyst and a cleavage stage embryo that had not been exposed to primary antibody during labelling, in order to demonstrate the specificity of the analysis tool used.***

In order to measure fluorescence intensity gradients across a single cell or ICM, the line selection tool was used, as detailed in figure 2.11.

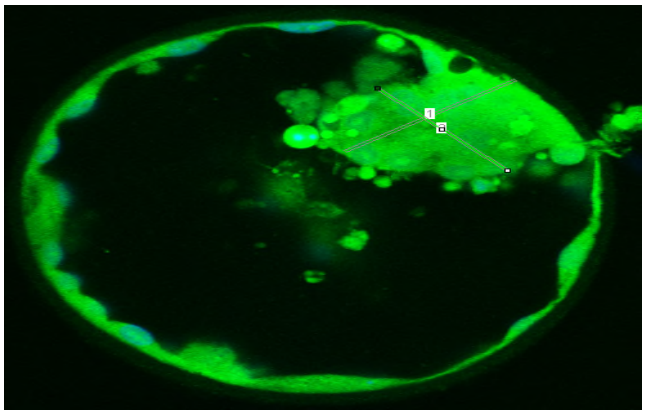

***Figure 2.11: Example of line technique to measure relative fluorescence intensity in a blastocyst ICM***

The numerical values generated in Image J were exported to Microsoft Excel databases for analysis, and graphical representations produced for ease of interpretation.

### *2.14 Time lapse monitoring*

Time lapse monitoring was undertaken to identify visual markers of embryo growth and morphology at key developmental stages, to improve our understanding of the temporal events involved in human pre-implantation embryo development.

During time lapse monitoring using the Cryo Innovation PRIMO Vision system (Parallabs), a major problem initially encountered was the movement of embryos out of the field of view. To overcome this, embryos were secured to the culture dish using Cell-Tak™ (BD Biosciences). Immediately prior to use, a stock solution containing 5µl Cell-Tak in 10µl 0.1M sodium bicarbonate ($NaHCO_3$) was prepared, and 5µl added to a Falcon 35mm culture dish (BD Biosciences). The Cell-Tak was allowed to air dry for a minimum of 20 minutes in the laminar flow hood, and the residue washed off with sterile water. The remaining footprint determined the position of the culture media drop, which was initially made with sperm preparation media (Origio) because its low protein constitution increased the adhesive qualities of the Cell-Tak. The drop was covered with sterile oil (Origio). The sperm preparation medium was then substituted with ~25µl ISM1 or BlastAssist, which was equilibrated in a 37°C/5% $CO_2$ incubator (Heraeus) for a minimum of two hours. Once equilibrated, the embryo was placed in the media drop, where the zona pellucida adhered to the Cell-Tak and remained secured in place. Embryos could be

easily removed from the Cell-Tak by applying gentle pressure with a denuding pipette.

61 zygotes and embryos were monitored using the PRIMO Vision (Parallabs) system placed inside a Heraeus 5% $CO_2$ incubator set to 37°C, see figure 2.12.

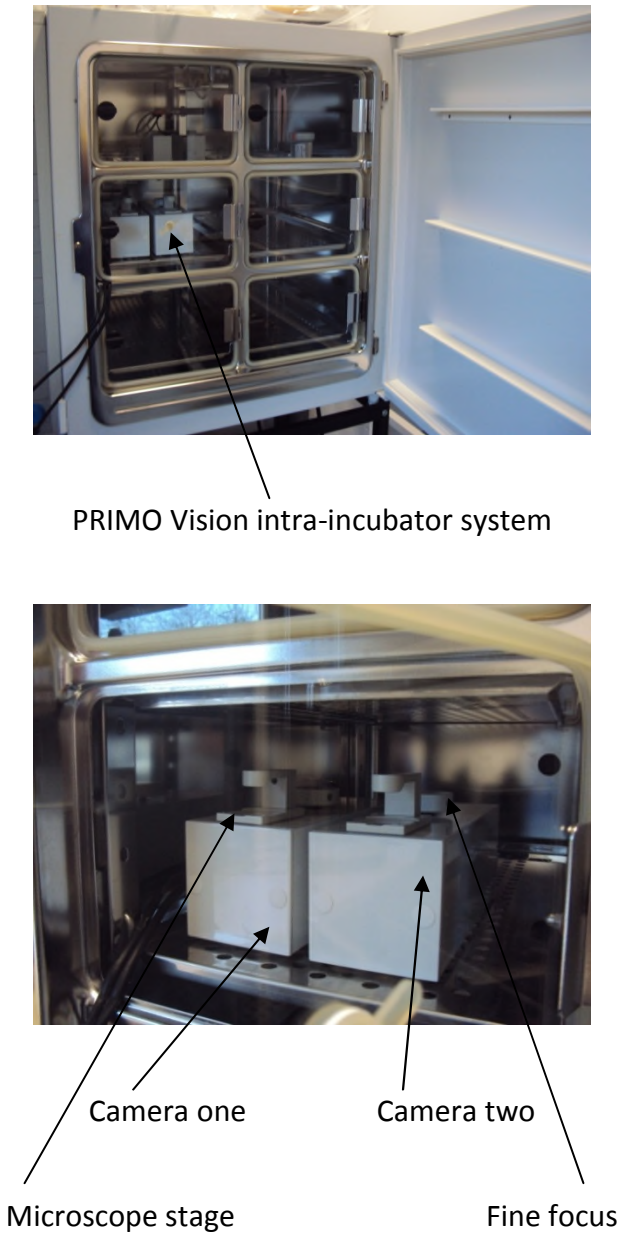


***Figure 2.12: PRIMO Vision intra-incubator continuous monitoring system***

The dish containing the embryo was placed on the microscope stage, and the integrated fine focus used to locate the embryo whilst viewing on the CryoEmbryo Capture software (Parallabs) installed on the attached laptop monitor. The interval time (minimum 10 minutes) and length of capture duration were specified, and a unique project code assigned to each time lapse sequence, followed by initiation of the programme. Embryos were assessed on-screen each day, and transferred to dishes containing fresh medium and Cell-Tak every two days, followed by fixation in 3.7% formaldehyde. Time lapse sequences were saved to the hard drive and analysed using CryoEmbryo Analysis software (Parallabs) and Image J. The data generated was exported to Microsoft Excel files.

Due to the poor quality of acquired images and data, this work was subsequently excluded from the final version of this thesis.

33 embryos were imaged using the Olympus IX81 (Olympus) inverted microscope with Solent Scientific integrated environment-controlled chamber, as shown in figure 2.13.

The chamber was pre-calibrated and set to 37°C/5% $CO_2$, and constantly monitored using an EasyLog USB data logger (Lascar Electronics, Salisbury, UK). Embryos were transferred into 10 µl drops of pre-equilibrated stage-appropriate media under oil in a Falcon 35mm culture dish (BD Biosciences). The dish was placed on the microscope stage inside the chamber and the embryos located at 100x magnification using the microscope eyepieces and fine focus. Once located, the magnification was increased to 200x and the camera switched on to enable viewing

of the microscopic field on the computer monitor. The focus was adjusted to optimise the on-screen image, and the CellM Experiment Manager used to specify the interval time (usually 5 minutes) and duration of capture required. Once the monitoring period was complete, the time lapse sequences were converted to Audio Video Interleave (AVI) files for analysis.

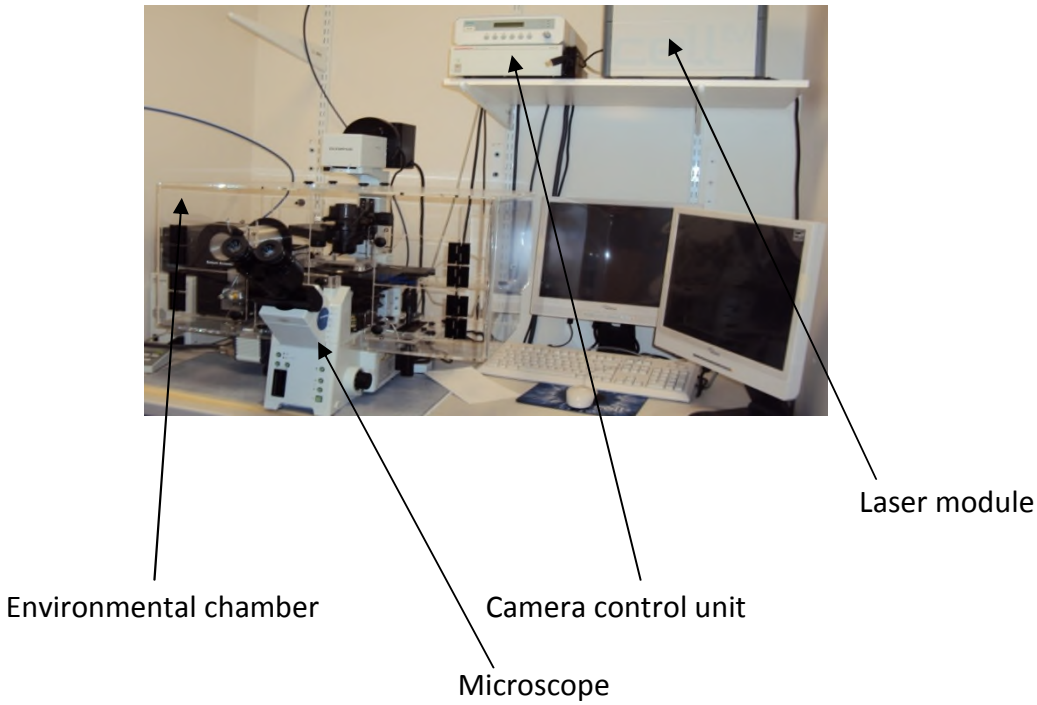


***Figure 2.13: Olympus IX81 microscope with Solent Scientific environmental chamber***

39 frozen-thawed research embryos and 403 freshclinical embryos were imaged using the Embryoscope (Unisense Fertilitech) self-contained embryo monitoring system, as shown in figure 2.14.


***Figure 2.14: Unisense Fertilitech EmbryoScope™ self-contained embryo monitoring system***

Sterile EmbryoSlides®, as shown in figure 2.15, were prepared by filling each microwell with ~1µl ISM1 or BlastAssist (Origio) culture medium using a plastic 135µm EZ-Squeeze™ denuding pipette (Research Instruments) to avoid scratching the bottom of the well, and topping up the medium in the well to 25µl using a Gilson pipette, to minimise the formation of bubbles. All 12 wells were covered with a 1.2ml layer of sterile light paraffin oil (Origio), and the EmbryoSlide equilibrated in a 37°C 5% $CO_2$ atmosphere for a minimum of 2 hours prior to use, according to the media manufacturer's protocol.

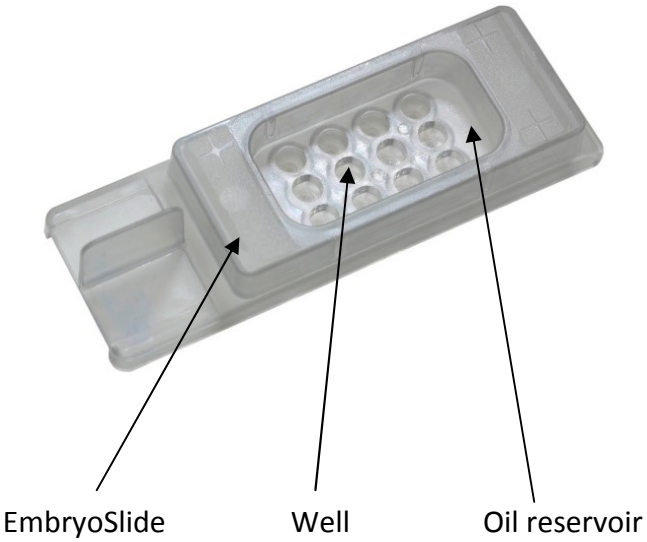


***Figure 2.15: Unisense Fertilitech EmbryoSlide®***

Embryos were loaded into the EmbryoSlide (Unisense Fertilitech) using a sterile plastic EZ-Squeeze denuding pipette (Research Instruments). The "add slide" function was selected on the EmbryoScope menu to prompt the next available slide holder to appear at the loading door, and the EmbryoSlide (Unisense Fertilitech) placed inside the chamber. The EmbryoScope software auto-focus function located each embryo within the individual well, before image acquisition commenced. Each embryo was imaged on seven focal planes every 20 minutes, and captured images were automatically saved using the EmbryoScope software, and converted to Audio Video Interleave (AVI) files to enable the development of each embryo to be visualised in a continuous time lapse video. Once the imaging period was complete, each embryo was manually annotated using the EmbryoScope (Fertilitech) software package. Using the EmbryoViewer, each cleavage division was inputted, along with the number of visible nuclei and degree of fragmentation, to allow temporal-dynamic changes in the developing embryo at specific time points to be identified.

The data generated was exported as a comma separated value (csv) file, and converted to a Microsoft Excel file for analysis.

### *2.15 Data analysis*

Microsoft Excel was used to analyse cleavage times, time spent at each developmental stage, compaction rate, cavitation rate, and blastocyst formation rate of all embryos. Dynamic properties of some embryos, such as fluctuations in the cytoplasm or membranes, and the rearrangement of blastomeres within the confines of the ZP were also observed.

The results were used to compare fresh and frozen embryos of varying quality and developmental stage, as well as the time lapse system used to acquire the data.

The two-tailed student's T test, independent group's T test, ANOVA, and Chi-square tests were used to determine significance depending upon the data sets being analysed.

### *2.16 Alteration of blastomere fate*

To investigate whether removal or damage of specific identifiable blastomeres from cleavage stage embryos had any effect on consequent development, time lapse monitoring of preimplantation embryos from day 1 to day 3 post- insemination was undertaken in the EmbryoScope (Fertilitech) to identify and track the first dividing cell. The daughters of the desired cell were then deliberately damaged using a micromanipulation technique similar to the ICSI procedure described in section 2.3, and further development of the embryo monitored by EmbryoScope (Fertilitech) time lapse imaging until day 5, 6 or 7. Assessment of themorphological

characteristics and developmental progress of the embryo were noted, before fixation in 3.7% formaldehyde.

Each embryo AVI file was annotated as described in section 2.13, and the data exported as a csv file before conversion to a Microsoft Excel file for analysis.

### *2.17 Culture of embryos with leptin protein*

To assess whether leptin affects human embryo development *in vitro*, day 4, 5 and 6 frozen-thawed embryos (n=14) were cultured with human leptin recombinant full length protein (ab13987) (Abcam) at a concentration of 1µg/ml or 20ng/ml in pre-equilibrated BlastAssist media (Origio) under sterile paraffin oil in a K-Systems G185 desktop incubator (Hunter Scientific) at 37°C/5% $CO_2$ for a period of 10 minutes, 20 minutes, 30 minutes, or 24 hours. Embryos were assessed for blastocyst development and quality, and then fixed in 1ml 3.7% formaldehyde.

To determine whether the expression of pSTAT3 was influenced by the presence of leptin, blastocysts that had been cultured with 20ng/ml human recombinant leptin were fixed in 3.7% formaldehyde and fluorescently labelled for pSTAT3 using a polyclonal antibody (TYR-705) as the primary antibody (Cell Signalling), and FITC conjugate (Sigma-Aldrich) as the secondary antibody, according to the method described in section 2.1.11.2. Embryos were imaged using the Zeiss LSM 510 confocal microscope (Zeiss).

Image stacks were imported into Image J, and analysed as described in section 2.13 using the elliptical selection tool and the RGB measurement plugin, in order to determine the relative fluorescence intensity. Measurements were taken in the cytoplasm and nuclei of the inner cell mass and trophectoderm cells, as shown in

figures 2.14 and 2.15. Each 1µm optical slice was analysed in turn from the top to the bottom of the z-stack.

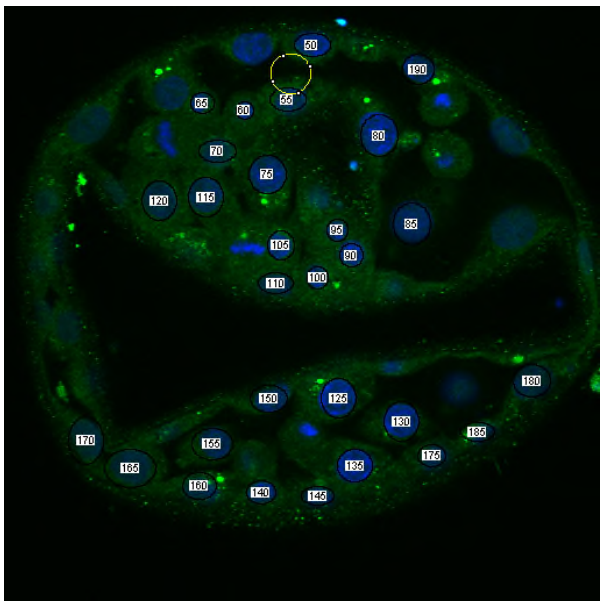


***Figure 2.16: Selection technique used to measure the relative fluorescence intensity in each nuclei of the trophectoderm in a blastocyst (selection tool shown in yellow)***

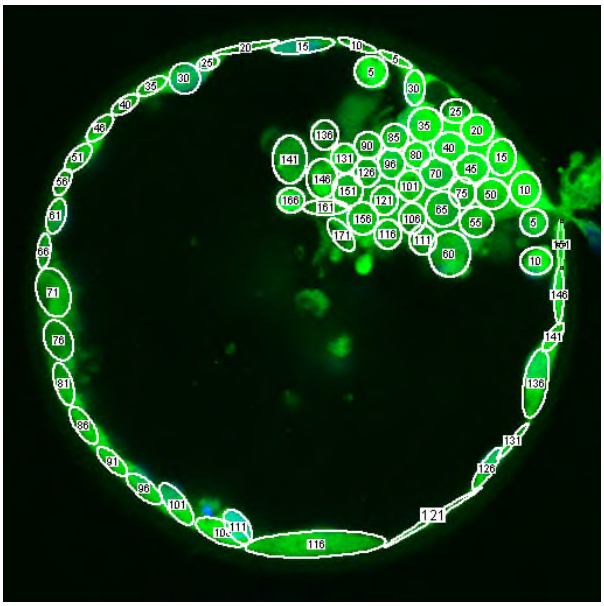

***Figure 2.17: Selection technique used to measure the relative fluorescence intensity in the cytoplasm and nuclei of the trophectoderm and inner cell mass of a blastocyst***

The pixel data generated was exported to Microsoft Excel files for analysis. The relative fluorescence intensity of FITC was measured separately in the inner cell mass and trophectoderm cytoplasm, and the inner cell mass and trophectoderm nuclei for comparison. Those embryos previously labelled for pSTAT3 without exposure to leptin protein were used as a control. Two-tailed student's t test was used to determine statistical significance.

### *2.18 Polymerase Chain Reaction*

In order to determine whether leptin receptor and SUMO-1 ribonucleic acid (RNA) was present on human oocytes and pre-implantation embryos, quantitative Real-Time Polymerase Chain Reaction (qRT-PCR) was performed on frozen-thawed oocytes (SUMO-1), zygotes and embryos (SUMO-1 and leptin receptor) at varying developmental stage and quality, obtained 1-7 days post-insemination.

#### *2.18.1 Cell Lysis*

The Ambion Single Cell-to-CT™ Kit (Life Technologies Ltd, Paisley, UK) Single Cell Lysis Solution, Single Cell DNase 1, and Single Cell Stop Solution were removed from the -20° freezer and thawed for approximately 5 minutes. For each oocyte/embryo, 9µl Single Cell Lysis Solution was mixed with 1µl DNase 1 (Life Technologies) in a sterile 0.5ml flat cap PCR tube (Starlab Group, Milton Keynes, UK). The zona pellucida of each oocyte/embryo was removed by rinsing through Acid Tyrodes Solution (Origio) and ISM1 medium (Origio) with a 135µm denuding pipette (Origio). The zona-free oocytes/embryos were added to the PCR tubes containing lysis/DNase solution and incubated for 5 minutes at room temperature. The cell lysis reaction was halted by adding 1µl Single Cell Stop Solution (Life Technologies) to each tube and incubated for a further 2 minutes at room temperature. The tubes were stored at -20°C until ready for processing.

### *2.18.2 RNA Reverse Transcription*

The Ambion Single Cell-to-CT™ Kit (Life Technologies) Single Cell VILO™RT Mix and the Single Cell SuperScript® RT were removed from the -20°C freezer and kept on ice.

When thawed, 3µl Single Cell VILO™ RT Mix (Life Technologies) was added to 1.5µl Single Cell SuperScript® (Life Technologies) per reaction in a sterile 0.5ml flat cap PCR tube (Life Technologies), and centrifuged to ensure all solution was mixed in the bottom of the tube. Each pre-prepared lysed cell sample tube was centrifuged prior to addition of 4.5µl RT reaction mix.

The sample tubes were centrifuged once more before transferring to a pre-heated Hybaid PCR Sprint Thermal Cycler (Thermo Scientific, Ma, USA). Reverse transcription of RNA to complementary deoxyribonucleic acid (cDNA) was achieved by running a three-step programme. Copying the RNA to produce a strand of cDNA was accomplished by holding the PCR tubes at 25°C for 10 minutes. Extending the copies of the resulting cDNA strand occurred at 42°C for 60 minutes, and the reverse transcriptase was stopped by holding at 85°C for 5minutes. Samples tubes were removed from the thermal cycler, allowed to cool, and kept at -20°C until ready to perform cDNA preamplification.

### *2.18.3 cDNA Preamplification*

In order to preamplify the cDNA prior to performing RT-PCR, lypholised primers for the detection of leptin receptor (Sigma) or SUMO-1 (Sigma) were resuspended in RNase/DNase free sterile water according to the required nanomolar concentration. Thesense primers, sequence 5'CTATGAGGACGAAAGCCAGAG3' (leptin receptor) and 5'TTTGTAAACCCCGGAGCGA3' (SUMO-1) were resuspended in 394µl, and the anti-sense primers, sequence5'GACTGAACTATTTATAAGCCCTTGT3' (leptin receptor) and 5'TTCAACTGAGGACTTGGGGG3' were resuspended in 404µl. The tubes were centrifuged to ensure complete mixing, and 2µl of each primer mix per reaction was added to 68µl of pH 8.0 Tris/EDTA buffer (TE buffer) (Applied Biosystems), to produce a final concentration of 20nmol.

### *2.18.4 Real-Time PCR*

For each reaction, 5µl of Ambion Single Cell PreAmp Mix (Applied Biosystems) was added to 6µl of the prepared primer mix in a sterile 0.5ml flat cap PCR tube (Life Technologies) and centrifuged. Finally, 11µl of the preamplification mixture was added to each cDNA sample. The sample tubes were centrifuged once more before transferring to a pre-heated Hybaid PCR Sprint Thermal Cycler (Thermo Scientific). Preamplification of cDNA was achieved by holding the temperature at 95°C for 10 minutes, then denaturing and extending the cDNA copies at 95°C for 15 seconds and 60°C for 4 minutes respectively. This cycle was repeated 14 times, followed by enzyme deactivation at 99°C for 10 minutes. The preamplified cDNA samples were

diluted 1:2 with RNase/DNase free water in sterile 0.5ml flat cap PCR tubes, centrifuged and stored on ice until ready to proceed with the RT-PCR step.

Lypholised primer and double-dye Taqman probe mixture for detection of leptin receptor or SUMO-1 (PrimerDesign Ltd, Southampton, UK) were resuspended in 330µl sterile RNase/DNase free water, then vortexed and centrifuged briefly to ensure complete resuspension. In a sterile 1.5ml flat cap PCR tube, 1µl of the primer/probe mixture was added to 10µl Precision-LR MasterMix and 4µl RNAse/DNAse free water per reaction. A Micro Amp Fast Optical 96-well Reaction Plate (Applied Biosystems) was prepared by reverse-pipetting 15µl primer/Mastermix into each well, and adding 5µl 1:10 diluted specific cDNA solution. Each reaction was performed in triplicate, and negative control wells were included containing only RNase/DNase free water to ensure cross contamination of the wells or sample had not occurred. The plate layout is shown in figure 2.18. For the SUMO-1 run, the plate layout was similar, although wells A1 and B1 contained oocyte cDNA solution, and subsequent wells in column 1 contained zygote stage, cleavage stage and blastocyst stage cDNA solutions.

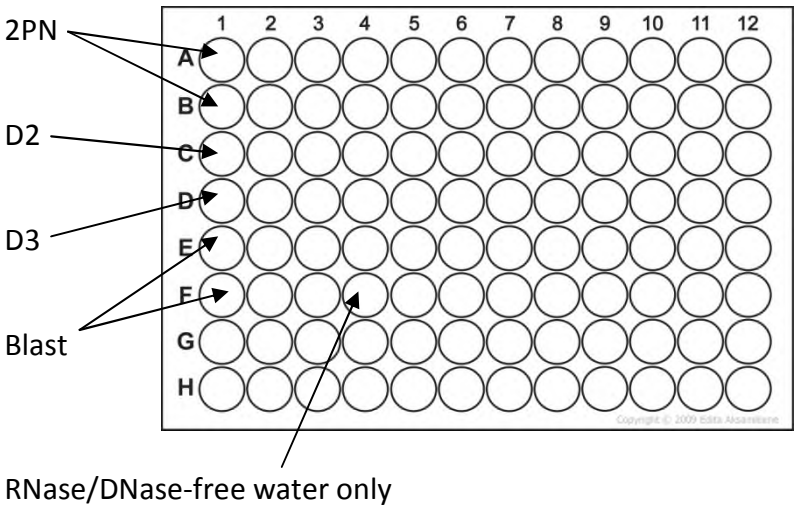


***Figure 2.18: Layout of 96-well PCR plate for detection of leptin receptor RNA.***

Once prepared, Thermal Seal RT2 optically transparent film (Sigma) was sealed around the top of the plate to cover all wells, and the plate centrifuged at 3000rpm for 7 minutes.

Amplification was achieved using an Applied Biosystems 7500 Fast Real Time PCR system (Life Technologies) at standard speed. Enzmye activation was attained by heating the plates at 95°C for 10 minutes, followed by denaturation at 95°C for 15 seconds and fluorogenic data collection at 60°C for 60 seconds. The cycle was repeated 50 times.

Data was collected and visualised using the integrated 7500 StepOne Software.

### *2.19 Extracellular Matrix Protein 3D implantation model*

Matrigel™ Basement Membrane Matrix (BD Biosciences) is a solubilised basement membrane preparation extracted from the Engelbreth-Holm-Swarm (EHS) mouse sarcoma, containing similar structural proteins and growth factors to the endometrial matrix (Ghaffari Novin *et al* 2007). In order to study cell adhesion and invasion, mimicking the implantation process *in vivo,* 19 embryos at days 4-7 post-insemination were cultured on Millicell (Millipore, Watford, UK) inserts containing a mixture of Matrigel (BD Biosciences) and BlastAssist (Origio) culture media in Corning Costar 24 well culture plates (Sigma-Aldrich).

Prior to commencing the implantation model experiments, the Matrigel was thawed overnight at 4°C. To ensure homogeneity in the reconstituted solution, the vial was swirled prior to dispensing into 250µl aliquots using pre-cooled pipettes, tips (Gilson Scientific, Luton, UK), and 0.5 ml micro tubes (Sarstedt, Leicester, UK) to minimise repeated freezing and thawing. The aliquots were then refrozen and stored at -20°C until required, when one aliquot of the solution was thawed at 4°C overnight.

Liquefied Matrigel (BD Biosciences) and pre-equilibrated BlastAssist (Origio) culture medium were mixed in a 1:1 ratio (100µl each) and layered onto the bottom of the Millicell insert. The insert was placed into a 24 well culture plate (Sigma-Aldrich) containing 500 µl BlastAssist (Origio) medium to ensure that the insert membrane was immersed, and equilibrated at 37°C/5% $CO_2$ for at least two hours, in accordance with the media manufacturer's instructions. Fresh and frozen-thawed

embryos at day 4-7 post-insemination were placed inside the Matrigel/culture medium and incubated at 37°C/5% $CO_2$. Embryos were visualised by light microscopy at 24-hour intervals to assess the adhesion and outgrowth during attachment and hatching of the blastocysts. Once the culture period was complete the permeable membrane on the bottom of the Millicell insert was detached using a fine gauge needle to cut around the edge, and the membrane and gel disc placed into a Falcon 50x9mm petri dish with snap-shut lid (BD Biosciences) and flooded with 3.7% formaldehyde in order to fix the whole mount.

### *2.20 Culture of embryos in conditioned medium*

In order to determine the effect of adhesion- and invasion- stage endometrium secretions on human preimplantation embryo marker profiles, day 5 and day 6 blastocysts were incubated with supernatant media from decidualised and non-decidualised human stromal cell cultures, or supernatant media from Ishikawa cell cultures, for varying time periods.

#### *2.20.1 Endometrial biopsy preparation and media collection*

Endometrial biopsies were collected from patients attending the recurrent miscarriage clinic at the CRM. The biopsies were prepared by transferring the tissue into 100mm Corning plastic culture dishes (Sigma-Alridch) and drawing off any excess fluid and mucus with a 1000µl Gilson pipette tip. Digestion of the tissue was achieved by mashing for 5 minutes using scalpel blades, adding 10mls filtered Dulbecco's Modified Eagle Medium (DMEM) F12 serum-free medium supplemented with 100µl collagenase and 100µl DNAse (Invitrogen), and incubating at 37°C/5%

$CO_2$ in Corning 25cm$^2$ flasks (Sigma-Aldrich) for one hour, shaking every 20 minutes to mix.

The enzymes were deactivated after one hour by adding DMEM F12 serum-supplemented media, and the cells spun down, resuspended and transferred to Corning 25cm$^2$ flasks (Sigma-Aldrich) for incubation at 37°C/5% $CO_2$ in air.

Cell cultures were checked every day, and media changed every two days until a convergent layer had grown on the bottom of the flask. The supernatant media removed from the cell cultures was collected in 5ml round-bottom tubes, aliquoted into 0.5ml eppendorf tubes, and stored at -80°C.

### *2.20.2 Blastocyst culture*

Frozen blastocysts at day 5 or 6 post-insemination were thawed as described in section 2.6, and incubated in pre-equilibrated BlastAssist media (Origio) under oil at 37°C/5% $CO_2$ for two hours.

Blastocysts (n=3) were exposed to stromal cell or Ishikawa cell- conditioned media for 10 minutes or 20 minutes, and immediately fixed in 3.7% formaldehyde. The embryos were labelled for pSTAT3 as described in section 2.11.2, imaged using confocal microscopy, and the z-stacks imported into Image J for analysis as described in section 2.13.

### *2.21 Image processing for creation of computer-generated models*

The confocal and time-lapse images acquired were exported in TIFF or AVI file format to the International Digital Laboratory, WMG, University of Warwick, and the School of Computing, Mathematics and Digital Technology, Manchester Metropolitan University.

Here, the images were pre-processed for 3-dimensional computer modelling and development of semi-automatic software tools using algorithms scripted in Matlab (MathWorks, Cambridge, UK). All image analysis and programme development was performed by colleagues at the University of Warwick, and Manchester Metropolitan University, using embryological datasets obtained as described in sections 2.12 and 2.14.

# Chapter Three

# Research Material

# Chapter Three

# Research Material

## *3.1 Embryos*

All embryos used or analysed in this project were originally created for patients undergoing assisted reproductive treatment at the Centre for Reproductive Medicine (CRM) Coventry, Leicester Fertility Centre (LFC), or Bath Fertility Centre (BFC).

During their preparation for treatment, patients are required to sign the HFEA MT/WT mandatory forms. This form included a question asking patients whether they agreed to be approached about research projects. Only patients who had agreed to be approached could be asked to take part in the project. Approximately 60% of patients attending the CRM for treatment during this project had consented to be approached regarding research projects. Of those patients who consented to be approached, an estimated 60% were informed of the project and given the opportunity to take part, as described in section 2.3. Of those approached, around 60% agreed to donate any arising surplus and/or abnormal oocytes and embryos that were not usable in their treatment. This equates to an uptake of <40% when considering the number of patients willing to be approached about the research project compared to the number patients agreeing to donate their gametes and embryos, and a maximum recruitment potential of <25% of all patients in treatment. It was also the case that, since many patients had to be approached long

in advance of the point at which it was known whether or not they had any surplus material available that could potentially be used for research, often patients were consented who subsequently had no material that was suitable for use in the research. The process of consenting was therefore time consuming and inefficient, but complied with all regulatory expectations.

A total of 445 embryos were donated for use in research procedures, such as fixing and fluorescent staining, and cell damage experiments (the experimental group). However, ~30% of these were not usable due to the embryos being degenerate, not recovered from the freezing straw, or not found in the transportation tube. Fresh oocytes and embryos accounted for 60% of the total, whilst 40% were frozen embryos. The details of the patient population providing this research material are the focus of this chapter.

Data from 924 embryos that were monitored using time lapse technology as part of routine clinical treatment were used for time lapse studies (the clinical group). Due to the relatively recent implementation of the Embryoscope™ as a clinical tool, only limited data about the couples donating these embryos was available at the time of writing this thesis, and therefore the only the details regarding patient age, aetiology, treatment type, number of oocytes retrieved, and urinary hCG pregnancy test in this group are included.

### *3.2 Patients*

In total, 165 couples were involved in donating the experimental material to the project, and 76 patients had their clinical embryo data analysed. The age of the female patients in the experimental arm ranged from 23-44 years, with a mean age of 34.6 (±4.05) years. BMI ranged from 17-42 kg/$m^2$, with an average 25.3 (±4.60) kg/$m^2$.

In the clinical group, the female age ranged from 25-41 years, with a mean age of 34.5 (±3.91) years.

Male factor infertility was the most prevalent specific aetiology in the experimental cohort of patients, with 50% of couples affected. This is a relatively high proportion in comparison to published data, although since 40% of the embryos used in this study were frozen surplus embryos, this is not entirely unexpected. Embryos derived from couples where male factor infertility predominates are more likely to be of superior quality, since there is no known female factor influencing the subfertility. Tubal disease accounted for 19% of infertility problems, and 11% of cases involved unexplained infertility. In 8% of cases, the aetiology of infertility was attributed to ovulatory dysfunction, and 5% to age-related decreased ovarian reserve. 2% of all female patients recruited for this study had been diagnosed with endometriosis, and 4% had been diagnosed with polycystic ovaries (PCO) as the major factor of infertility. This is considerably lower than that reported in the general population, which is estimated at up to 20% (Sirmans and Pate 2014), although similar occurrence of PCO has been reported in previous studies (Bahceci and Ulug 2004).

The variation in the occurrence of PCO as a cause of infertility suggests that there are several factors influencing the infertility status of these patients. Pre-chemotherapy fertility preservation accounted for 1% of the patients involved in this study.

In the clinical group, 62% of patients had a female factor as the predominant underlying cause of infertility, 36% male factor, and 2% unexplained. This high incidence of female factor may be due to the nature of the patients opting for time lapse imaging, for instance those who have previously had an unsuccessful cycle and who would benefit from the additional information about their embryo development provided by the generated images. Poor embryo development may be related to reduced oocyte quality, and thus would be indicative of female-related factors.

65% of couples in the research cohort presented with primary infertility, compared to 35% of couples with secondary infertility.

### *3.3 Treatments*

The majority of couples (52%) who donated research embryos for this project were attempting their first fresh cycle of IVF or ICSI treatment. Other couples were embarking on a second (32%), third (14%), fourth (5%) or fifth (6%) fresh attempt. One couple had previously had five fresh attempts, and the embryos donated to this project were created during their sixth fresh cycle. The chance of a live birth reportedly increases with cumulative cycles of ART, using fresh and frozen embryos (McLernon *et al* 2016).

Most of the couples undergoing treatment were having ICSI (60%), which is consistent with the high incidence of male infertility in the recruited cohort. Standard IVF accounted for 38% of treatments, whilst 2% of couples opted for an IVF/ICSI split.

In the clinical group, the treatment type was virtually identical to the research group, with 60% of the couples having ICSI. This does not correlate with the lower percentage of male factor patients, but may be explained by a higher number of couples with a previously failed cycle electing for ICSI as a precaution against poor fertilisation rates, for those with low oocyte numbers, or for patients with several factors contributing to their infertility, but for whom female factors predominate.

### *3.4 Lifestyle*

Female patients who admitted to smoking comprised 6% of the total for whom this information was available, whilst 2% claimed to be former smokers. More than twice as many male patients (15%) admitted to smoking. However, this may not be reliable, because NHS funding criteria often specify that those funded must be non-smokers. No tests or further investigations are routinely carried out to verify non-smoking status. The number of smokers in this study is too small to study any potential link between smoking and treatment outcome, however female smoking has been linked to reduced ovarian response and lower clinical pregnancy rates in ART cycles (Freour *et al* 2008).

Alcohol use was commonplace in this patient group, with 87% of females and 83% of males consuming alcohol. Females drinking more than the government recommended limit of 14 units per week comprised 11% of alcohol consumers,

whilst 17% of males were drinking more than 21 units of alcohol per week. A pregnancy rate of only 11% was observed when the female partner consumed more than 14 units of alcohol per week, although the number of subjects in this category was small (n=9).

### *3.5 Number of oocytes collected*

The number of oocytes collected from each patient in the research group varied from 3-68, with a median of 11, and in the clinical group from 2-26, with a median of 9. The numbers of oocytes at the top end of the range are extremely large; however the number of patients with high oocyte numbers was minimal. Clearly, the patients studied had surplus material so low responders who had low numbers of oocytes collected were under-represented in this group. The optimal number of oocytes required from a fresh ART cycle to maximise cumulative live birth rate has previously been reported as 10 or more (Drakopoulos *et al* 2016). I found no significant correlations between the numbers of oocytes collected and the female patient age, female BMI, primary versus secondary infertility, attempt number, or treatment type. Neither was the number of oocytes collected linked to pregnancy result. These findings are in contrast to published data, where the number of oocytes retrieved decreases with patient age (Tan *et al* 2014; Drakopoulos *et al* 2016), and is reportedly strongly correlated with live birth rate (Sunkara *et al* 2011). There was a trend towards an increased number of oocytes collected for those couples where male factor infertility was the predominant aetiology, although the difference was not significant.

These unexpected results may reflect the cohort of patients included in the research group, who generally had a better prognosis by default due to them having surplus material available, and/or frozen embryos. This group of patients is therefore not representative of the general IVF population.

### *3.6 Embryo development and utilisation*

The number of zygotes formed following insemination in the research group ranged from 0-42, with an average of 6.7 (±4.45), and the overall fertilisation rate was 55%. The majority of patients had 2 embryos transferred (76%), whilst 28% of patients had a single embryo transfer. One patient aged 44 years had 3 embryos transferred on day 5 (1x early blastocyst; 2x morula), resulting in a biochemical pregnancy. Transfer of 3 embryos is discouraged by the HFEA, although is permitted in exceptional circumstances for women aged 40 years or over. No suitable embryos were available to transfer in 4% of couples who took part in this study.

The first priority for all patients is to have any surplus good quality embryos cryopreserved. It is only after cryopreservation of any suitable embryos has taken place that other embryos can be considered for research use. The number of embryos frozen in each cycle varied from 0-12, not including those cycles requiring all zygotes or embryos to be frozen electively (n=3) in order to avoid a transfer at that time, for example due to cancer therapy or adverse endometrial environment. The total embryo utilisation rate, which takes into account the percentage of embryos transferred or cryopreserved in each cycle, ranged from 0-100% (average = 52%).

### *3.7 Outcomes*

In total, 47% of patients involved in the research arm of this study had a positive urinary hCG test in the fresh cycle in which the donated embryos were created 12-14 days post-transfer, depending upon the developmental stage of the embryo transferred. Seven weeks post-transfer, 75% of those patients had a foetal heart beat detected by ultrasound scan. Biochemical pregnancy was diagnosed in 16% of cases at this time, whilst 9% of patients suffered a miscarriage after the seven week scan. The multiple pregnancy rate for this group of patients was 33%.

Increasing patient age was correlated with a decline in pregnancy rate in this group of patients, as shown in figure 3.1.

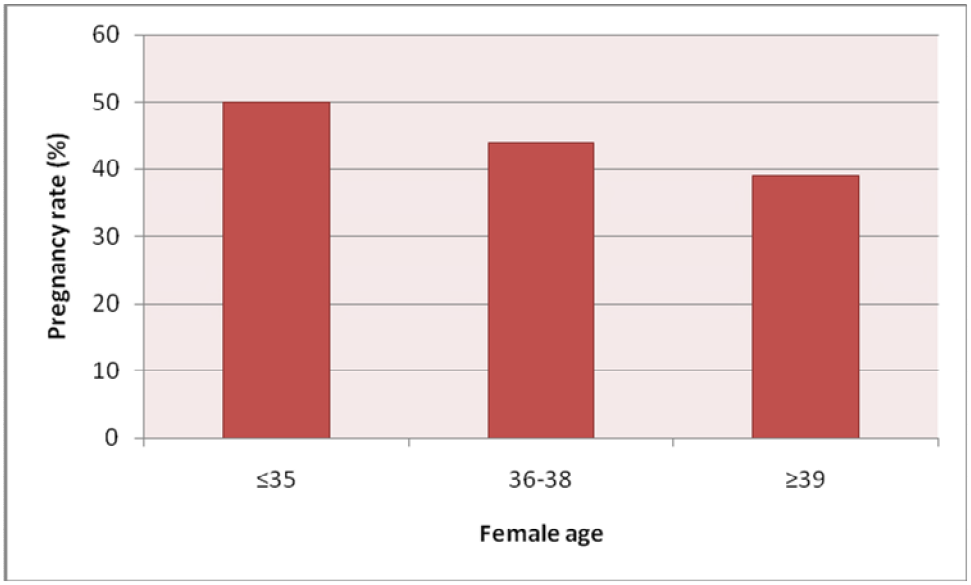


***Figure 3.1: Bar chart to show patient age versus urinary hCG result. Increasing patient age is correlated with decreasing positive pregnancy result***

The percentage of embryos utilised in each cycle was positively correlated with pregnancy, as shown in figure 3.2.

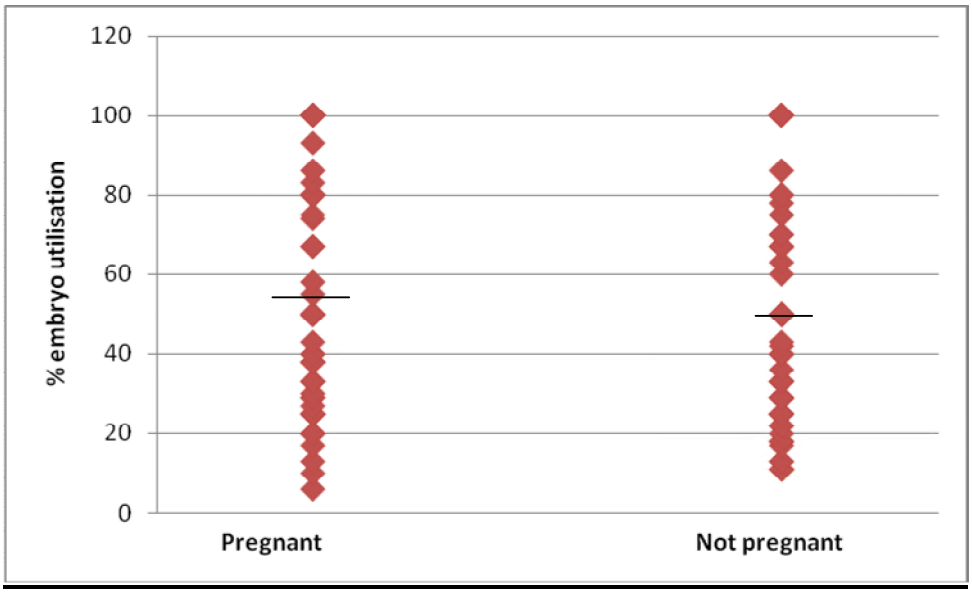


***Figure 3.2: Scatter plot showing the embryo utilisation rate (%) versus the urinary hCG result. A higher utilisation rate correlates with positive pregnancy result***

Additionally, the higher percentage of embryos utilised in each cycle was associated with ongoing pregnancy. Those patients who had a lower embryo utilisation rate were significantly more likely to suffer a biochemical pregnancy or a miscarriage than those with a higher embryo utilisation rate (*p=0.004; two-tailed t test).

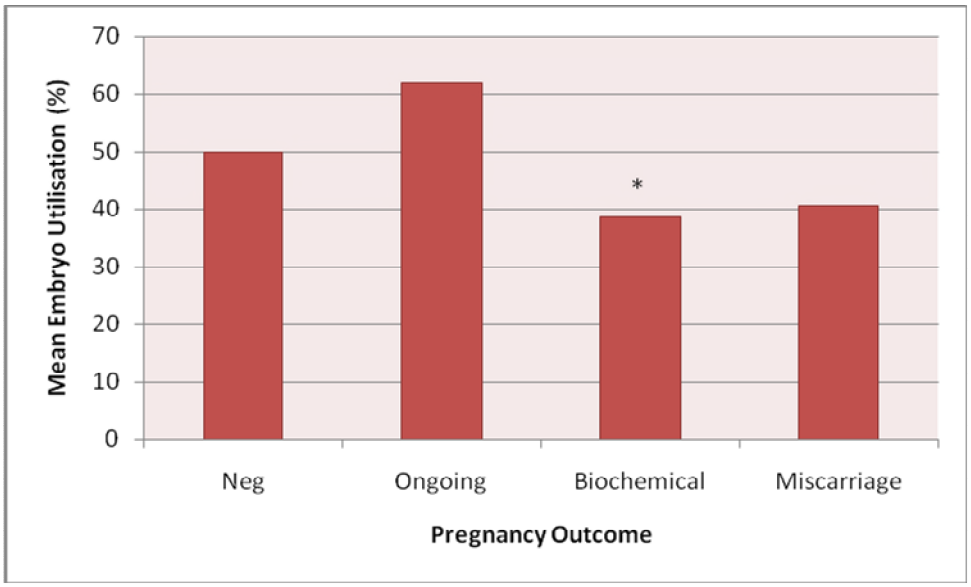


***Figure 3.3: Bar chart showing the mean embryo utilisation rate (%) versus the pregnancy outcome. A higher rate of embryo utilisation is correlated with successful pregnancy outcome***

For the clinical group of patients, whose embryos were monitored in the Embryoscope (Unisense Fertilitech) and whose outcomes were reported, the overall pregnancy rate was 49%.

Analysis of the number of embryos frozen in each cycle shows that positive pregnancy is associated with embryo cryopreservation. The mere fact that there are embryos available to freeze seems more important than the number of embryos *per se*, as 60% of patients who had embryos frozen became pregnant. The majority of patients (72%) with no embryos to freeze did not become pregnant.

The following four chapters will summarise how each embryo was utilised during the course of this project, and the results obtained from the associated experiments and analysis.

# Chapter Four

# Potential Molecular and Morphological Markers of Human Embryo Viability

# Chapter Four

# Potential Molecular and Morphological Markers of Human Embryo Viability

## *4.1 Introduction*

Several morphokinetic markers of human preimplantation embryo viability, which relate to the morphology and rate of developmental progression, have been identified. These markers are routinely visualised during embryo culture in the clinical IVF laboratory to assist in the identification and selection of those embryos that are most likely to result in a pregnancy (Montag et al 2013). These are considered to be non-invasive, as the need for manipulation of the embryos is minimal when assessing morphology. In addition, a number of invasive methods of predicting human preimplantation embryo viability also exist, including polar body, blastomere, and trophectoderm biopsy for preimplantation genetic diagnosis (Montag *et al* 2013). The ultimate goal in clinical embryology is to be able to accurately predict the implantation potential of a single embryo using the least invasive methods possible. Time lapse imaging is an emerging non-invasive technology used to identify cleavage patterns and temporal behaviour in developing embryos, and this is investigated in more detail in chapter six of this thesis.

Fragmentation is a common occurrence in human embryos, and may be a permanent feature or a transient episode during preimplantation embryonic development (Van Blerkom et al 2001). Fragments may be associated with

apoptosis, during which large aggregations of chromatin form on the inner nuclear membrane of cells, condensation of the cytoplasm occurs, and indentations of the cytoplasmic membranes are observed. Following fragmentation of the nucleus, the apoptotic cell breaks down into membrane-bound bodies which may contain fragments of the nucleus (Hardy 1999). Apoptotic cells in human preimplantation embryos have been identified, and are characterised by nuclear membrane blebbing, condensation of chromatin, vacuoles in the cytoplasm, and fragmentation of the nuclei and cytoplasm (Hardy 1999; Brison 2000; Chi *et al* 2011). These may be associated with micronuclei, which may be seen frequently in human embryos during clinical observation; however, a link with embryo quality had not previously been explored at the time of initiating this project. Additionally, fragmentation occurring as a direct consequence of apoptosis has been previously dismissed (Antczak and Van Blerkom 1999). A significantly higher proportion of chromosomal abnormalities have been identified in blastocysts derived from poorer quality cleavage-stage embryos in comparison with those developing from good quality embryos (Hardarson et al 2003). Furthermore, blastocysts arising from poor morphology day two embryos had significantly fewer cells at the blastocyst stage than those arising from good quality day two embryos (Hardarson et al 2003). More recently, chromosome-containing fragments and micronuclei within developing human embryos have been shown to contribute to embryonic aneuploid status (Chavez et al 2012).

The number of cells within the human blastocyst is broadly associated with viability. In early studies of human blastocysts, the number of TE cells remained largely

unchanged between day 5 and day 6, but had doubled by day 7. Conversely, the number of ICM cells doubled between day 5 and day 6 but remained unchanged on day 7. The proportion of ICM cells ranged from one third to one half of the total cell number depending upon the number of days since insemination (Hardy et al 1989).

The occurrence of human monozygotic twins is increased following assisted reproductive treatment (Edwards *et al* 1986; Behr *et al* 2000), and significantly increased when blastocysts are transferred compared to the transfer of cleavage stage embryos (Milki *et al* 2003). One suggested mechanism for this phenomenon is the development of two inner cell masses in the blastocoelic cavity (Meintjes *et al* 2001). One study observing the behaviour of mouse blastocysts with double inner cell masses found that each inner cell mass continued to develop after hatching (Chida 1990). Additionally, the characterisation of monozygotic twins identifies four types depending upon the time of embryonic division, with type II being derived from a separation of a single inner cell mass into two. This is the most commonly occurring (~80%) of all monozygotic twin types (Hogenson 2013).

Excluded cells, which exhibit poor interaction with other embryonic cells, are commonly seen in compacting and cavitating stage preimplantation embryos (Hardy et al 1996). Early electron microscopy studies of abnormal mouse embryos showed that one or more large excluded cells, possessing the structural characteristics of 8-cell stage blastomeres, were present at the blastocyst stage. The excluded cells were usually confined to the periphery of the blastocyst, although they were occasionally observed within the blastocoel (Calarco and Perdersen 1976). These are likely to be cells that have arrested at some point during the development of

the embryo, and are banished into the perivitelline space during compaction, excluding them from becoming part of the eventual blastocyst (Hardarson *et al* 2012). Cells at the cleavage stages are not necessarily identical, with variations in both chromosomal and cytoplasmic components evident. It is unknown whether these cells may be a response to abnormality, for example, allowing improved distribution of what material is present, or an abnormality *per se*. However, when compaction and cavitation occur in human embryos, substantial rearrangements are also noted (Mihajlovic *et al* 2015).

Non-invasive markers currently offer limited information about embryonic molecular constitution, which normally requires invasive analysis. Conversely, invasive analysis cannot be directly related to developmental potential, since this cannot be measured following invasive testing. Proposed molecular markers of embryo viability include the integrity of the actin cytoskeleton and the polar distribution of the closely-associated regulatory proteins leptin and STAT3 (Antczak and Van Blerkom 1997).

Actin is a ubiquitous contractile protein which has key roles in cellular shape and motility (Small et al 1999). The uniformity of the actin cytoskeleton is an indicator of the quality of preimplantation embryos (Levy et al 1998; Wang et al 1999). Initially, actin was selected for this project in order to highlight and visualise the borders between cells with a view to developing computer-generated models of human embryo development. The results reported in this chapter are therefore secondary to the initial purpose of actin staining.

Polarisation refers to the non-uniform organisation of components of the oocyte and embryo, and is believed to underlie the ability of the early embryo to differentiate into two cell types at the blastocyst stage (Edwards and Beard 1997). Polarity in oocytes can be identified by reference to the polar body positions (Gardner 1997; Garello *et al* 1999), but cytoplasmic rotations may make these assessments unreliable.

Leptin and STAT3 have previously been shown to have a polarised distribution in the oocytes of mice and humans, and to be distributed differentially between blastomeres of cleavage stage human embryos (Antczak and Van Blerkom 1997). Leptin, the product of the mouse *obese (ob)* gene, is a 16-kDa non-glycosylated peptide hormone synthesised primarily by adipocytes, with the characteristics of a secreted protein (Zhang *et al* 1994). Leptin is associated with the activation of STAT3, during which Janus kinases catalyse the phosphorylation of cytoplasmic STAT3 via the Jak/STAT signalling pathway, forming homo- and/or heterodimers which translocate to the nucleus and activate transcription of target genes (Duncan *et al* 1997). The use of leptin and STAT3 labelling during this project was aimed at investigating whether these polarised markers were affected by or associated with embryo quality. Such molecular markers cannot be detected using conventional light microscopy as applied in the clinical setting. Instead, specialised fluorescent stains and microscopy techniques are required in order to highlight the target marker (Lichtman and Conchello 2005). Unlike time lapse imaging, these techniques preclude live cell imaging, since fixation of the embryos is required prior to staining, and therefore these methods are considered highly invasive and non-compatible

with continued embryo development. For this reason, it is impossible to fully quantify how the distribution of proteins within human preimplantation embryos directly relates to achievement of pregnancy. However, examining the distribution of structural and cytoplasmic proteins within three-dimensional reconstructions of human embryos under experimental conditions may help to increase our understanding of the mechanisms of development, which can be used to advantage in the clinical IVF laboratory.

## *4.2 Aims*

The aims of the experiments presented in this chapter were:

To detect and confirm the distribution of the actin cytoskeleton in cleavage stage, compacting, and arrested human preimplantation embryos and blastocysts.

To establish whether the regulatory proteins STAT3 and leptin are polarised within human oocytes and preimplantation embryos, and whether their distribution differs in relation to the position of the polar body in metaphase II stage oocytes and oocytes that have failed to fertilise, and between the cells of the trophectoderm and the inner cell mass.

To determine the number of cells in the inner cell mass and the trophectoderm in human blastocysts during *in vitro* development, and to consider morphological characteristics of cleavage stage embryos and blastocysts and their relationship with quality and possible clinical outcomes.

## *4.3 Methods*

171 human oocytes and embryos of varying developmental stage and quality were fixed and stained with fluorescent probes to determine the distribution of actin, STAT3, pSTAT3 and leptin, as described in section 2.11, and imaged using confocal microscopy with standardised settings, as described in section 2.12. Relative fluorescence intensities were measured using Image J with techniques validated using positive and negative controls, as described in section 2.13**.** Morphological features of stained and unstained blastocysts, such as free cells, excluded cells, cytoplasmic projections, and double ICMs were identified, and cell numbers in the ICM and TE of blastocysts were determined.

## *4.4 Results*

### *4.4.1 Actin*

A total of 26 frozen-thawed and 24 fresh embryos were fixed and labelled with AlexaFluor® 488 phalloidin in order to visualise the actin cytoskeleton, and mounted in DAPI medium to highlight the nuclear chromatin, as described in section 2.11.1.

Figure 4.1 shows the pattern of actin distribution in poor quality fresh cleavage stage embryos. Figure 4.1 (a) shows two images of a day four embryo with five cells. There are clear borders around each blastomere and around individual fragments. Note the appearance of the nucleus in the top cell in figure 4.1 (a), this may be disorganised chromatin or poorly organised mitotic chromosomes. Figure 4.1 (b) shows a day four fresh embryo with a large arrested cell. There are distinct actin borders visible around the edges of the intact cells, and around the morphologically normal cell nuclei. There is no discernible actin border surrounding the fragmented/mitotic chromosomes of the nucleus in the arrested cell.

*(a)*

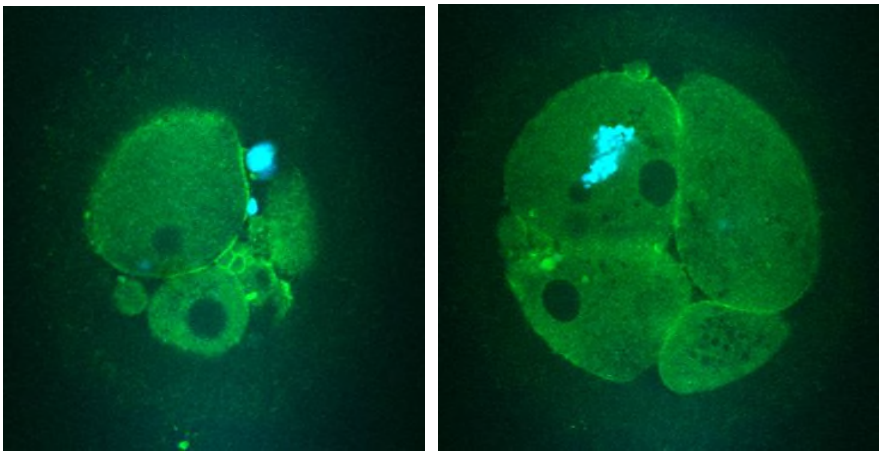

*(b)*

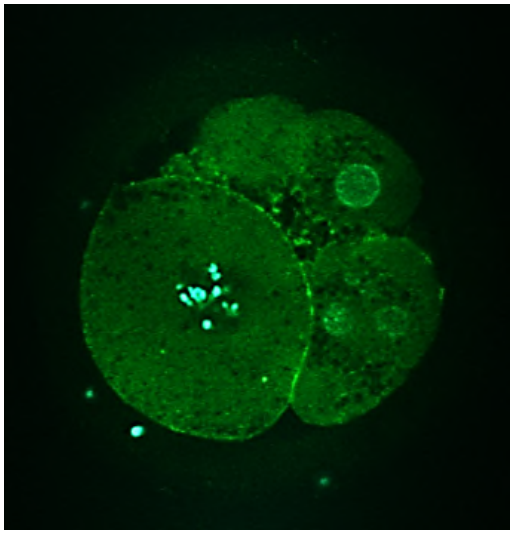

***Figure 4.1: Confocal images showing actin distribution in (a) fresh 5-cell arrested embryo (b) fresh 4-cell embryo with a large arrested cell on the left hand side of the image. Distinct actin borders are seen around each cell, intact nuclei, and small individual fragments, but not around the disorganised chromatin of the fragmenting/mitotic nuclei***

The patient who donated the embryos in figure 4.1 did not have an embryo transfer during the fresh cycle, so the implantation potential of the sibling embryos is not known.

Figure 4.2 shows confocal images of day two frozen-thawed embryos of varying quality. There are no distinct actin borders around the individual blastomeres or the cell nuclei. The cell survival rates were 2/2 (100%, a) and 3/4 (75%, b), thus both embryos in this example would be deemed clinically viable post-thaw. Each of the cells visible is mononucleated and both polar bodies are also identifiable in these images. Both of the embryo donors became pregnant after embryo transfer in the fresh cycle.

*(a)*

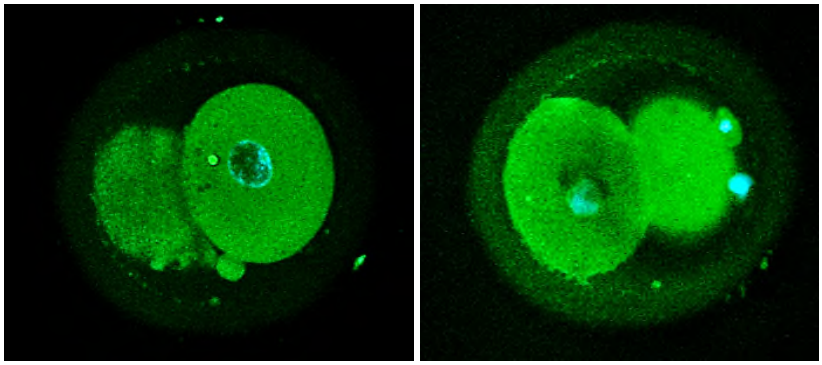

*(b)*

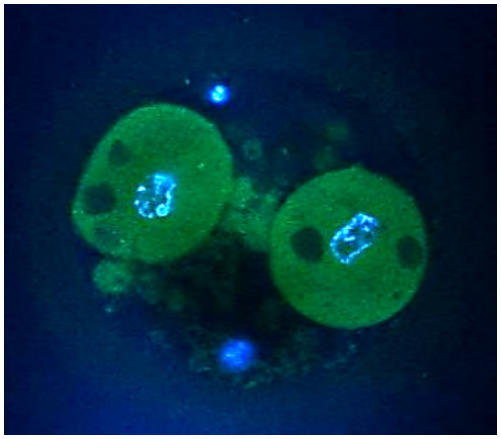

***Figure 4.2: Confocal images showing actin distribution in the cells of (a) 2-cell frozen-thawed embryo (b) 3-cell frozen-thawed embryo. The cytoplasmic actin distribution is non-uniform, and the blastomeres lack a distinct actin border***

Figure 4.3 shows examples of actin distribution patterns in morphologically normal appearing day two and day three frozen-thawed embryos. All of the embryos have clear actin boundaries around the individual blastomeres. The percentage cell survival for the embryos were 75% (c) 85% (f) and 100% (a), (b), (d), (e) respectively, thus each of these embryos would have been deemed viable upon thawing according to our clinical laboratory protocols. The fresh cycles of the three patients who donated these particular embryos all resulted in live births.

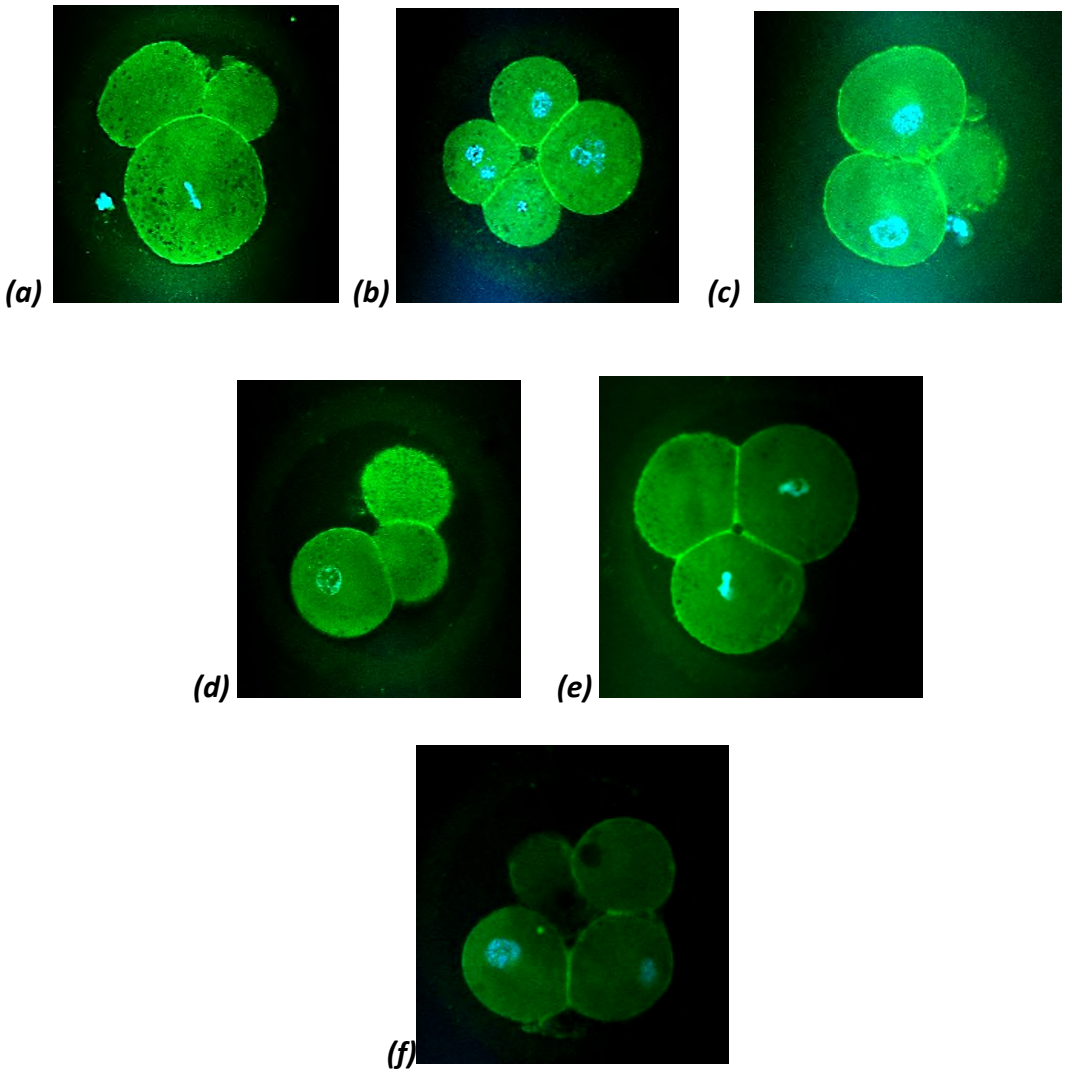


***Figure 4.3: Confocal images showing (a) a day 3 frozen-thawed morphologically normal appearing embryo with chromosomes apparently well aligned in metaphase, (b) a day 3 frozen-thawed embryo with some multi-nucleated cells (c) a day 2 frozen-thawed embryo, (d) a day 2 frozen-thawed embryo, (e) a day 2 frozen-thawed embryo (f) a day 2 frozen-thawed embryo***

Figure 4.4 shows confocal images of a day four fresh compacting embryo. There is actin fluorescence at the periphery and at the junctions between cells, which are beginning to flatten against one another. The areas lacking in fluorescence are vacuoles, and some stained areas of fragmentation can be observed in the perivitelline space.

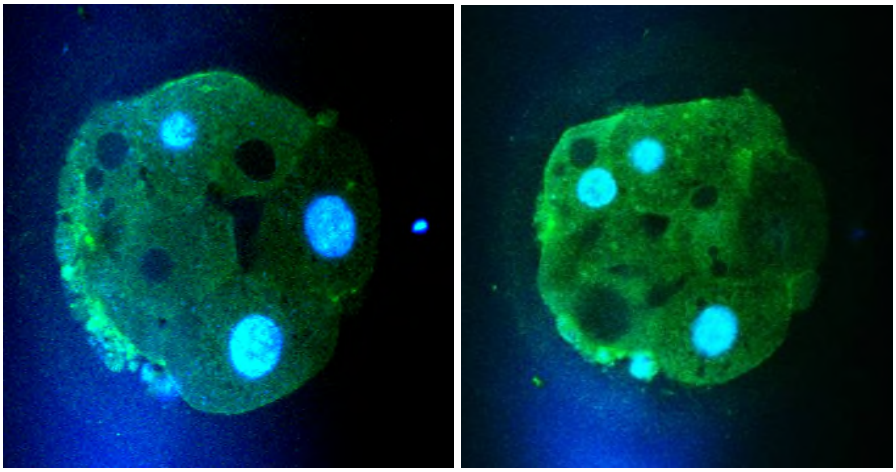

***Figure 4.4: Confocal images showing actin distribution in a compacting day 4 fresh embryo. There is actin fluorescence seen at the periphery and junctions between cells. The differences in image intensity are due to the focal z-plane***

Figure 4.5 shows day six fresh blastocysts at varying degrees of expansion. Actin staining is most intense at the junctions between cells but is variable from cell to cell. This is noticeable in both the trophectoderm and the inner cell mass.

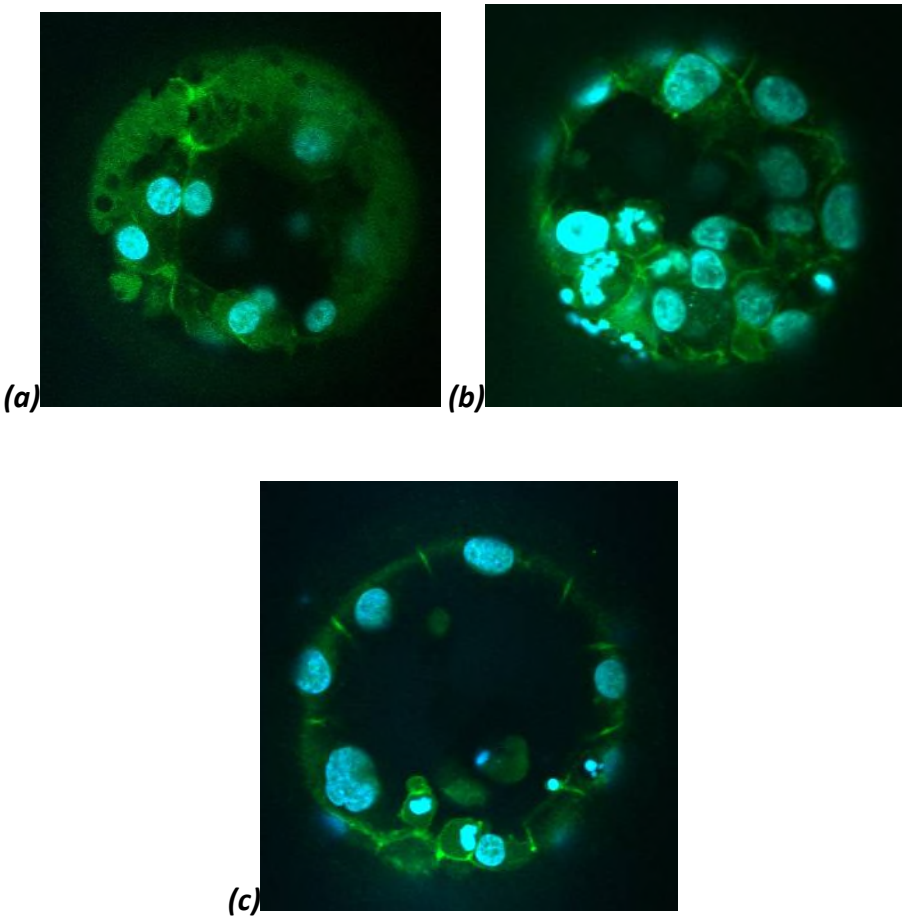


***Figure 4.5: Confocal images showing actin borders around individual cells of the trophectoderm and inner cell mass of (a) a day 6 fresh early blastocyst (b) a day 6 fresh 1CC grade blastocyst, and (c) a day 6 fresh hatching blastocyst***

The variability of actin staining and the lack of consistent findings even within embryos of apparently similar morphology, did not allow it to be used as a reliable cell surface marker for modelling purposes, nor did it have any potential as a useful viability marker in embryos.

### *4.4.2 Leptin, STAT3 and pSTAT3 distribution*

A total of 121 oocytes and human preimplantation embryos were fluorescently labelled in order to visualise the regulatory proteins leptin, STAT3 and pSTAT3, as described in section 2.11.2.

Fluorescently labelled cleavage stage embryos were analysed to investigate whether there were differing levels of leptin and STAT3 between individual cells. However, since the analysis was deemed to be incorrectly executed, these results have not been included in this chapter.

***Distribution of leptin in unfertilised oocytes***

Leptin distribution was measured in mature oocytes that had been exposed to spermatozoa, but had failed to fertilise, herein referred to as 0PNs. The fluorescence intensity of the leptin staining was determined at the periphery and centre of the 0PNs, and near and opposite the polar body using Image J software, as described in section 2.13. The results are shown in figure 4.6. There was a significantly higher level of leptin staining at the periphery of the 0PNs compared to the central area ($p=0.001$; Student's t-test). There was no difference in the distribution of leptin near and opposite the polar body.

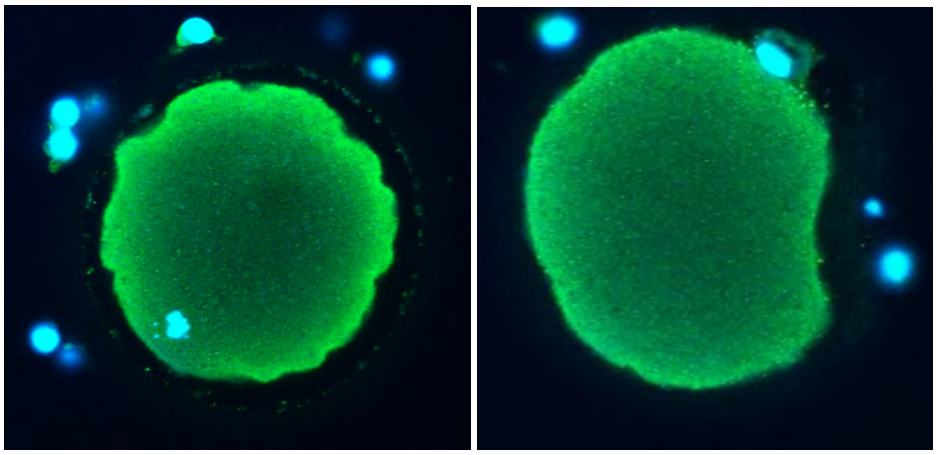

***Figure 4.6: Distribution of leptin at the periphery versus the centre, and beneath the polar body versus opposite the polar body in unfertilised mature oocytes. There is a distinct pattern of leptin distribution between the periphery and centre of the 0PNs, but no discernible difference between the region under the polar body versus the area directly opposite the polar body***

***Distribution of leptin in cleavage stage embryos***

Leptin distribution within the cell was assessed by measuring the fluorescence intensity at the periphery and the perinuclear region of each individual cell. The results show generally higher expression of leptin at the periphery of each cell in comparison to the perinuclear region, as summarised in figure 4.7.

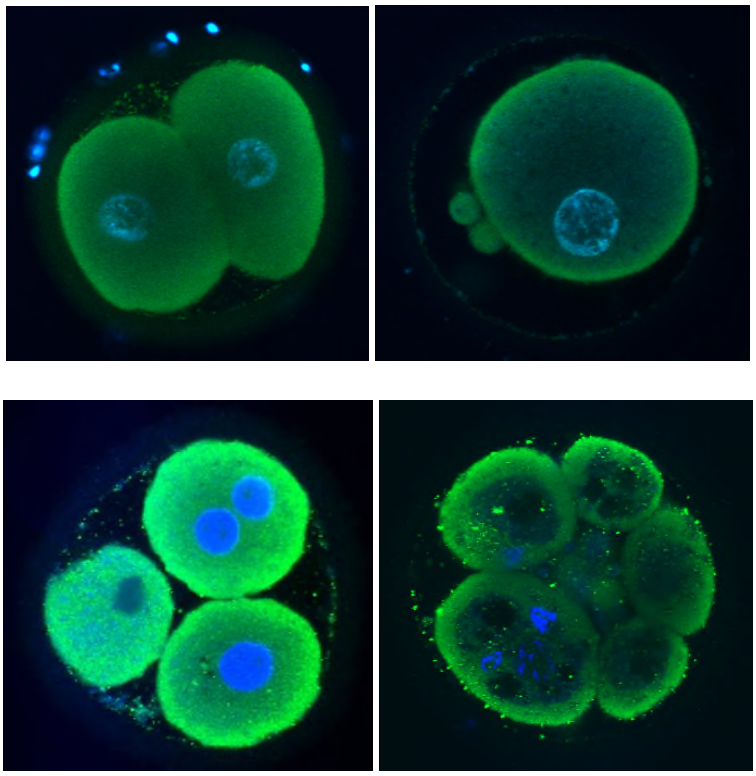

***Figure 4.7: Intracellular leptin distribution in cleavage stage embryos. There is evidence of higher leptin levels at the edge of each cell in comparison to the perinuclear region***

***Distribution of leptin in blastocysts***

Leptin was measured in the inner cell mass and the trophectoderm cells using Image J, to establish whether there was a differential distribution between the two cell populations. The images, as demonstrated in figure 4.8 (a) and (b), show a trend towards higher levels of leptin in the trophectoderm compared to the inner cell mass, although this is not true for all blastocysts, as seen in figure 4.8 (c).

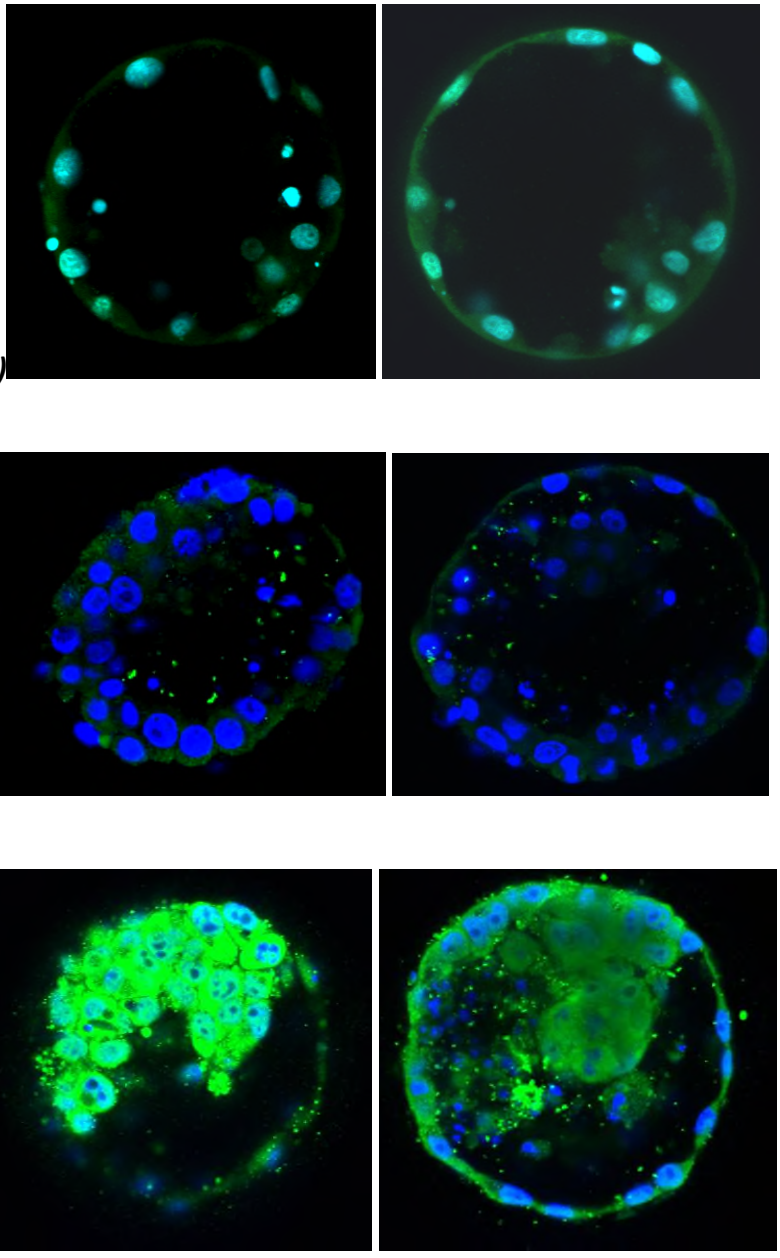


***Figure 4.8: Confocal images showing examples of the distribution of leptin (green) in (a) day 6 fresh 2BB (b) day 7 fresh 4CC (c) day 7 fresh 2CC blastocysts***

The results are summarised in graphical form in figure 4.9. There does not appear to be a link between expansion status or blastocyst quality and leptin expression levels.

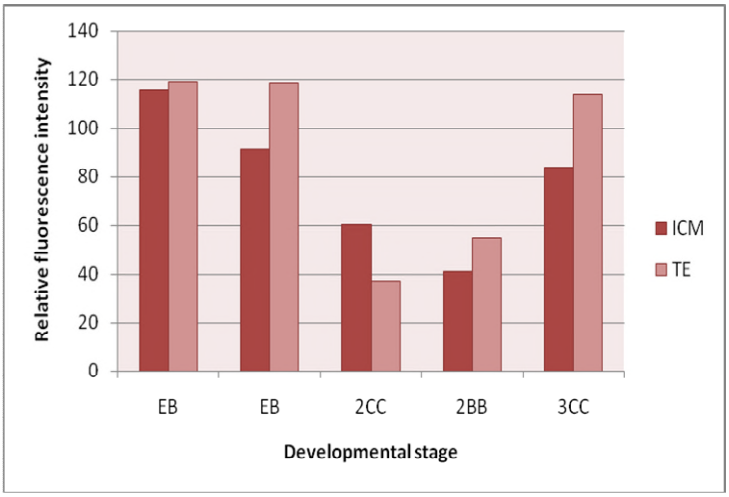


***Figure 4.9: The distribution of leptin in the inner cell mass relative to the trophectoderm in blastocysts of varying degrees of expansion and quality. Whilst there was a trend towards higher levels of leptin in the TE compared to the ICM, there were no significant differences and no correlation between leptin distribution and the stage of development***

***Distribution of STAT3 in unfertilised oocytes***

STAT3 distribution at the periphery and the centre of unfertilised mature oocytes (0PNs) was determined to establish whether there was a differential distribution of STAT3 within the cytoplasm of oocytes exposed to spermatozoa, but which failed to fertilise. There appeared to be higher levels of STAT3 at the periphery of 0PNs in comparison to the central region, similar to leptin distribution, however, these differences were not significant. Also similar to leptin, there was no apparent difference in STAT3 levels directly beneath the polar body compared to the region directly opposite the polar body in 0PNs. These results are summarised in figure 4.10.

*(a)* 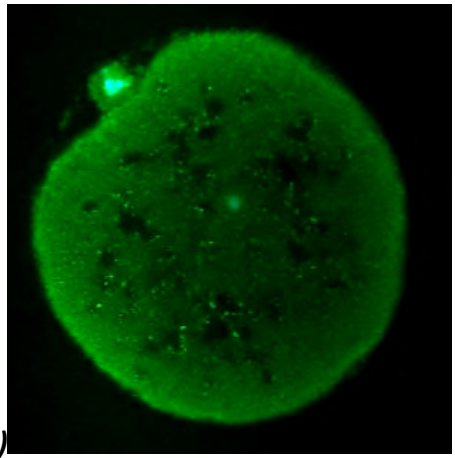 *(b)* 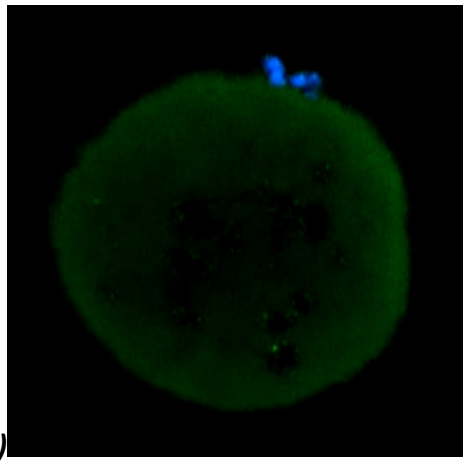

***Figure 4.10: Distribution of STAT3 at the periphery versus the centre, and beneath the polar body as compared to opposite the polar body in unfertilised mature oocytes (a) (b). There appeared to be more STAT3 at the periphery compared to the centre of the 0PNs, however these differences were insignificant. There was no discernible difference between the region under the polar body and the area directly opposite the polar body***

***Distribution of STAT3 in cleavage stage embryos***

STAT3 distribution was determined intracellularly by measuring the fluorescence intensity at the periphery (edge) and the perinuclear region of each individual cell. In contrast to leptin distribution in cleavage stage embryos, there was a trend towards higher levels of STAT3 at the perinuclear region of the cell in comparison to the periphery of the cell in some embryos, as summarised in figure 4.11.

***(a)*** 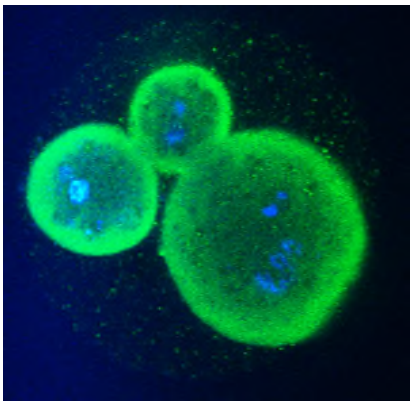 ***(b)*** 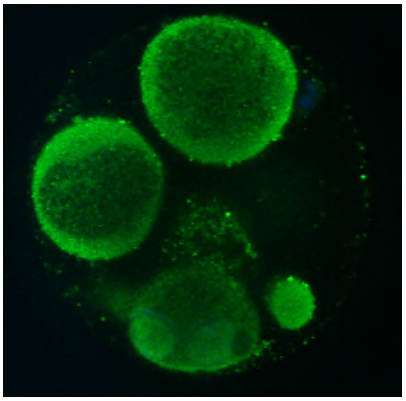

***Figure 4.11: Cleavage stage embryos fluorescently labelled to identify the distribution of STAT3 between individual cells (a) day seven fresh 5 cell (b) day seven fresh 5 cell***

***Distribution of STAT3 in blastocysts***

Blastocysts labelled with anti-STAT3 antibodies (see figure 4.12) were assessed to determine whether there was a differential distribution of STAT3 between the inner cell mass and the trophectoderm. There was a non-significant trend towards higher expression of STAT3 in the ICM compared to the TE cells, which was in contrast to the distribution of leptin in blastocysts.

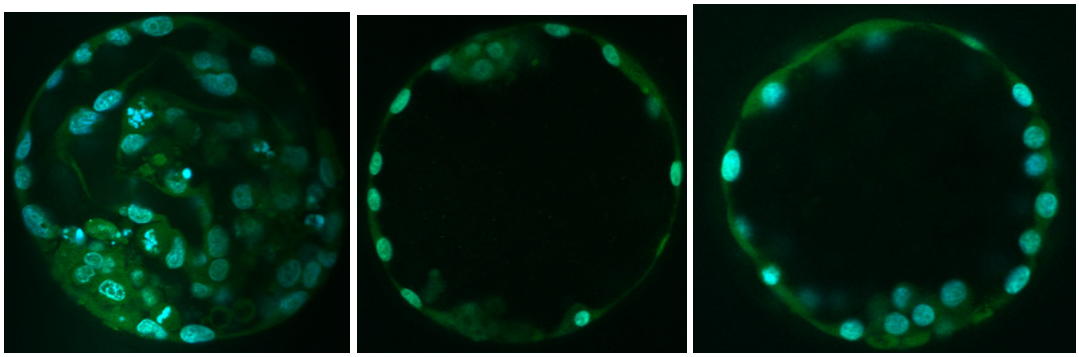

***Figure 4.12: Confocal images of blastocysts of varying degrees of expansion and quality fluorescently labelled for STAT3 (green). There was a trend for higher levels of STAT3 in the ICM compared to the TE, although the differences were not significant, and there was no apparent relationship between STAT3 distribution and the stage of development***

The results are summarised in graphical form in figure 4.13. There does not appear to be a link between expansion status or blastocyst quality and STAT3 expression levels.

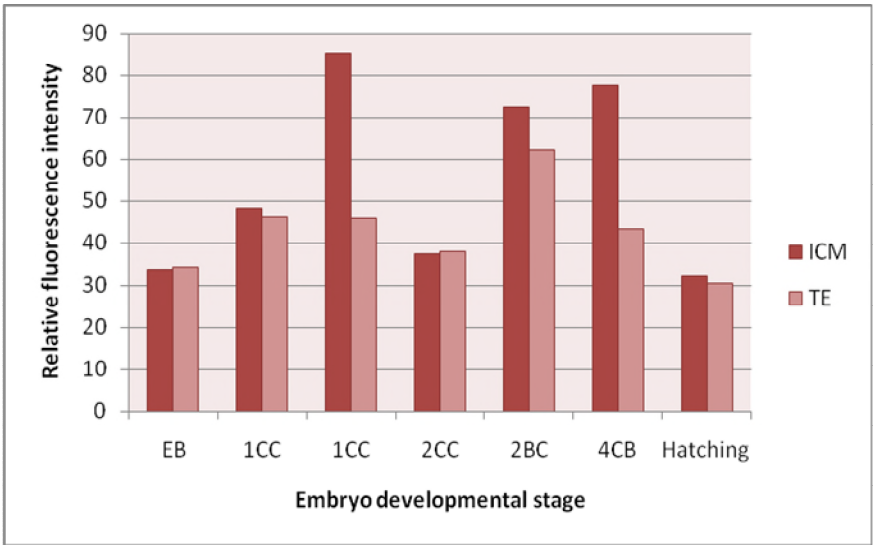


***Figure 4.13: The distribution of STAT3 in the inner cell mass relative to the trophectoderm in blastocysts of varying degrees of expansion and quality. Whilst there was a trend towards higher levels of STAT3 in the ICM compared to the TE, there were no significant differences and no correlation between STAT3 distribution and the stage of development***

***Distribution of pSTAT3 in unfertilised oocytes and cleavage stage embryos***

pSTAT3 distribution at the periphery and the centre of mature unfertilised oocytes (0PNs), and at the periphery and in the perinuclear region of cleavage stage embryo blastomeres was determined to establish whether there was a differential distribution of cytoplasmic pSTAT3. There was no distinct pattern of distribution between the regions, and levels of pSTAT3 were similar at all measured points. There was little staining of pSTAT3 in 0PNs or cleavage stage embryos. These results are summarised in figure 4.14.

*(a)*

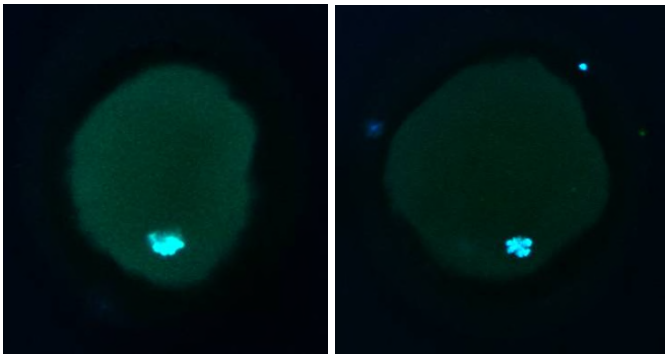

*(b)*

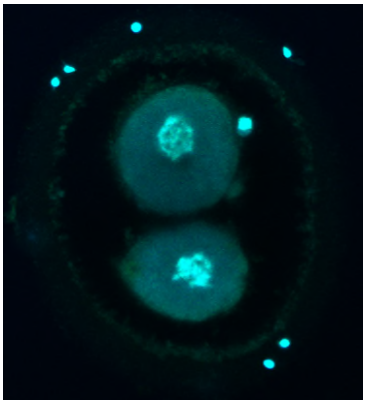

***Figure 4.14: The distribution of pSTAT3 at (a) the periphery and centre of 0PNs, or beneath the polar body versus opposite the polar body and (b) at the periphery and perinuclear regions of individual blastomeres. There was no discernible pattern of distribution, and the levels were generally similar at all measured points***

***Distribution of pSTAT3 in blastocysts***

Blastocysts of varying quality and at differing degrees of expansion were fluorescently labelled to determine whether there was a differential distribution of pSTAT3 in the inner cell mass versus the trophectoderm. Similar to the distribution pattern of non-phosphorylated STAT3, there was a trend towards higher levels of pSTAT3 in the ICM than the TE, although they were not significantly different. These results are summarised in figure 4.15.

***(a)*** 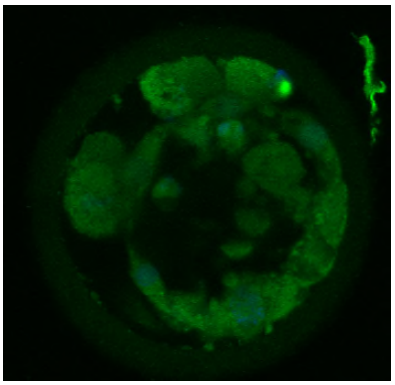 ***(b)*** 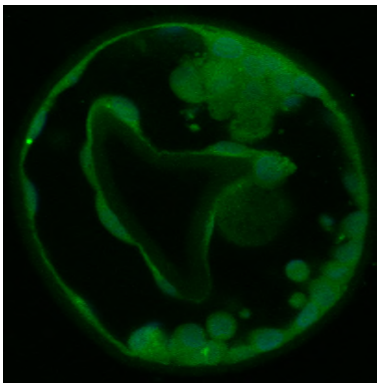

***(c)*** 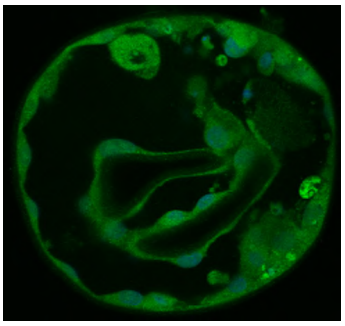

***Figure 4.15: Confocal images of (a) day 7 fresh 2DC blastocyst (b) day 6 fresh 1CC blastocyst (c) day 6 fresh 1CC blastocyst, fluorescently labelled for pSTAT3***

The results are summarised in graphical form in figure 4.16. There does not appear to be a link between expansion status or blastocyst quality and pSTAT3 expression levels.

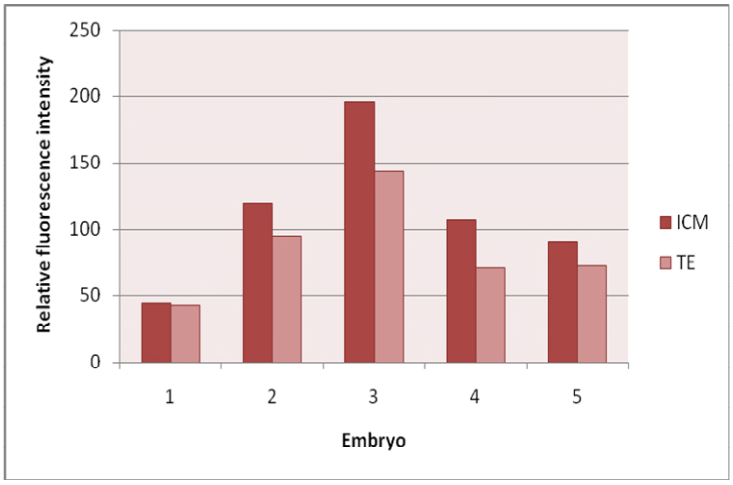


***Figure 4.16: The distribution of pSTAT3 in the inner cell mass relative to the trophectoderm in blastocysts of varying degrees of expansion and quality. Whilst there was a trend towards higher levels of pSTAT3 in the ICM compared to the TE, there were no significant differences and no correlation between pSTAT3 distribution and the stage of development***

***Negative controls***

To ensure that the labelling for leptin, STAT3 and pSTAT3 was specific, cleavage stage embryos and blastocysts were fluorescently stained using the same protocol as described in 2.11.2, but with the primary antibody step omitted. Examples of confocal images are shown in figure 4.17.

***(a)*** 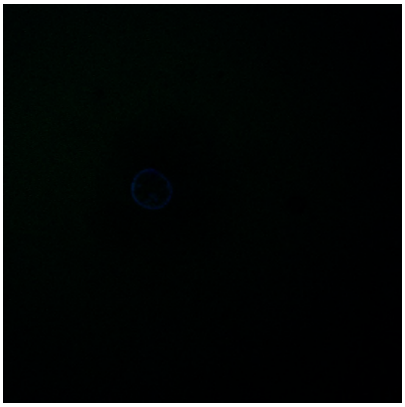 ***(b)*** 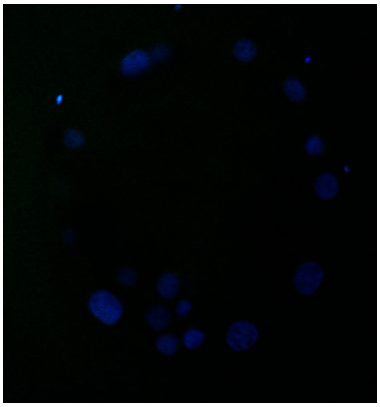

***Figure 4.17: Confocal images of (a) cleavage stage and (b) blastocyst stained with secondary antibody only, and mounted in DAPI media***

### *4.4.3 OCT-4 and JC-1 staining*

A small number of embryos and blastocysts were labelled with OCT-4 to investigate whether it was present in cells of the ICM and TE of blastocysts. An example is shown in figure 4.18 (a). Additionally, cleavage stage embryos were stained with JC-1 to assess the distribution of polarised mitochondria. An example is shown in figure 4.18 (b).

These experiments were discontinued, and the remaining fluorescence labelling work focussed on leptin, STAT3, and pSTAT3.

***(a)*** 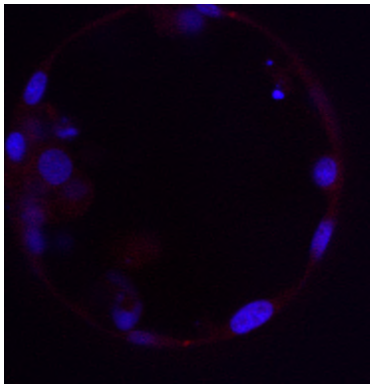 ***(b)*** 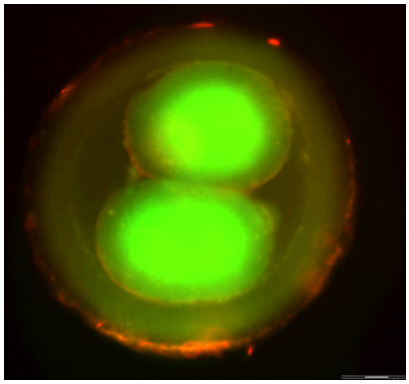

***Figure 4.18 (a) blastocyst labelled with OCT-4 antibodies and (b) a cleavage stage embryo labelled to detect mitochondrial distribution***

### *4.4.4 Free cells*

Approximately 38% of the blastocysts analysed in this study contained cells in the blastocoelic cavity that were not attached to the inner cell mass or the trophectoderm, herein referred to as free cells. Since they were most obviously visible in the confocal images of blastocysts fluorescently labelled with pSTAT3, the levels of pSTAT3 in free cells were measured in relation to the levels in the ICM and TE. The level of pSTAT3 in free cells was similar to those observed in the ICM cells of blastocysts, as summarised in figure 4.19. Additionally, time lapse image sequences indicate that free cells originate from the ICM of expanding blastocysts. Examples are shown in figure 4.20.

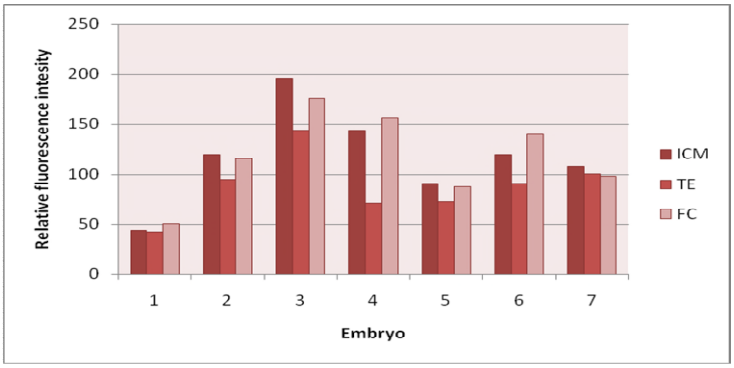


***Figure 4.19: Bar graph showing the relative fluorescence intensities of pSTAT3 staining in ICM, TE and free cells (FC). The ICM and FC have similar fluorescent staining profiles***

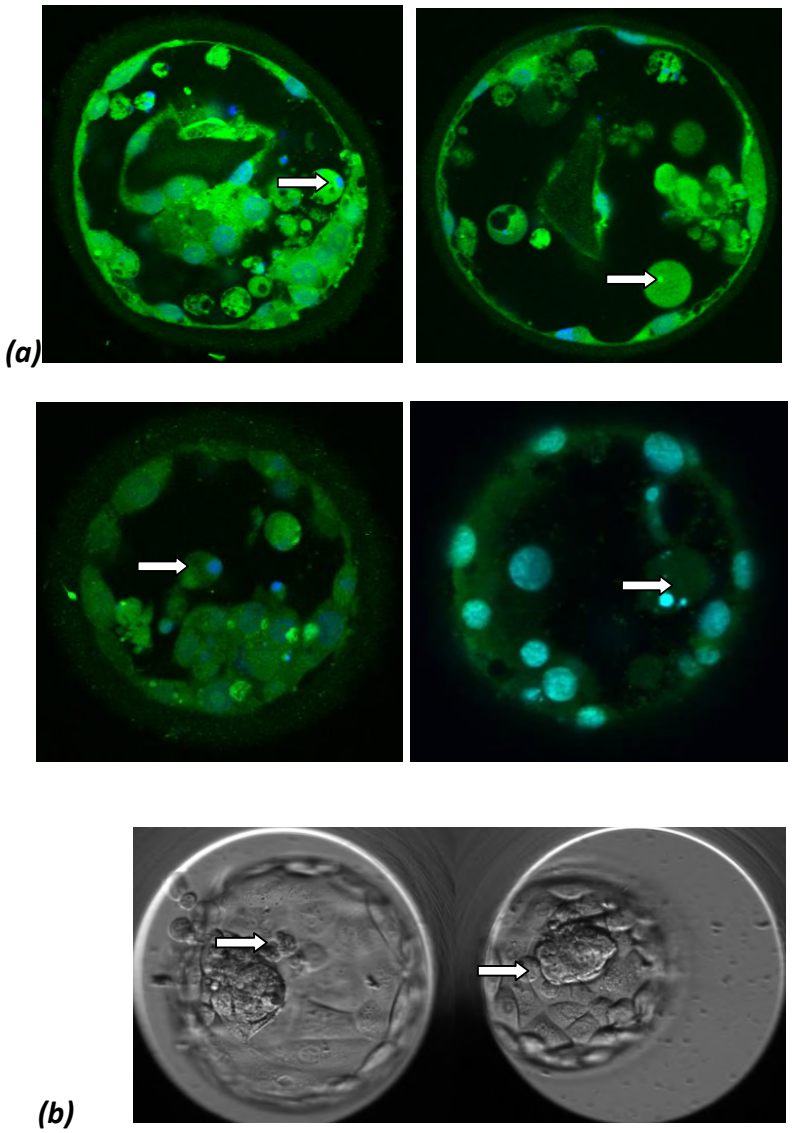


***Figure 4.20: (a) confocal images showing fluorescently labelled blastocysts with free cells in the blastocoelic cavity and (b) time lapse images showing the free cells originating from the ICM of live blastocysts. White arrows indicate location of free cells***

### *4.4.5 Excluded cells*

Excluded cells were observed in 36% of blastocysts analysed in this study, predominantly in the space between the trophectoderm and the *zona pellucida*, having been expelled outwards prior to or during expansion of the blastocyst. Occasionally excluded cells were seen in the blastocoelic cavity. Examples are shown in figure 4.21.

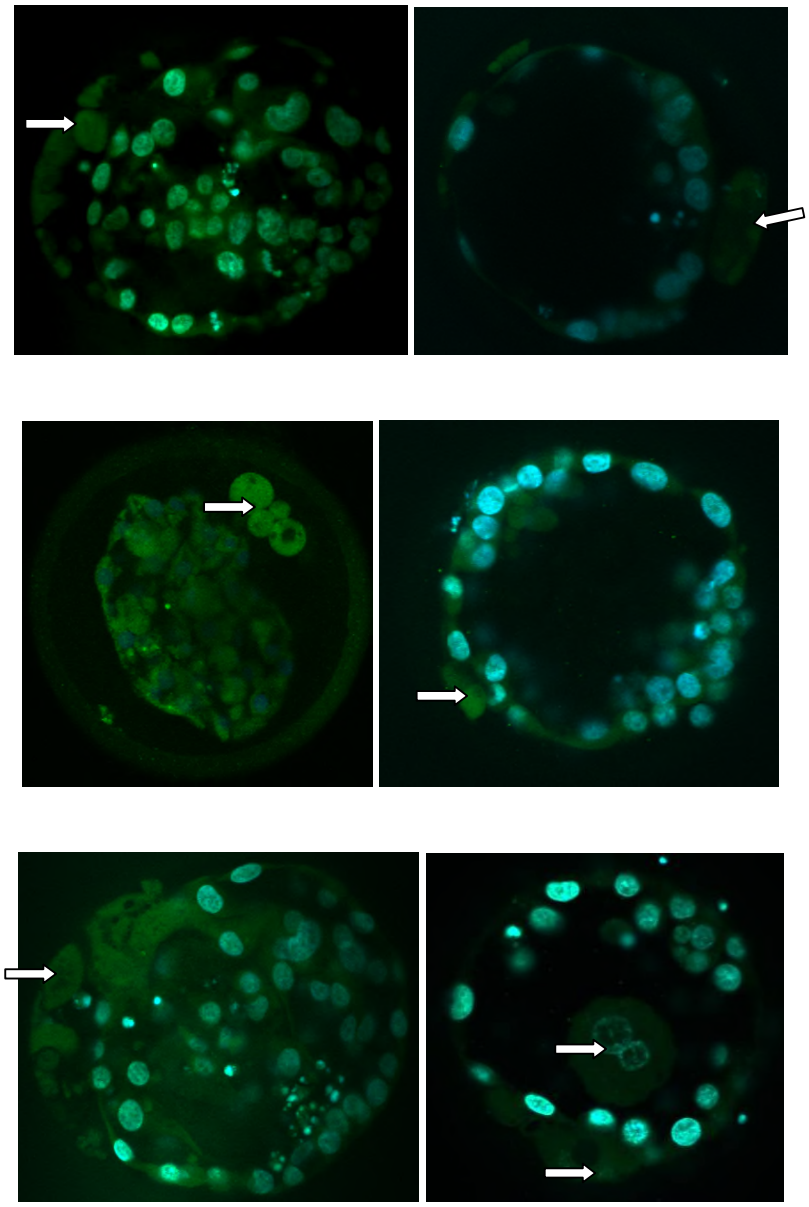

***Figure 4.21: Confocal images of fluorescently labelled blastocysts at varying degrees of expansion and quality showing cells extruded into the perivitelline space, or in one example, into the blastocoelic cavity. White arrows indicate location of extruded cells***

### *4.4.6 Cell numbers in blastocysts*

A total of 25 fresh and frozen-thawed blastocysts of varying degrees of expansion and quality were assessed for cell numbers in the ICM and the TE. The mean number of cells in the whole blastocyst was 118.76 (±48.73), in the ICM was 21.28 (±12.3) and in the TE was 97.48 (±41.0), so approximately one fifth of the cells in the blastocyst were allocated to the ICM. Figure 4.22(a) shows the number of cells in the ICM versus the TE in all blastocysts, and figure 4.22(b) shows the numbers of cells in the ICM versus the TE in day 5, day 6 and day 7 blastocysts. The results imply a decrease in the cell numbers of the ICM, the TE and the blastocyst as a whole from day 5 to day 7 post-insemination, however it is likely that this is an artefact of the material selected as available for research.

*(a)*

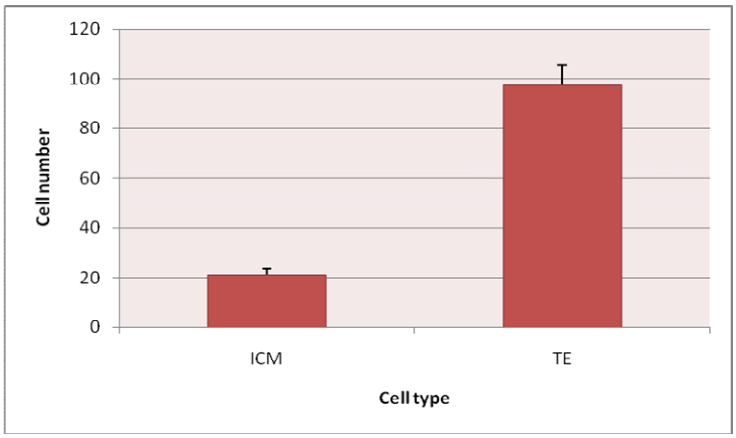


*(b)*

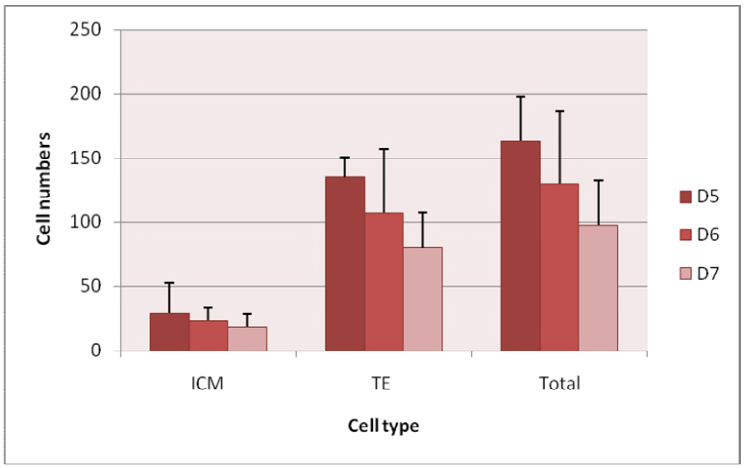


***Figure 4.22: (a) the number of cells in the ICM and the TE. Approximately one fifth of cells in the blastocyst were allocated to the ICM (b) the number of cells in the blastocyst according to day of culture post-insemination***

### *4.4.7 Cytoplasmic projections*

Approximately 30% of blastocysts in this study were observed to have cytoplasmic projections that tethered the inner cell mass to the polar TE and mural TE by traversing the blastocoelic cavity. Interestingly, these projections were more common in the morphologically better quality blastocysts. Examples are shown in figure 4.23.

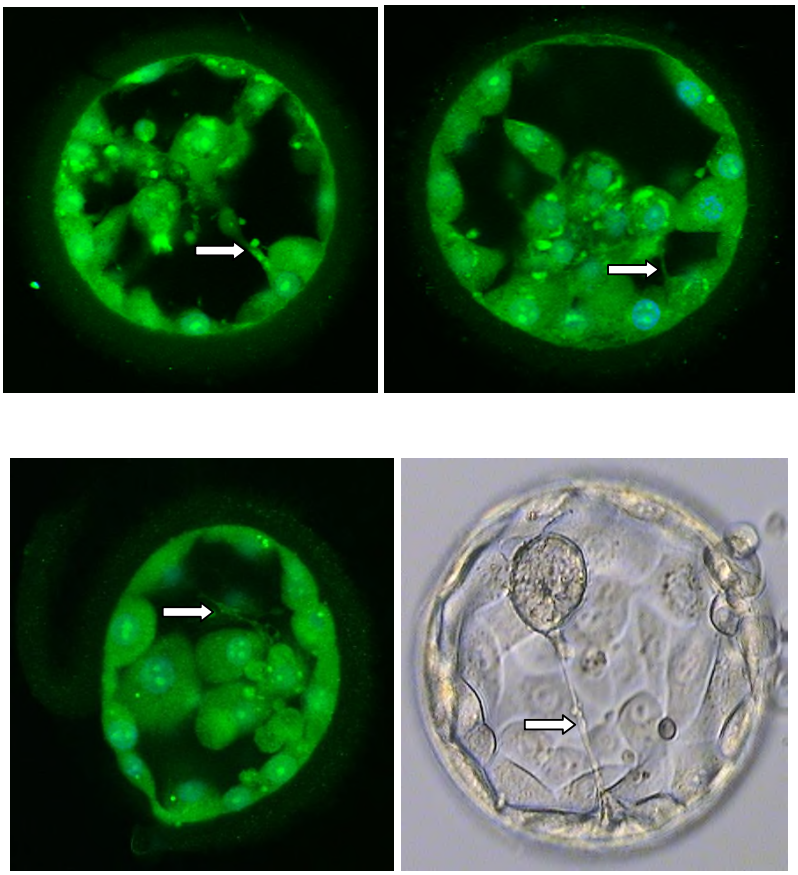

***Figure 4.23: Confocal (labelled green) and brightfield (greyscale) images of human blastocysts with cytoplasmic strings connecting the ICM to the TE. White arrows indicate location of cytoplamsic projections.***

### *4.4.8 Double ICM*

Double inner cell masses were observed in several blastocysts (~5%) labelled with fluorescent markers. Sometimes, the two ICMs were seen in entirely different planes, although in some blastocysts they were clearly visible within the same confocal plane. Examples of double ICMs are shown in figure 4.24.

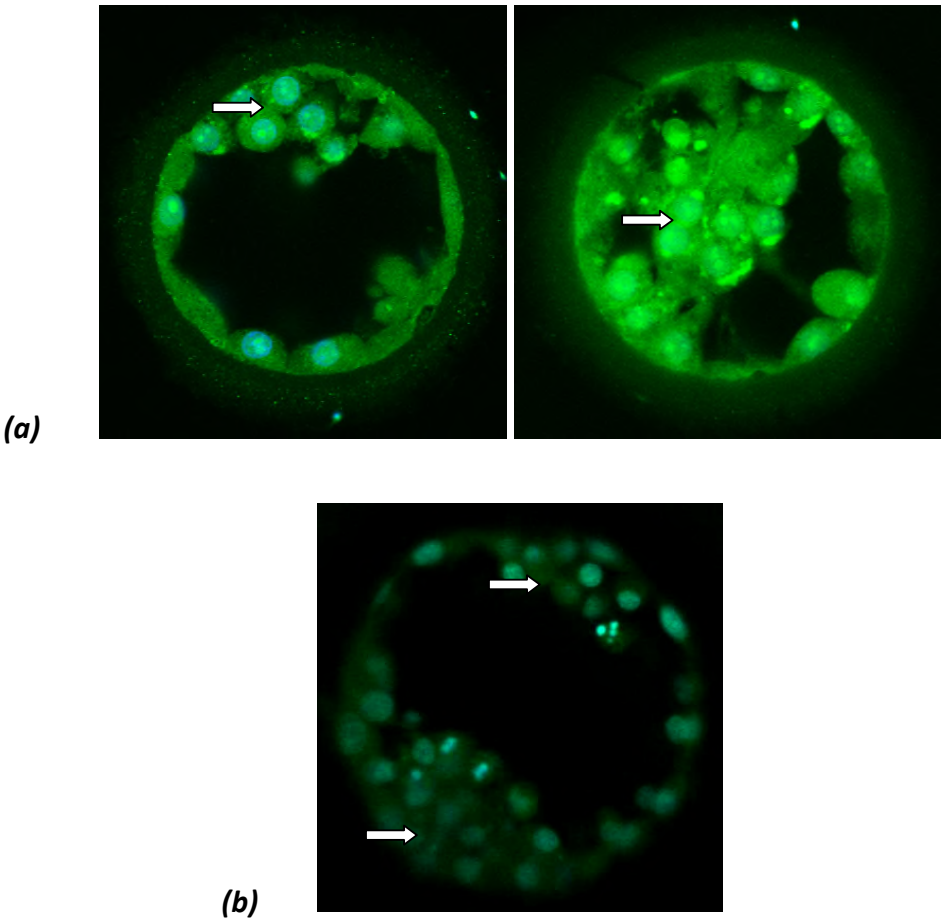

***(a)***

***(b)***

***Figure 4.24: Confocal images of fluorescently labelled blastocysts showing double inner cell masses. The ICMs are visible in two entirely different planes (a) or in the same plane (b). White arrows indicate location of ICM 1 and ICM 2***

### *4.4.9 Micronuclei and chromatin-containing fragments*

Micronuclei were observed in fresh and frozen cleavage stage embryos regardless of apparent morphological quality. Fragments containing chromatin were visible in fresh and frozen cleavage stage embryos and blastocysts. Examples are shown in figure 4.25.

***(a)*** 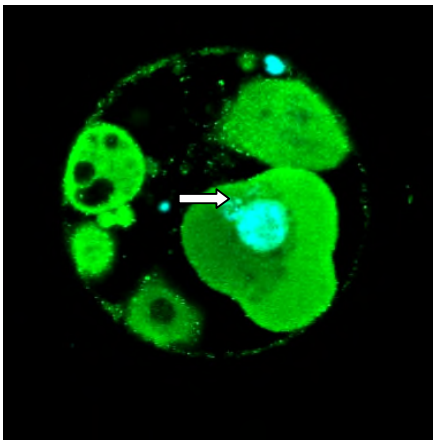 ***(b)*** 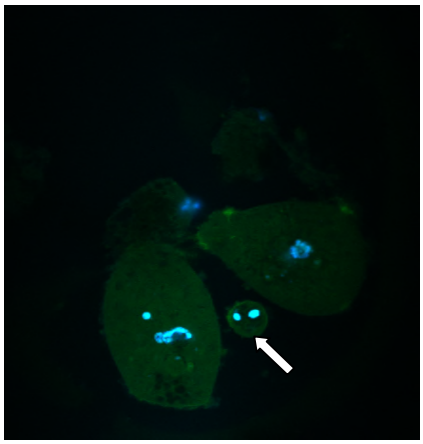

***Figure 4.25: Poor quality cleavage stage embryos with (a) micronucleus and (b) chromatin-containing fragments. White arrows indicate the locations of micronucleus and chromatin-containing fragment***

## *4.5 Discussion*

Many studies on the structure and function of the actin cytoskeleton have been conducted using the oocytes and embryos of several species, including chick (Sanger 1975), pig (Wang *et al* 1999), horse (Tharasanit *et al* 2005), *Caenorhabditis elegans* (Wang *et al* 2005), *Xenopus laevis* (Danilchik and Brown 2008), and mouse (Sanfins *et al* 2015), however studies using human gametes and embryos are scarce.

Actin has been identified in immature (germinal vesicle) and mature (metaphase II) human oocytes, and whilst mature oocytes have a highly organised cortically arranged actin framework with an intense accumulation at the spindle pole, immature oocytes do not, suggesting a role for actin in the extrusion of the first polar body upon progression to metaphase II (Coticchio *et al* 2014). One study of the cytoskeletal actin distribution in fresh and cryopreserved cleavage stage human embryos using fluorescence scanning confocal microscopy, showed that that the actin cortex in the blastomeres of good quality human preimplantation embryos was uniformly distributed, and that poor quality or degenerate embryos demonstrated a disorganised actin cortex, with irregular or completely disrupted cellular membranes (Levy *et al* 1998). A comparison of the developmental potential of *in vitro* versus *in vivo* matured mouse oocytes determined that fertilisation rate, synchronous cleavage, and blastocyst development were adversely affected by *in vitro* maturation. The cleavage of embryos critically depends upon the stable association of blastomeres and failure of their adherence during compaction can result in developmental defects (Danilchik and Brown 2008). Studies of the

structural changes associated with expected human preimplantation embryo development show a pronounced cellular compaction around four days post-insemination, evidenced by the flattening of blastomeres against one another. Non-compacted cells were also frequently present in these embryos (Nikas et al 1996). Furthermore, the cytoplasmic strings, or filopodia, seen connecting the ICM to the TE in the early and expanded blastocyst of the mouse, were confirmed to contain actin (Salas-Vidal and Lomeli 2004).

The results in this study tend to confirm these findings, as poor quality cleavage stage embryos displayed disorganised actin cytoskeletons around the blastomeres and the nuclei. The ability of an embryo to cleave in a regular fashion may be impaired by poor actin structure, thus resulting in unequal sized cells and the inability to compact effectively, impeding the development of the embryo to the blastocyst stage. Conversely, those embryos with well organised actin matrices, are able to cleave evenly, compact efficiently, and expand into blastocysts based upon the actions of their cytoskeletal proteins. However, actin was not found to be sufficiently clearly and reliably localised to use as a cell edge marker for modelling of embryos in 3D, or for use as a quality indicator, so no further work on this protein was undertaken in this thesis. Instead focus was shifted to leptin and STAT3, given reports of their polarised distribution which may have functional correlates in development.

Previously, STAT3 and leptin have been reported to be co-localised in mouse and human oocytes and cleavage stage embryos (Antzcak and Ven Blerkom, 1997), however in this work, STAT3 and leptin appear to be co-localised only in human

oocytes. In embryos there appeared to be no consistent co-localised distribution pattern, and in blastocysts STAT3 and leptin were localised to regions to differing extents. Interestingly, STAT3 was repeatedly more concentrated at perinuclear regions in cleavage stage embryos and blastocysts. This may be because STAT3 translocates to the nucleus after activation to enable targeted gene transcription, and therefore may be located nearer to the nucleus in readiness for rapid movement. Alternatively, this could be an artefact of STAT3 having recently translocated out of the nucleus after deactivation.

Consistent, but non-significantly, higher levels of STAT3 and pSTAT3 in the ICM compared to the TE as observed in the blastocysts analysed here may emphasise the role of STAT3 in implantation. *In utero*, the blastocyst is positioned with the ICM orientated towards the endometrium in readiness for attachment and invasion of the trophoblast, which is a prerequisite for implantation (Weimar *et al* 2013). Human studies of implantation are scarce due to the practical difficulties of obtaining human endometrium and embryos, however the relationship between STAT3 and implantation in murine models has been extensively investigated. Ablation of STAT3 in the uterine epithelium of mice resulted in total implantation failure due to an inability of the blastocyst to attach to the endometrium, and demonstrates that STAT3 is critical in the process of implantation (Pawar *et al* 2013; Sun *et al* 2013), whilst dysregulation of the LIF- STAT3 pathway via induction of diabetes in mice resulted in a significant reduction in implantation (Wang *et al* 2015).

The majority of fresh embryos used in the fluorescent staining experiments in this project were arrested or poor quality, since they were surplus to patient treatment requirements and therefore unsuitable for transfer or cryopreservation. This may have had an effect on the distribution of markers previously found to be polarised in human oocytes and embryos, and may not be representative of normally developing, good quality human embryos. Conversely, the non-polar distribution of the identified proteins may in part explain the arrest or poor quality of the embryos shown here, as abnormal development is known to be related to aberrant cleavage and unequal division of cytoplasm in daughter cells (Prados *et al* 2012).

Free cells, which were seen exclusively in the fluid-filled cavity of expanding blastocysts, had a non-degenerate appearance and a uniform shape. The observation that free cells have a similar pSTAT3 staining profile to cells of the ICM, and that they were observed being expelled from the ICM in time lapse image sequences, suggests that they may originate from the ICM. Excluded cells were observed in 36% of blastocysts analysed in this study, most often identified as degenerating cells expelled outwards into the perivitelline space between the embryo proper and the ZP prior to the commencement of cavitation. Occasionally, large multi-nucleated cells were observed in the blastocoelic cavity. It is possible that excluded cells and free cells are left out of the developing embryo as a result of an innate corrective mechanism, to ensure that abnormal cells are not included in the fully expanded blastocyst, and therefore are not part of the implanting embryo. This theory is supported by a previous publication, where chromosomal

abnormalities were found to exist in 38.8% of good quality human blastocysts (Fragouli *et al* 2008).

The proportion of cells allocated to the ICM and the TE were similar to previous reports, with approximately one fifth of cells in the blastocyst allocated to the ICM, however, the total number and the proliferation of the ICM and TE cells over time differed to previously published results (Hardy *et al* 1989). In this study the mean number of cells in the ICM was 28.33 (±24.21) on day 5, 23.1 (±10.73) on day 6, and 18 (±9.9) on day 7. The TE contained on average 135.33 (±15.9) on day 5, 107.3 (±50) on day 6, and 79.83 (±27.6) on day 7. This is in contrast to previously published results, where the ICM reportedly contained an average of 20 (±4) on day 5, 41.9 (±5) on day 6, and 46 (±10.2) on day 7, and the TE contained an average of 37.9 (±6) on day 5 to 80.6 (±15.2) on day 7 (Hardy *et al* 1989). In this study the total mean number of cells in fully expanded blastocysts was 163.7 (±33.8) on day 5, 130.4 (±56.3) on day 6, and 97.8 (± 35) on day 7, whereby in the reference report, the blastocyst as a whole contained 58.3 (±8.1) cells on day 5, 82.2 (±7.8) on day 6, and 126.2 (±21) on day 7 (Hardy *et al* 1989). The differences in cell number over time may be explained by the improvements in the techniques and culture systems used for blastocyst culture during recent years, with a general acceptance that day 5 is the optimal day of blastocyst expansion in modern clinical embryology laboratories (Gardner *et al* 1998). More rapid development of larger numbers of cells by day 5 might be expected in response to improvements in culture media over the years between the two studies. The results in this study also concur with a previous report on the developmental behaviour of cells in mouse blastocysts,

where the proliferative ability of TE cells during development of the early blastocyst depends on interaction with the cells of the ICM, and declines following the migration of the polar TE to the side of the blastocoelic cavity furthest away from the ICM, the so-called mural region (Copp, 1978). This may explain the declining TE cell numbers in the human blastocysts studied here.

The cytoplasmic projections connecting the cells of the ICM to both the mural and polar TE in the blastocysts in this study have previously been observed in around 40% of *in vivo* derived mouse blastocysts, where those projections traversing the fluid-filled cavity of the blastocoels were purported to aid in the continued division of TE cells following their migration to the abembryonic pole via a direct communication mechanism (Salas-Vidal and Lomeli 2004). This is a similar percentage to those seen in the human blastocysts in this project (~30%), however cytoplasmic projections were noted in the majority of *in vitro* cultured mouse blastocysts, suggesting that *in vitro* culture may have a stabilising influence on their structure. In the mouse, the assembly of these structures was apparently actively maintained in the increasingly expanding blastocyst, as observed using time lapse imaging, suggesting that they have a function, perhaps in enabling mural TE cells to continue to divide when necessary, despite their distance from the ICM (Salas-Vidal and Lomeli 2004). Interestingly in this study, the majority of blastocysts that had cytoplasmic projections from the ICM to the TE were of superior morphological quality, and therefore despite previous assumptions that cytoplasmic “strings” are indicative of reduced viability (Scott 2000), it is possible that these blastocoel-traversing structures are in fact an indicator of increased implantation potential.

Further research to investigate the clinical pregnancy rate following transfer of blastocysts containing cytoplasmic strings is needed in order to clarify this.

Higher order gestations are commonly associated with *in vitro* fertilisation, most notably due to the practice of replacing more than one embryo at the time of transfer. In recent years, the HFEA has produced guidelines on the acceptable percentage of multiple pregnancies resulting from fertility treatments with the introduction of the Multiple Births Minimisation Strategy (HFEA, 2009) and consequently, there have been moves to limit the numbers of embryos transferred simultaneously. The incidence of monozygotic (MZ) twinning resulting from transfer of a single embryo in IVF has been reported as approximately 1.1% to 2.3%, whereas monozygotic twins occur naturally in around 0.4% of pregnancies (Vaughan *et al* 2016; Aston *et al* 2008). This may indicate an increasing incidence of MZ twins after IVF, however, not all clinics report similar data and an effect of certain combinations of culture media and laboratory and clinical protocols may be one explanation. The mechanism by which MZ twinning occurs is not well defined, although the most likely reason is thought to be via the splitting of the ICM or the formation of two ICMs in the blastocyst (Saito *et al* 2000). Alternatively, double ICMs may result from the continuation of cell division at the mural TE via cytoplasmic projections. There are four types of MZ twinning, defined by the developmental stage at which the embryo splits. Type II occurs where the ICM divides during day 4-8 of development, and is the most commonly occurring (Hogenson 2013). Extended embryo culture beyond 4 days post-insemination and PGD following blastomere biopsy are reported to be risk factors for MZ twinning

(Vaughan *et al* 2016). In the work presented here, double ICMs were observed in a small proportion of human blastocysts (~5%), at a rate similar to that reported in murine blastocysts (Chida *et al* 1990). Since these blastocysts were fixed and/or not transferred, it is not known whether the presence of a double ICM would necessarily result in a monozygotic twin pregnancy, and it would be unethical to transfer double ICM blastocysts actively in order to confirm whether this is indeed the case, since MZ twins have higher risks for both mother and babies than other pregnancies. It would seem sensible, therefore, to avoid selecting blastocysts with an obvious double ICM for transfer to the uterine cavity during ART procedures, unless no other suitable options were available.

The appearance of micronuclei and chromosome-containing fragments has previously been reported. These are thought to reflect the aneuploid status of many human preimplantation embryos (Chavez *et al* 2012). The authors hypothesised that missing chromosomes in the developing embryo may have been contained within fragments during cleavage, and that these distinct fragments originated from micronuclei (Chavez *et al* 2012). Blastomeres containing micronuclei have also been reported in mosaic human embryos, and their presence is deemed to be a mechanism of mitotic aneuploidy generation which may result in the arrested development of preimplantation human embryos (Kort *et al* 2015). Indeed, the embryos in this study which were found to contain micronuclei and chromatin-containing fragments were generally of poor quality and had arrested in their development at the cleavage stage. It may therefore be prudent to avoid selecting cleavage stage embryos exhibiting such characteristics for uterine transfer

due to the significantly increased risk of aneuploidy, and the known association with poor implantation potential (Kort *et al* 2015).

# Chapter Five

## Investigating the possible role of STAT3 activation in human embryo-endometrial communication

# Chapter Five

# Investigating the possible role of STAT3 activation in human embryo-endometrial communication

## *5.1 Introduction*

Leptin, the product of the *obese (ob)* gene, is a 16-kDa non-glycosylated regulatory peptide hormone synthesised by several cell types, including adipose tissue (Zhang *et al* 1994) and human placenta (Senaris *et al* 1997). Leptin is known to regulate body weight by increasing energy expenditure and decreasing appetite (Messinis and Milingos 1999), and has roles in reproductive function (Cervero *et al* 2005) and early embryo development (Kawamura *et al* 2002). Leptin deficient *ob/ob* mice are sterile due to a point mutation in the *ob* gene, rendering them incapable of synthesising functional leptin (Zhang *et al* 1994), and resulting in complete lack of circulating leptin (Malik *et al* 2001). Interestingly, administration of human recombinant leptin to sterile homozygous *ob/ob* female mice can correct their infertility (Chehab *et al* 1996), and withdrawal of exogenous leptin treatment following detection of the copulatory plug in *ob/ob* mice does not have an adverse affect on implantation or foetal growth (Mounzih *et al* 1998). Leptin is secreted by human blastocysts, and is present in human midsecretory endometrium (Gonzalez *et al* 2000), and pre-ovulatory human follicular fluid (Cioffi *et al* 1997).

Leptin binds to specific receptors (OB-R) on the cell membrane, which may be of the long or short form (Tartaglia 1997). Both variants are present in the human

endometrium (Kitawaki *et al* 2000), granulosa cells and cumulus oophorus complexes (Cioffi *et al* 1997). The long form of leptin receptor ($OB\text{-}R_L$) is reported to possess signalling capacity (Ghilardi and Skoda 1997; Wang *et al* 1997), in contrast to its truncated isoforms which lack the intracellular domain (Campfield *et al* 1996; Ghilardi and Skoda 1997). Leptin receptor mRNA is expressed in the human ovary (Karlsson *et al* 1997), granulosa and cumulus cells (Cioffi *et al* 1997), suggesting a role for leptin in reproductive function. The expression of leptin receptor mRNA in human endometrium peaks during the early secretory phase (Kitawaki *et al* 2000), and is also expressed in human mid secretory phase endometrium, which is the time when implantation occurs (Gonzalez *et al* 2000), suggesting that leptin may have a possible role in endometrial-blastocyst interaction and early human development.

Leptin is known to be an activator of STAT3, during which Janus kinases catalyse the phosphorylation of cytoplasmic STAT3 via the receptor-mediated Jak/STAT signalling pathway, forming homo- and/or heterodimers which translocate to the nucleus and activate transcription of target genes (Duncan *et al* 1997). STAT3 is implicated in successful apposition, adhesion and penetration of the luminal epithelium by the trophoblast of the hatched blastocyst in rodents and humans (Cheng *et al* 2001). High levels of STAT3 in the glandular and luminal epithelium, and phosphorylated STAT3 (pSTAT3) in the luminal epithelium were detected in mice during peri-implantation on day four of pregnancy. Furthermore, strong p-STAT3 staining was observed in the luminal epithelium and in the stroma surrounding the blastocyst at the site of implantation on day five, suggesting that

STAT3 has some involvement in the establishment of early pregnancy in mice (Teng *et al* 2004). Activation of STAT3 in mouse endometrium occurs only during the implantation window on day 4 post-fertilisation (Cheng *et al* 2001), and moreover, inhibition of STAT3 activation in murine endometrium significantly reduces implantation rates (Catalano *et al* 2005). Unexplained infertility refers to the ~30% of couples who are unable to conceive, but whose fertility investigations reveal no obvious abnormality in either partner (Evers 2002). Interestingly, significantly lower levels of p-STAT3 have been reported in the glandular epithelial endometrium of infertile women with unexplained infertility (Dimitriadis *et al* 2007). Couples with diagnosed male factor infertility were excluded from the study, whilst all female participants had regular menstrual cycles, and no evidence of endometriosis, anovulation, or tubal defects, thus increasing the possibility that the cause of the subfertility may be related to oocyte and embryo developmental factors or endometrial dysfunction, and reinforcing the possibility of a role for activated STAT3 (pSTAT3) in the acquisition of uterine receptivity (Dimitriadis *et al* 2007). Activated STAT3 has also been observed in the trophectoderm and inner cell mass of mouse blastocysts, and in the cell membrane of blastocysts that have been exposed to leptin (Fedorcsak and Storeng 2003), and has been detected in endometrial tissues proximal to the blastocyst implantation site in mice (Teng *et al* 2004), reinforcing the potential role of pSTAT3 in implantation.

## *5.2 Aims*

The aim of this work was to establish whether STAT3 activation may represent a mechanism by which the embryo and endometrium communicate at implantation. Human recombinant leptin protein was tested as a potential medium supplement to promote the activation of STAT3 in human preimplantation blastocysts, and the optimal time of exposure to leptin protein in order to activate STAT3 was determined. The ICM and TE cells were compared in terms of their responses to leptin, and different expression patterns in the nucleus versus the cytoplasm were analysed. The presence of leptin receptor mRNA on human blastocysts was then investigated in order to determine whether the leptin system plays a role in the activation of STAT3. Finally, the interaction between embryos and Ishikawa cells, as a model of the endometrial epithelium, was tested using exposure to spent culture media.

## *5.3 Methods*

Thirteen blastocysts were fixed and stained with anti-pSTAT3 antibodies without exposure to human recombinant leptin protein, and fourteen blastocysts were fixed and stained with anti-pSTAT3 antibodies following exposure to human recombinant leptin protein for 10 minutes, 20 minutes, 30 minutes or 24 hours, as described in section 2.17. Two blastocysts were cultured with stromal cell-enriched medium, and two blastocysts were cultured with Ishikawa cell-enriched medium, and labelled with anti-pSTAT3 antibodies after fixation, as described in section 2.20. All fixed and labelled embryos were imaged using confocal microscopy with standardised

settings, as described in section 2.12. Relative fluorescence intensities were measured using Image J with techniques validated using positive and negative controls, as described in section 2.13.

Two normally fertilised zygotes, two cleavage stage embryos and two blastocysts were subjected to qRT-PCR to detect the presence of long-form leptin receptor mRNA, and two oocytes, two normally fertilised zygotes, two cleavage stage embryos and two blastocysts were subjected to qRT-PCR for the detection of SUMO mRNA, as described in section 2.18.

## *5.4 Results*

### *5.4.1 Activated STAT3 distribution in human embryos not exposed to human recombinant leptin protein*

A total of 10 frozen-thawed day 5, and 3 fresh day 7 blastocysts of varying quality were fixed without exposure to human recombinant leptin protein, and stained with FITC-conjugated anti-pSTAT3 antibodies as described in section 2.11.2. The embryos were imaged using confocal microscopy and the relative fluorescence intensity of the FITC and DAPI measured using Image J, as described in section 2.12 and 2.13.

Figure 5.1 shows examples of single plane confocal images of blastocysts that were not exposed to leptin protein. The images show the presence of pSTAT3 in the cytoplasm and nuclei of the cells (green), and chromatin in the nuclei of the cells (blue). The intensity of pSTAT3 staining in the embryos is highly variable despite standardisation of image capture. Figure 5.2 shows the relative fluorescence

intensity of pSTAT3 staining in the cytoplasm and nuclei of the ICM and TE of blastocysts not exposed to human recombinant leptin protein, measured using Image J, as described in section 2.14.

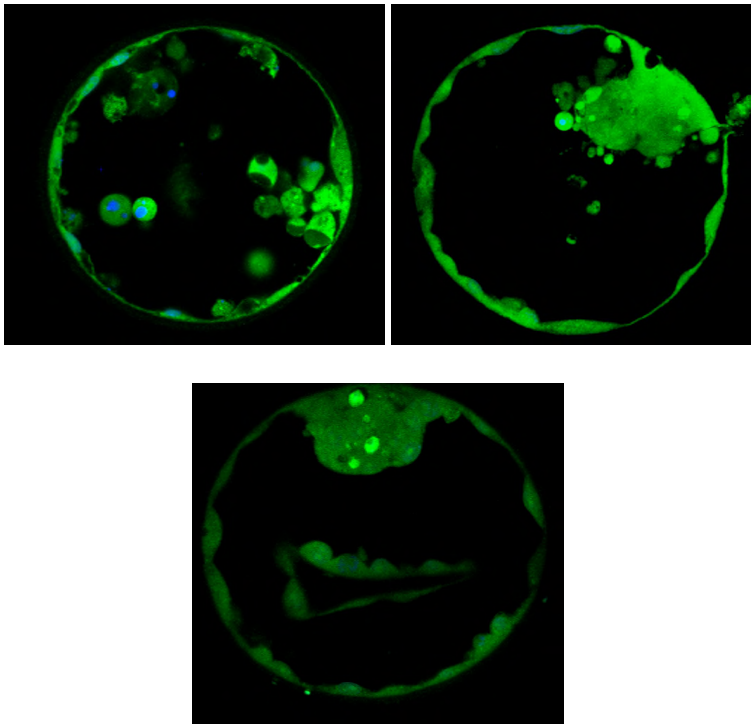

***Figure 5.1: Confocal images of blastocysts stained with FITC-conjugated anti-pSTAT3 antibody and mounted in DAPI media, without exposure to leptin protein***

Figure 5.2 shows these results in graphical form.

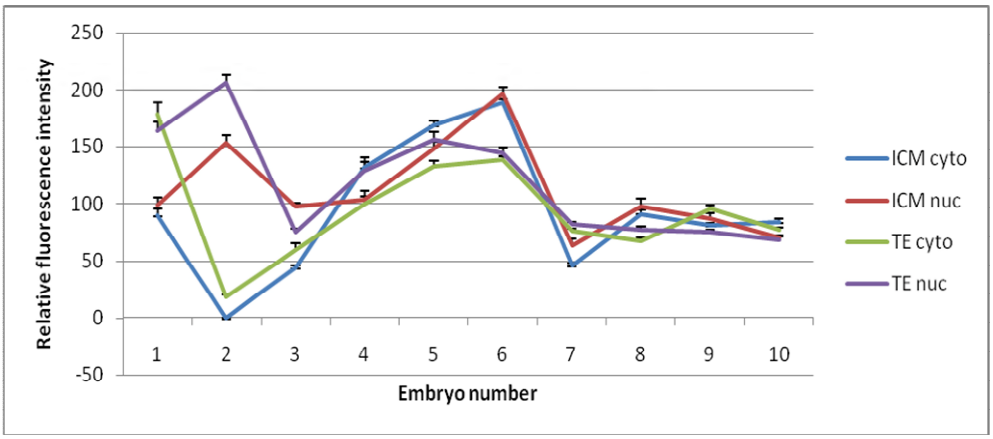


***Figure 5.2: Distribution of pSTAT3 in the cytoplasm (cyto) and nuclei (nuc) of the ICM and TE cells in blastocysts not exposed to leptin protein***

### *5.4.2 Activated STAT3 distribution in human embryos exposed to human recombinant leptin protein*

Four frozen-thawed morula stage embryos were cultured with 1µg/ml human recombinant leptin protein for 24 hours. All embryos degenerated, and therefore the exposure concentration was reduced.

Ten frozen-thawed embryos, from day 4 to day 7 post-insemination, were cultured with 20ng/ml human recombinant leptin protein for 10 minutes, 20 minutes, 30 minutes or 24 hours, as described in section 2.17. The embryos were fixed and stained with FITC-conjugated anti-pSTAT3 antibodies, and imaged using confocal microscopy, as described in sections 2.11 and 2.12. Relative fluorescence intensities

were measured in the cytoplasm and nuclei of all cells in the ICM and TE using Image J, as described in section 2.13.

Figure 5.3 shows single plane confocal images of human frozen-thawed blastocysts cultured with 20ng/ml human recombinant leptin protein for varying lengths of time before being fixed and stained with FITC-conjugated anti-pSTAT3 antibodies. Balstocyst (a) was cultured for 10 minutes, (b) was cultured for 20 minutes, and (c) was cultured for 30 minutes. In all blastocysts there was an upregulation of pSTAT3 staining in the cytoplasm, high intensity staining in the perinuclear regions, and distinct brightly stained spots in the nuclei of ICM and TE cells, when compared to blastocysts that had not been cultured with leptin protein.

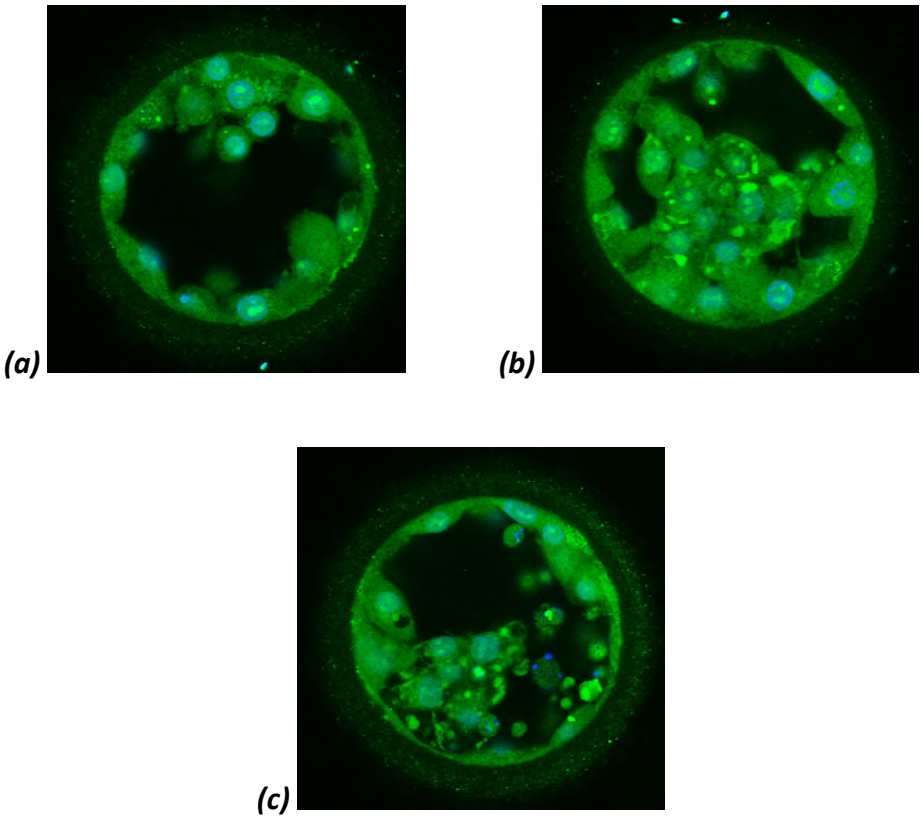


***Figure 5.3: Confocal images of human frozen-thawed blastocysts cultured with 20ng/ml leptin protein for (a) 10 minutes, (b) 20 minutes and (c) 30 minutes, and labelled with FITC-conjugated anti-pSTAT3 antibody***

Figure 5.4 shows single plane confocal images of frozen-thawed blastocysts cultured with 20ng/ml human recombinant leptin protein for 24 hours. The pattern of pSTAT3 staining was similar to that observed in the control embryos, with lower levels of pSTAT3 present in the cytoplasm and nuclei of cells, and residual bright spots of staining in the perinuclear regions.

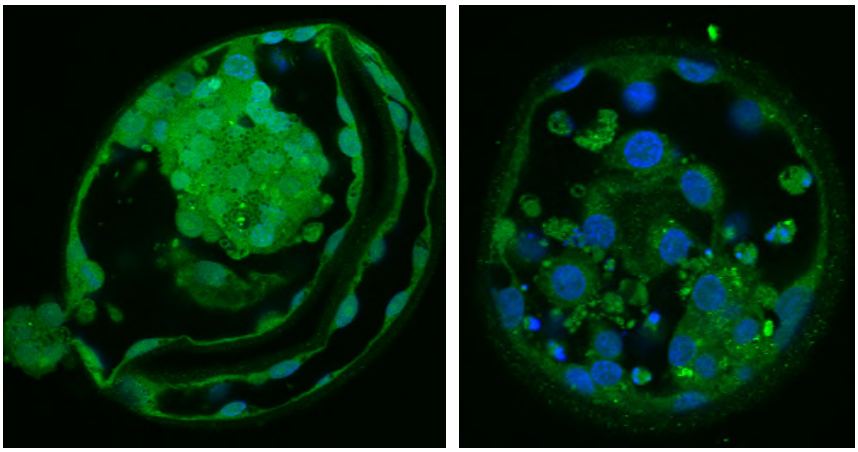

***Figure 5.4: Confocal images of frozen-thawed human blastocysts cultured with 20ng/ml human recombinant leptin protein for 24 hours, stained with FITC-conjugated anti-pSTAT3 antibody***

Figure 5.5 shows the mean relative intensity values for pSTAT3 fluorescence in the nuclei and cytoplasm of the ICM cells in human blastocysts cultured with or without 20ng/ml human recombinant leptin protein for 10 minutes, 20 minutes, 30 minutes or 24 hours. There was a significantly lower level of pSTAT3 in the ICM nuclei and cytoplasm of control embryos in comparison to embryos that were exposed to leptin protein for any of the exposure times (*p=0.008; two-tailed t-test).

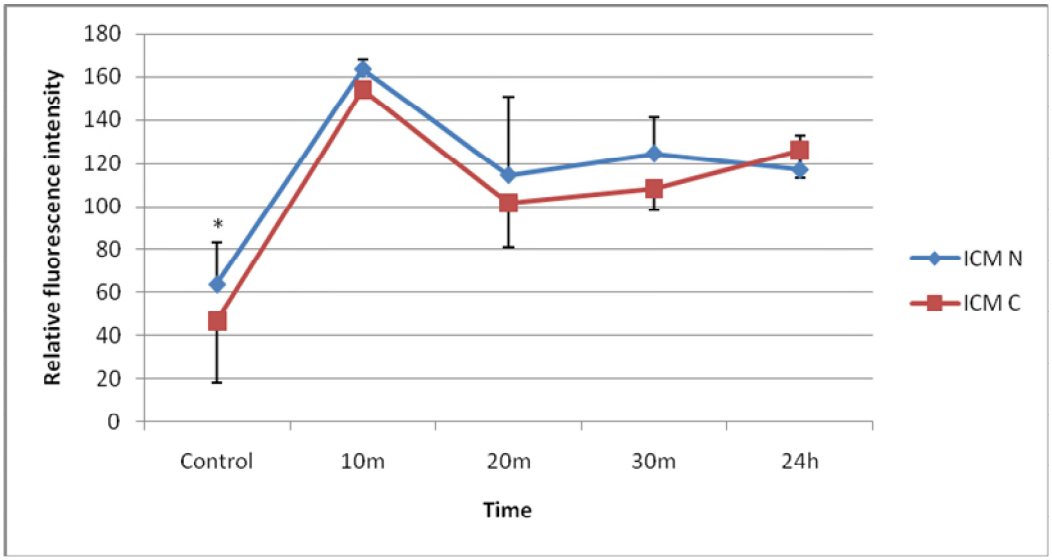


***Figure 5.5: Mean relative intensity values for pSTAT3 fluorescence in the nuclei (N) and cytoplasm (C) of the ICM in human blastocysts. Control = not exposed to leptin protein***

Figure 5.6 shows the mean relative intensity values for pSTAT3 fluorescence in the nuclei and cytoplasm of the TE cells in human blastocysts cultured with or without 20ng/ml human recombinant leptin protein for 10 minutes, 20 minutes, 30 minutes or 24 hours. There were no significant differences in the levels of pSTAT3 in the TE nuclei and cytoplasm of control embryos in comparison to embryos that were exposed to leptin protein. There was a non-significant increase in fluorescence intensity at 10, 20 and 30 minutes, however levels had returned to pre-exposure levels by the 24-hour exposure time.

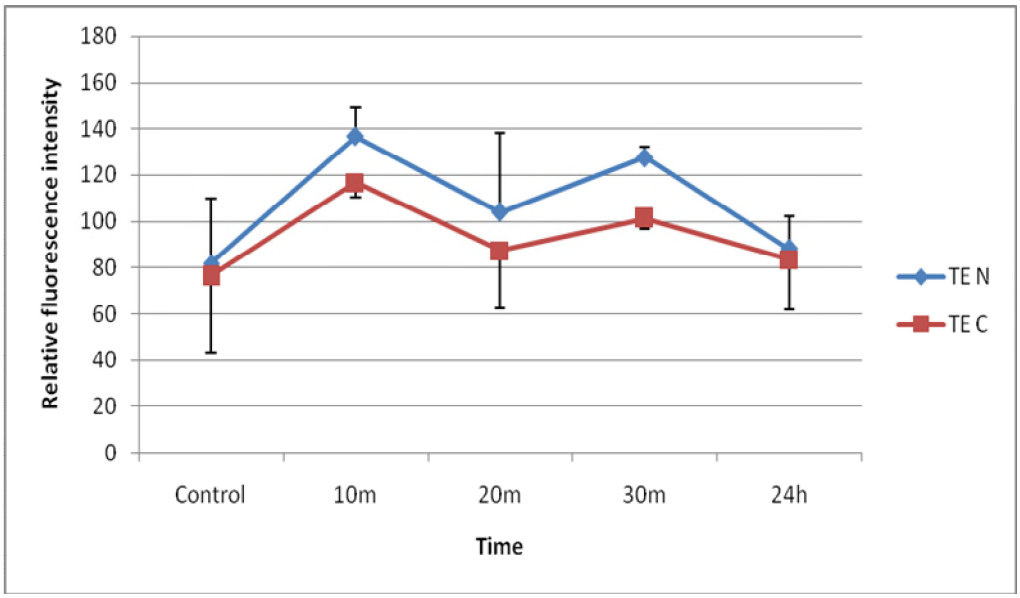


***Figure 5.6: Mean relative intensity values for pSTAT3 fluorescence in the nuclei (N) and cytoplasm (C) of the TE of human blastocysts. Control = not exposed to leptin protein***

There were higher or equal levels of pSTAT3 in the ICM in comparison to the TE at all exposure times, although these differences were not significant.

### *5.4.3 Effect of human recombinant leptin protein on blastocyst cell numbers*

Following exposure to human recombinant leptin protein, as described in section 2.17, the cell numbers in the ICM and the TE of blastocysts were counted and compared to those that had not been exposed.

The average ICM cell number for blastocysts not exposed to leptin protein was 20.94 (±10.02) compared to 26.13 (±15.7) for blastocysts that had been exposed. This difference was not significant. The average number of cells in the TE for blastocysts that had not been exposed to leptin protein was 87.4 (±10.02) compared to 119 (±33.09) for those blastocysts which had been exposed. This difference was approaching significance (p=0.06; two-tailed t-test). The results are summarised in figure 5.7.

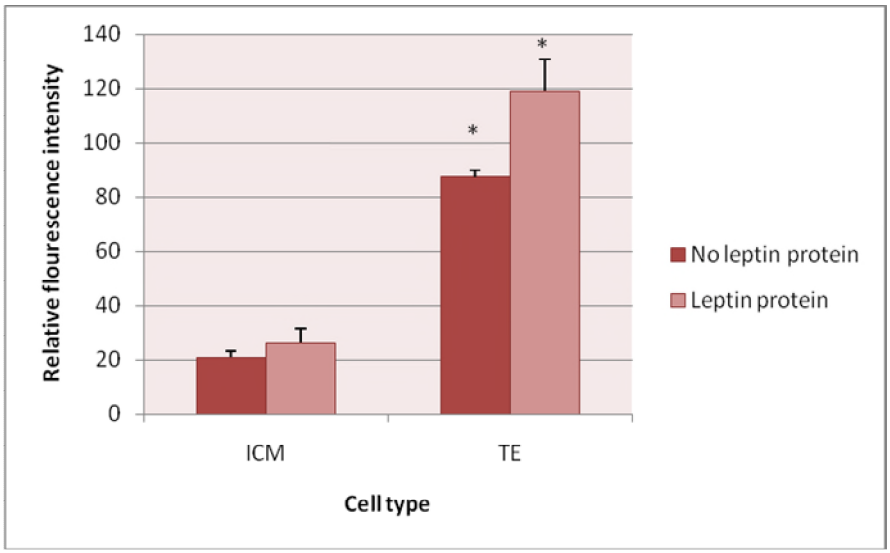


***Figure 5.7: Cell numbers in the ICM versus the TE in blastocysts exposed to human recombinant leptin protein compared to blastocysts that were not exposed***

### *5.4.4 Culture of human blastocysts with stromal cell-enriched medium*

Two blastocysts were cultured with stromal cell-enriched medium (1x10 minutes, 1x20 minutes), and two blastocysts were cultured with Ishikawa cell-enriched medium (1x10 minutes, 1x20 minutes).

The levels of pSTAT3 present were similar to those in blastocysts exposed to leptin protein for 24 hours. There was an increase in pSTAT3 levels in the cytoplasm of the ICM and TE in blastocysts exposed to Ishikawa cell-enriched medium compared to those exposed to stromal cell-enriched medium (see figure 5.9), however there were no significant differences observed within or between cell types. Further investigative work is necessary.

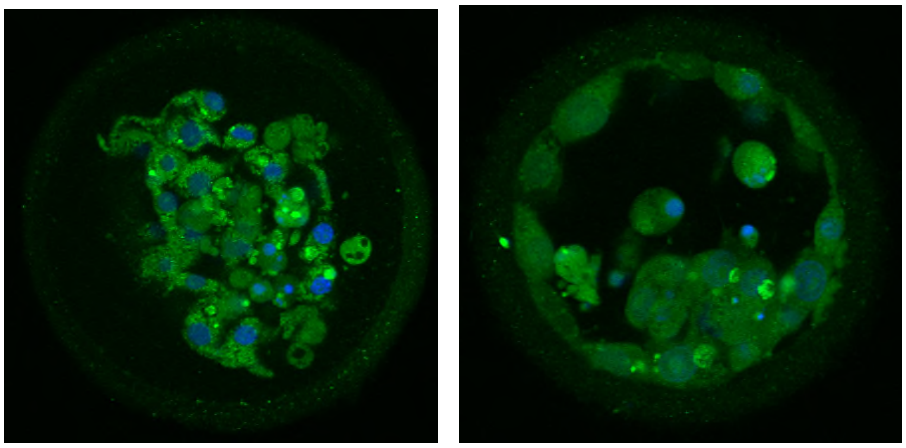

***Figure 5.8: (a) day 6 frozen-thawed blastocyst cultured with Ishikawa cell-enriched medium for 10 minutes (b) day 5 frozen-thawed blastocyst cultured with stromal cell-enriched medium for 10 minutes, stained with FITC-conjugated anti-pSTAT3 antibody and mounted in DAPI media.***

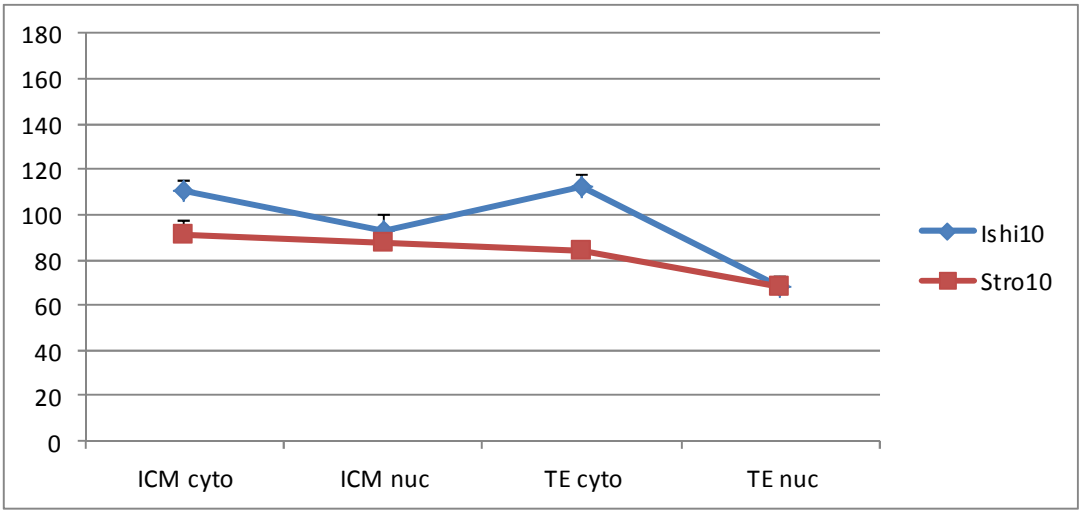


***Figure 5.9: Relative fluorescence intensity of pSTAT3 staining in the ICM cytoplasm (cyto), ICM nulcei (ICM nuc), TE cytoplasm (cyto), and TE nuclei (nuc) in blastocysts exposed to Ishikawa cells (Ishi10) and stromal cells (Stro10) for 10 minutes***

### *5.4.5 Quantitative Reverse Transcription Polymerase Chain Reaction (qRT-PCR) for the detection of long-form leptin receptor mRNA in human zygotes, cleavage stage embryos and blastocysts*

Two normally fertilised zygotes, two cleavage stage embryos, and two blastocysts were thawed and subjected to qRT-PCR for the detection of leptin receptor mRNA, as described in section 2.19.

Figure 5.10 shows the level of long form leptin receptor ($LEPR_L$) mRNA at each developmental stage. A higher level of leptin receptor mRNA was detected at the blastocyst stage, in comparison to both pronuclear and cleavage stages, however these differences were not significant.

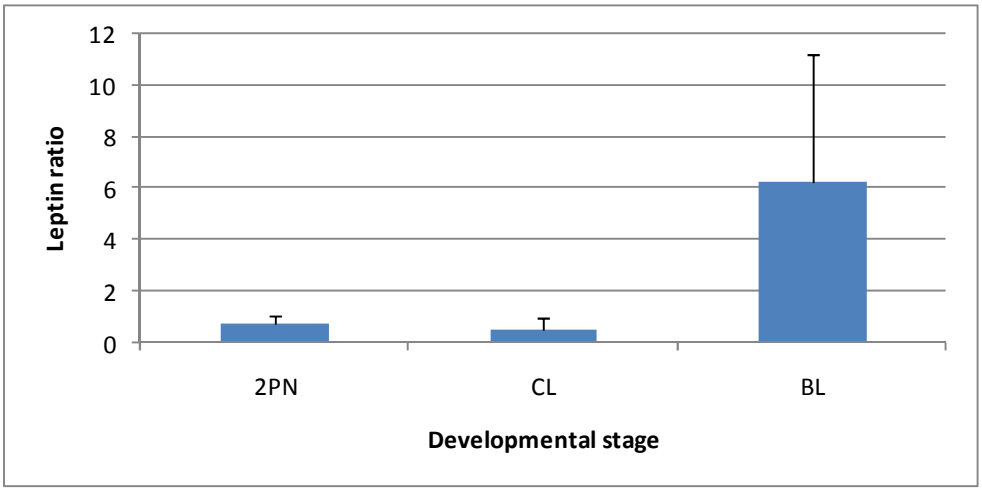


***Figure 5.10: Comparison of the amount of $LEPR_L$ mRNA in frozen-thawed pronucleates (2PN), cleavage stage embryos (CL), and blastocysts (BL)***

To demonstrate specificity, two oocytes (Metaphase) two normally fertilised zygotes (2PN), two cleavage stage embryos (CL), and two blastocysts (BL) were thawed and subjected to qRT-PCR for the detection of SUMO mRNA, as described in section 2.19. Figure 5.11 shows the level of SUMO mRNA at each developmental stage. There was an increase in the level of SUMO mRNA at the zygote stage compared to all other stages.

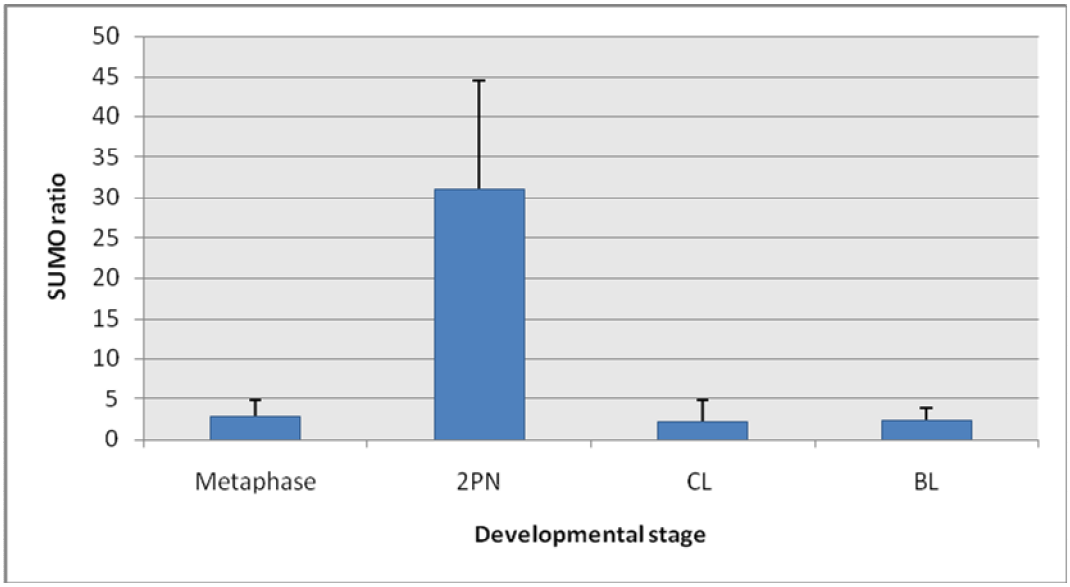


***Figure 5.11: Comparison of the level of SUMO mRNA in frozen-thawed oocytes (Metaphase), pronucleates (2PN), cleavage stage embryos (CL), and blastocysts (BL). Error bars represent the standard error of the mean***

## *5.5 Discussion*

This work suggests for the first time that exogenous human recombinant leptin activates STAT3 via the leptin receptor in human blastocysts, inducing translocation of cytoplasmic pSTAT3 to the nucleus. This finding is in agreement with a previous report in which exposure of mouse oocytes to recombinant leptin led to an increase in the phosphorylation of STAT3 (Matsuoka *et al* 1999). However, the human embryos used during these experiments were variable in their stages of development and morphological quality, and were cultured using a range of culture media and conditions. Some of the embryos in the non-exposed group were fresh, whilst all of the embryos in the exposed group were frozen-thawed. Additionally, whilst some of the frozen-thawed embryos were slow-frozen, others had been vitrified. Therefore, caution must be applied when interpreting these results, particularly when comparing those embryos which had been exposed to leptin protein with those that had not been exposed to leptin protein.

The effect of leptin protein on the activation of STAT3 in human blastocysts observed using a concentration of 20ng/ml was not seen when the concentration was increased to 1µg/ml, when all exposed embryos degenerated. This may be due to the lower concentration of 20ng/ml more closely representing physiological levels of leptin, as measured in blood serum obtained from the umbilical cords of newborn humans (19.9ng/ml) (Matsuda *et al* 1997), and may indicate a toxic effect of leptin on human blastocysts at higher concentrations.

The observed up-regulation of STAT3 activation in human blastocysts by leptin protein suggests that human blastocysts have the long form of transmembrane leptin receptor, since the truncated forms lack the signalling properties of the long form (Wang *et al* 1997). The long form of leptin receptor mRNA and protein have also been detected in mouse metaphase II oocytes (Matsuoka *et al* 1999), and total leptin receptor mRNA has been previously detected in human oocytes and preimplantation embryos (Cervero *et al* 2004), although distinction between the short and long forms was not made. When verifying the presence of leptin receptor mRNA in human preimplantation embryos in this work using qRT-PCR, primers for the specific detection of the long form of the receptor were used, thus confirming this theory. In order to ensure that the qRT-PCR was detecting the specified target gene, a control plate was prepared with primers directed against SUMO, a small polypeptide implicated in nuclear integrity, chromosome segregation and embryonic viability in mice (Nacerddine *et al* 2005), which showed higher levels of SUMO mRNA in pronucleates in comparison to cleavage stage embryos and blastocysts, thus confirming detection of specific target genes.

Ishikawa cells, derived from human endometrial adenocarcinoma (Nishida *et al* 1985) represent a robust model of normal functioning endometrial epithelium during the implantation window (Castlebaum *et al* 1997), and therefore may be expected to exert a similar effect to leptin protein upon the activation of STAT3 in human embryos at the time of implantation. Stromal cells regulate human epithelial growth and differentiation, and are used here as a control. The results showing no significant increase in activation of STAT3 in human blastocysts cultured with

Ishikawa-cell enriched media in comparison to blastocysts cultured with stromal cell-enriched media are likely due to the small numbers involved, due to the limited availability of embryos, and warrants further investigation.

The upregulation of pSTAT3 in the ICM of blastocysts exposed to human recombinant leptin protein resonates with a previous finding that several genes involved in the Jak-STAT signalling pathway were upregulated in the ICM of bovine blastocysts (Ozawa *et al* 2012). This may indicate that the activation of STAT3 by leptin via the Jak-STAT pathway is important for the regulation of ICM function, in a similar way to the promotion of cell differentiation in ICM-derived cells by leukaemia inhibitory factor (LIF) in mice, which also acts via the Jak-STAT signalling pathway (Smith *et al* 1992), and is a known activator of STAT3 (Auernhammer and Melmed 2000). The transient effect of exogenous leptin protein on the activation of STAT3 observed in this work may be explained by the short half-life of human recombinant leptin. This has previously been reported as 60 minutes when monitored in the circulation of mice after injection, with circulating leptin levels becoming undetectable 7 hours post-injection (Chehab *et al* 1997).

Since activated STAT3 is implicated in invasive cell behaviour including implantation (Teng *et al* 2004), and leptin is reported to promote blastocyst attachment and adhesion during implantation in mice (Yang *et al* 2006), these results may provide important insights into the molecular mechanisms involved in human implantation.

# Chapter Six

# Analysis of Time Lapse Images of Live Human Preimplantation Embryos

# Chapter Six

# Analysis of Time Lapse Images of Live Human Preimplantation Embryos

## *6.1 Introduction*

Normal fertilisation is usually evidenced by two abutting pronuclei, centrally located in the ooplasm, and observed approximately 16-20 hours after insemination (Payne *et al* 1997). Visible markers of embryo growth and morphology at key developmental stages include appearance, disappearance, number and positioning of pronuclei and nuclei (Payne *et al* 1997; Garello *et al* 1999), embryo cleavage rate, cell number (Lemmen *et al* 2008), cell shape, blastomere orientation (Edwards and Beard 1997), fragmentation, blastocyst development rate, and blastocyst inner cell mass location (Hardarson *et al* 2003). These indicators of embryo quality are routinely assessed microscopically in the clinical embryology laboratory at intervals of approximately 24 hours in order to select the embryo deemed most suitable for uterine transfer (Prados *et al* 2012) although increasingly, time-lapse video microscopy is applied.

Hatching of the blastocyst from the ZP is the final stage of human preimplantation embryo development, and is believed to be essential for attachment and subsequent implantation *in utero* (Ren *et al* 2013). Interaction between the blastocyst and the endometrium are necessary to facilitate implantation in the optimal uterine location, and in the correct polar orientation to enable successful establishment and continuation of pregnancy (Achache and Revel 2006).

Approximately 7% of human oocytes in IVF fertilise abnormally, exhibiting multiple pronuclei (MPN) (Balakier 1993) which have been previously discussed in this thesis. Some MPN embryos have developmental capacity that includes the ability to form a blastocyst, although the majority arrest prior to differentiation and many will harbour chromosomal and structural aberrations. While most MPN embryos fail to implant, the small proportion that do implant may result in spontaneous abortion, or the occasional birth of a triploid foetus which dies at birth (Balakier 1993). A further possible consequence is modification of the genetic complement resulting in the formation of a hydatidiform mole (Edwards *et al* 1992) which may lead to choriocarcinoma (Magrath *et al* 1971). For this reason, MPN zygotes created during clinical treatment cycles are routinely discarded rather than transferred. Consequently, the proportion of MPN implantations after IVF is lower than in the natural population.

The high variability of cell cleavage timings and appearance during embryo development has been widely reported, moreover embryo morphology can change markedly within a few hours (Montag et al 2011). Evaluating such a dynamic process once daily as is routine in many clinical IVF laboratories, may therefore result in important developmental events being overlooked and the incorrect grading of good quality embryos as poor quality or *vice versa* (Lemmen *et al* 2008). One of the ways in which these challenges are being addressed is via the use of time lapse imaging. Time lapse microscopy, usually involving the acquisition of images at intervals of between 5 and 20 minutes, enables observation of preimplantation embryo development during the entire culture period from fertilisation through to

blastocyst, whilst maintaining the stable culture conditions required for optimal embryo growth (Kirkegaard *et al* 2012).Collecting images at multiple focal planes is superior because it enables details that would otherwise be out of focus to be documented and analysed. The presence of a computerised record of images for every embryo facilitates direct comparisons between individual embryos, and the analysis of trends and characteristics associated with particular outcomes. It is possible to return to images later to evaluate new prospective markers of potential importance for development.

Integrated time lapse monitoring systems such as the Embryoscope have been shown to be comparable to traditional $CO_2$ incubators, with no reported adverse effects on embryo quality and viability (Cruz *et al* 2011). Furthermore, selecting embryos for transfer with the assistance of time lapse monitoring may result in an estimated 20% increase in clinical pregnancy rate, in comparison to standard morphological grading alone (Meseguer *et al* 2012).

In order to assess the genetic complement of an oocyte or embryo directly, a sample of genetic material has to be acquired for analysis (Hardy *et al* 1990). This may be achieved by removing polar bodies from oocytes, one or more blastomeres from cleavage stage embryos, or by harvesting a few cells of the trophectoderm from blastocysts (Kirkegaard *et al* 2012). Currently, the most common method of collecting DNA for PGD is via blastomere biopsy (Harper *et al* 2010). This method was initially found to have no adverse effect on the development of human preimplantation embryos to the blastocyst stage (Hardy *et al* 1990), however, there is evidence to suggest a significant influence on blastocyst formation when

comparing the removal of one versus two blastomeres from day 3 embryos (Goossens *et al* 2008). Some research indicates that there may be a developmental delay in mouse embryos after biopsy (Duncan *et al* 2009), and recent research using time lapse imaging suggests that biopsied human embryos reach the compacting, cavitating, and blastocyst stages significantly later than non-biopsied controls (Kirkegaard *et al* 2012).

In some animal species, such as flies and frogs, the spatial arrangement of the pre-implantation embryo is known to be important for its developmental potential. Polarised development from the fertilised egg to the implanting embryo gives rise to the eventual axes of the organism, a fundamental requirement for normal function. It has been proposed that the position of the animal pole in the oocyte, containing nuclear material and indicated by the first polar body, establishes the first embryonic axis (Edwards and Beard 1997). After the first division along the meridian of the pronuclei, the first dividing blastomere of the newly formed 2-cell embryo forms a cleavage furrow along the meridian axis prior to division into daughter cells which pass through the embryonic and vegetal poles. The second-cleaving blastomere then rotates and divides transversely, resulting in the classical "crosswise" arrangement observed in normal 4-cell embryos (Edwards and Beard 1997). Disruption of normal cleavage could lead to interruption of axis formation, and thus embryonic developmental delay or lethality, which may have some implication when selecting which blastomere(s) to remove for PGD screening.

## *6.2 Aims*

The aims of this work were to identify potential markers of embryo viability and predictors of embryo development by assessment of human preimplantation embryos using time lapse monitoring.

The potential effect of deliberately damaging the daughters of the first dividing cell at the third cleavage division (4-8 cells) with respect to ensuing cleavage patterns and blastocyst formation was also investigated, to determine whether damage of specific blastomeres may impact on axis establishment and subsequent embryo development.

Finally, the initial site of blastocyst hatching from the ZP with respect to the position of the inner call mass was examined, to establish whether there was any association between the site of hatching and pregnancy potential.

## *6.3 Methods*

536 human live preimplantation embryos were imaged using a selection of time lapse imaging systems, as described in detail in section 2.14, with varying degrees of success. Known indicators of embryo quality, including cell cleavage timings, blastomere dynamics, and blastocyst formation were analysed and compared in both fresh and frozen-thawed embryos. Identification and deliberate damage of the daughters of the first-dividing cell was executed as described in section 2.16, and the development of the embryos monitored using advanced time lapse technology.

## *6.4 Results*

### *6.4.1 Analysis of time lapse images acquired using the Embryoscope self-contained monitoring system*

Initially, a total of 40 fresh embryos arising during clinical treatment and 39 frozen-thawed research embryos at various developmental stages (day 1 - day 6) were imaged every 10 or 20 minutes for up to 6 days in the Unisense FertiliTech Embryoscope ™self-contained embryo monitoring system, to assess development *in vitro*, as described in section 2.14. A further 401 fresh clinical embryos were analysed later, following establishment of the Embryoscope ™ as a clinical tool at the CRM. Unfortunately, due to the paucity of embryos frozen in early development and then donated to research, the same number of frozen embryos could not be assessed.

### *6.4.2 Arrested embryos*

A total of 25 fresh embryos and 15 frozen embryos from the small initial cohort, recorded in a pre-clinical study of the Embryoscope™, arrested at various developmental stages during the culture period. Figure 6.1 shows the specific stage at which fresh and frozen-thawed embryos arrested; 1-4 cell, 5-8 cell, compaction, or cavitation.

A significantly higher proportion of frozen embryos arrested at the 1-4 cell stage in comparison to fresh embryos (*p = 0.01; 2-sample t-test).

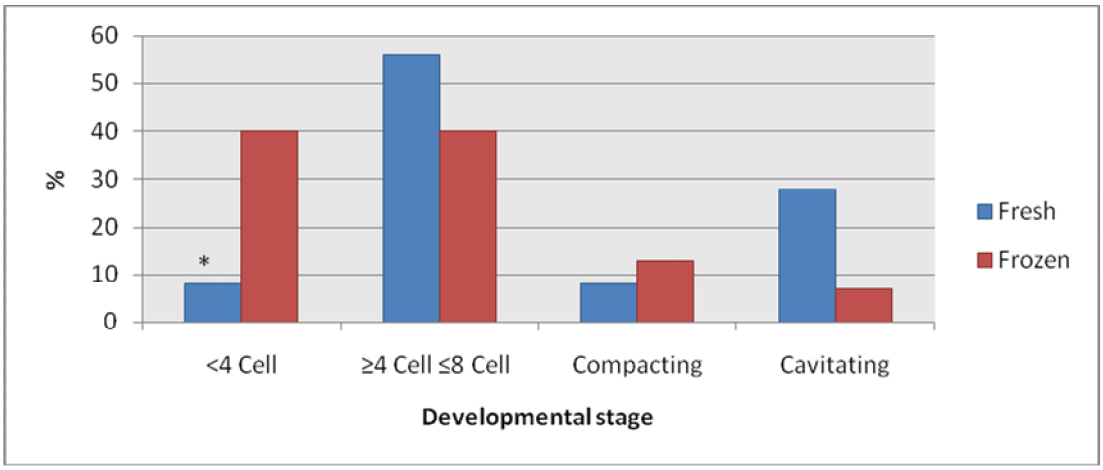


***Figure 6.1: Comparison of the developmental stages at which fresh and frozen-thawed embryos arrested during culture in the Embryoscope time lapse incubator***

### *6.4.3 Embryo cleavage*

A total of 441 fresh, normally fertilised embryos, created using standard IVF or ICSI for CRM patients were cultured in the Embryoscope from day 1 post-insemination (2PN) until day 6 in order to assess embryo cleavage completion timings and the time spent at each developmental stage. The clinical pregnancy rate for these patients was 49%.

A total of 39 donated frozen embryos ranging from day 1 to day 4 were thawed and cultured in the Embryoscope until day 6 in order to assess embryo cleavage rates and time spent at each developmental stage. Embryos were created using standard

IVF or ICSI, and were cryopreserved or vitrified at varying stages of development, according to the requirements of the patient during the fresh treatment cycle. These embryos were not transferred, and therefore the implantation potential of these embryos is unknown.

Figure 6.2 shows the mean time taken to complete cleavage in all fresh embryos. The mean first cleavage time was 27.98 (±4.62) hours post-insemination, and the mean blastocyst formation time was 116.0 (±13.93) hours post-insemination.

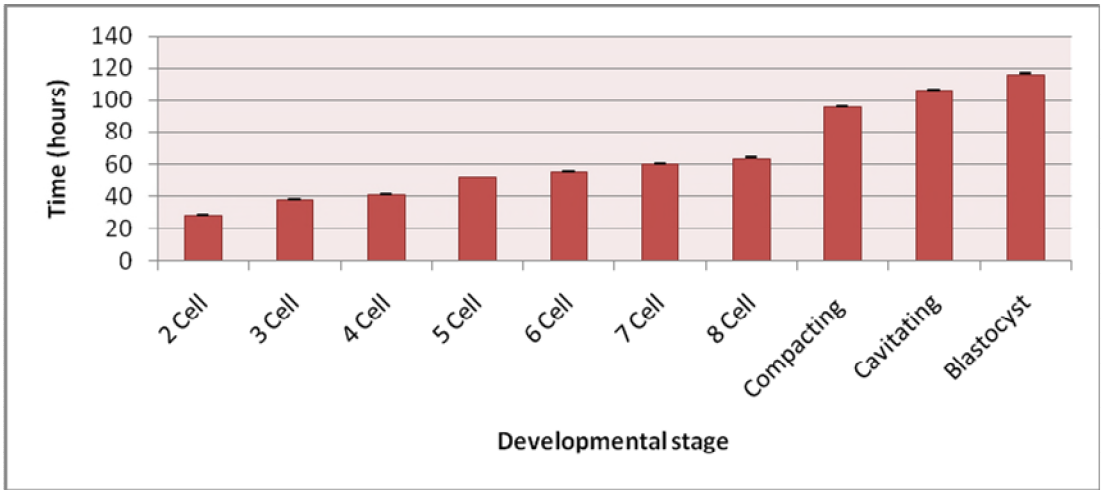


***Figure 6.2 : Mean cleavage completion times in all fresh embryos. The mean first cleavage time was 27.98 (±4.62) hours post-insemination, and the mean blastocyst formation time was 116.0 (±13.93) hours post-insemination Error bars represent standard error of the mean***

Figure 6.3 shows the mean time taken to complete cleavage in all frozen embryos. The mean first cleavage time was 33.8 (±6.8) hours post-insemination, and the mean blastocyst formation time was 136.6 (±36.12) hours post-insemination.

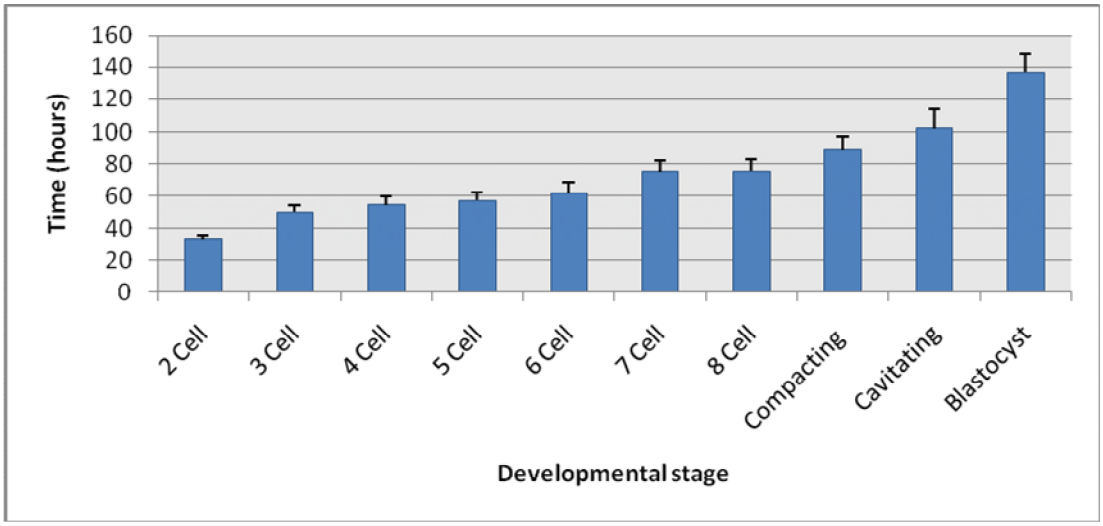


***Figure 6.3: Mean cleavage completion times in all frozen embryos. Error bars represent standard error of the mean. The mean first cleavage time was 33.8 (±6.8) hours post-insemination, and the mean blastocyst formation time was 136.6 (±36.12) hours post-insemination***

Figure 6.4 shows the comparison between the mean cleavage completion times in all frozen and fresh embryos. Fresh embryos completed cleavage into 2 cell, 3 cell, 4 cell, 7 cell and 8 cell, and formed blastocysts at a significantly faster rate than frozen embryos (*p=<0.001; independent groups t-test between means). All other differences in cleavage rates, compaction, and cavitation were insignificant between the two groups.

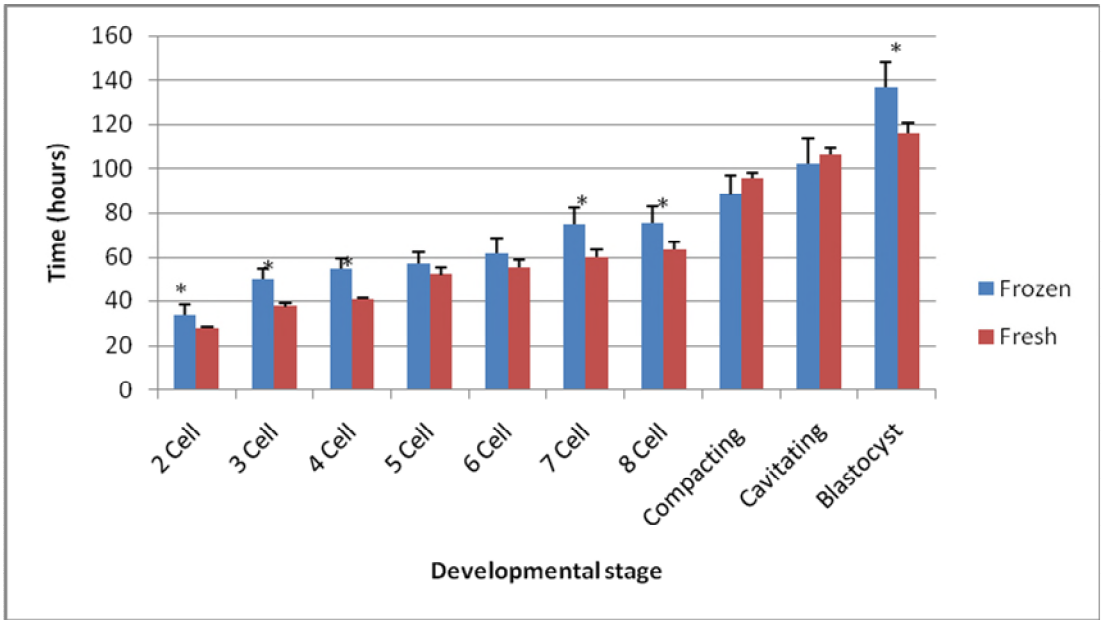


***Figure 6.4: Mean cleavage completion time in all frozen versus fresh embryos. Error bars represent standard error of the mean. Fresh embryos completed cleavage into 2 cell, 3 cell, 4 cell, 7 cell and 8 cell, and formed blastocysts at a significantly faster rate than frozen embryos (*p=<0.001; independent groups t-test between means). All other differences in cleavage rates, compaction, and cavitation were insignificant between the two groups***

Figure 6.5 shows the cleavage completion times in all frozen embryos created using standard IVF versus those created using ICSI. The embryos created using standard IVF were significantly slower to complete cleavage into two cells (42.70±11.8 vs 32.64 ±4.30) (*p=0.05; unpaired t-test), three cells (66.62 ±13.0 vs 41.74 ±6.71) and four cells (66.95 ±18.42 vs 44.06 ±5.5) (**p=0.002; unpaired t-test) than embryos created using ICSI. Whilst ICSI embryos developed generally faster than IVF embryos, the differences were not significant from the 5-cell stage to the blastocyst stage.

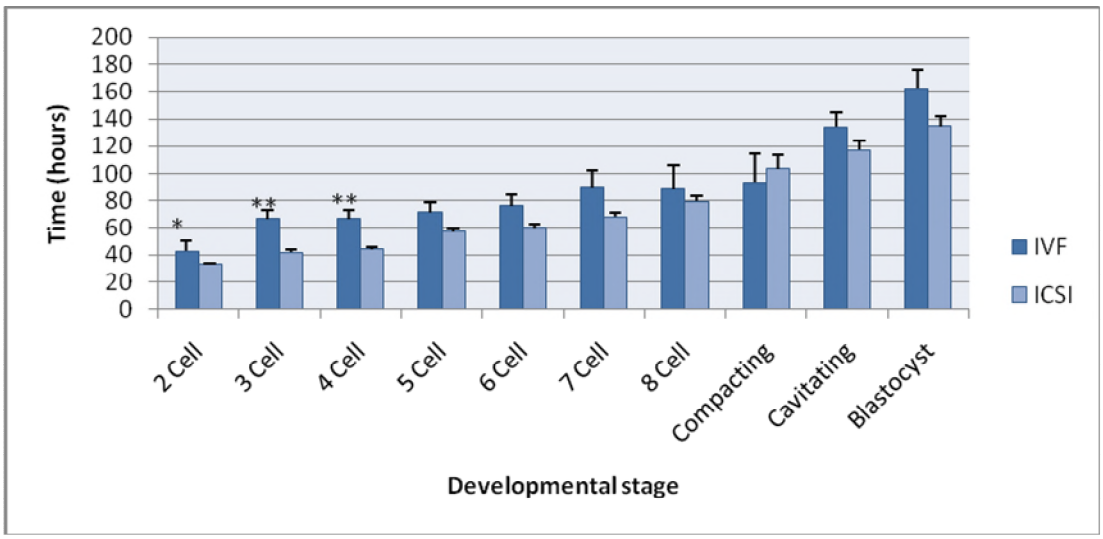


***Figure 6.5: Mean cleavage completion times in all frozen IVF versus ICSI embryos. Error bars represent standard error of the mean. The embryos created using standard IVF were significantly slower to complete cleavage into two cells (42.70±11.8 vs 32.64 ±4.30) (*p=0.05; unpaired t-test), three cells (66.62 ±13.0 vs 41.74 ±6.71) and four cells (66.95 ±18.42 vs 44.06 ±5.5) (**p=0.002; unpaired t-test) than embryos created using ICSI. Whilst ICSI embryos developed generally faster than IVF embryos, the differences were not significant from the 5-cell stage to the blastocyst stage***

### *6.4.4 Time spent at each developmental stage*

Figure 6.6 shows the mean time spent at each developmental stage in all fresh embryos. Fresh embryos spent an average of 27.8 hours at the 1 cell stage. Embryos spent significantly longer at developmental stages involving even cell numbers (2 cell, 4 cell, 6 cell, 8 cell) in comparison to those involving odd cell numbers (3 cell, 5 cell, 7 cell) (a vs b; p = 0.02; independent groups t-test).

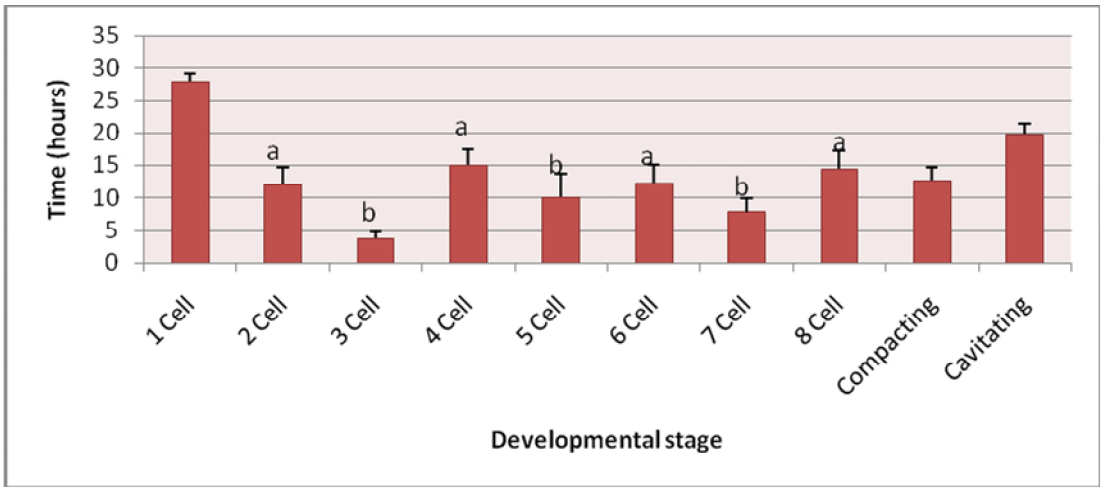


***Figure 6.6: Mean time spent at each developmental stage in all fresh embryos. Error bars represent the standard error of the mean. (a vs b; p = 0.02; independent groups t-test)***

Figure 6.7 shows the mean time spent at each developmental stage in all frozen embryos. Frozen embryos spent an average of 29.2 hours at the 1 cell stage. Embryos spent significantly longer at developmental stages involving even cell numbers (2 cell, 4 cell, 6 cell, 8 cell) in comparison to those involving odd cell numbers (3 cell, 5 cell, 7 cell) (a vs b; p = 0.02; independent groups t-test).

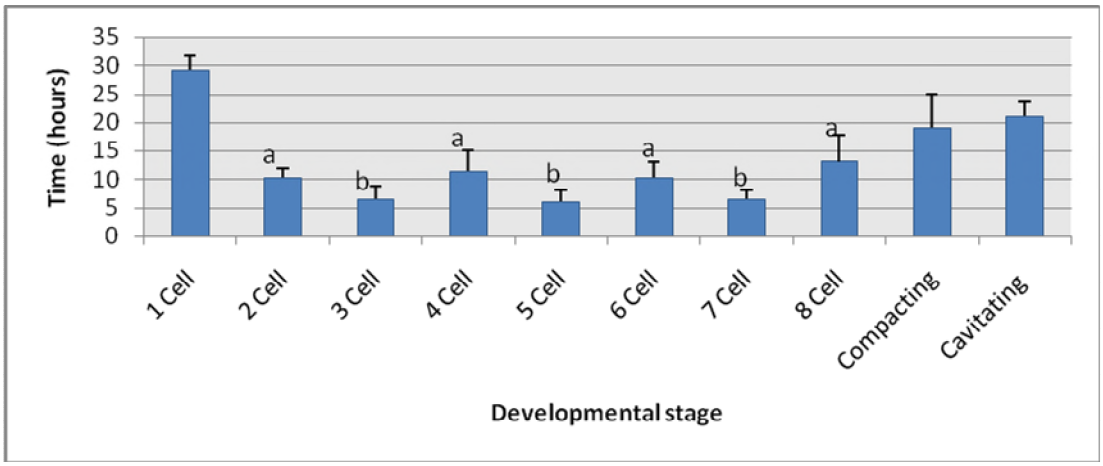


***Figure 6.7: Mean time spent at each stage of development in all frozen embryos. Error bars represent the standard error of the mean. (a vs b; p = 0.02; independent groups t-test)***

In order to reflect different culture conditions and to allow for the time taken to freeze and thaw the embryos, figure 6.8 shows a comparison of the absolute cleavage timings of fresh and frozen embryos at each developmental stage. There are no significant differences between fresh and frozen embryos.

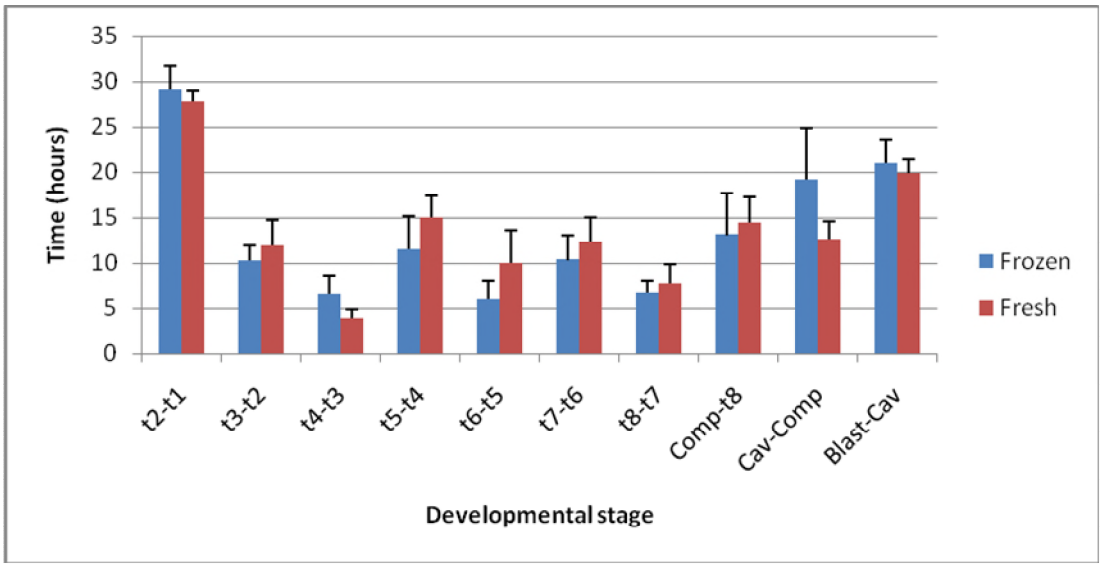


***Figure 6.8: Absolute cleavage times at each developmental stage in frozen versus fresh embryos. Error bars represent the standard error of the mean. There were no significant differences inthe mean time spent at each developmental stage between the frozen and fresh embryos***

### *6.4.5 Blastocyst development*

The proportion of fresh embryos developing to blastocyst was 34% and the proportion of frozen embryos developing to blastocyst was 29%.

Figure 6.9 shows the mean cleavage completion times in fresh embryos arresting before the blastocyst stage, versus those developing to the blastocyst stage. Embryos that became blastocysts completed cleavage into 2 cells and 4 cells significantly faster than those not developing to blastocyst (*p=0.03; independent groups t-test). All other differences in cleavage completion times were insignificant.

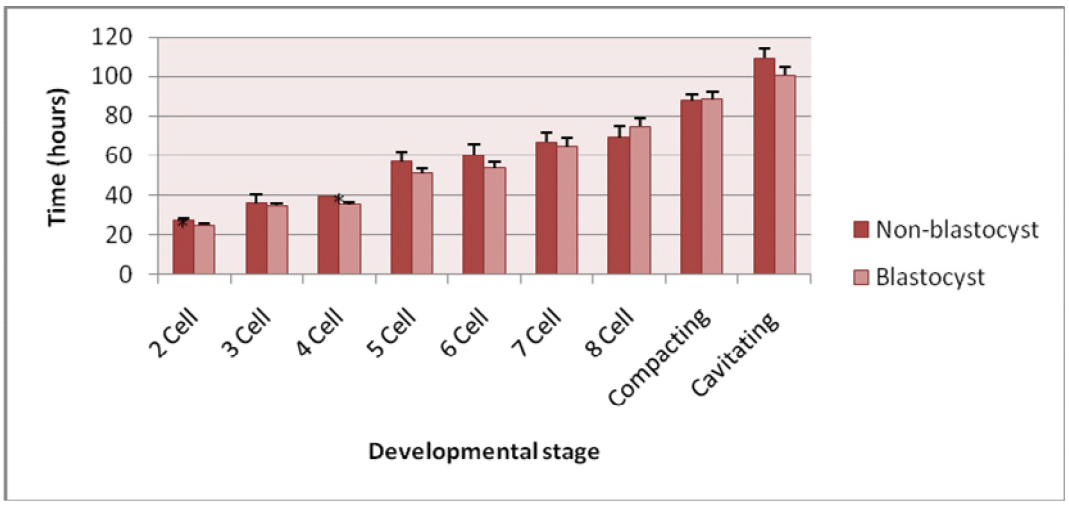


***Figure 6.9: Mean cleavage completion rates in fresh embryos not developing to the blastocyst stage versus developing to the blastocyst stage. Error bars represent the standard error of the mean. Embryos that became blastocysts completed cleavage into 2 cells and 4 cells significantly faster than those not developing to blastocyst (*p=0.03; independent groups t-test).All other differences in cleavage completion times were insignificant***

Figure 6.10 shows the mean time spent at each developmental stage in fresh embryos that arrested prior to the blastocyst stage versus those embryos that reached the blastocyst stage. Embryos that developed to blastocyst spent a significantly shorter time at the 1-cell stage (*) and a significantly longer time at the 7-cell stage (**) (p=0.02; independent groups t-test) than embryos that did not develop to blastocyst.

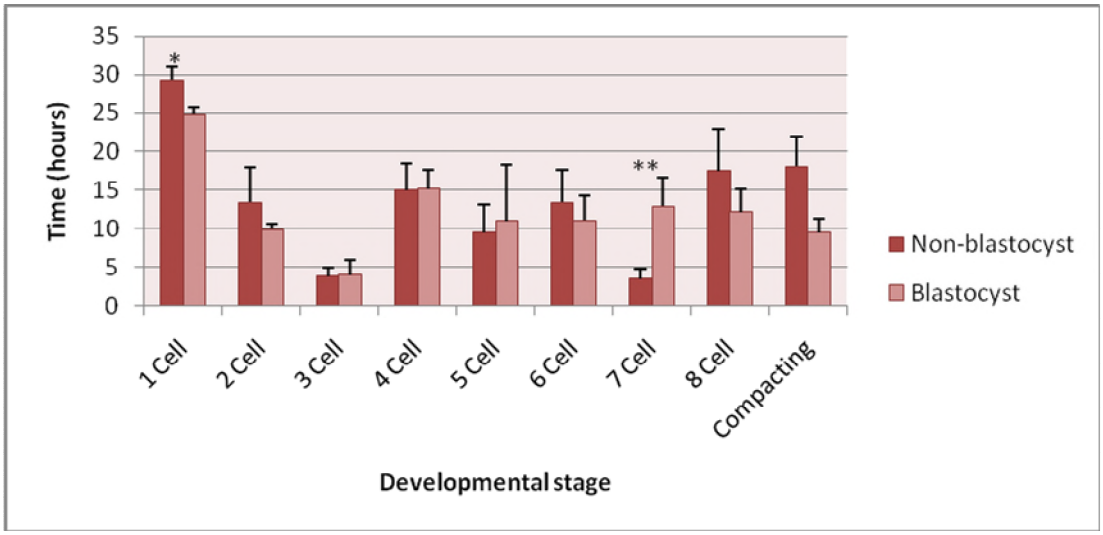


***Figure 6.10: Mean time spent at each developmental stage in all fresh embryos not developing to blastocyst versus developing to blastocyst.Error bars represent the standard error of the mean. Embryos that developed to blastocyst spent a significantly shorter time at the 1-cell stage (*) and a significantly longer time at the 7-cell stage (**) (p=0.02; independent groups t-test) than embryos that did not develop to blastocyst.***

Figure 6.11 shows the mean cleavage completion times in frozen embryos arresting before the blastocyst stage, versus embryos developing to the blastocyst stage.Frozen embryos developing to blastocyst completed developmental stages from three-cell to cavitating on average 20.2 hours later than embryos not developing to blastocyst. The differences were not significant.

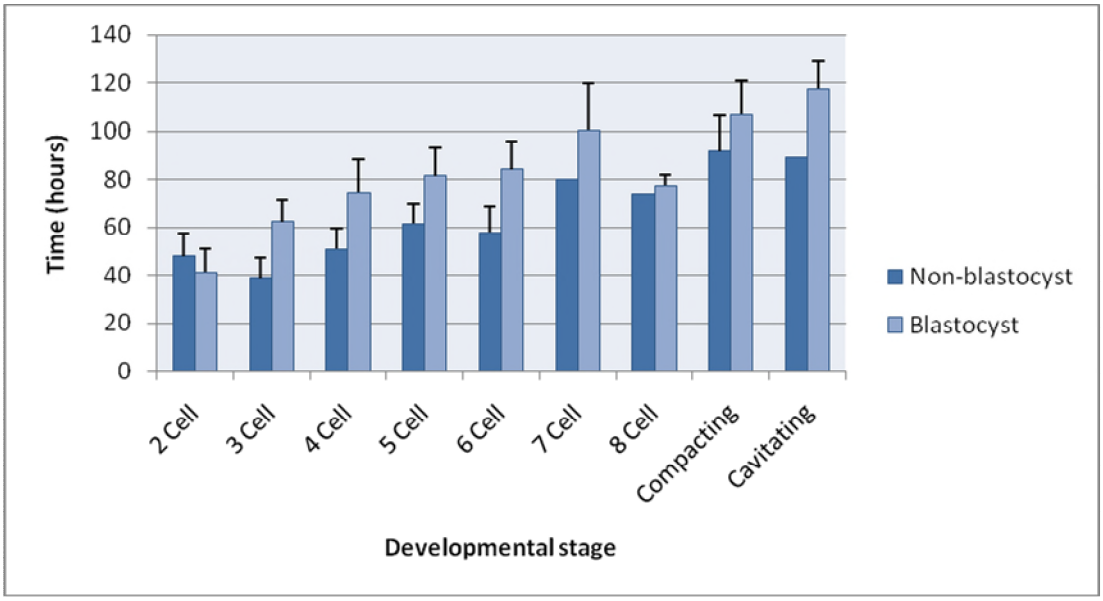


***Figure 6.11: Mean cleavage completion rates in frozen embryos not developing to the blastocyst stage versus frozen embryos developing to the blastocyst stage.Error bars represent the standard error of the mean. Frozen embryos developing to blastocyst completed developmental stages from three-cell to cavitating on average 20.2 hours later than embryos not developing to blastocyst. The differences were not significant***

Figure 6.12 shows the mean time spent at each developmental stage in frozen embryos that arrested prior to the blastocyst stage versus those embryos that reached the blastocyst stage. The times were highly variable, and no significant differences were observed.

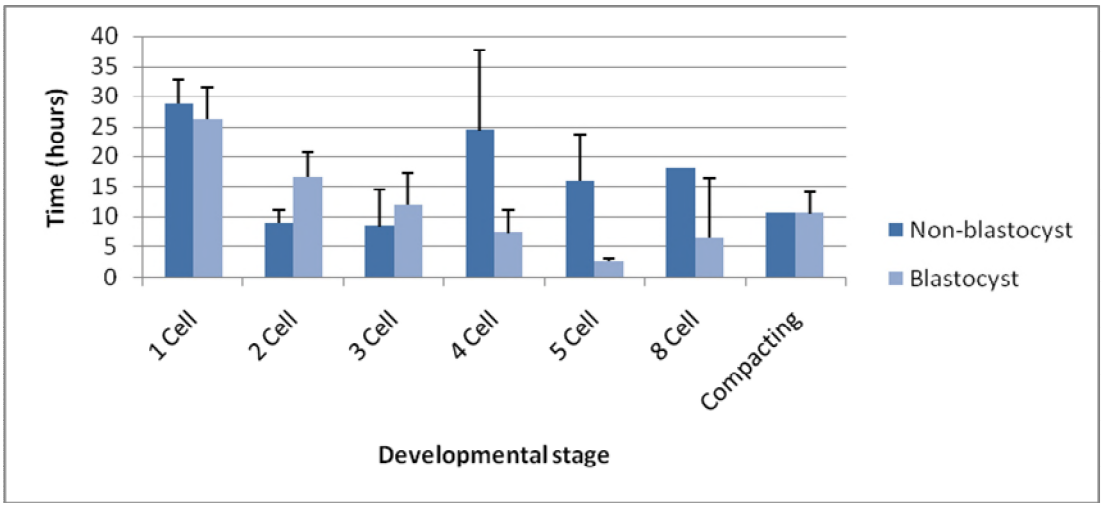


***Figure 6.12: Mean time spent at each developmental stage in frozen embryos not developing to blastocyst versus frozen embryos developing to blastocyst. Error bars represent the standard error of the mean. The times were highly variable, and no significant differences were observed***

### *6.4.6 Blastocyst hatching*

Analysis of the initial hatching sites in blastocysts, where hatching blebs were identified in relation to the position of the inner cell mass in fresh embryos on day 5 and day 6, showed that hatching is initiated by trophectoderm (TE) at various sites relative to the inner cell mass in an apparently unpredictable fashion *in vitro.*

Twenty three hatching blastocysts were observed following culture in the Embryoscope for five or six days post-insemination. Eight blastocysts hatched from the mural TE directly opposite the ICM, ten hatched near the ICM, and five hatched directly adjacent to the ICM. Occasionally, hatching blebs were observed at more than one site. Figure 6.5.1 shows examples of hatching sites (a) in close proximity to the ICM (b) opposite the ICM (c) at multiple consecutive sites.

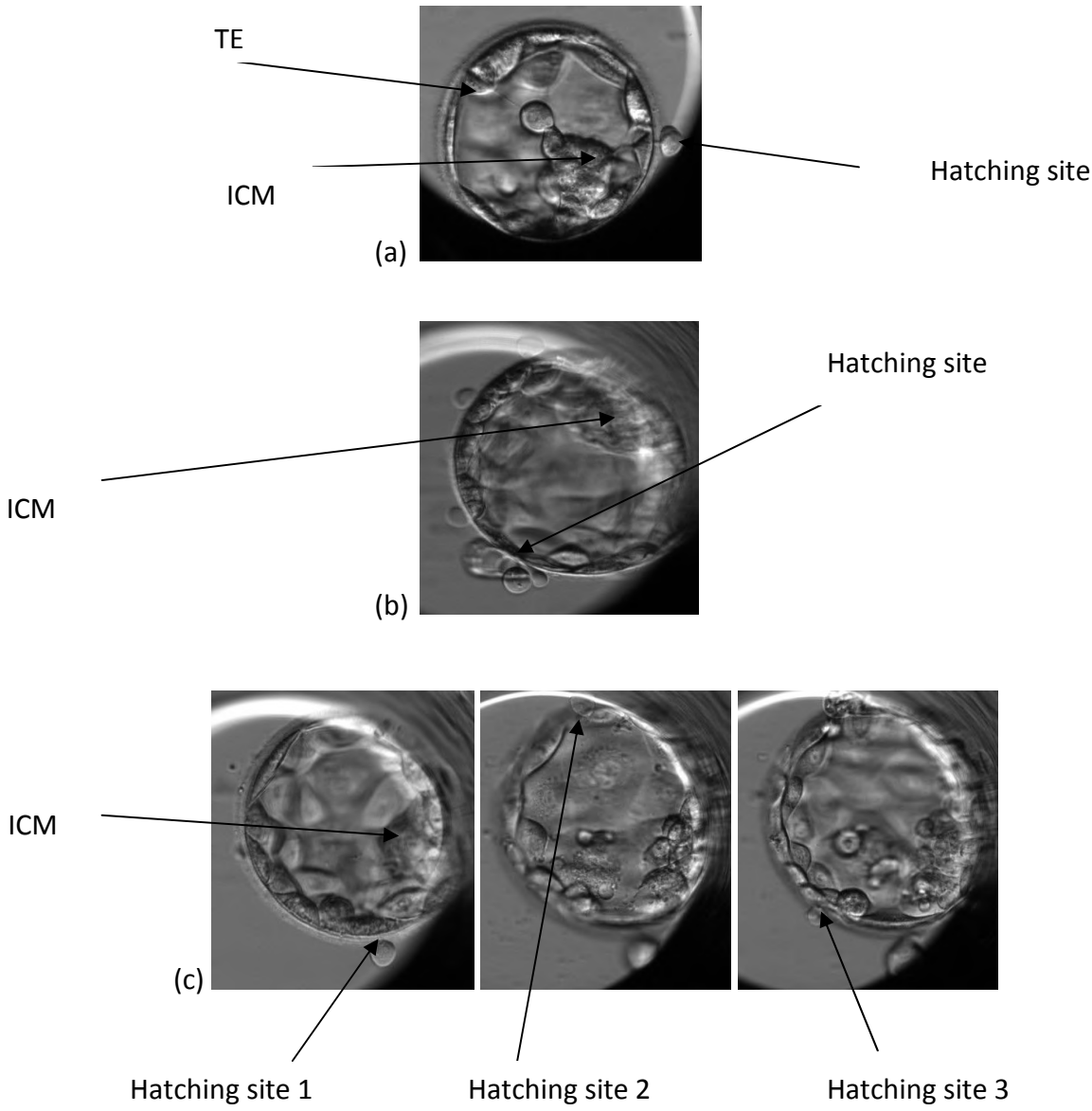


***Figure 6.13: Hatching sites in three different blastocysts (a) in close proximity to the ICM (b) opposite the ICM (c) at multiple consecutive sites***

Six of the hatching blastocysts observed were transferred in elective single embryo transfers, resulting in five pregnancies testing positive for urinary hCG two weeks later. Four fetal hearts were detected by abdominal ultrasound seven weeks post-transfer. There was no apparent pattern in the site of hatching in those blastocysts resulting in pregnancy compared to those that did not.

### *6.4.7 Development of human preimplantation embryos following blastomere damage*

Following deliberate damage to one or two daughters of the first-dividing cell at the 7-8 cell stage, all embryos (n=9) reached the compaction stage, 89% reached the cavitation stage, and 67% developed to blastocyst. In the control, non-damaged embryos (n=10) 47% reached the compaction stage, 33% reached the cavitation stage, and 27% developed to blastocyst.

Figure 6.14 shows the time to completion of each developmental stage in non-damaged, pre- damaged and post-damaged embryos. There were no significant differences between the groups.

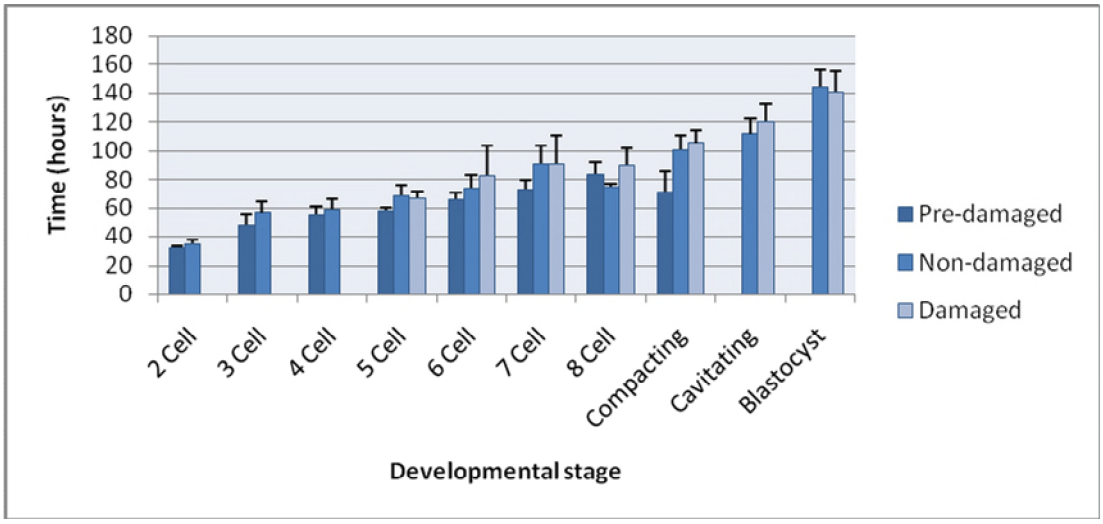


***Figure 6.14: Average time to cleavage completion in all non-damaged, pre-damaged and post-damaged embryos. Error bars represent the standard error of the mean. There were no significant differences between the groups***

Embryos utilised in these experiments were created using either standard IVF or ICSI. Figure 6.15 shows that the average cleavage completion times in non-damaged embryos created using IVF were slower than those created using ICSI at all stages of development, with significant differences seen at the 4-cell, 6-cell and 7-cell stages of development (p=*0.008; p**=0.001; p***=0.05; two-tailed t-test).

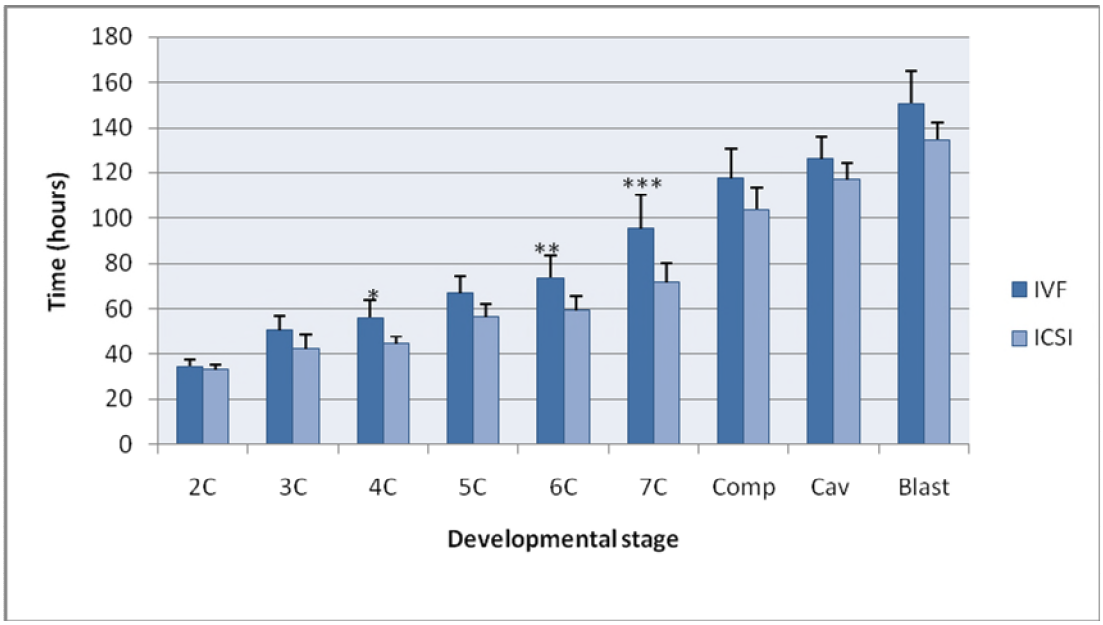


***Figure 6.15: Average time to cleavage completion in non-damaged embryos created with IVF versus ICSI. Error bars represent the standard error of the mean. The average cleavage completion times in non-damaged embryos created using IVF were slower than those created using ICSI at all stages of development, with significant differences seen at the 4-cell, 6-cell and 7-cell stages of development (p=*0.008; p**=0.001; p***=0.05; two-tailed t-test)***

Figure 6.16 shows the average completion times of the compacting and cavitating stages in damaged embryos created using IVF versus ICSI. The IVF embryos completed compaction and cavitation faster than ICSI embryos, in contrast to non-damaged embryos, although the differences were not significant.

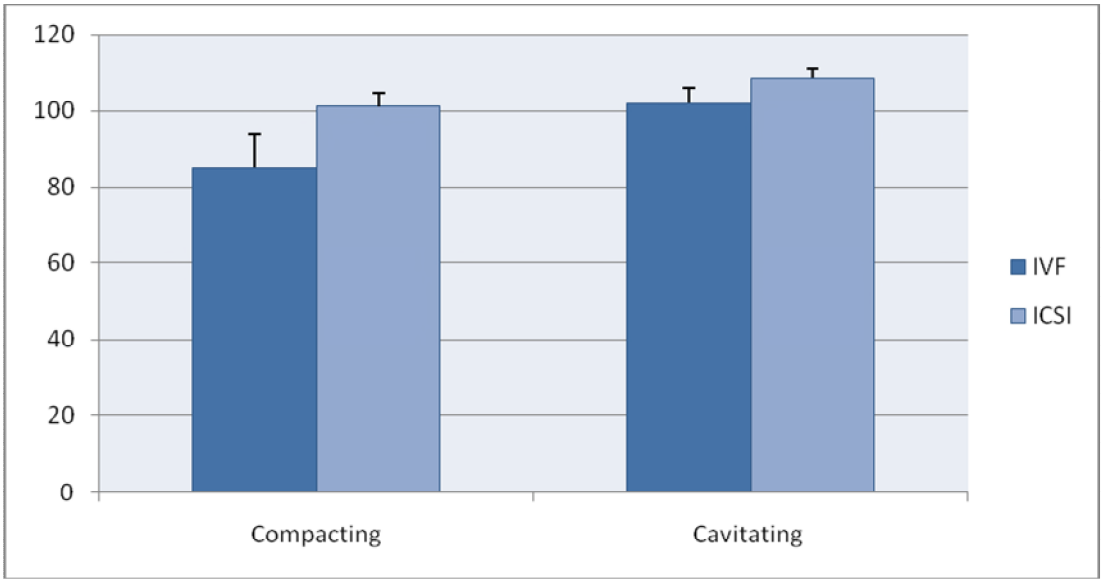


***Figure 6.16: Average time to cleavage completion in damaged embryos created with IVF versus ICSI. Error bars represent the standard error of the mean. The IVF embryos completed compaction and cavitation faster than ICSI embryos, in contrast to non-damaged embryos, although the differences were not significant***

Figure 6.17 shows the time spent at each developmental stage in pre- or non-damaged embryos compared to damaged embryos. Those with damaged blastomeres spent a similar period of time at all stages of development, but commenced compaction earlier and blastulation later than non-damaged embryos. These differences were not significant.

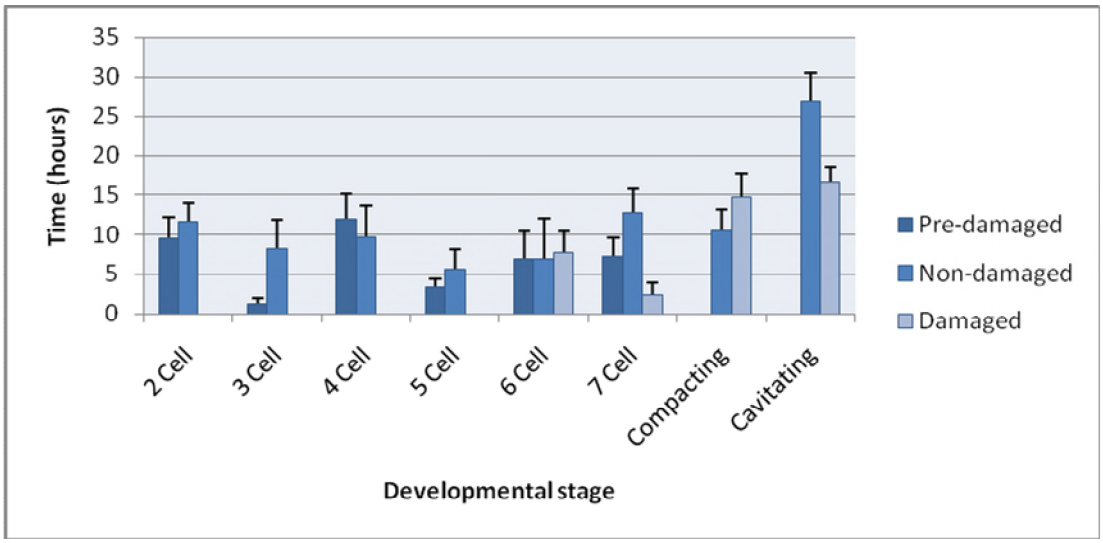


***Figure 6.17: Average time spent at each developmental stage in and pre- and non-damaged embryos in comparison to damaged embryos. Error bars represent the standard error of the mean. Those with damaged blastomeres spent a similar period of time at all stages of development, but commenced compaction earlier and blastulation later than non-damaged embryos. These differences were not significant***

### *6.4.8 Cleavage patterns in abnormally fertilised zygotes*

Figure 6.20 shows an interesting observation made during the first cleavage division of a tripronucleate into a two-cell embryo following the fusion of the three pronuclei and the formation of a “Y-shaped” centrally-located blastomere arrangement. Consequent fusion of two of the blastomeres resulted in the formation of a two-cell embryo which subsequently arrested. This embryo was observed using the Cell IQ system which was also trialled for embryo culture. It was determined as unsuitable because, first, the plate moved and so the embryo did not remain in a stable position for viewing, and second, because the focal plane was fixed, and third, because the gas control was suboptimal. However, it was a useful system for time-lapse observation of cell monolayers (data not shown).

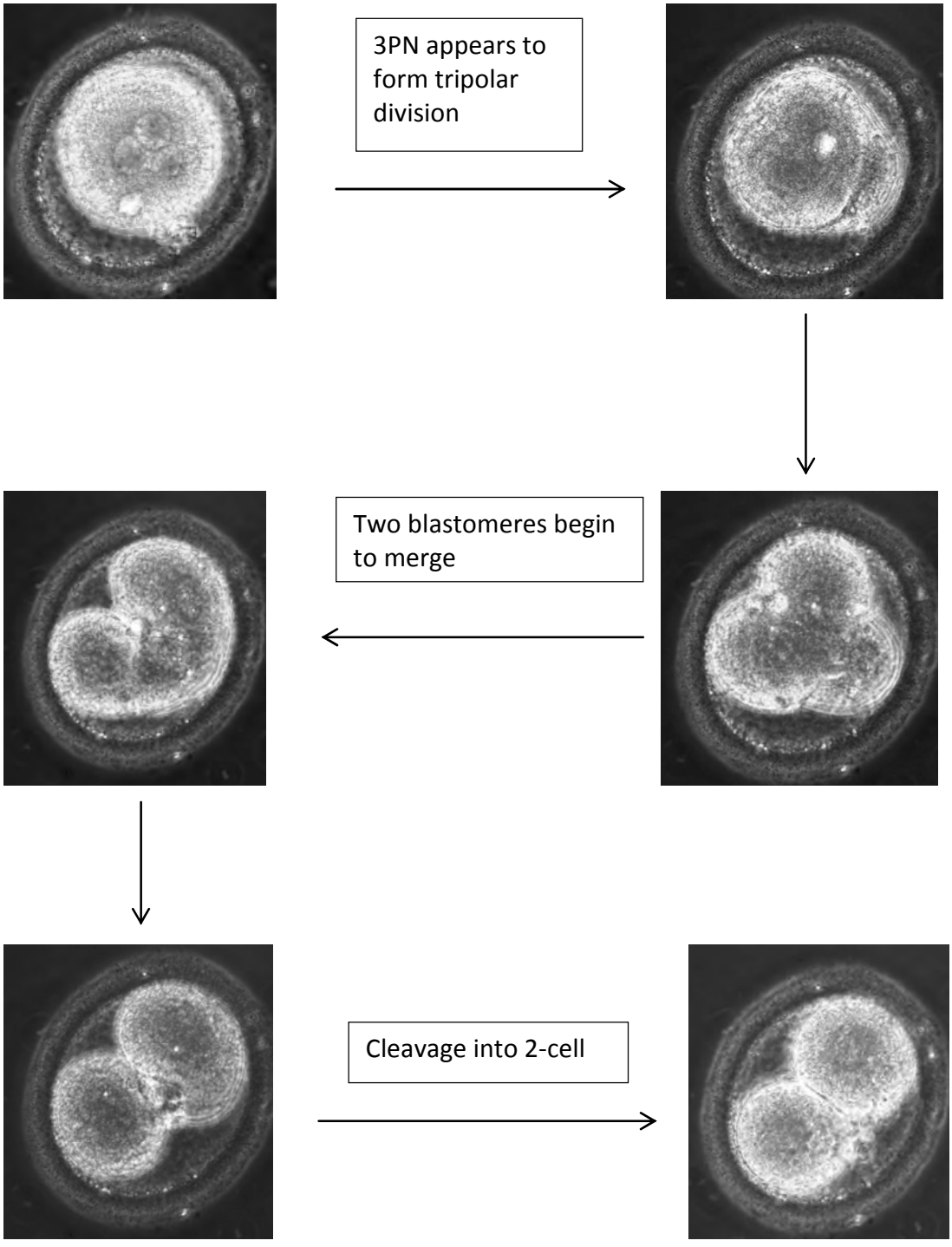


***Figure 6.18: Cleavage of a tripronucleate into a two-cell embryo***

A total of 47 abnormally fertilised fresh embryos were cultured in the Embryoscope (Fertilitech) for up to six days post-insemination, in order to determine whether their cleavage patterns differed from normally fertilised zygotes.

Figure 6.22 shows the mean cleavage completion times in fresh 1PN patient zygotes, multiple-PN (MPN) zygotes, and 2PN zygotes. No significant differences were observed between 1PN and MPN zygotes. Abnormally fertilised oocytes were significantly slower at completing compaction than normally fertilised oocytes (p=*0.0001; unpaired t-test). No other significant differences were noted.

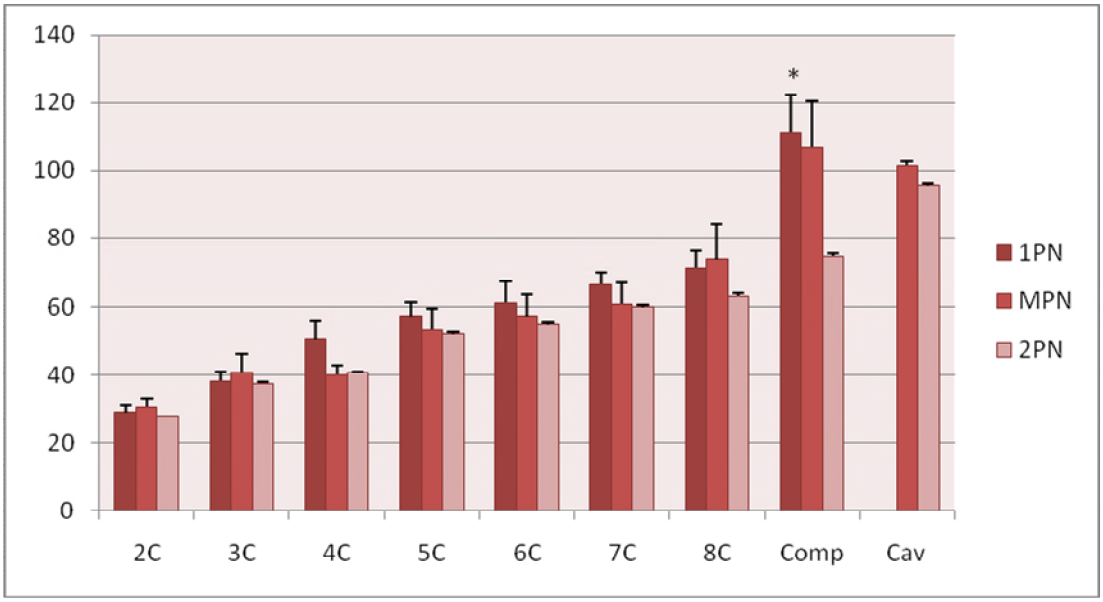


***Figure 6.19: The mean cleavage completion times in 1PN, MPN and2PN zygotes. Error bars represent standard error of the mean. No significant differences were observed between 1PN and MPN zygotes. Abnormally fertilised oocytes were significantly slower at completing compaction than normally fertilised oocytes (p=0.0001; unpaired t-test). No other significant differences were noted***

Figure 6.23 shows the mean time spent at each developmental stage in fresh 1PN patient zygotes, multiple-PN (MPN) zygotes and 2PN zygotes. There were no significant differences observed.

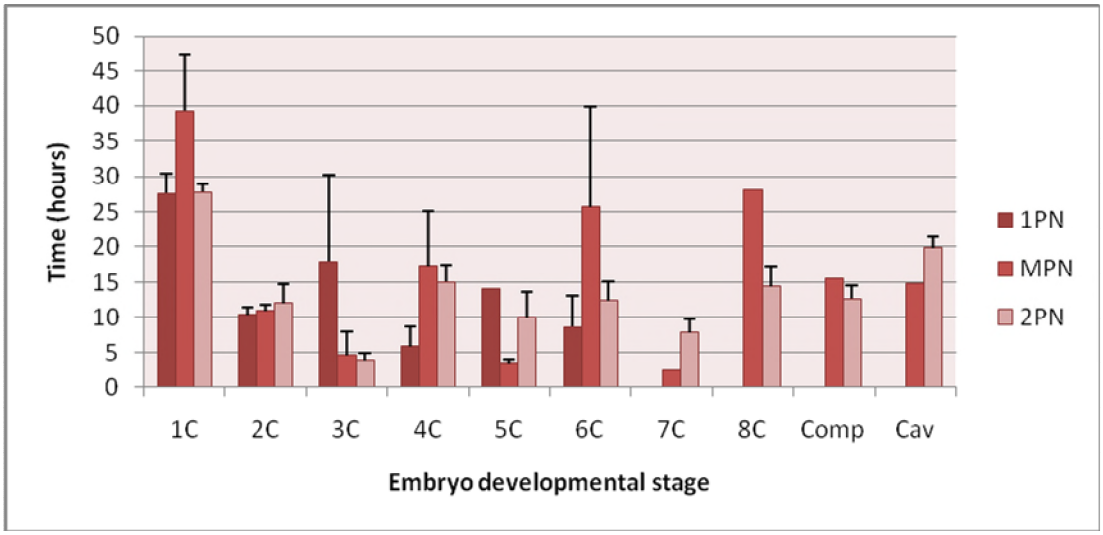


***Figure 6.20: The mean time spent at each developmental stage in 1PN versus MPN zygotes. Error bars represent standard error of the mean. There were no significant differences observed***

These results reinforce the importance of correctly identifying abnormally fertilised oocytes, and de-selecting them for uterine transfer, since early development of embryos derived from singular or multiple pronucleates is not noticeably aberrant when compared to normally fertilised oocytes.

## 6.5 *Discussion*

Time lapse imaging has been used for several years in research to study the temporal dynamics of embryo development (Payne *et al* 1997) although recently, advancements in technology have resulted in time lapse imaging being introduced into routine clinical laboratory practice (Kirkegaard *et al* 2012). Time-lapse monitoring of embryos at frequent intervals from fertilisation to blastocyst formation provides invaluable information regarding embryo kinetics that might otherwise be overlooked using traditional 24-hourly evaluation methods. It also allows precise measurement of the time at which key events in embryonic development take place, such as pronuclear appearance and disappearance, and specific cleavage divisions.

The variation in the timing of first cleavage in fresh zygotes into two-cell embryos (25-33 hours post insemination) has been previously noted (Capmany *et al* 1996), and cleavage of fresh zygotes into two-cells 25-29 hours post-insemination, is positively associated with achievement of clinical pregnancy (Shoukir *et al* 1997; Sakkas *et al* 1998; Lundin *et al* 2001; Bos-Mikich *et al* 2001), with slower-developing embryos having less prospect of initiating pregnancy. The time taken to complete cleavage from one-cell into two-cells in fresh embryos developing to blastocyst was significantly faster than in those not developing to blastocyst (24.9±2.9 vs 27.4±3.5 hours), which supports the use of early cleavage as an indicator of embryo viability. In addition, completion of division from three-cells to four-cells was significantly

faster in fresh embryos developing to blastocyst versus arresting embryos (35.8±3.0 vs 39.3±5.7 hours). Meseguer *et al* (2011) reported that fresh embryos that went on to form blastocysts spent a significantly shorter time at the one-cell stage than embryos that did not form blastocysts, and furthermore the time taken to complete cleavage from two to three cells, three to four cells, and four to five cells, was significantly positively associated with implantation (Meseguer *et al* 2011).

In my study, the incidence of blastocyst formation in fresh and frozen embryos was 34% and 29% respectively, similar to results reported elsewhere (Dal Canto 2012). Both fresh and frozen embryos that did not form blastocysts, arrested at a range of developmental stages from two-cell to cavitation, however, the majority arrested between two- and eight-cells, in concordance with Wong *et al* (2010).

The mean time to completion of cleavage of fresh one-cell two-pronucleate zygotes into two cell embryos was 26.4 (±3.44) hours, which is in agreement with previously published data (Bos-Mikich *et al* 2001), and in frozen-thawed pronucleates was 33.8 (±6.8) hours. This delay observed in cryopreserved pronucleate embryos is in contrast to other authors who reported that cryopreservation did not retard human embryo development (Wong *et al* 2010). My study utilised a lower number of embryos than Wong et al (2010) because the availability of frozen pronucleate embryos for use in research was limited due to changes in cryopreservation policies. However, when cleavage stage embryos which had divided into 2-8 cells prior to cryopreservation were included for temporal developmental analysis, a slower rate of further cleavage was also observed. Interestingly, Macas et al (1998) reported significantly slower cleavage in frozen-thawed ICSI-generated zygotes in comparison

to frozen-thawed IVF-generated zygotes, a difference not noted in non-frozen zygotes (Macas*et al* 1998). The authors postulated that the mechanism of cell division was adversely affected due to freezing after syngamy had occurred in some of these zygotes (Macas*et al* 1998). This appears to contradict an earlier study by Wright *et al*, which found that a significantly higher number of zygotes frozen at ≥ 29 hours after oocyte retrieval went on to implant in comparison to zygotes frozen <29 hours after oocyte recovery. They suggested that this may be due to the completion of pronuclear migration prior to syngamy, and the concomitant embryonic organisation and implanting capacity of the zygote (Wright *et al* 1990).

In my study, frozen embryos were slower to complete all cleavage stages and blastocoel formation compared to fresh embryos, and these timings were significantly slower during the first three cleavages from one to two-cell (42.2±18.7 vs 26.4±3.4 hours), two to three-cell (53.4±19.4 vs 35.7±7.6 hours), and three to four cell (54.5±22.1 vs 38.1±5.2 hours). Frozen embryos developing to blastocyst completed all divisions from three-cell to eight-cell stage on average 19.7 hours later, compaction 15.3 hours later, and cavitation 28.1 hours later than embryos not developing to blastocyst. However, when the absolute cleavage timings between fresh and frozen embryos were compared, there were no significant differences. The lack of significance of these results is most likely due to the high variability in cleavage completion times in frozen-thawed embryos. The putative developmental delay of frozen-thawed embryos compared to fresh embryos observed in the time to each stage of cleavage completion in this project may be indicative of an adverse effect of cryopreservation on embryo development in humans, similar to that

observed in mice (Uechi*et al* 1997), but is most likely due to different culture conditions and the time taken to freeze and thaw the embryos. Additionally, human frozen-thawed embryos have been previously seen to develop at a slower rate than fresh embryos, regardless of their chromosomal status, although implantation rates were not different after fresh or frozen embryo transfer (Edirisinghe *et al* 2005).

In addition, it has been reported that the time taken for embryos to initiate compaction and blastulation was significantly slower in aneuploid embryos in comparison to euploid embryos (Campbell *et al* 2013). It has been reported that cryopreservation may induce mitotic chromosomal abnormalities in human embryos (Iwarsson *et al* 1999) which could partly explain the delay in frozen-thawed embryo development that I observed.

In this project, frozen-thawed embryos were significantly more likely to arrest at the 1-4 cell stages when compared to fresh embryos. However, the frozen embryo cohort included partially intact embryos with ≥50% surviving blastomeres. Since the implantation potential of frozen-thawed embryos is related to the post-thaw cell survival (Edgar *et al* 2000; Guerif *et al* 2002) and resumption of mitosis after thawing (Guerif *et al* 2002; Van Landuyt *et al* 2013; Gallardo *et al* 2016), it follows that the inclusion of the partially intact embryos in this analysis may have had an influence on the results observed. A significantly reduced implantation rate has been reported following transfer of partially intact embryos compared to fully intact embryos (Van den Abeel *et al* 1997; Edgar *et al* 2000; Guerif *et al* 2002). Furthermore, a maximum of 89% of partially intact frozen-thawed embryos resume cleavage following thawing and overnight culture (Van Landuyt *et al* 2013; Gallardo

*et al* 2016), therefore those embryos with damaged blastomeres, and those which did not resume mitosis after thawing will have had an impact on the number of arrested embryos at this early stage of development. Nevertheless, the similarities in developmental arrest in the 4-8 cell, compaction, and cavitation stages echo the findings that post-thaw embryos that continue to cleave have an implantation potential comparable to fresh embryos (Edgar *et al* 2000).

Little research has been conducted on the effect of freezing on subsequent cleavage patterns, although frozen-thawed cleavage stage embryos that continued to divide during a 24 hour culture period post-thaw were significantly more likely to result in a live birth after uterine transfer, compared to those not cleaving during the same period (Van der Elst *et al* 1997; Guerif *et al* 2002). These studies stipulated that one or more blastomeres must have divided during the time between thawing and transfer (24 and 20 hours respectively), but these authors did not include details of the number of divisions that the embryos completed, and it is not clear how quickly the embryos were cleaving, however it appears that frozen embryos that do not display further cleavage after thawing do not have the capacity to implant (Van der Elst *et al* 1997). The time to completion of cytokinesis, defined as the final step before full division into separate blastomeres, and the time between appearance of the cleavage furrow and completion of cleavage into two distinct daughter cells, have been shown to be predictors of blastocyst development in frozen-thawed embryos (Wong *et al* 2010). The results in this study suggest that cleavage completion times are an indicator of embryo viability. Synchronous divisions have been associated with significantly higher chances of implantation (Lemmen*et al*

2008). Thus, embryos cleaving from 2 cells to 4 cells, or from 4 cells to 8 cells, within a short time period are considered to have synchronous cleavages.

Both fresh and frozen embryos remained at developmental stages involving even cell numbers significantly longer than those stages involving odd numbers. Fresh embryos that developed to blastocyst spent a significantly shorter time at the one-cell stage than those that did not develop to blastocyst, confirming the results of Sakkas *et al* 1998. These embryos also spent a significantly longer time at the seven-cell stage, supporting the idea that synchronous division is associated with embryo viability, and in agreement with previous findings published by Meseuger *et al* (2011).

There were no such significant differences observed in the time spent at each developmental stage in frozen embryos that developed to blastocyst in comparison to those that did not develop to blastocyst, and the times were highly variable. This may be explained by the relatively low number of embryos in this group compared to the fresh group, as well as the potential chromosomal disturbances caused by cryopreservation (Iwarsson *et al* 1999). An increase in aberrant cell cleavage times is thought to be related to the different numbers of chromosomes present in the blastomeres of euploid versus aneuploid human embryos, which have variable chromosome segregation timings, manifesting as diverse cell division timings (Chavez *et al* 2012).Therefore it is possible that cryopreserved embryos may exhibit more asynchronous divisions, as previously seen in aneuploid embryos (Apryshko*et al* 2010), and may explain the differences observed between fresh and frozen embryos in this project.

Oocytes inseminated via conventional IVF are reportedly slower to cleave than their ICSI-inseminated counterparts (Plachot 2000; Lemmen *et al* 2008).This is thought to be due to the necessity of the sperm to infiltrate the cumulus cell complex, bind to the ZP and penetrate the oolemma during standard IVF. During ICSI, these steps are circumvented by removal of the cumulus cells, mechanical breach of the zona pellucida, and direct injection of the sperm into the ooplasm (Cruz *et al* 2013), resulting in a 2-4 hour difference in the timing of pronuclear fading and time to first cleavage between IVF and ICSI embryos (Plachot 2000). The results in this study confirm these findings, with frozen embryos created using ICSI cleaving significantly faster from the two-cell to the four-cell stage than frozen embryos created using IVF.

Early events in embryo cleavage lay the foundations for later development. For example, it is reported that the orientation of the first cleavage division along the AV axis tends to be perpendicular to the embryonic-abembryonic axis of the future embryo (Bischoff *et al* 2008). Furthermore, following the first cleavage division along the meridian of the pronuclear axis, the first dividing blastomere of the newly formed 2-cell will form a cleavage furrow along the meridian axis prior to division into daughter cells which pass through the embryonic and vegetal poles. The second-cleaving blastomere then rotates and divides transversely, resulting in the classical “crosswise” 4-cell arrangement observed in normally cleaving embryos (Edwards and Beard 1997). Further evidence that that cleavage planes are regulated rather than random is apparent from the observation that asymmetrically dividing cells contribute more frequently to the ICM than the TE in mice (Bischoff *et al*

2008). It is therefore possible that blastomeres rearrange themselves within the ZP in order to position themselves in the correct orientation for subsequent cleavage and distribution of cells into ICM or TE lineages. Those embryos with blastomeres in the incorrect orientation due to a lack of reorganisation of cells may potentially be more prone to delayed or non-existent establishment of polarity and consequent embryonic developmental arrest and lethality, thus explaining the differences observed in blastomere rearrangements in cleaving versus non-cleaving embryos. The ability of embryos to develop to blastocyst is not adversely affected following deliberate damage of the daughters of the first dividing cell, and in fact this appeared to improve blastocyst formation. This may be due to the distinct sample population used, since all embryos in this experiment were frozen surplus embryos from clinical ART cycles, and were therefore good quality, and not necessarily representative of a typical embryo cohort. Nevertheless, these findings are in agreement with previously published data, which reported that the biopsy of one to three blastomeres of the eight-cell embryo did not adversely affect human preimplantation development *in vitro*, with an increase in blastocyst formation observed in the biopsied group compared to the intact group (Hardy *et al* 1990). Later studies appeared to confirm the results of Hardy *et al* (1990), reporting that biopsy of one, two or three cells from embryos initially containing between four and seven cells does not impede developmental competence (Van de Velde *et al* 2000), and the removal of one or two cells from day three embryos at the six-cell to compacting stages of development does not affect live birth rates (Goossens *et al* 2008). However, others dispute this, reporting significantly reduced blastocyst

formation originating from eight-cell embryos with two cells removed compared to intact controls, and significantly reduced live birth rates compared to embryos with one cell removed (De Vos*et al* 2009). I had hypothesised that this discrepancy might be due to the unequal nature of blastomeres at the 8-cell stage; however, my experiments have shown that destruction of the two leading cells in an 8-cell embryo is not detrimental.

The time to completion of all stages of development was similar in post-damaged embryos compared to non-damaged embryos, in agreement with a previously published report, which found no differences in the time to completion of the two- to the eight-cell stage in biopsied versus non-biopsied embryos (Kirkegaard *et al* 2012). There was an interesting difference observed in the time to completion of the compaction and cavitation stages in embryos created using standard IVF in comparison to ICSI, whereby the IVF embryos completed these stages faster than ICSI embryos. This is in contrast to the usual pattern of IVF embryos cleaving at a slower pace than ICSI embryos, and may be due to the embryos "catching up" following damage of cells at the cleavage stage. The time spent at each developmental stage from the five-cell to the expansion of the blastocoel was not significantly different in damaged versus non-damaged embryos. This is in contrast to Kirkegaard *et al* (2012), who found that embryos spent significantly longer at the stage at which they were biopsied, although all other stages were not different.

In this project cells were damaged by aspiration of the cytoplasm rather than completely removed, thus the results may be more comparable to post-thaw blastomere degeneration than biopsy, and there remains a possibility that the

detritus of the damaged cells affected the surviving cells of the embryo, resulting in altered cleavage patterns. It is important to note that damaging the cells by piercing with an ICSI injecting needle prior to removing the cytoplasm may not be the ideal model for blastomere biopsy, since some cellular products may remain due to the leakage following membrane rupture. Studies investigating the viability of day 2 frozen-thawed embryos found significantly higher implantation, clinical pregnancy, and live birth rates following transfer of fully intact frozen-thawed cleavage stage embryos in comparison to partially intact frozen-thawed cleavage stage embryos, suggesting that the co-existence of damaged and non-damaged blastomeres is detrimental to embryo implantation potential (Van den Abeel *et al* 1997; Guerif *et al* 2002). These results were in agreement with the finding that fully intact day 2 frozen-thawed embryos had implantation rates comparable to their fresh counterparts, and significantly higher than the partially intact day 2 frozen-thawed embryos (Edgar *et al* 2000). It is therefore possible that, although the blastocyst development rate of the embryos in this project was apparently unaffected by blastomere damage, the implantation potential of those embryos may have been compromised. Since these blastocysts were fixed and not transferred, this remains unknown. Furthermore, the cytoplasm from the damaged cells in this study was removed by aspiration rather than left within the embryo, which may have lessened the deleterious effects. The toxic effect of damaged blastomeres on the intact blastomeres is reportedly increased at earlier developmental stages (2-cell and 4-cell) (Van den Abeel *et al* 1997), and therefore the impact of damaged blastomeres may have been lower in these experiments, since damage occurred at the 7-cell and

8-cell stages. Interestingly, the implantation potential of day 3 fully intact and partially intact frozen-thawed embryos was similar, providing that mitosis resumed in the 24 hours following thawing (Van Landuyt *et al* 2013), although this is not in agreement with a more recent study, which found that fully intact day 3 embryos had a significantly higher implantation rate than partially intact day 3 embryos, even if a post-thaw resumption in mitosis was observed (Gallardo *et al* 2016).

Some studies have reported aberrant behaviour in blastocysts derived from biopsied embryos around the time of hatching in mice (Ugajin *et al* 2010) and humans (Kirkegaard *et al* 2012). In this project, however, the blastocysts were fixed on day five or six for use in immunofluorescent labelling experiments, as described in section 2.11. Therefore, it is not possible to assess the effect of cell damage on hatching in these embryos.

As far as is known, this is the first study to identify and damage specifically the daughters of the first dividing cell and monitor the ongoing development of the embryo thereafter. Ideally, further work to identify and damage the daughters of the slowest dividing cell would be performed to assess whether a different effect on embryo development was apparent. This may provide valuable information regarding which blastomeres to remove prior to PGD after time lapse monitoring. Unfortunately, the limited availability of human cleavage stage frozen embryos, combined with a change in clinical practice, did not allow for these further studies.

The mechanisms of blastocyst hatching *in vitro*, in the absence of endometrial influences, are reportedly different to those hatching *in vivo* (Gonzales and Bavister

1995). Human blastocysts have previously been observed as usually hatching away from the ICM pole (Sathananthan 2003), however, the blastocysts in this study had seemingly unpredictable hatching sites, which were not indicative of subsequent pregnancy. This observation is in agreement with the findings of one group, who concluded that implantation, pregnancy and live birth rates were not influenced by the site of assisted hatching in vitrified-warmed blastocysts (Ren *et al* 2013). Transfer of spontaneously hatching or hatched blastocysts resulted in a significantly higher pregnancy and live birth rate when compared to transfer of non-hatched, expanded blastocysts in clinical practice (Chimote *et al* 2013). These results accord with my observation of an 80% pregnancy rate after transfer of a single hatching blastocyst, however the number of cases was small.

In this project, F-actin has been shown by immunofluorescence to form part of the structural cytoskeleton of individual cells in the human embryo (see chapter four). The actin cytoskeleton provides support to maintain the shape of cells, and is reorganised during and after mitosis to promote centrosome separation and completion of cell division (Heng and Koh 2010). Disruption of the integrity of the actin cytoskeleton due to cryopreservation of mouse embryos has been demonstrated to adversely affect embryo development beyond the first cleavage, hypothesised to be due to increased rigidity of the cytoskeleton (Hosu *et al* 2008). Therefore, it is possible that a disorganised cytoskeletal structure prevents mitosis and leads to embryonic arrest, as implied by the lack of membrane oscillations in non-cleaving embryos in these experiments.

It has been previously reported that the viscosity of the ooplasm is correlated with embryonic development and pregnancy rate, whereby oocytes with less viscous cytoplasm develop into superior quality blastocysts and result in a higher incidence of clinical pregnancy (Ebner *et al* 2003). This is thought to be due to the promotion of microtubule organisation and movement of pronuclei through the ooplasm to their central abutting position prior to syngamy (Ebner *et al* 2003). The pattern of cytoplasmic movements in newly-fertilised mouse oocytes has been shown to be an indicator of embryo quality, where faster cytoplasmic movements were predictive of cell number on day four of development and live birth potential (Ajduk*et al* 2011). Therefore, the cytoplasmic movements observed in the cleaving embryos in this project may be indicative of a less viscous cytoplasm pertaining to the correct organisation of intracellular microtubules necessary for the advancement of mitosis in viable embryos.

Cleavage of tripronucleate zygotes may involve an apparently normal division pattern, with cleavage into two cells then four cells, however others have been observed to divide into two cells with a simultaneously extruded cytoplasmic mass, which does not participate further, resulting in a diploid embryo (Kola *et al* 1987). Time lapse monitoring has allowed much greater insight into the complexities of embryonic behaviour than previously realised. Many tripronucleate zygotes exhibit a unique cleavage pattern, dividing directly into three equivalent sized cells via a tripolar spindle, with chromosomes arranging into a Y-shape in the centre of the zygote, although further division of these blastomeres involves bipolar spindles, so the embryo then divides from 3-cell to 6-cell to 12-cell. The unusual pattern of

division seen in figure 6.21, whereby the embryo formed a tripolar spindle but actually cleaved into two distinct cells upon completion of cytokinesis, would not have been observed without the use of time lapse imaging, and the embryo may have been scored as a regularly dividing two-cell during assessment, despite the presence of a tripolar spindle. One recent study reported that normally fertilised zygotes cleaving directly from one cell into three cells were significantly less likely to implant compared to those cleaving from one cell into two cells, prompting the authors to recommend disregarding such embryos when selecting which to transfer (Rubio *et al* 2012). Therefore, the use of time lapse imaging may prove invaluable in identifying abnormally developing, and therefore non-viable, embryos. This may improve clinical ART success rates via the avoidance ofsuch embryos in the process of choosing embryos for uterine transfer.

In conclusion, cleavage timings and blastomere activity in human preimplantation embryos can be used as a predictor of viability. Cryopreservation may delay post-thaw embryo development, whilst the percentage of surviving cells after thawing is more indicative of subsequent development than the number of cells at the time of freezing. The site of hatching in preimplantation blastocysts with respect to the location of the ICM is not predictive of pregnancy outcome. Damaging the daughters of the first-dividing cell does not adversely affect ongoing embryo development in good quality embryos. Abnormally fertilised oocytes do not display significantly different cleavage timings during development to the blastocyst stage. Time lapse monitoring is a useful tool to aid the identification of the most viable

embryos, and may prove invaluable in improving implantation and live birth rates in clinical IVF treatment cycles.

# Chapter Seven

## Developing a computer-assisted model of embryos at different stages of preimplantation development

# Chapter Seven

# Developing a computer-assisted model of embryos at different stages of preimplantation development

## 7.1 *Introduction*

The use of computer software for the development of advanced image processing systems has led to an increase in the application of digital imaging to human medicine. Medical visualisation describes the generation of three-dimensional (3D) models using digital algorithms, based upon living specimens, to increase the understanding of biological structures and their functions (Klauschen *et al* 2009).

Commonly used image processing techniques include segmentation, thresholding and 3D reconstruction. Segmentation is the division of an image into smaller distinct regions that share certain detectable characteristics, such as cell nuclei, using boundaries to create a set of separated images from which data may be obtained (Chalana and Kim, 1997). Segmentation of cell nuclei is notoriously difficult due to the non-uniform distribution, overlapping, and clustering of some nuclei (Oritz De Soloranzo *et al* 1999). Thresholding involves isolating the image proper from the background noise by identifying an upper and a lower pixel threshold, and comparing each region of interest with the pre-determined threshold values (Chang *et al* 2000). Edge detection segmentation can be used to create three dimensional images, and combined with three dimensional rendering, allows for detailed analysis of image structures (Rogowska 2000).

The number, shape and size of individual blastomeres and cell nuclei in human preimplantation embryos are markers of quality, and high developmental potential is indicated by embryos with symmetrical cell division, equally sized spherical blastomeres (Racowsky *et al* 2010), and a single regularly shaped nucleus per cell (Kort *et al* 2015). Measurement of blastomere size using static, multi-plane, semi-automated morphology assessment software has provided evidence that an increasing degree of fragmentation is correlated with a significant decrease in cell size, and multinuclearity is related to an increased cell size (Hnida *et al* 2004). However, more precise and sophisticated markers are necessary in order to aid in identifying the most viable embryos in a cohort.

The nuclear to cell volume ratio remains constant in normally dividing cells, even when the cell size is altered as a result of cell cleavage. However, the mechanism by which the cell to nuclear volume ratio is controlled is unclear, and disturbance of the ratio may be indicative of abnormal or unequal cell cleavage resulting in retarded embryo development (Webster *et al* 2009). Therefore, visualisation of the number, shape and size of blastomeres and nuclei provides valuable information about the potential viability of the embryo, and may help us to understand the mechanisms of developmental failure.

A fourth dimension, namely 'time', is also a critical factor in assessing embryo quality and potential for pregnancy because the timeliness of specific stages of development is important to coordinate with the endometrial preparation for receptivity and the woman's menstrual cycle. Hence, there is increasing use of spatio-temporal imaging in the clinical IVF laboratory. Consequently, time lapse

monitoring of human preimplantation embryo development is increasing, and the volume of data available from these images is potentially huge. However, annotating Embryoscope™ time lapse images is time consuming and subjective, and carries a high intra-operator variance (Sundvall *et al* 2013). Fully automated cell tracking systems, such as Eeva™ are also not completely reliable, particularly when abnormally cleaving or highly fragmented embryos are being monitored, and often embryologists are required to manually input cell cleavages to obtain a more accurate result. In addition, concerns remain about how completely any fully automated system can replicate the decisions and interpretations that would be made by a trained and experienced human operator. There is also concern that computer-generated algorithms cannot be safely applied across all laboratories, since there are many variables, including culture media systems and incubation conditions (Mantikou *et al* 2013; Swain 2014). The implementation of a semi-automated system may be the ideal solution, affording the clinical team a time-saving option, whilst still requiring human input in ambiguous cases, thereby allowing embryo development to be more accurately tracked.

## *7.2 Aims*

The aims of this chapter are:

To explore different options for computer-assisted image analysis of human embryos at different stages of development and using different of image types.

To apply the most effective semi automated computer-assisted options to investigate the nuclear to cell ratio in cleavage stage human preimplantation embryos, and the nuclear volumes of different cell lineages in blastocysts, using data derived from a semi-automated computer programme developed in collaboration with colleagues at the Warwick Digital Laboratory, and Manchester University School of Computing.

## *7.3 Methods*

Fixed and stained human oocytes and preimplantation embryos were imaged using confocal microscopy with standardised settings, as described in section 2.12, and exported to Dr Silvester Czanner at the Warwick Digital Laboratory for processing, alongside his own research group. I worked closely with Dr Czanner's group, to generate models that were intended to closely correspond to the biological and clinical interpretation of the embryo images. The first student involved was University of Warwick undergraduate James Michael, who began to set up methods to process the images that I provided. Figure 7.1 shows the flowchart constructed by James to summarise the procedures involved in the image processing pathway.

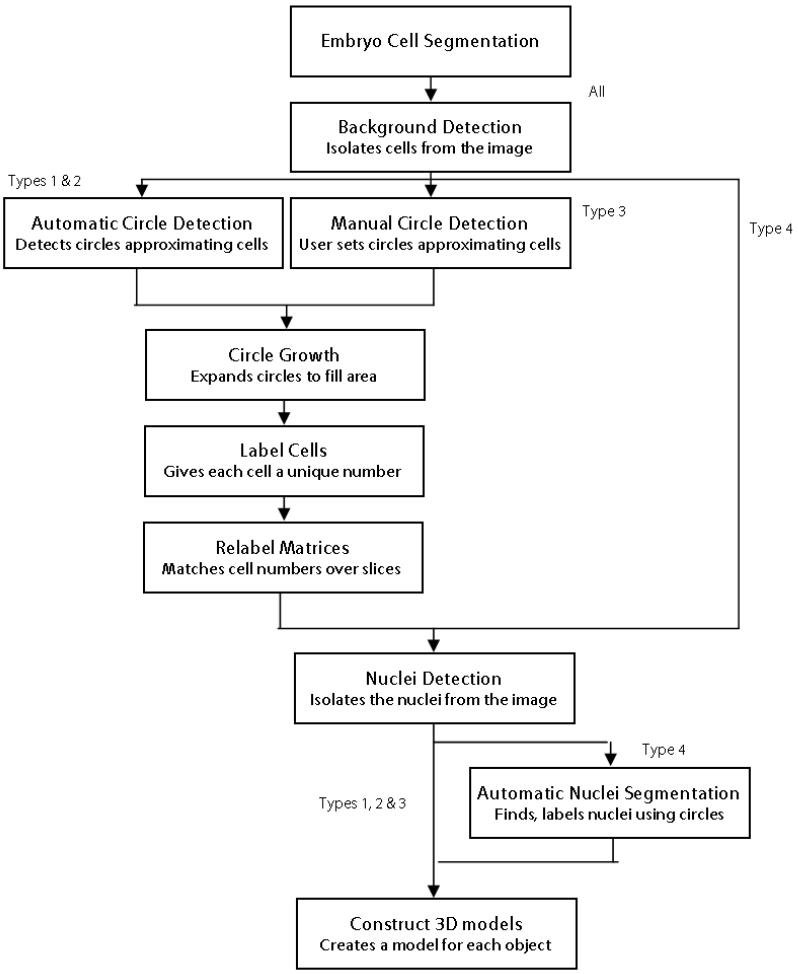


***Figure 7.1: Flow chart depicting the procedures involved in creating three-dimensional models of human preimplantation embryos from confocal images.***

***Courtesy of James Michael.***

### *7.4 Results*

The early intention of this project was to create a three-dimensional (3D) virtual embryo using data derived from confocal image stacks of preimplantation human embryos labelled with fluorescent probes. After fixing and labelling the embryos, as described in section 2.11, I obtained multi-plane images using confocal microscopy (see section 2.12). Data for a single embryo was available as a series of colour TIFF files, each 512 pixels square. These images were stored together in individual directories, and each image corresponded to a separate location on the z-axis. In each original confocal image, blastomeres were coloured green (FITC), nuclei blue (DAPI), and the background black. Each image is associated with a degree of background noise as a result of out of focus fluorescence, which interferes with the image resolution. Therefore, there is a need to pre-process the data to remove noise and isolate the blastomeres from the background.

### *7.4.1 Segmentation of the embryo*

This section details the early attempts at edge detection and segmentation of the images, and refinement of the process to improve output. Segmentation of human preimplantation embryos began with simple single-cell images and progressed to images of multi-cellular embryos, as shown in figure 7.2. Figure 7.2 (a) and (b) shows the results of background detection (red line), additional edge detection (pink lines), concave point detection (cyan circles), segmentation by connecting concave points (white line), and detection of nuclei (yellow lines), with varying results. Figure 7.2 (b) shows good segmentation of the cell boundary and chromatin-containing bodies, although the polar body visible at the 11 o'clock position has not been correctly identified as being separate from the cell. Figure 7.2 (c) shows reasonable outer edge detection for the blastomeres, but poor segmentation. The blastomeres are separated by manual segmentation, although this is a poor attempt, limited by the sensitivity of the mouse. Background noise in the centre of the image shown in 7.2 (d) caused some incorrect pixel readings, leading to inaccurate image segmentation, whilst better results were attained when the background noise was reduced, although further reduction of the background noise resulted in one of the blastomeres not being fully segmented. Figure 2.7 (e) demonstrates the effect of a large amount of background noise, caused by confocal detection of the blue colour of the DAPI mounting media. This also makes detection of the nuclei difficult. Although the cell edges were detected in this image, the result is generally poor. The image represented in figure 7.2 (f) also had a large

amount of blue background noise; however by adjusting the parameters, a much improved result could be achieved. Although the edges of all blastomeres were separated from the background in this image, the cell boundaries were not fully segmented. Adjustments to further refine the segmentation tool shows a successfully segmented two-cell embryo, as shown in figure 7.2 (g).

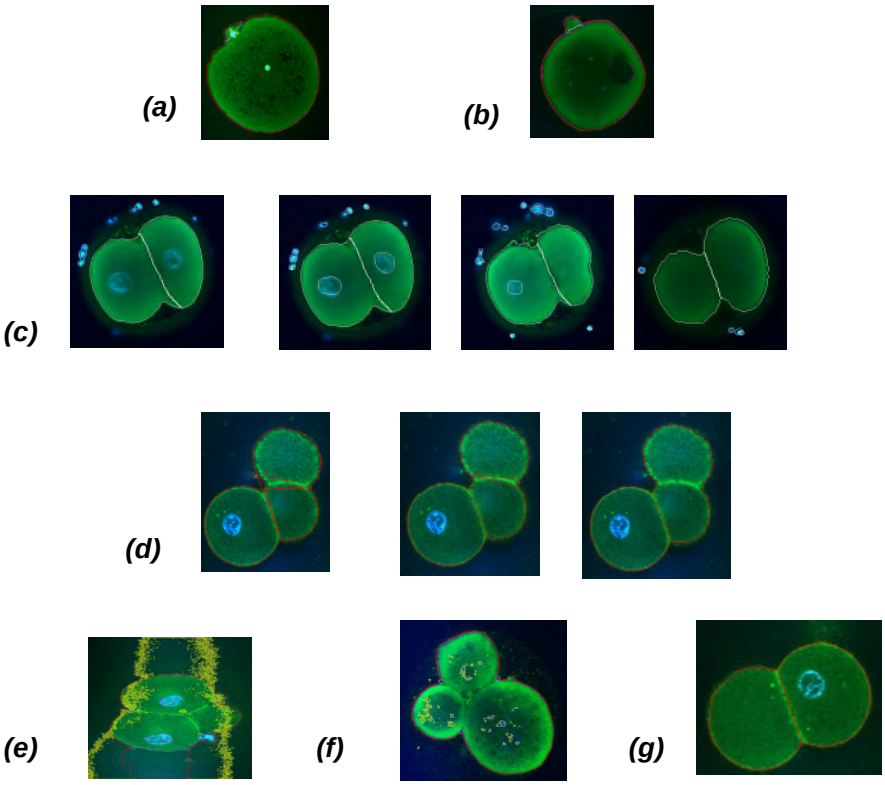


***Figure 7.2: Segmentation of confocal images of human preimplantation embryos at various stages of development.***

Figure 7.3 (a-c) shows early results of the edge detection method on confocal images of fluorescently labelled blastocysts, showing poor detection of the whole cells due to low contrast between cellular and background fluorescence, but well-detected nuclei. Figure 7.3 (d) is an attempt at background detection of an early blastocyst using an alternative technique.

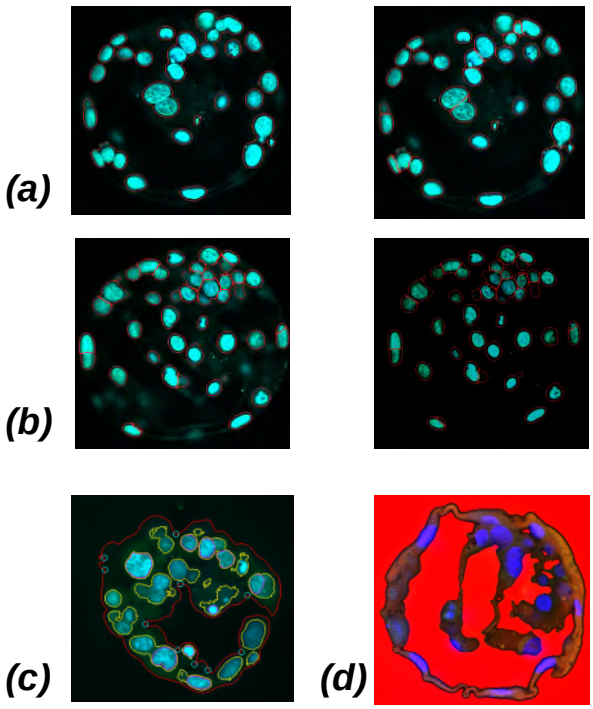


***Figure 7.3: Edge detection in confocal images of human preimplantation blastocysts at various stages of development.***

Following successful background and edge detection, circles approximating individual cells and polar bodies were expanded and allocated a specific arbitrary colour. Figure 7.4 shows examples of the colour-coding using this technique.

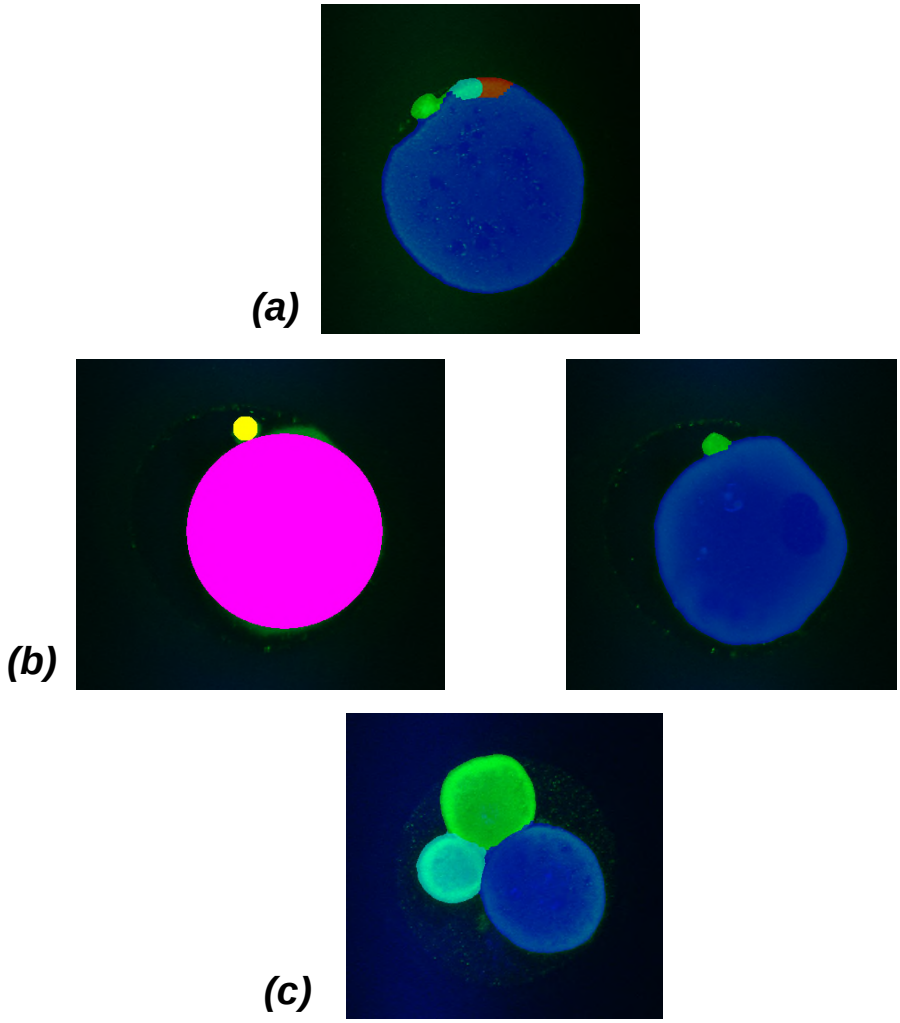


***Figure 7.4: Circle detection, growth and colour coding of oocytes (a), (b) and the individual blastomeres of an embryo (c).***

### *7.4.2 Visualising the three-dimensional structure of the embryo*

A certain amount of trial and error was necessary to manually adjust the image parameters, in order to gain segmented images that appeared correct by eye. At this stage, automation could not account for the wide variability in image quality and type, however, with manual intervention, appropriately segmented images could be achieved.

Using these segmented images, three-dimensional versions were created, to demonstrate the spatial structure of oocytes, cleavage stage embryos and blastocysts. Figure 7.5 shows the preliminary results. Figure 7.5 (d) shows an early 3D model of individual blastomeres in a cleavage stage embryo, constructed using the edge detection method. Some slices are incomplete, giving the impression that some parts of the cells are missing. Figure 7.5 (e) demonstrates 3D modelling of all of the nuclei present in a complete z-stack of a blastocyst, constructed using the edge detection process.

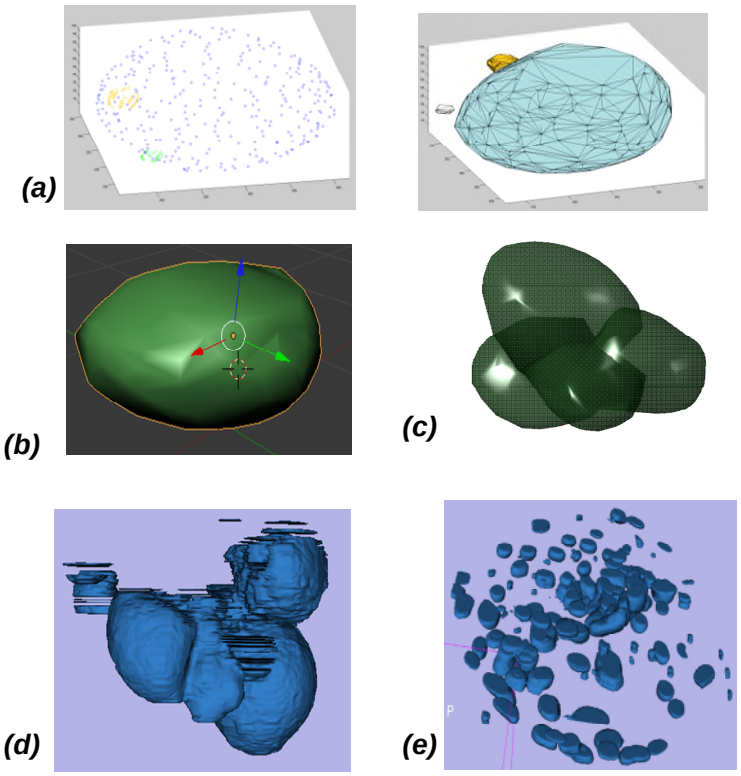


***Figure 7.5: Three-dimensional plotting and rendering of segmented images of oocytes (a), (b), blastomeres of an embryo (c), (d) and the nuclei in a blastocyst (e)***

### *7.4.3 Investigating the cell to nuclear volume in fixed specimens*

The programming inititated by James Michael was continued by University of Warwick MSc student Kieran Rafferty, resulting in the production of a segmentation editor tool using concave corners to segment embryo images (Rafferty *et al* 2012). Dr Czanner then moved away from Warwick to Manchester Metropolitan University and Anna Mölder, a postgraduate researcher in his group, proceeded to improve the segmenter and editor tool in order to facilitate the analysis of the confocal images of embryos at various stages of development. For the preliminary stages of this work using an early version of the software, four cleavage stage embryos and six blastocysts that I had previously fixed and stained with actin, anti-STAT3 and anti-leptin antibodies and imaged using the confocal microscope, were analysed using the semi-automated embryo segmenter tool (Rafferty *et al* 2012). This development improved the ability to resolve close and overlapping signals such as cells or nuclei such that, despite the software having a number of practical drawbacks and requiring labour-intensive manual modification of the 'automatically' analysed images, it was neverhteless possible then to address the aim of analysing cell and nuclear volumes.

The cell and nuclear volumes of cleavage stage embryos, and the nuclear volumes of cells identified as distinct populations in blastocysts, were measured and compared. The cell populations identified were ICM and TE cells.

Figure 7.6 shows the cell volume (voxels) versus the nuclear volume (voxels) in cleavage stage embryos. All blastomeres anaylsed were mononuclear, although a

small number of blastomeres did contain micronuclei (n=2), however these were ignored for the purpsose of this analysis.The nuclei in the 2-cell embryos (n=2) comprised 1.9-2.5% of the total cell volume (mean=2.2%), whilst in a 4-cell embryo (n=2), the nuclei comprised 2.4-5.7% of the total cell volume (mean=3.4%). Figure 7.6 (a) shows a day 2 frozen-thawed embryo where nucleus 1 comprises 2.5% of cell 1 and nucleus 2 comprises 1.9% of cell 2. Figure 7.6 (b) shows a day 2 fresh embryo, where nucleus 1 comprises 2.1% of cell 1 and nucleus 2 comprises 2.1% of cell 2. Figure 7.6 (c) shows a day 2 frozen embryo, with nucleus 1 comprising 2.5% of cell 1, nucleus 2 comprising 2.9% of cell 2, nucleus 3 comprising 2.4% of cell 3, and nucleus 4 comprising 3.0% of cell 4. Figure 7.6 (d) shows a day 2 fresh 4-cell embryo derived from a 3PN, where nucleus 1 comprises 5.7% of cell 1, nucleus 2 comprises 4.1% of cell 2, nucleus 3 comprises 3.3% of cell 3, and nucleus 4 comprises 3.4% of cell 4.

The size of the cells versus the size of the nuclei is generally consistent, with smaller cells having smaller nuclei relative to their volume. The exception in this example is the 4-cell embryo derived from a 3PN, where the nucleus of cell 1 comprises almost double the volume of the cell, and the nucleus of cell 2 comprises approximately one third more of the volume of the cell, compared to the other two cells, which are comparable to the cell/nuclear volume seen in 2PN embryos.

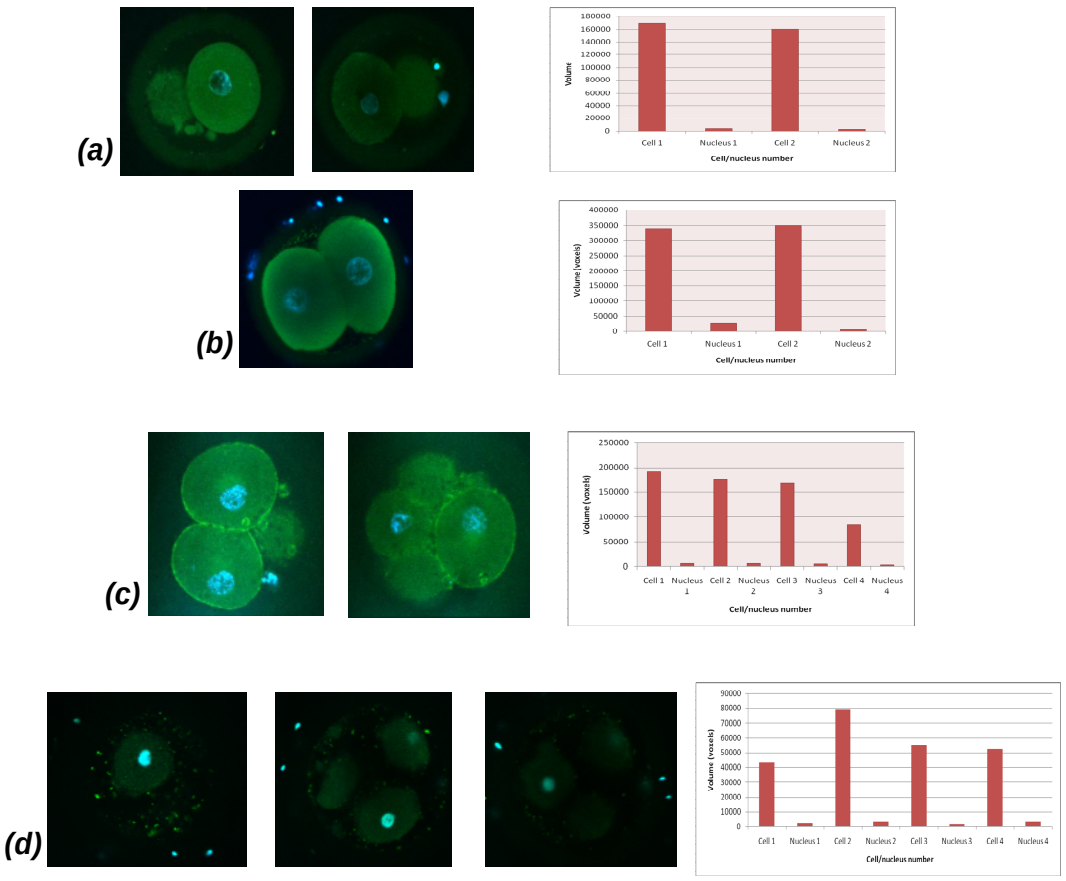


***Figure 7.6: Cell volumes versus nuclear volumes in cleavage stage embryos. The embryos were fluorescently labelled with actin (green), anti-STAT3 or anti-leptin antibodies, and DAPI (blue)***

### *7.4.5 Investigating the nuclear volumes in blastocysts*

Figure 7.7 shows the differences in the nuclear volumes of cells in the ICM versus the TE. There is a trend towards smaller nuclei in the ICM in comparison to the TE in all blastocysts analysed. Figure 7.7 (a) shows a day 7 fresh blastocyst in which the ICM cell nuclei are 26% of the volume of TE cells (or 74% smaller), although this difference is not significant ($p = 1.99$; students t-test). Figure 7.7 (b) shows a day 6 fresh blastocyst with two distinct inner cell masses. The nuclei in ICM1 are 48% smaller than those of the TE ($p=3.7$; students t-test), and the nuclei in ICM2 are 30% smaller than the nuclei of the TE ($p=0.005$; students t-test). The inner nuclei, defined as those furthest away from the TE inside the blastocoel, are visibly smaller than the outer nuclei in the ICM. Figure 7.7 (c) shows the nuclei in the ICM versus the TE of a day 7 fresh blastocyst. The nuclei in the ICM measure 20% smaller than those in the TE, and appear visibly so ($p=0.05$; students t-test). Figure 7.7 (d) shows the differences in the nuclei of the ICM compared to the TE in a day 7 fresh blastocyst. The nuclei in the ICM are 35% smaller than the nuclei in the TE ($p = 0.005$; student's t-test). Figure 7.7 (e) shows a day 7 fresh blastocyst in which the volume of the ICM nuclei are 34% smaller than those of the TE ($p = 0.001$; students t-test).

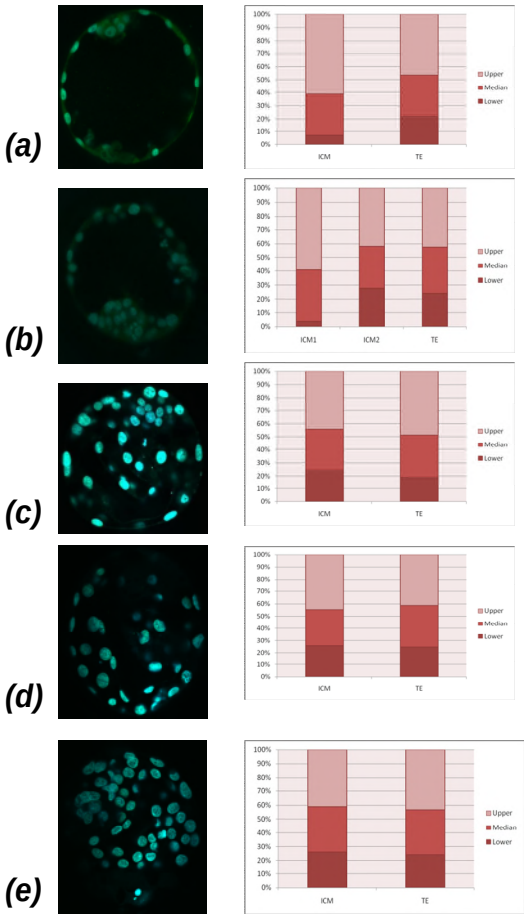


***Figure 7.7: Nuclear volumes in the ICM versus the TE of fresh blastocysts. ICM nuclei are genrally smaller than TE cells in all blastocysts analysed***

### *7.4.5 Developing a semi-automated embryo analysis tool using live cell time lapse imaging*

Following implementation of the Embryoscope™ in the clinical Embryology laboratory at CRM, and the subsequent increase in time lapse data available, I collected suitable images and exported them to my colleague Anna Mölder at Manchester Metropolitan University for processing. I worked closely with Anna regarding the biological and clinical aspects of development of human preimplantation embryos, current morphological markers of embryo quality, and culture conditions in our laboratory. Images generated from live cells have much less contrast than those from confocal microscope with fluorescent staining, so whilst similar approaches were used, refined sensitivity was needed.

The primary aim was to utilise two-dimensional data from fixed cell confocal images in combination with brightfield live cell images to construct simple three-dimensional models of human embryos at varying stages of development (Mölder *et al* 2016), in order to allow the visualisation of embryos in greater detail. Confocal images were segmented as previously described (Rafferty *et al* 2012), and reconstructed into three-dimensional models, as shown in section 7.4.2. Manual selection of the ZP, individual blastomeres, and cell nuclei using the embryo segmenter tool allowed for the visualisation of embryos in three dimensions, whilst also permitting the study of connectivity between blastomeres (Mölder *et al* 2016).

A further complexity of live cell imaging is that the embryoscope has up to 9 planes of focus through the z-stack of the embryo at ~20µm thickness, but a maximum of 7 of these can be utilised without detriment to the embryo due to excessive exposure to imaging. The degree of detail in the z-stacks was therefore greatly reduced in comparison to the confocal versions, and extensive processing to remove out of focus signals was necessary.

Further development of the preliminary program was undertaken to allow the semi-automated detection of cell boundaries and nuclei in greyscale images obtained from consecutive frames of live embryo images, using localised variation in the distribution of brightfield image intensity. This would potentially permit faster and more standardised analysis of large volumes of time lapse image data, with a view to eventually identifying key developmental processes to aid in the selection of viable preimplantation embryos for uterine transfer in the clinical setting. Optical conversion of light and dark gradients on an even grey background results in the edges of the images becoming the most prominent feature, and an increase in the number of cell boundaries as the embryo divides results in a change in the distribution of image intensity. The compaction stage of embryo development is characterised by a loss of distinct cell boundaries, and a subsequent decrease in the intensity of the greyscale, whilst cavitation causes an increase in intensity as the edges of the cavity become apparent, followed by a decrease with the expansion of the blastocoel (Mölder *et al* 2014). With this in mind, a region of interest in the optimal focal plane was selected at each developmental stage, and the intensity of the greyscale calculated in consecutive images using maximum and minimum

variance. Superior quality embryos had a distinctive pattern of variance, with a step-wise increase until a decrease at the compaction stage, and a further increase as the blastocyst formed. Those embryos which were morphologically inferior, or which exhibited chaotic cleavage or fragmentation had a greatly increased maximal and minimal variance in the greyscale, and a much less ordered pattern (Mölder *et al* 2014).

The computer-generated semi-automated analysis was compared to manual annotations in order to determine the accuracy of the cell tracking during development from syngamy to blastocyst formation. For the early developmental stages up to 8 cells, the accuracy of both the computational analysis and the manual analysis in detecting cell divisions were approximately 75%, although semi-automated detection of blastocyst formation was less accurate, generating a false positive result in ~28% of embryos (Mölder *et al* 2014). This work demonstrated that semi-automated detection of key developmental events in human preimplantation embryos may assist in the analysis of large volumes of time lapse data to enable the clinical embryologist to reduce the amount of time spent annotating images, and focus on fine tuning the process of embryo selection. Throughout the development of the program, I provided clinical expertise in the acquisition and interpretation of images, tested the reliability of the semi-automated programme, annotated embryo images used in the programme and validated each prototype version.

## *7.5 Discussion*

The visualisation of biological specimens in three-dimensions is a useful tool when attempting to understand the mechanisms of development and/or abberant behaviours. The investigation of the structure of complex multi-cellular specimens, with the added bonus of accurate spatial resolution, is made possible with the application of computational modelling (Klauschen *et al* 2009). Further development of the semi-automated analysis tool may assist in generating reliable and quantitative data to increase understanding of cell division patterns in relation to clinical outcomes, and may improve our ability to select the most viable embryos from a cohort from an early stage of development. This in turn will allow us to predict embryos most likely to develop into a blastocyst, thus reducing multiple gestations and maintaining clinical pregnancy and live birth rates, and improving our outcomes with subsequent frozen embryo transfer cycles.

The development of semi-automated analysis of human embryo images is a desirable prospect, particularly considering the increasing use of time lapse technologies in clinical IVF laboratories worldwide. Annotation of images currently involves a great deal of time and patience, and there is variability in the opinions of operators in terms of the timings of completion of cell cleavage divisions, commencement of compaction and cavitation, and expansion of the blastocoelic cavity (Sundvall *et al* 2013). Those time lapse systems offering a semi-automated analysis function are limited in their accuracy since they rely on the variations in

light intensity gradients that occur during cell cleavage, which are sometimes confused with the occurrence of fragmentation and cellular reabsorption. The use of dark field microscopy in such systems decreases the contrast of the images, making it difficult to accurately correct the automated cell tracking manually when necessary.

Eukaryotic cells have the ability to regulate their size and maintain nuclear volumes that are appropriate to their developmental stage (Huber and Gerace 2007). Throughout the cell cycle of budding yeast, the nucleus increases in volume (Umen 2005), and during the synthesis (S) phase, asynchronously growing mutant variants maintain their constant nuclear/cell ratio at ~8% volume (Jorgensen *et al* 2007).

Studies regarding the nuclear/cell volume ratio in human preimplantation embryos are scarce. In this project, as the cell number in cleavage stage human embryos increases with each division round, there is a trend towards a higher percentage of the cell being taken up by the nucleus. This is not unexpected, as although the cell numbers are increasing, the voume of the embryo as a whole remains the same until the commencement of cavitation (Hardarson *et al* 2012). This is commensurate with murine studies, which demonstrated that whilst the cytoplasmic volume of the embryo remains constant throughtout preimplantation development, the nucleo-cytoplasmic ratio increases exponentially (Aiken *et al* 2004; Wennekamp *et al* 2013). A previous study has demonstrated that no significant differences exist between chromosomally normal and chromosomally abnormal embryos with regard to nuclear diameter, blastomere diameter, or nuclear/cell ratio. However, the group did conclude that nuclei with missing

chromosomes were significantly smaller than those with extra chromosomes (Agerholm *et al* 2008). In this study, the embryo derived from a tripronucleate zygote, known to have an abnormal chromosome complement, had two cells with a higher cell to nuclear volume than those derived from normal 2PN zygotes. This may be due to unequal division of the daughter cells during the first cleavage round as a result of a tripolar spindle. The embryo derived from the 3PN zygote is of much poorer quality than those derived from 2PNs, which may also explain the aberrant cell to nuclear ratio.

Uneven embryo cleavage is negatively associated with implantation and pregnancy rates, with those dividing unevenly having a higher likelihood of chromosomal abnormalities and a higher number of multinucleated cells, which may interfere with cytoskeletal function and cellular division (Hardarson *et al* 2001). The resulting unequal distribution of cytoplasmic material in the daughter cells, particularly in the case of polarised proteins, may cause disruption of embryonic axis establishment, and may partially explain poor embryo development. Fragmentation is a commonly used indicator of embryo viability (Hardarson *et al* 2003). Increasing degrees of fragmentation in cleavage stage human embryos have been associated with a significant reduction in total blastomere volume (Hnida *et al* 2004). Additionally, binucleated blastomeres are reportedly significantly larger than their mononucleated counterparts, indicating that uneven cell size may be associated with multinucleation (Agerholm *et al* 2008), and embryos containing non-uniformly sized blastomeres were more likely to be aneuploid and binucleated (Hardarson *et al* 2001).

Labelling fixed embryos with DAPI allows the visualisation of nuclear chromatin, providing data on numbers of normal and abnormal nuclei, which are indicators of embryo viability (Hardy 1999). Normal cell nuclei are characterised by a regular rounded shape, with an even distribution of chromatin, whilst abnormal or degenerating nuclei have fragmented or condensed chromatin, and may be irregular in shape. Nuclei undergoing mitosis, the separation of chromosomes in the nucleus prior to cell division, have a distinctive non-regular appearance.

During the transition to blastocyst, the human preimplantation embryo undergoes compaction of the blastomeres, followed by cavitation and allocation of the cells into two distinct cell populations; the inner cell mass and the trophectoderm (Hardarson *et al* 2012). Cell division during expansion of the blastocyst increases during this process, and the average good quality blastocyst contains upwards of 80 cells (Matsuura *et al* 2010). The results in this project indicate that some cells in the blastocyst divide at a faster rate than others, and that these may be preferentially allocated to the ICM.

# Chapter Eight

# General Discussion and Conclusions

# Chapter Eight

## General Discussion and Conclusions

The initial idea for this project was to develop a computer-generated virtual embryo using visual and mathematical data obtained from images of human preimplantation oocytes, embryos and blastocysts, produced using fluorescently labelled antibodies and high resolution confocal microscopy. The markers selected would also provide insights into possible quality indicators and polarity markers of embryos. Preliminary work conducted by my supervisor Professor Geraldine Hartshorne suggested that the borders of cells in the preimplantation human embryo could be sufficiently highlighted using fluorescent labelling of the cytoskeletal protein F-actin. Whilst the resulting images were deemed unsuitable for the development of computer-based models due to excessive variability, the experiments did emphasise the importance of the actin cytoskeleton in the maintenance of human preimplantation embryo development. Poor quality cleavage stage embryos, such as those with slow or arrested development and irregular shaped cells, had a disorganised actin cytoskeleton surrounding the blastomeres, and actin-bound fragments. Good quality embryos displaying normal temporal development and evenly shaped cells had distinct actin borders around each blastomere and nucleus at the cleavage stage, at the flattened junctions of compacting cells, and around the cells of the ICM and TE in blastocysts. Since actin is known to have an important role in the regulation of cell division (Heng and Koh

2010), it follows that the integrity of the actin cytoskeleton is important for normal embryo development.

The purpose of investigating the distribution of leptin and STAT3 in human oocytes, embryos and blastocysts, was to determine whether their previously reported differential distribution within and between cells in both human and mouse (Antczak and Van Blerkom 1997), could be used as a potential marker of polarisation in preimplantation embryo development. This may have provided evidence as to whether the allocation of cells to the ICM and TE in the blastocyst may be pre-determined. Analysis of the images showed that, in agreement with published data, leptin and STAT3 are co-localised in oocytes, with higher levels of fluorescence at the periphery of the cell in comparison to the central cytoplasmic region. However, in contrast, there was no difference in the fluorescence intensity of either protein at the site of the PB versus the area opposite the PB. Similarly, in cleavage stage embryos, leptin fluorescence was more intense at the periphery of each blastomere than in the perinuclear region, whilst STAT3 fluorescence was more intense in the perinuclear region compared to the peripheral region. In the blastocyst, leptin staining was increased in the TE compared to the ICM, and conversely STAT3 was increased in the ICM versus the TE. Therefore, whilst there appears to be differential distribution of leptin and STAT3 within cytoplasmic domains in the unfertilised oocyte and blastomeres of the cleavage stage embryo, and in the ICM and TE cells of the blastocyst, the differences were non-significant, and they did not seem to be co-localised after the first cell division, thus the results

published by Antczak and Van Blerkom (1997) were not reproduced here and could not be built upon in analysing polarity in human embryonic development.

Leptin, acting via the long form of the leptin receptor OB-$R_L$, is known to be an activator of STAT3, and activation of STAT3 in mouse oocytes can be induced by exposure to exogenous recombinant leptin (Matsuoka *et al* 1999). In this project, pSTAT3 fluorescence was observed at low levels of intensity in the ICM and TE of human blastocysts, as has been previously reported in the mouse (Fedorcsak and Storeng 2003). Exposure of human blastocysts to exogenous human recombinant leptin protein for 10 minutes or more led to a significant increase in the relative fluorescence intensity of pSTAT3 in the nuclei and cytoplasm of ICM cells, but not in the cells of the TE. Interestingly, there was a significant increase in the total number of TE cells in blastocysts that had been exposed to human recombinant leptin protein for 10 minutes or more, which is in agreement with previously published mouse data (Kawamura *et al* 2002).

The detection of OB-$R_L$ mRNA was confirmed in human pronucleate, cleavage stage embryos and blastocysts. A non-significant increase in OB-$R_L$ mRNA levels was seen in the blastocyst in comparison to pronucleate and cleavage stage embryos.

A number of interesting morphological features were observed in the fluorescently labelled blastocysts. Free cells were seen in the blastocoelic cavity of around one third of the blastocysts studied in this project. The similarities in relative fluorescence intensity of pSTAT3 staining between these cells and those of the ICM, along with the analysis of time-lapse image sequences, suggest that these cells

originate from the ICM in human blastocysts. A similar proportion of blastocysts exhibited excluded cells in the space between the trophectoderm and the ZP, and these differed to free cells in that they had little fluorescent staining and were degenerate in appearance. It is possible that both free cells and excluded cells are part of an inherent self-correcting mechanism that excludes abnormal cells from the implanting blastocyst. Cytoplasmic projections were seen in around one-third of blastocysts, often traversing the entire diameter of the blastocoelic cavity, and linking the ICM to the TE. One interesting theory is that they may serve as a direct communication mechanism to maintain cell division of the mural TE following migration to the abembryonic pole (Salas-Vidal and Lomeli 2004). Whilst previously published data has suggested that these are indicative of reduced embryo viability (Scott 2000), the majority of blastocysts with cytoplasmic projections in this project were of superior quality, which certainly warrants further studies into the implantation potential of such blastocysts. Double ICMs were observed in approximately 5% of blastocysts, and have previously been linked with the incidence of a monozygotic multiple order pregnancy (Meintjes *et al* 2001), suggesting this as a useful morphological marker during selection of blastocysts prior to uterine transfer. Micronuclei and chromosome-containing fragments may be indicative of aneuploidy in human embryos (Chavez *et al* 2012), and may result in developmental arrest (Kort *et al* 2015), thus the presence of micronuclei and chromosome-containing fragments in cleavage stage embryos in this project may also be utilised as a de-selection tool during microscopic assessment in the clinical embryology laboratory.

During the course of this project, decades after they were first proposed, time lapse incubators of sufficient quality became available as a tool that could be applied clinically for the monitoring and selection of embryos. The preliminary work in chapter six of this thesis formed the basis of validation and implementation of time lapse monitoring into clinical practice at the CRM.

Time lapse analysis of fresh and frozen-thawed human preimplantation embryos showed that frozen-thawed embryos completed cleavages at a slower rate than fresh embryos, significantly at the 2-cell, 3-cell, 4-cell, 7-cell and 8-cell completion times, and at the commencement of blastocyst development. Frozen embryos have previously been reported to develop at a slower rate than fresh, regardless of their chromosomal status (Edirisinghe *et al* 2005). Frozen embryos created using standard IVF developed at a significantly slower rate until the 5-cell stage, which is in agreement with previous studies showing a delay in development after IVF in comparison to ICSI derived embryos, particularly at the early cleavage stage (Van Landuyt *et al* 2005). Fresh embryos that developed into blastocysts completed cleavage into 2-cell and 4-cell significantly faster, and spent a significantly shorter time at the 1-cell stage, emphasising the importance of early cleavage as a marker of human embryo viability (Sakkas *et al* 1998). In contradiction to other reports, those embryos developing into blastocysts spent a significantly longer time at the 7-cell stage than those that arrested (Cetinkaya *et al* 2015), although published reports into specific investigations of the 7-cell stage of development are rare, and most concentrate on the total time taken to develop from the 5-cell to the 8-cell stage (Desai *et al* 2014).

Time lapse monitoring has provided insight into fascinating embryo behaviours which would ordinarily be missed during microscopic assessment at 24-hourly intervals, such as blastocyst collapse and expansion prior to hatching (Marcos *et al* 2015). Blastocyst hatching is initiated by the TE, and whilst hatching from the polar region near the ICM was once considered more common, and indeed superior (Sathananthan *et al* 2003), analysis of the spontaneous site of hatching in relation to the position of the ICM in this project has shown that the initial site of hatching in relation to ICM position has no apparent influence on clinical pregnancy and implantation rates.

Removal of blastomeres from cleavage stage embryos for PGD is routine practice in clinical embryology, and is reported not to be detrimental to continued development (Brodie *et al* 2012); however knowing which cell to remove may prove important for the future development of the embryo. In this project, time lapse imaging was used to identify and track the first-dividing cell of a two-cell embryo, and specifically damage the daughters of that cell in order to investigate whether this would potentially disrupt the polar axes and affect blastocyst formation. The blastocyst development rate did not appear to be affected in the damaged embryos, and whilst they did commence compaction earlier and cavitation later than non-damaged embryos, the differences were non-significant. It would have been interesting to repeat the experiments with focus on the slowest-dividing daughter cells; however the paucity of available zygotes unfortunately prevented this.

Several observations in the earliest of the time lapse studies presented in this thesis appeared to predict embryo cleavage. Ruffling of the blastomere membranes, cellular cytoplasmic movements, and rearrangement of blastomeres within the ZP occurred in a significantly higher proportion of cryopreserved embryos that subsequently cleaved, in comparison to those that did not. These findings are in contrast to others (Athayde Wirka *et al* 2014); however the results described were based upon relatively poor quality images from a time lapse system in development, the use of which was subsequently discontinued in our lab.

The use of fluorescent images obtained during this project in the development of three-dimensional computer-generated models was not as successful as originally predicted. However, they laid the foundations for structural studies (Rafferty *et al* 2013), and along with manual analysis of time lapse image sequences, we were able to begin developing predictive algorithms of human embryo development (Mölder *et al* 2015; Mölder *et al* 2016).

The usefulness of temporal and spatial images may be improved by combining the findings of both. The analysis of the developmental timings of abnormally fertilised oocytes (1PN or MPN) in comparison with normally fertilised oocytes (2PN) showed no significant differences in the cleavage completion times, although 2PNs did complete compaction significantly faster than MPNs. Investigation of the cell to nuclear volume in a 4-cell embryo derived from a 3PN using semi-automated software, showed that the cell to nuclear volume seemed greater than in 4-cell embryos derived from 2PNs. This suggests that, although the development of abnormally fertilised embryos is indistinguishable from that of normally fertilised

embryos by morphokinetics, they may be severely chromosomally compromised, thus reinforcing the importance of identifying such embryos during fertilisation assessment in the clinical embryology laboratory.

Human preimplantation embryo development is complex and unpredictable. The findings of the research conducted during this project show that, whilst our understanding of the growth and developmental mechanisms of human preimplantation embryos has improved since the birth of Louise Brown (Steptoe and Edwards 1978), there is still much to learn. In particular, my research has highlighted the need for further studies of polarity in human embryos, the lack of markers of developmental functionality, and the potential of computer-assisted image analysis to improve our understanding and selection based upon quality of embryos in the clinical setting.

Human embryos are curious and fascinating. New and exciting technologies are constantly emerging, and more research into this extraordinary area of medicine is essential to allow us to continue our mission to improve outcomes for our ever-expanding patient population.

# Chapter Nine

# References

## Chapter Nine

## References


1. American Society for Reproductive Medicine 57th annual meeting. October 20-25, 2001. Orlando, Florida, USA. Abstracts. *Fertil Steril.* 2001;76(3 Suppl):S1-288.

2. Abrahamsohn PA, Zorn TM. Implantation and decidualization in rodents. *J Exp Zool.*1993;266(6):603-628.

3. Abusheikha N, Salha O, Sharma V, Brinsden P, Abusheika N. Monozygotic twinning and IVF/ICSI treatment: a report of 11 cases and review of literature. *Hum Reprod Update.*2000;6(4):396-403.

4. Achache H, Revel A. Endometrial receptivity markers, the journey to successful embryo implantation. *Hum Reprod Update.* 2006;12(6):731-746.

5. Aiken CE, Swoboda PP, Skepper JN, Johnson MH. The direct measurement of embryogenic volume and nucleo-cytoplasmic ratio during mouse pre-implantation development.*Reproduction.* 2004;128(5):527-535.

6. Ajduk A, Zernicka-Goetz M. Polarity and cell division orientation in the cleavage embryo: from worm to human. *Mol Hum Reprod.* 2015.

7. Alikani M, Olivennes F, Cohen J. Microsurgical correction of partially degenerate mouse embryos promotes hatching and restores their viability. *Hum Reprod.* 1993;8(10):1723-1728.

8. Almeida PA, Bolton VN. The relationship between chromosomal abnormality in the human preimplantation embryo and development in vitro. *Reprod Fertil Dev.* 1996;8(2):235-241.

9. Embryology ASiRMaESIGo. The Istanbul consensus workshop on embryo assessment: proceedings of an expert meeting. *Hum Reprod.* 2011;26(6):1270-1283.

10. Andersen AN, Goossens V, Ferraretti AP, et al. Assisted reproductive technology in Europe, 2004: results generated from European registers by ESHRE. *Hum Reprod.*2008;23(4):756-771.

11. Antczak M, Van Blerkom J. Oocyte influences on early development: the regulatory proteins leptin and STAT3 are polarized in mouse and human oocytes and differentially distributed within the cells of the preimplantation stage embryo. *Mol Hum Reprod.*1997;3(12):1067-1086.

12. Antczak M, Van Blerkom J. Temporal and spatial aspects of fragmentation in early human embryos: possible effects on developmental competence and association with the differential elimination of regulatory proteins from polarized domains. *Hum Reprod.*1999;14(2):429-447.

13. Arias-Alvarez M, García-García RM, Torres-Rovira L, González-Bulnes A, Rebollar PG, Lorenzo PL. Influence of leptin on in vitro maturation and steroidogenic secretion of cumulus-oocyte complexes through JAK2/STAT3 and MEK 1/2 pathways in the rabbit model. *Reproduction.* 2010;139(3):523-532.

14. Armstrong S, Vail A, Mastenbroek S, Jordan V, Farquhar C. Time-lapse in the IVF-lab: how should we assess potential benefit? *Hum Reprod.* 2015;30(1):3-8.

15. Arnold JT, Kaufman DG, Seppälä M, Lessey BA. Endometrial stromal cells regulate epithelial cell growth in vitro: a new co-culture model. *Hum Reprod.* 2001;16(5):836-845.

16. Ashwood-Smith MJ, Edwards RG. DNA repair by oocytes. *Mol Hum Reprod.* 1996;2(1):46-51.

17. Aston KI, Peterson CM, Carrell DT. Monozygotic twinning associated with assisted reproductive technologies: a review. *Reproduction.* 2008;136(4):377-386.

18. Athayde Wirka K, Chen AA, Conaghan J, et al. Atypical embryo phenotypes identified by time-lapse microscopy: high prevalence and association with embryo development.*Fertil Steril.* 2014;101(6):1637-1648.e1631-1635.

19. Azzarello A, Hoest T, Mikkelsen AL. The impact of pronuclei morphology and dynamicity on live birth outcome after time-lapse culture. *Hum Reprod.* 2012;27(9):2649-2657.

20. Bahceci M, Ulug U. Does underlying infertility aetiology impact on first trimester miscarriage rate following ICSI? A preliminary report from 1244 singleton gestations.*Hum Reprod.* 2005;20(3):717-721.

21. Balaban B, Urman B, Ata B, et al. A randomized controlled study of human Day 3 embryo cryopreservation by slow freezing or vitrification: vitrification is associated with higher survival, metabolism and blastocyst formation. *Hum Reprod.* 2008;23(9):1976-1982.

22. Balaban B, Urman B, Isiklar A, et al. The effect of pronuclear morphology on embryo quality parameters and blastocyst transfer outcome. *Hum Reprod.* 2001;16(11):2357-2361.

23. Balaban B, Urman B, Yakin K, Isiklar A. Laser-assisted hatching increases pregnancy and implantation rates in cryopreserved embryos that were allowed to cleave in vitro after thawing: a prospective randomized study. *Hum Reprod.* 2006;21(8):2136-2140.

24. Balakier H. Tripronuclear human zygotes: the first cell cycle and subsequent development. *Hum Reprod.* 1993;8(11):1892-1897.

25. Banerjee K, Resat H. Constitutive activation of STAT3 in breast cancer cells: A review.*Int J Cancer.* 2016;138(11):2570-2578.

26. Bavister BD. Culture of preimplantation embryos: facts and artifacts. *Hum Reprod Update.* 1995;1(2):91-148.

27. Bazrgar M, Gourabi H, Valojerdi MR, Yazdi PE, Baharvand H. Self-correction of chromosomal abnormalities in human preimplantation embryos and embryonic stem cells. *Stem Cells Dev.* 2013;22(17):2449-2456.

28. Becker S, Groner B, Müller CW. Three-dimensional structure of the Stat3beta homodimer bound to DNA. *Nature.* 1998;394(6689):145-151.

29. Behr B, Fisch JD, Racowsky C, Miller K, Pool TB, Milki AA. Blastocyst-ET and monozygotic twinning. *J Assist Reprod Genet.* 2000;17(6):349-351.

30. Bensdorp AJ, Tjon-Kon-Fat RI, Bossuyt PM, et al. Prevention of multiple pregnancies in couples with unexplained or mild male subfertility: randomised controlled trial of in vitro fertilisation with single embryo transfer or in vitro fertilisation in modified natural cycle compared with intrauterine insemination with controlled ovarian hyperstimulation.*BMJ.* 2015;350:g7771.

31. Biggers JD, Borland RM, Powers RD. Transport mechanisms in the preimplantation mammalian embryo. *Ciba Found Symp.* 1977(52):129-153.

32. Bischof P, Campana A. A model for implantation of the human blastocyst and early placentation. *Hum Reprod Update.* 1996;2(3):262-270.

33. Bischoff M, Parfitt DE, Zernicka-Goetz M. Formation of the embryonic-abembryonic axis of the mouse blastocyst: relationships between orientation of early cleavage divisions and pattern of symmetric/asymmetric divisions. *Development.* 2008;135(5):953-962.

34. Bolton H, Graham SJ, Van der Aa N, et al. Mouse model of chromosome mosaicism reveals lineage-specific depletion of aneuploid cells and normal developmental potential. *Nat Commun.* 2016;7:11165.

35. Bos-Mikich A, Mattos AL, Ferrari AN. Early cleavage of human embryos: an effective method for predicting successful IVF/ICSI outcome. *Hum Reprod.* 2001;16(12):2658-2661.

36. Brezinova J, Oborna I, Svobodova M, Fingerova H. Evaluation of day one embryo quality and IVF outcome--a comparison of two scoring systems. *Reprod Biol Endocrinol.*2009;7:9.

37. Brison DR. Apoptosis in mammalian preimplantation embryos: regulation by survival factors. *Hum Fertil (Camb).* 2000;3(1):36-47.

38. Brodie D, Beyer CE, Osborne E, Kralevski V, Rasi S, Osianlis T. Preimplantation genetic diagnosis for chromosome rearrangements - one blastomere biopsy versus two blastomere biopsy. *J Assist Reprod Genet.* 2012;29(8):821-827.

39. Calarco PG. Polarization of mitochondria in the unfertilized mouse oocyte. *Dev Genet.*1995;16(1):36-43.

40. Calarco PG, Pedersen RA. Ultrastructural observations of lethal yellow (Ay/Ay) mouse embryos. *J Embryol Exp Morphol.* 1976;35(1):73-80.

41. Campbell A, Fishel S, Bowman N, Duffy S, Sedler M, Hickman CF. Modelling a risk classification of aneuploidy in human embryos using non-invasive morphokinetics.*Reprod Biomed Online.* 2013;26(5):477-485.

42. Capalbo A, Wright G, Elliott T, Ubaldi FM, Rienzi L, Nagy ZP. FISH reanalysis of inner cell mass and trophectoderm samples of previously array-CGH screened blastocysts shows high accuracy of diagnosis and no major diagnostic impact of mosaicism at the blastocyst stage. *Hum Reprod.* 2013;28(8):2298-2307.

43. Capmany G, Taylor A, Braude PR, Bolton VN. The timing of pronuclear formation, DNA synthesis and cleavage in the human 1-cell embryo. *Mol Hum Reprod.* 1996;2(5):299-306.

44. Carnegie J, Claman P, Lawrence C, Cabaca O. Can Matrigel substitute for Vero cells in promoting the in-vitro development of mouse embryos? *Hum Reprod.* 1995;10(3):636-641.

45. Carver J, Martin K, Spyropoulou I, Barlow D, Sargent I, Mardon H. An in-vitro model for stromal invasion during implantation of the human blastocyst. *Hum Reprod.*2003;18(2):283-290.

46. Castelbaum AJ, Ying L, Somkuti SG, Sun J, Ilesanmi AO, Lessey BA. Characterization of integrin expression in a well differentiated endometrial adenocarcinoma cell line (Ishikawa). *J Clin Endocrinol Metab.* 1997;82(1):136-142.

47. Catalano RD, Johnson MH, Campbell EA, Charnock-Jones DS, Smith SK, Sharkey AM. Inhibition of Stat3 activation in the endometrium prevents implantation: a nonsteroidal approach to contraception. *Proc Natl Acad Sci U S A.* 2005;102(24):8585-8590.

48. Cauffman G, Verheyen G, Tournaye H, Van de Velde H. Developmental capacity and pregnancy rate of tetrahedral- versus non-tetrahedral-shaped 4-cell stage human embryos. *J Assist Reprod Genet.* 2014;31(4):427-434.

49. Cervero A, Horcajadas JA, Domínguez F, Pellicer A, Simón C. Leptin system in embryo development and implantation: a protein in search of a function. *Reprod Biomed Online.* 2005;10(2):217-223.

50. Cervero A, Horcajadas JA, MartIn J, Pellicer A, Simón C. The leptin system during human endometrial receptivity and preimplantation development. *J Clin Endocrinol Metab.*2004;89(5):2442-2451.

51. Cetinkaya M, Pirkevi C, Yelke H, Colakoglu YK, Atayurt Z, Kahraman S. Relative kinetic expressions defining cleavage synchronicity are better predictors of blastocyst formation and quality than absolute time points. *J Assist Reprod Genet.* 2015;32(1):27-35.

52. Cha KY, Chian RC. Maturation in vitro of immature human oocytes for clinical use. *Hum Reprod Update.* 1998;4(2):103-120.

53. Cha KY, Koo JJ, Ko JJ, Choi DH, Han SY, Yoon TK. Pregnancy after in vitro fertilization of human follicular oocytes collected from nonstimulated cycles, their culture in vitro and their transfer in a donor oocyte program. *Fertil Steril.* 1991;55(1):109-113.

54. Chalana V, Kim Y. A methodology for evaluation of boundary detection algorithms on medical images. *IEEE Trans Med Imaging.* 1997;16(5):642-652.

55. Chang EM, Song HS, Lee DR, Lee WS, Yoon TK. In vitro maturation of human oocytes: Its role in infertility treatment and new possibilities. *Clin Exp Reprod Med.* 2014;41(2):41-46.

56. Chang SG, Yu B, Vetterli M. Spatially adaptive wavelet thresholding with context modeling for image denoising. *IEEE Trans Image Process.* 2000;9(9):1522-1531.

57. Chavez SL, Loewke KE, Han J, et al. Dynamic blastomere behaviour reflects human embryo ploidy by the four-cell stage. *Nat Commun.* 2012;3:1251.

58. Chehab FF, Lim ME, Lu R. Correction of the sterility defect in homozygous obese female mice by treatment with the human recombinant leptin. *Nat Genet.* 1996;12(3):318-320.

59. Chehab FF, Mounzih K, Lu R, Lim ME. Early onset of reproductive function in normal female mice treated with leptin. *Science.* 1997;275(5296):88-90.

60. Chen AA, Tan L, Suraj V, Reijo Pera R, Shen S. Biomarkers identified with time-lapse imaging: discovery, validation, and practical application. *Fertil Steril.* 2013;99(4):1035-1043.

61. Cheng JG, Chen JR, Hernandez L, Alvord WG, Stewart CL. Dual control of LIF expression and LIF receptor function regulate Stat3 activation at the onset of uterine receptivity and embryo implantation. *Proc Natl Acad Sci U S A.* 2001;98(15):8680-8685.

62. Chi HJ, Koo JJ, Choi SY, Jeong HJ, Roh SI. Fragmentation of embryos is associated with both necrosis and apoptosis. *Fertil Steril.* 2011;96(1):187-192.

63. Chida S. Monozygous double inner cell masses in mouse blastocysts following fertilization in vitro and in vivo. *J In Vitro Fert Embryo Transf.* 1990;7(3):177-179.

64. Child TJ, Henderson AM, Tan SL. The desire for multiple pregnancy in male and female infertility patients. *Hum Reprod.* 2004;19(3):558-561.

65. Child TJ, Phillips SJ, Abdul-Jalil AK, Gulekli B, Tan SL. A comparison of in vitro maturation and in vitro fertilization for women with polycystic ovaries. *Obstet Gynecol.*2002;100(4):665-670.

66. Chimote NM, Chimote NN, Nath NM, Mehta BN. Transfer of spontaneously hatching or hatched blastocyst yields better pregnancy rates than expanded blastocyst transfer. *J Hum Reprod Sci.* 2013;6(3):183-188.

67. Cohen J. Sorting out chromosome errors. *Science.* 2002;296(5576):2164-2166.

68. Cohen J, Elsner C, Kort H, et al. Impairment of the hatching process following IVF in the human and improvement of implantation by assisting hatching using micromanipulation. *Hum Reprod.* 1990;5(1):7-13.

69. Copp AJ. Interaction between inner cell mass and trophectoderm of the mouse blastocyst. I. A study of cellular proliferation. *J Embryol Exp Morphol.* 1978;48:109-125.

70. Coticchio G, Guglielmo MC, Albertini DF, et al. Contributions of the actin cytoskeleton to the emergence of polarity during maturation in human oocytes. *Mol Hum Reprod.*2014;20(3):200-207.

71. Cruz M, Gadea B, Garrido N, et al. Embryo quality, blastocyst and ongoing pregnancy rates in oocyte donation patients whose embryos were monitored by time-lapse imaging. *J Assist Reprod Genet.* 2011;28(7):569-573.

72. Dal Canto M, Coticchio G, Mignini Renzini M, et al. Cleavage kinetics analysis of human embryos predicts development to blastocyst and implantation. *Reprod Biomed Online.*2012;25(5):474-480.

73. Dale PO, Tanbo T, Abyholm T. In-vitro fertilization in infertile women with the polycystic ovarian syndrome. *Hum Reprod.* 1991;6(2):238-241.

74. Danilchik MV, Brown EE. Membrane dynamics of cleavage furrow closure in Xenopus laevis. *Dev Dyn.* 2008;237(3):565-579.

75. De Kretzer D, Dennis P, Hudson B, et al. Transfer of a human zygote. *Lancet.*1973;2(7831):728-729.

76. de Melo-Martin I. On cloning human beings. *Bioethics.* 2002;16(3):246-265.

77. De Vos A, Janssens R, Van de Velde H, et al. The type of culture medium and the duration of in vitro culture do not influence birthweight of ART singletons. *Hum Reprod.*2015;30(1):20-27.

78. De Vos A, Staessen C, De Rycke M, et al. Impact of cleavage-stage embryo biopsy in view of PGD on human blastocyst implantation: a prospective cohort of single embryo transfers. *Hum Reprod.* 2009;24(12):2988-2996.

79. Denver RJ, Bonett RM, Boorse GC. Evolution of leptin structure and function.*Neuroendocrinology.* 2011;94(1):21-38.

80. Desai N, Ploskonka S, Goodman LR, Austin C, Goldberg J, Falcone T. Analysis of embryo morphokinetics, multinucleation and cleavage anomalies using continuous

time-lapse monitoring in blastocyst transfer cycles. *Reprod Biol Endocrinol.* 2014;12:54.

81. Dey SK, Lim H, Das SK, et al. Molecular cues to implantation. *Endocr Rev.*2004;25(3):341-373.

82. Dimitriadis E, Sharkey AM, Tan YL, Salamonsen LA, Sherwin JR. Immunolocalisation of phosphorylated STAT3, interleukin 11 and leukaemia inhibitory factor in endometrium of women with unexplained infertility during the implantation window. *Reprod Biol Endocrinol.* 2007;5:44.

83. Do DV, Ueda J, Messerschmidt DM, et al. A genetic and developmental pathway from STAT3 to the OCT4-NANOG circuit is essential for maintenance of ICM lineages in vivo.*Genes Dev.* 2013;27(12):1378-1390.

84. Drakopoulos P, Blockeel C, Stoop D, et al. Conventional ovarian stimulation and single embryo transfer for IVF/ICSI. How many oocytes do we need to maximize cumulative live birth rates after utilization of all fresh and frozen embryos? *Hum Reprod.*2016;31(2):370-376.

85. Duncan FE, Stein P, Williams CJ, Schultz RM. The effect of blastomere biopsy on preimplantation mouse embryo development and global gene expression. *Fertil Steril.*2009;91(4 Suppl):1462-1465.

86. Duncan SA, Zhong Z, Wen Z, Darnell JE. STAT signaling is active during early mammalian development. *Dev Dyn.* 1997;208(2):190-198.

87. Ebner T, Tritscher K, Mayer RB, et al. Quantitative and qualitative trophectoderm grading allows for prediction of live birth and gender. *J Assist Reprod Genet.* 2016;33(1):49-57.

88. Edgar DH, Bourne H, Speirs AL, McBain JC. A quantitative analysis of the impact of cryopreservation on the implantation potential of human early cleavage stage embryos.*Hum Reprod.* 2000;15(1):175-179.

89. Edirisinghe R, Jemmott R, Allan J. Comparison of growth rates of fresh and frozen-thawed embryos according to chromosomal status. *J Assist Reprod Genet.* 2005;22(7-8):295-300.

90. Edwards RG, Crow J, Dale S, Macnamee MC, Hartshorne GM, Brinsden P. Pronuclear, cleavage and blastocyst histories in the attempted preimplantation diagnosis of the human hydatidiform mole. *Hum Reprod.* 1992;7(7):994-998.

91. Edwards RG, Mettler L, Walters DE. Identical twins and in vitro fertilization. *J In Vitro Fert Embryo Transf.* 1986;3(2):114-117.

92. El-Toukhy T, Khalaf Y, Braude P. IVF results: optimize not maximize. *Am J Obstet Gynecol.* 2006;194(2):322-331.

93. Law ETFoEa. 6. Ethical issues related to multiple pregnancies in medically assisted procreation. *Hum Reprod.* 2003;18(9):1976-1979.

94. Evers JL. Female subfertility. *Lancet.* 2002;360(9327):151-159.

95. Evsikov S, Verlinsky Y. Mosaicism in the inner cell mass of human blastocysts. *Hum Reprod.* 1998;13(11):3151-3155.

96. Farooqi IS, O'Rahilly S. New advances in the genetics of early onset obesity. *Int J Obes (Lond).* 2005;29(10):1149-1152.

97. Fatemi HM, Popovic-Todorovic B. Implantation in assisted reproduction: a look at endometrial receptivity. *Reprod Biomed Online.* 2013;27(5):530-538.

98. Fedorcsák P, Storeng R. Effects of leptin and leukemia inhibitory factor on preimplantation development and STAT3 signaling of mouse embryos in vitro. *Biol Reprod.* 2003;69(5):1531-1538.

99. Fernandez Gallardo E, Spiessens C, D'Hooghe T, Debrock S. Effect of embryo morphology and morphometrics on implantation of vitrified day 3 embryos after warming: a retrospective cohort study. *Reprod Biol Endocrinol.* 2016;14(1):40.

100. Flaherty SP, Payne D, Matthews CD. Fertilization failures and abnormal fertilization after intracytoplasmic sperm injection. *Hum Reprod.* 1998;13 Suppl 1:155-164.

101. Flaherty SP, Payne D, Swann NJ, Mattews CD. Aetiology of failed and abnormal fertilization after intracytoplasmic sperm injection. *Hum Reprod.* 1995;10(10):2623-2629.

102. Fragouli E, Lenzi M, Ross R, Katz-Jaffe M, Schoolcraft WB, Wells D. Comprehensive molecular cytogenetic analysis of the human blastocyst stage. *Hum Reprod.*2008;23(11):2596-2608.

103. Freour T, Masson D, Mirallie S, et al. Active smoking compromises IVF outcome and affects ovarian reserve. *Reprod Biomed Online.* 2008;16(1):96-102.

104. Fulka J, Kárníková L, Moor RM. Oocyte polarity: ICSI, cloning and related techniques.*Hum Reprod.* 1998;13(12):3303-3305.

105. Gardner DK. Changes in requirements and utilization of nutrients during mammalian preimplantation embryo development and their significance in embryo culture.*Theriogenology.* 1998;49(1):83-102.

106. Gardner DK, Lane M. Culture of viable human blastocysts in defined sequential serum-free media. *Hum Reprod.* 1998;13 Suppl 3:148-159; discussion 160.

107. Gardner DK, Lane M, Stevens J, Schlenker T, Schoolcraft WB. Blastocyst score affects implantation and pregnancy outcome: towards a single blastocyst transfer. *Fertil Steril.*2000;73(6):1155-1158.

108. Gardner RL. The early blastocyst is bilaterally symmetrical and its axis of symmetry is aligned with the animal-vegetal axis of the zygote in the mouse. *Development.*1997;124(2):289-301.

109. Gardner RL. Specification of embryonic axes begins before cleavage in normal mouse development. *Development.* 2001;128(6):839-847.

110. Gerris J, De Neubourg D, Mangelschots K, Van Royen E, Van de Meerssche M, Valkenburg M. Prevention of twin pregnancy after in-vitro fertilization or intracytoplasmic sperm injection based on strict embryo criteria: a prospective randomized clinical trial. *Hum Reprod.* 1999;14(10):2581-2587.

111. Gerris J, Van Royen E. Avoiding multiple pregnancies in ART: a plea for single embryo transfer. *Hum Reprod.* 2000;15(9):1884-1888.

112. Gianaroli L, Cristina Magli M, Ferraretti AP, et al. Reducing the time of sperm-oocyte interaction in human in-vitro fertilization improves the implantation rate. *Hum Reprod.*1996;11(1):166-171.

113. Gianaroli L, Magli MC, Cavallini G, et al. Predicting aneuploidy in human oocytes: key factors which affect the meiotic process. *Hum Reprod.* 2010;25(9):2374-2386.

114. Gonzales DS, Bavister BD. Zona pellucida escape by hamster blastocysts in vitro is delayed and morphologically different compared with zona escape in vivo. *Biol Reprod.*1995;52(2):470-480.

115. González RR, Simón C, Caballero-Campo P, et al. Leptin and reproduction. *Hum Reprod Update.* 2000;6(3):290-300.

116. Goolam M, Scialdone A, Graham SJ, et al. Heterogeneity in Oct4 and Sox2 Targets Biases Cell Fate in 4-Cell Mouse Embryos. *Cell.* 2016;165(1):61-74.

117. Goossens V, De Rycke M, De Vos A, et al. Diagnostic efficiency, embryonic development and clinical outcome after the biopsy of one or two blastomeres for preimplantation genetic diagnosis. *Hum Reprod.* 2008;23(3):481-492.

118. Grossmann M, Calafell JM, Brandy N, et al. Origin of tripronucleate zygotes after intracytoplasmic sperm injection. *Hum Reprod.* 1997;12(12):2762-2765.

119. Guerif F, Bidault R, Cadoret V, Couet ML, Lansac J, Royere D. Parameters guiding selection of best embryos for transfer after cryopreservation: a reappraisal. *Hum Reprod.* 2002;17(5):1321-1326.

120. Hansis C, Grifo JA, Krey LC. Oct-4 expression in inner cell mass and trophectoderm of human blastocysts. *Mol Hum Reprod.* 2000;6(11):999-1004.

121. Hansis C, Tang YX, Grifo JA, Krey LC. Analysis of Oct-4 expression and ploidy in individual human blastomeres. *Mol Hum Reprod.* 2001;7(2):155-161.

122. Hardarson T, Caisander G, Sjögren A, Hanson C, Hamberger L, Lundin K. A morphological and chromosomal study of blastocysts developing from morphologically suboptimal human pre-embryos compared with control blastocysts. *Hum Reprod.* 2003;18(2):399-407.

123. Hardarson T, Hanson C, Sjögren A, Lundin K. Human embryos with unevenly sized blastomeres have lower pregnancy and implantation rates: indications for aneuploidy and multinucleation. *Hum Reprod.* 2001;16(2):313-318.

124. Hardarson T, Löfman C, Coull G, Sjögren A, Hamberger L, Edwards RG. Internalization of cellular fragments in a human embryo: time-lapse recordings. *Reprod Biomed Online.*2002;5(1):36-38.

125. Hardarson T, Lundin K, Hamberger L. The position of the metaphase II spindle cannot be predicted by the location of the first polar body in the human oocyte. *Hum Reprod.*2000;15(6):1372-1376.

126. Hardarson T, Van Landuyt L, Jones G. The blastocyst. *Hum Reprod.* 2012;27 Suppl 1:i72-91.

127. Hardy K. Cell death in the mammalian blastocyst. *Mol Hum Reprod.* 1997;3(10):919-925.

128. Hardy K. Apoptosis in the human embryo. *Rev Reprod.* 1999;4(3):125-134.

129. Hardy K, Handyside AH, Winston RM. The human blastocyst: cell number, death and allocation during late preimplantation development in vitro. *Development.*1989;107(3):597-604.

130. Hardy K, Hooper MA, Handyside AH, Rutherford AJ, Winston RM, Leese HJ. Non-invasive measurement of glucose and pyruvate uptake by individual human oocytes and preimplantation embryos. *Hum Reprod.* 1989;4(2):188-191.

131. Hardy K, Martin KL, Leese HJ, Winston RM, Handyside AH. Human preimplantation development in vitro is not adversely affected by biopsy at the 8-cell stage. *Hum Reprod.* 1990;5(6):708-714.

132. Hardy K, Warner A, Winston RM, Becker DL. Expression of intercellular junctions during preimplantation development of the human embryo. *Mol Hum Reprod.* 1996;2(8):621-632.

133. Harper JC, Coonen E, De Rycke M, et al. ESHRE PGD Consortium data collection X: cycles from January to December 2007 with pregnancy follow-up to October 2008. *Hum Reprod.* 2010;25(11):2685-2707.

134. Hassold T, Chen N, Funkhouser J, et al. A cytogenetic study of 1000 spontaneous abortions. *Ann Hum Genet.* 1980;44(Pt 2):151-178.

135. Hassold T, Hall H, Hunt P. The origin of human aneuploidy: where we have been, where we are going. *Hum Mol Genet.* 2007;16 Spec No. 2:R203-208.

136. Hassold T, Hunt P. To err (meiotically) is human: the genesis of human aneuploidy. *Nat Rev Genet.* 2001;2(4):280-291.

137. Haxton MJ, Black WP. The aetiology of infertility in 1162 investigated couples. *Clin Exp Obstet Gynecol.* 1987;14(2):75-79.

138. Heng YW, Koh CG. Actin cytoskeleton dynamics and the cell division cycle. *Int J Biochem Cell Biol.* 2010;42(10):1622-1633.

139. Herrid M, Nguyen VL, Hinch G, McFarlane JR. Leptin has concentration and stage-dependent effects on embryonic development in vitro. *Reproduction.* 2006;132(2):247-256.

140. Herrid M, Palanisamy SK, Ciller UA, et al. An updated view of leptin on implantation and pregnancy: a review. *Physiol Res.* 2014;63(5):543-557.

141. Hiraoka K, Kinutani M, Kinutani K. Blastocoele collapse by micropipetting prior to vitrification gives excellent survival and pregnancy outcomes for human day 5 and 6 expanded blastocysts. *Hum Reprod.* 2004;19(12):2884-2888.

142. Hlinka D, Kaľatová B, Uhrinová I, et al. Time-lapse cleavage rating predicts human embryo viability. *Physiol Res.* 2012;61(5):513-525.

143. Hnida C, Engenheiro E, Ziebe S. Computer-controlled, multilevel, morphometric analysis of blastomere size as biomarker of fragmentation and multinuclearity in human embryos. *Hum Reprod.* 2004;19(2):288-293.

144. Hosu BG, Mullen SF, Critser JK, Forgacs G. Reversible disassembly of the actin cytoskeleton improves the survival rate and developmental competence of cryopreserved mouse oocytes. *PLoS One.* 2008;3(7):e2787.

145. Huber MD, Gerace L. The size-wise nucleus: nuclear volume control in eukaryotes. *J Cell Biol.* 2007;179(4):583-584.

146. Hull MG, Glazener CM, Kelly NJ, et al. Population study of causes, treatment, and outcome of infertility. *Br Med J (Clin Res Ed).* 1985;291(6510):1693-1697.

147. Ji YZ, Bomsel M, Jouannet P, Wolf JP. Modifications of the human oocyte plasma membrane protein pattern during preovulatory maturation. *Mol Reprod Dev.*1997;47(1):120-126.

148. Jones GM, Cram DS, Song B, et al. Gene expression profiling of human oocytes following in vivo or in vitro maturation. *Hum Reprod.* 2008;23(5):1138-1144.

149. Jorgensen P, Edgington NP, Schneider BL, Rupes I, Tyers M, Futcher B. The size of the nucleus increases as yeast cells grow. *Mol Biol Cell.* 2007;18(9):3523-3532.

150. Kalu E, Thum MY, Abdalla H. Reducing multiple pregnancy in assisted reproduction technology: towards a policy of single blastocyst transfer in younger women. *BJOG.*2008;115(9):1143-1150.

151. Kamel RM. Assisted reproductive technology after the birth of louise brown. *J Reprod Infertil.* 2013;14(3):96-109.

152. Khalaf Y, El-Toukhy T, Coomarasamy A, Kamal A, Bolton V, Braude P. Selective single blastocyst transfer reduces the multiple pregnancy rate and increases pregnancy rates: a pre- and postintervention study. *BJOG.* 2008;115(3):385-390.

153. Kirkegaard K, Agerholm IE, Ingerslev HJ. Time-lapse monitoring as a tool for clinical embryo assessment. *Hum Reprod.* 2012;27(5):1277-1285.

154. Kirkegaard K, Hindkjaer JJ, Ingerslev HJ. Human embryonic development after blastomere removal: a time-lapse analysis. *Hum Reprod.* 2012;27(1):97-105.

155. Kirkegaard K, Sundvall L, Erlandsen M, Hindkjær JJ, Knudsen UB, Ingerslev HJ. Timing of human preimplantation embryonic development is confounded by embryo origin. *Hum Reprod.* 2016;31(2):324-331.

156. Kitawaki J, Koshiba H, Ishihara H, Kusuki I, Tsukamoto K, Honjo H. Expression of leptin receptor in human endometrium and fluctuation during the menstrual cycle. *J Clin Endocrinol Metab.* 2000;85(5):1946-1950.

157. Klauschen F, Qi H, Egen JG, Germain RN, Meier-Schellersheim M. Computational reconstruction of cell and tissue surfaces for modeling and data analysis. *Nat Protoc.*2009;4(7):1006-1012.

158. Kola I, Trounson A, Dawson G, Rogers P. Tripronuclear human oocytes: altered cleavage patterns and subsequent karyotypic analysis of embryos. *Biol Reprod.* 1987;37(2):395-401.

159. Kuliev A, Cieslak J, Ilkevitch Y, Verlinsky Y. Chromosomal abnormalities in a series of 6,733 human oocytes in preimplantation diagnosis for age-related aneuploidies. *Reprod Biomed Online.* 2003;6(1):54-59.

160. Lee JH, Kim TH, Oh SJ, et al. Signal transducer and activator of transcription-3 (Stat3) plays a critical role in implantation via progesterone receptor in uterus. *FASEB J.*2013;27(7):2553-2563.

161. Lee MJ, Lee RK, Lin MH, Hwu YM. Cleavage speed and implantation potential of early-cleavage embryos in IVF or ICSI cycles. *J Assist Reprod Genet.* 2012;29(8):745-750.

162. Lemmen JG, Agerholm I, Ziebe S. Kinetic markers of human embryo quality using time-lapse recordings of IVF/ICSI-fertilized oocytes. *Reprod Biomed Online.* 2008;17(3):385-391.

163. Levens ED, Whitcomb BW, Hennessy S, James AN, Yauger BJ, Larsen FW. Blastocyst development rate impacts outcome in cryopreserved blastocyst transfer cycles. *Fertil Steril.* 2008;90(6):2138-2143.

164. Levy DE, Lee CK. What does Stat3 do? *J Clin Invest.* 2002;109(9):1143-1148.

165. Levy R, Benchaib M, Cordonier H, Souchier C, Guerin JF. Laser scanning confocal imaging of abnormal or arrested human preimplantation embryos. *J Assist Reprod Genet.*1998;15(8):485-495.

166. Li RQ, Ouyang NY, Ou SB, et al. Does reducing gamete co-incubation time improve clinical outcomes: a retrospective study. *J Assist Reprod Genet.* 2016;33(1):33-38.

167. Li X, Kato Y, Tsunoda Y. Comparative analysis of development-related gene expression in mouse preimplantation embryos with different developmental potential. *Mol Reprod Dev.* 2005;72(2):152-160.

168. Lichtman JW, Conchello JA. Fluorescence microscopy. *Nat Methods.* 2005;2(12):910-919.

169. Liu J, Wang W, Sun X, et al. DNA microarray reveals that high proportions of human blastocysts from women of advanced maternal age are aneuploid and mosaic. *Biol Reprod.* 2012;87(6):148.

170. Lundin K, Bergh C, Hardarson T. Early embryo cleavage is a strong indicator of embryo quality in human IVF. *Hum Reprod.* 2001;16(12):2652-2657.

171. Macas E, Imthurn B, Borsos M, Rosselli M, Maurer-Major E, Keller PJ. Impairment of the developmental potential of frozen-thawed human zygotes obtained after intracytoplasmic sperm injection. *Fertil Steril.* 1998;69(4):630-635.

172. Machtinger R, Racowsky C. Culture systems: single step. *Methods Mol Biol.*2012;912:199-209.

173. Madaschi C, de Souza Bonetti TC, de Almeida Ferreira Braga DP, Pasqualotto FF, Iaconelli A, Borges E. Spindle imaging: a marker for embryo development and implantation. *Fertil Steril.* 2008;90(1):194-198.

174. Magrath IT, Golding PR, Bagshawe KD. Medical presentations of choriocarcinoma. *Br Med J.* 1971;2(5762):633-637.

175. Maheshwari A, Hamilton M, Bhattacharya S. Should we be promoting embryo transfer at blastocyst stage? *Reprod Biomed Online.* 2016;32(2):142-146.

176. Malik NM, Carter ND, Murray JF, Scaramuzzi RJ, Wilson CA, Stock MJ. Leptin requirement for conception, implantation, and gestation in the mouse. *Endocrinology.*2001;142(12):5198-5202.

177. Mandelbaum J. Oocytes. *Hum Reprod.* 2000;15 Suppl 4:11-18.

178. Mandelbaum J, Belaïsch-Allart J, Junca AM, et al. Cryopreservation in human assisted reproduction is now routine for embryos but remains a research procedure for oocytes.*Hum Reprod.* 1998;13 Suppl 3:161-174;discussion175-167.

179. Mantikou E, Youssef MA, van Wely M, et al. Embryo culture media and IVF/ICSI success rates: a systematic review. *Hum Reprod Update.* 2013;19(3):210-220.

180. Marcos J, Pérez-Albalá S, Mifsud A, Molla M, Landeras J, Meseguer M. Collapse of blastocysts is strongly related to lower implantation success: a time-lapse study. *Hum Reprod.* 2015;30(11):2501-2508.

181. Margalioth EJ, Ben-Chetrit A, Gal M, Eldar-Geva T. Investigation and treatment of repeated implantation failure following IVF-ET. *Hum Reprod.* 2006;21(12):3036-3043.

182. Martikainen H, Tiitinen A, Tomás C, et al. One versus two embryo transfer after IVF and ICSI: a randomized study. *Hum Reprod.* 2001;16(9):1900-1903.

183. Matsuda J, Yokota I, Iida M, et al. Serum leptin concentration in cord blood: relationship to birth weight and gender. *J Clin Endocrinol Metab.* 1997;82(5):1642-1644.

184. Matsuoka T, Tahara M, Yokoi T, et al. Tyrosine phosphorylation of STAT3 by leptin through leptin receptor in mouse metaphase 2 stage oocyte. *Biochem Biophys Res Commun.* 1999;256(3):480-484.

185. Matsuura K, Hayashi N, Takiue C, Hirata R, Habara T, Naruse K. Blastocyst quality scoring based on morphologic grading correlates with cell number. *Fertil Steril.*2010;94(3):1135-1137.

186. McLernon DJ, Maheshwari A, Lee AJ, Bhattacharya S. Cumulative live birth rates after one or more complete cycles of IVF: a population-based study of linked cycle data from 178 898 women. *Hum Reprod.* 2016;31(3):572-581.

187. Merchant R, Gandhi G, Allahbadia GN. In vitro fertilization/intracytoplasmic sperm injection for male infertility. *Indian J Urol.* 2011;27(1):121-132.

188. Merhi Z, Buyuk E, Berger DS, et al. Leptin suppresses anti-Mullerian hormone gene expression through the JAK2/STAT3 pathway in luteinized granulosa cells of women undergoing IVF. *Hum Reprod.* 2013;28(6):1661-1669.

189. Meseguer M, Herrero J, Tejera A, Hilligsøe KM, Ramsing NB, Remohí J. The use of morphokinetics as a predictor of embryo implantation. *Hum Reprod.* 2011;26(10):2658-2671.

190. Meseguer M, Rubio I, Cruz M, Basile N, Marcos J, Requena A. Embryo incubation and selection in a time-lapse monitoring system improves pregnancy outcome compared with a standard incubator: a retrospective cohort study. *Fertil Steril.* 2012;98(6):1481-1489.e1410.

191. Milewski R, Kuć P, Kuczyńska A, Stankiewicz B, Łukaszuk K, Kuczyński W. A predictive model for blastocyst formation based on morphokinetic parameters in time-lapse monitoring of embryo development. *J Assist Reprod Genet.* 2015;32(4):571-579.

192. Milki AA, Jun SH, Hinckley MD, Behr B, Giudice LC, Westphal LM. Incidence of monozygotic twinning with blastocyst transfer compared to cleavage-stage transfer.*Fertil Steril.* 2003;79(3):503-506.

193. Min JK, Hughes E, Young D, et al. Elective single embryo transfer following in vitro fertilization. *J Obstet Gynaecol Can.* 2010;32(4):363-377.

194. Mir P, Mateu E, Mercader A, et al. Confirmation rates of array-CGH in day-3 embryo and blastocyst biopsies for preimplantation genetic screening. *J Assist Reprod Genet.*2016;33(1):59-66.

195. Miyata H, Matsubayashi H, Fukutomi N, Matsuba J, Koizumi A, Tomiyama T. Relevance of the site of assisted hatching in thawed human blastocysts: a preliminary report.*Fertil Steril.* 2010;94(6):2444-2447.

196. Mölder A, Drury S, Costen N, Hartshorne GM, Czanner S. Semiautomated analysis of embryoscope images: Using localized variance of image intensity to detect embryo developmental stages. *Cytometry A.* 2015;87(2):119-128.

197. Mölder A, Drury S, Costen N, Hartshorne GM, Czanner S. Three dimensional visualisation of microscope imaging to improve understanding of human embryo development. ©Springer International Publishing Switzerland L. Linsen *et al* (eds) *Visualisationin Medicine and Life Sciences III*, Mathematics and Visualisation.

198. Montag M, Liebenthron J, Köster M. Which morphological scoring system is relevant in human embryo development? *Placenta.* 2011;32 Suppl 3:S252-256.

199. Montag M, Toth B, Strowitzki T. New approaches to embryo selection. *Reprod Biomed Online.* 2013;27(5):539-546.

200. Morales DA, Bengoetxea E, Larrañaga P, et al. Bayesian classification for the selection of in vitro human embryos using morphological and clinical data. *Comput Methods Programs Biomed.* 2008;90(2):104-116.

201. Motrich RD, Olmedo JJ, Molina R, Tissera A, Minuzzi G, Rivero VE. Uric acid crystals in the semen of a patient with symptoms of chronic prostatitis. *Fertil Steril.*2006;85(3):751.e751-751.e754.

202. Mounzih K, Lu R, Chehab FF. Leptin treatment rescues the sterility of genetically obese ob/ob males. *Endocrinology.* 1997;138(3):1190-1193.

203. Mounzih K, Qiu J, Ewart-Toland A, Chehab FF. Leptin is not necessary for gestation and parturition but regulates maternal nutrition via a leptin resistance state. *Endocrinology.*1998;139(12):5259-5262.

204. Munné S, Sandalinas M, Escudero T, et al. Improved implantation after preimplantation genetic diagnosis of aneuploidy. *Reprod Biomed Online.* 2003;7(1):91-97.

205. Nacerddine K, Lehembre F, Bhaumik M, et al. The SUMO pathway is essential for nuclear integrity and chromosome segregation in mice. *Dev Cell.* 2005;9(6):769-779.

206. Nagy ZP, Janssenswillen C, Janssens R, et al. Timing of oocyte activation, pronucleus formation and cleavage in humans after intracytoplasmic sperm injection (ICSI) with testicular spermatozoa and after ICSI or in-vitro fertilization on sibling oocytes with ejaculated spermatozoa. *Hum Reprod.* 1998;13(6):1606-1612.

207. Nagy ZP, Liu J, Joris H, et al. The influence of the site of sperm deposition and mode of oolemma breakage at intracytoplasmic sperm injection on fertilization and embryo development rates. *Hum Reprod.* 1995;10(12):3171-3177.

208. Nagy ZP, Liu J, Joris H, Devroey P, Van Steirteghem A. Time-course of oocyte activation, pronucleus formation and cleavage in human oocytes fertilized by intracytoplasmic sperm injection. *Hum Reprod.* 1994;9(9):1743-1748.

209. Nakahara T, Iwase A, Goto M, et al. Evaluation of the safety of time-lapse observations for human embryos. *J Assist Reprod Genet.* 2010;27(2-3):93-96.

210. Nakamura H, Kimura T, Koyama S, et al. Mouse model of human infertility: transient and local inhibition of endometrial STAT-3 activation results in implantation failure.*FEBS Lett.* 2006;580(11):2717-2722.

211. National Institute for Health and Care Excellence (NICE) Fertility: guideline CG156, 2014.

212. Neubourg DD, Mangelschots K, Van Royen E, et al. Impact of patients' choice for single embryo transfer of a top quality embryo versus double embryo transfer in the first IVF/ICSI cycle. *Hum Reprod.* 2002;17(10):2621-2625.

213. Niakan KK, Han J, Pedersen RA, Simon C, Pera RA. Human pre-implantation embryo development. *Development.* 2012;139(5):829-841.

214. Nijs M, Van Steirteghem AC. Assessment of different isolation procedures for blastomeres from two-cell mouse embryos. *Hum Reprod.* 1987;2(5):421-424.

215. Nikas G, Ao A, Winston RM, Handyside AH. Compaction and surface polarity in the human embryo in vitro. *Biol Reprod.* 1996;55(1):32-37.

216. Nishida M, Kasahara K, Kaneko M, Iwasaki H, Hayashi K. [Establishment of a new human endometrial adenocarcinoma cell line, Ishikawa cells, containing estrogen and progesterone receptors]. *Nihon Sanka Fujinka Gakkai Zasshi.* 1985;37(7):1103-1111.

217. Ortiz de Solórzano C, García Rodriguez E, Jones A, et al. Segmentation of confocal microscope images of cell nuclei in thick tissue sections. *J Microsc.* 1999;193(Pt 3):212-226.

218. Ozawa M, Sakatani M, Yao J, et al. Global gene expression of the inner cell mass and trophectoderm of the bovine blastocyst. *BMC Dev Biol.* 2012;12:33.

219. Özgür K, Berkkanoğlu M, Bulut H, Isikli A, Coetzee K. Higher clinical pregnancy rates from frozen-thawed blastocyst transfers compared to fresh blastocyst transfers: a retrospective matched-cohort study. *J Assist Reprod Genet.* 2015;32(10):1483-1490.

220. Palermo G, Joris H, Devroey P, Van Steirteghem AC. Pregnancies after intracytoplasmic injection of single spermatozoon into an oocyte. *Lancet.* 1992;340(8810):17-18.

221. Palmieri SL, Peter W, Hess H, Schöler HR. Oct-4 transcription factor is differentially expressed in the mouse embryo during establishment of the first two extraembryonic cell lineages involved in implantation. *Dev Biol.* 1994;166(1):259-267.

222. Pandian Z, Templeton A, Serour G, Bhattacharya S. Number of embryos for transfer after IVF and ICSI: a Cochrane review. *Hum Reprod.* 2005;20(10):2681-2687.

223. Papale L, Fiorentino A, Montag M, Tomasi G. The zygote. *Hum Reprod.* 2012;27 Suppl 1:i22-49.

224. Papi M, Brunelli R, Sylla L, et al. Mechanical properties of zona pellucida hardening. *Eur Biophys J.* 2010;39(6):987-992.

225. Paula-Lopes FF, Boelhauve M, Habermann FA, Sinowatz F, Wolf E. Leptin promotes meiotic progression and developmental capacity of bovine oocytes via cumulus cell-independent and -dependent mechanisms. *Biol Reprod.* 2007;76(3):532-541.

226. Pavone ME, Innes J, Hirshfeld-Cytron J, Kazer R, Zhang J. Comparing thaw survival, implantation and live birth rates from cryopreserved zygotes, embryos and blastocysts.*J Hum Reprod Sci.* 2011;4(1):23-28.

227. Pawar S, Starosvetsky E, Orvis GD, Behringer RR, Bagchi IC, Bagchi MK. STAT3 regulates uterine epithelial remodeling and epithelial-stromal crosstalk during implantation. *Mol Endocrinol.* 2013;27(12):1996-2012.

228. Payne D, Flaherty SP, Barry MF, Matthews CD. Preliminary observations on polar body extrusion and pronuclear formation in human oocytes using time-lapse video cinematography. *Hum Reprod.* 1997;12(3):532-541.

229. Perona RM, Wassarman PM. Mouse blastocysts hatch in vitro by using a trypsin-like proteinase associated with cells of mural trophectoderm. *Dev Biol.* 1986;114(1):42-52.

230. Pierce GB, Arechaga J, Muro C, Wells RS. Differentiation of ICM cells into trophectoderm.*Am J Pathol.* 1988;132(2):356-364.

231. Pinborg A, Loft A, Schmidt L, Andersen AN. Morbidity in a Danish national cohort of 472 IVF/ICSI twins, 1132 non-IVF/ICSI twins and 634 IVF/ICSI singletons: health-related and social implications for the children and their families. *Hum Reprod.*2003;18(6):1234-1243.

232. Plachot M. Fertilization. *Hum Reprod.* 2000;15 Suppl 4:19-30.

233. Plachta N, Bollenbach T, Pease S, Fraser SE, Pantazis P. Oct4 kinetics predict cell lineage patterning in the early mammalian embryo. *Nat Cell Biol.* 2011;13(2):117-123.

234. Prados FJ, Debrock S, Lemmen JG, Agerholm I. The cleavage stage embryo. *Hum Reprod.*2012;27 Suppl 1:i50-71.

235. Pribenszky C, Mátyás S, Kovács P, Losonczi E, Zádori J, Vajta G. Pregnancy achieved by transfer of a single blastocyst selected by time-lapse monitoring. *Reprod Biomed Online.* 2010;21(4):533-536.

236. Racowsky C, Vernon M, Mayer J, et al. Standardization of grading embryo morphology.*Fertil Steril.* 2010;94(3):1152-1153.

237. Rawlings JS, Rosler KM, Harrison DA. The JAK/STAT signaling pathway. *J Cell Sci.*2004;117(Pt 8):1281-1283.

238. Reichman DE, Politch J, Ginsburg ES, Racowsky C. Extended in vitro maturation of immature oocytes from stimulated cycles: an analysis of fertilization potential, embryo development, and reproductive outcomes. *J Assist Reprod Genet.* 2010;27(7):347-356.

239. Ren X, Liu Q, Chen W, Zhu G, Zhang H. Effect of the site of assisted hatching on vitrified-warmed blastocyst transfer cycles: a prospective randomized study. *J Assist Reprod Genet.* 2013;30(5):691-697.

240. Renjini AP, Titus S, Narayan P, Murali M, Jha RK, Laloraya M. STAT3 and MCL-1 associate to cause a mesenchymal epithelial transition. *J Cell Sci.* 2014;127(Pt 8):1738-1750.

241. Richter KS, Harris DC, Daneshmand ST, Shapiro BS. Quantitative grading of a human blastocyst: optimal inner cell mass size and shape. *Fertil Steril.* 2001;76(6):1157-1167.

242. Roberts R, Iatropoulou A, Ciantar D, et al. Follicle-stimulating hormone affects metaphase I chromosome alignment and increases aneuploidy in mouse oocytes matured in vitro. *Biol Reprod.* 2005;72(1):107-118.

243. Robertson JA. Extending preimplantation genetic diagnosis: the ethical debate. Ethical issues in new uses of preimplantation genetic diagnosis. *Hum Reprod.* 2003;18(3):465-471.

244. Roesner S, Von Wolff M, Eberhardt I, Beuter-Winkler P, Toth B, Strowitzki T. In vitro maturation: a five-year experience. *Acta Obstet Gynecol Scand.* 2012;91(1):22-27.

245. Rosen MP, Shen S, Dobson AT, Fujimoto VY, McCulloch CE, Cedars MI. Triploidy formation after intracytoplasmic sperm injection may be a surrogate marker for implantation. *Fertil Steril.* 2006;85(2):384-390.

246. Rubio C, Rodrigo L, Mercader A, et al. Impact of chromosomal abnormalities on preimplantation embryo development. *Prenat Diagn.* 2007;27(8):748-756.

247. Rubio I, Kuhlmann R, Agerholm I, et al. Limited implantation success of direct-cleaved human zygotes: a time-lapse study. *Fertil Steril.* 2012;98(6):1458-1463.

248. Saito H, Tsutsumi O, Noda Y, Ibuki Y, Hiroi M. Do assisted reproductive technologies have effects on the demography of monozygotic twinning? *Fertil Steril.* 2000;74(1):178-179.

249. Sakkas D, Percival G, D'Arcy Y, Sharif K, Afnan M. Assessment of early cleaving in vitro fertilized human embryos at the 2-cell stage before transfer improves embryo selection.*Fertil Steril.* 2001;76(6):1150-1156.

250. Sakkas D, Shoukir Y, Chardonnens D, Bianchi PG, Campana A. Early cleavage of human embryos to the two-cell stage after intracytoplasmic sperm injection as an indicator of embryo viability. *Hum Reprod.* 1998;13(1):182-187.

251. Salas-Vidal E, Lomelí H. Imaging filopodia dynamics in the mouse blastocyst. *Dev Biol.*2004;265(1):75-89.

252. Sallam HN, Sadek SS, Agameya AF. Assisted hatching--a meta-analysis of randomized controlled trials. *J Assist Reprod Genet.* 2003;20(8):332-342.

253. Salumets A, Tuuri T, Mäkinen S, et al. Effect of developmental stage of embryo at freezing on pregnancy outcome of frozen-thawed embryo transfer. *Hum Reprod.*2003;18(9):1890-1895.

254. Sanfins A, Plancha CE, Albertini DF. Pre-implantation developmental potential from in vivo and in vitro matured mouse oocytes: a cytoskeletal perspective on oocyte quality.*J Assist Reprod Genet.* 2015;32(1):127-136.

255. Sanger JW. Changing patterns of actin localization during cell division. *Proc Natl Acad Sci U S A.* 1975;72(5):1913-1916.

256. Saravelos SH, Zhang T, Chung JP, et al. Monochorionic quadramniotic and triamniotic pregnancies following single embryo transfers: two case reports and a review of the literature. *J Assist Reprod Genet.* 2016;33(1):27-32.

257. Sathananthan AH. Ultrastructural changes during meiotic maturation in mammalian oocytes: unique aspects of the human oocyte. *Microsc Res Tech.* 1994;27(2):145-164.

258. Sathananthan H, Menezes J, Gunasheela S. Mechanics of human blastocyst hatching in vitro. *Reprod Biomed Online.* 2003;7(2):228-234.

259. Savulescu J, Dahl E. Sex selection and preimplantation diagnosis: a response to the Ethics Committee of the American Society of Reproductive Medicine. *Hum Reprod.*2000;15(9):1879-1880.

260. Schoolcraft WB, Gardner DK, Lane M, Schlenker T, Hamilton F, Meldrum DR. Blastocyst culture and transfer: analysis of results and parameters affecting outcome in two in vitro fertilization programs. *Fertil Steril.* 1999;72(4):604-609.

261. Schultz GA, Heyner S. Growth factors in preimplantation mammalian embryos. *Oxf Rev Reprod Biol.* 1993;15:43-81.

262. Schwärzler P, Zech H, Auer M, et al. Pregnancy outcome after blastocyst transfer as compared to early cleavage stage embryo transfer. *Hum Reprod.* 2004;19(9):2097-2102.

263. Scott LA. Oocyte and embryo polarity. *Semin Reprod Med.* 2000;18(2):171-183.

264. Scott LA, Smith S. The successful use of pronuclear embryo transfers the day following oocyte retrieval. *Hum Reprod.* 1998;13(4):1003-1013.

265. Scott L, Alvero R, Leondires M, Miller B. The morphology of human pronuclear embryos is positively related to blastocyst development and implantation. *Hum Reprod.*2000;15(11):2394-2403.

266. Sermon K, Van Steirteghem A, Liebaers I. Preimplantation genetic diagnosis. *Lancet.*2004;363(9421):1633-1641.

267. Shapiro BS, Daneshmand ST, Garner FC, Aguirre M, Thomas S. Large blastocyst diameter, early blastulation, and low preovulatory serum progesterone are dominant predictors of clinical pregnancy in fresh autologous cycles. *Fertil Steril.* 2008;90(2):302-309.

268. Sherard J, Bean C, Bove B, et al. Long survival in a 69,XXY triploid male. *Am J Med Genet.* 1986;25(2):307-312.

269. Shoukir Y, Campana A, Farley T, Sakkas D. Early cleavage of in-vitro fertilized human embryos to the 2-cell stage: a novel indicator of embryo quality and viability. *Hum Reprod.* 1997;12(7):1531-1536.

270. Shoukir Y, Chardonnens D, Campana A, Sakkas D. Blastocyst development from supernumerary embryos after intracytoplasmic sperm injection: a paternal influence?*Hum Reprod.* 1998;13(6):1632-1637.

271. Sirmans SM, Pate KA. Epidemiology, diagnosis, and management of polycystic ovary syndrome. *Clin Epidemiol.* 2013;6:1-13.

272. Small J, Rottner K, Hahne P, Anderson KI. Visualising the actin cytoskeleton. *Microsc Res Tech.* 1999;47(1):3-17.

273. Smith AG, Nichols J, Robertson M, Rathjen PD. Differentiation inhibiting activity (DIA/LIF) and mouse development. *Dev Biol.* 1992;151(2):339-351.

274. Stecher A, Vanderzwalmen P, Zintz M, et al. Transfer of blastocysts with deviant morphological and morphokinetic parameters at early stages of in-vitro development: a case series. *Reprod Biomed Online.* 2014;28(4):424-435.

275. Steptoe PC, Edwards RG. Reimplantation of a human embryo with subsequent tubal pregnancy. *Lancet.* 1976;1(7965):880-882.

276. Steptoe PC, Edwards RG. Birth after the reimplantation of a human embryo. *Lancet.*1978;2(8085):366.

277. Stigliani S, Persico L, Lagazio C, Anserini P, Venturini PL, Scaruffi P. Mitochondrial DNA in Day 3 embryo culture medium is a novel, non-

invasive biomarker of blastocyst potential and implantation outcome. *Mol Hum Reprod.* 2014;20(12):1238-1246.

278. Stokes PJ, Hawkhead JA, Fawthrop RK, et al. Metabolism of human embryos following cryopreservation: implications for the safety and selection of embryos for transfer in clinical IVF. *Hum Reprod.* 2007;22(3):829-835.

279. Strom CM, Ginsberg N, Rechitsky S, et al. Three births after preimplantation genetic diagnosis for cystic fibrosis with sequential first and second polar body analysis. *Am J Obstet Gynecol.* 1998;178(6):1298-1306.

280. Strömberg B, Dahlquist G, Ericson A, Finnström O, Köster M, Stjernqvist K. Neurological sequelae in children born after in-vitro fertilisation: a population-based study. *Lancet.*2002;359(9305):461-465.

281. Sugawara A, Sato B, Bal E, Collier AC, Ward MA. Blastomere removal from cleavage-stage mouse embryos alters steroid metabolism during pregnancy. *Biol Reprod.*2012;87(1):4, 1-9.

282. Sugimura S, Akai T, Somfai T, et al. Time-lapse cinematography-compatible polystyrene-based microwell culture system: a novel tool for tracking the development of individual bovine embryos. *Biol Reprod.* 2010;83(6):970-978.

283. Sun X, Bartos A, Whitsett JA, Dey SK. Uterine deletion of Gp130 or Stat3 shows implantation failure with increased estrogenic responses. *Mol Endocrinol.*2013;27(9):1492-1501.

284. Sunkara SK, Rittenberg V, Raine-Fenning N, Bhattacharya S, Zamora J, Coomarasamy A. Association between the number of eggs and live birth in IVF treatment: an analysis of 400 135 treatment cycles. *Hum Reprod.* 2011;26(7):1768-1774.

285. Swain JE. Decisions for the IVF laboratory: comparative analysis of embryo culture incubators. *Reprod Biomed Online.* 2014;28(5):535-547.

286. Swain JE, Dunn RL, McConnell D, Gonzalez-Martinez J, Smith GD. Direct effects of leptin on mouse reproductive function: regulation of follicular, oocyte, and embryo development. *Biol Reprod.* 2004;71(5):1446-1452.

287. Takeda K, Noguchi K, Shi W, et al. Targeted disruption of the mouse Stat3 gene leads to early embryonic lethality. *Proc Natl Acad Sci U S A.* 1997;94(8):3801-3804.

288. Tan TY, Lau SK, Loh SF, Tan HH. Female ageing and reproductive outcome in assisted reproduction cycles. *Singapore Med J.* 2014;55(6):305-309.

289. Tao J, Tamis R, Fink K, Williams B, Nelson-White T, Craig R. The neglected morula/compact stage embryo transfer. *Hum Reprod.* 2002;17(6):1513-1518.

290. Tarín JJ, Vendrell FJ, Ten J, Cano A. Antioxidant therapy counteracts the disturbing effects of diamide and maternal ageing on meiotic division and chromosomal segregation in mouse oocytes. *Mol Hum Reprod.* 1998;4(3):281-288.

291. Tarkowski AK, Suwinska A, Czolowska R, O d enski W. Individual blastomeres of 16- and 32-cell mouse embryos are able to develop into foetuses and mice. *Dev Biol.*2010;348(2):190-198.

292. Tartaglia LA. The leptin receptor. *J Biol Chem.* 1997;272(10):6093-6096.

293. Tartaglia LA, Dembski M, Weng X, et al. Identification and expression cloning of a leptin receptor, OB-R. *Cell.* 1995;83(7):1263-1271.

294. Taylor A. ABC of subfertility: extent of the problem. *BMJ.* 2003;327(7412):434-436.

295. Templeton A, Morris JK. Reducing the risk of multiple births by transfer of two embryos after in vitro fertilization. *N Engl J Med.* 1998;339(9):573-577.

296. Teng CB, Diao HL, Ma XH, Xu LB, Yang ZM. Differential expression and activation of Stat3 during mouse embryo implantation and decidualization. *Mol Reprod Dev.*2004;69(1):1-10.

297. Teranishi A, Kuwata A, Fumino T, Hamai H, Shigeta M. A theoretical model for single blastocyst transfer. *J Assist Reprod Genet.* 2009;26(6):327-334.

298. Tharasanit T, Colenbrander B, Stout TA. Effect of cryopreservation on the cellular integrity of equine embryos. *Reproduction.* 2005;129(6):789-798.

299. Truchet S, Chebrout M, Djediat C, Wietzerbin J, Debey P. Presence of permanently activated signal transducers and activators of transcription in nuclear interchromatin granules of unstimulated mouse oocytes and preimplantation embryos. *Biol Reprod.*2004;71(4):1330-1339.

300. Umen JG. The elusive sizer. *Curr Opin Cell Biol.* 2005;17(4):435-441.

301. Van Blerkom J, Davis P, Alexander S. A microscopic and biochemical study of fragmentation phenotypes in stage-appropriate human embryos. *Hum Reprod.*2001;16(4):719-729.

302. Van Blerkom J, Henry G. Cytogenetic analysis of living human oocytes: cellular basis and developmental consequences of perturbations in chromosomal organization and complement. *Hum Reprod.* 1988;3(6):777-790.

303. Van de Velde H, De Vos A, Sermon K, et al. Embryo implantation after biopsy of one or two cells from cleavage-stage embryos with a view to preimplantation genetic diagnosis. *Prenat Diagn.* 2000;20(13):1030-1037.

304. Van den Abbeel E, Camus M, Van Waesberghe L, Devroey P, Van Steirteghem AC. Viability of partially damaged human embryos after cryopreservation. *Hum Reprod.*1997;12(9):2006-2010.

305. Van den Abbeel E, Balaban B, Ziebe S, et al. Association between blastocyst morphology and outcome of single-blastocyst transfer. *Reprod Biomed Online.*2013;27(4):353-361.

306. Van der Elst J, Van den Abbeel E, Vitrier S, Camus M, Devroey P, Van Steirteghem AC. Selective transfer of cryopreserved human embryos with further cleavage after thawing increases delivery and implantation rates. *Hum Reprod.* 1997;12(7):1513-1521.

307. Van Landuyt L, De Vos A, Joris H, Verheyen G, Devroey P, Van Steirteghem A. Blastocyst formation in in vitro fertilization versus intracytoplasmic sperm injection cycles: influence of the fertilization procedure. *Fertil Steril.* 2005;83(5):1397-1403.

308. Van Landuyt L, Van de Velde H, De Vos A, et al. Influence of cell loss after vitrification or slow-freezing on further in vitro development and implantation of human Day 3 embryos. *Hum Reprod.* 2013;28(11):2943-2949.

309. Van Montfoort AP, Dumoulin JC, Kester AD, Evers JL. Early cleavage is a valuable addition to existing embryo selection parameters: a study using single embryo transfers. *Hum Reprod.* 2004;19(9):2103-2108.

310. van Tol HT, van Eerdenburg FJ, Colenbrander B, Roelen BA. Enhancement of Bovine oocyte maturation by leptin is accompanied by an upregulation in mRNA expression of leptin receptor isoforms in cumulus cells. *Mol Reprod Dev.* 2008;75(4):578-587.

311. Vanderzwalmen P, Bertin G, Debauche C, et al. Births after vitrification at morula and blastocyst stages: effect of artificial reduction of the blastocoelic cavity before vitrification. *Hum Reprod.* 2002;17(3):744-751.

312. Vaughan DA, Ruthazer R, Penzias AS, Norwitz ER, Sakkas D. Clustering of monozygotic twinning in IVF. *J Assist Reprod Genet.* 2016;33(1):19-26.

313. Verlinsky Y, Rechitsky S, Evsikov S, et al. Preconception and preimplantation diagnosis for cystic fibrosis. *Prenat Diagn.* 1992;12(2):103-110.

314. Vincent C, Pickering SJ, Johnson MH. The hardening effect of dimethylsulphoxide on the mouse zona pellucida requires the presence of an oocyte and is associated with a reduction in the number of cortical granules present. *J Reprod Fertil.* 1990;89(1):253-259.

315. Virant-Klun I, Knez K, Tomazevic T, Skutella T. Gene expression profiling of human oocytes developed and matured in vivo or in vitro. *Biomed Res Int.* 2013;2013:879489.

316. Volarcik K, Sheean L, Goldfarb J, Woods L, Abdul-Karim FW, Hunt P. The meiotic competence of in-vitro matured human oocytes is influenced by donor age: evidence that folliculogenesis is compromised in the reproductively aged ovary. *Hum Reprod.*1998;13(1):154-160.

317. Walker MC, Murphy KE, Pan S, Yang Q, Wen SW. Adverse maternal outcomes in multifetal pregnancies. *BJOG.* 2004;111(11):1294-1296.

318. Wang J, Sauer MV. In vitro fertilization (IVF): a review of 3 decades of clinical innovation and technological advancement. *Ther Clin Risk Manag.* 2006;2(4):355-364.

319. Wang TS, Gao F, Qi QR, et al. Dysregulated LIF-STAT3 pathway is responsible for impaired embryo implantation in a Streptozotocin-induced diabetic mouse model. *Biol Open.* 2015;4(7):893-902.

320. Wang WH, Abeydeera LR, Han YM, Prather RS, Day BN. Morphologic evaluation and actin filament distribution in porcine embryos produced in vitro and in vivo. *Biol Reprod.*1999;60(4):1020-1028.

321. Wang Y, Kuropatwinski KK, White DW, et al. Leptin receptor action in hepatic cells. *J Biol Chem.* 1997;272(26):16216-16223.

322. Weber RJ, Pedersen RA, Wianny F, Evans MJ, Zernicka-Goetz M. Polarity of the mouse embryo is anticipated before implantation. *Development.* 1999;126(24):5591-5598.

323. Webster M, Witkin KL, Cohen-Fix O. Sizing up the nucleus: nuclear shape, size and nuclear-envelope assembly. *J Cell Sci.* 2009;122(Pt 10):1477-1486.

324. Weimar CH, Post Uiterweer ED, Teklenburg G, Heijnen CJ, Macklon NS. In-vitro model systems for the study of human embryo-endometrium interactions. *Reprod Biomed Online.* 2013;27(5):461-476.

325. Wen L, Craig J, Dyce PW, Li J. Cloning of porcine signal transducer and activator of transcription 3 cDNA and its expression in reproductive tissues. *Reproduction.*2006;132(3):511-518.

326. Wennekamp S, Mesecke S, Nédélec F, Hiiragi T. A self-organization framework for symmetry breaking in the mammalian embryo. *Nat Rev Mol Cell Biol.* 2013;14(7):452-459.

327. Werner P, Hussy N, Buell G, Jones KA, North RA. D2, D3, and D4 dopamine receptors couple to G protein-regulated potassium channels in Xenopus oocytes. *Mol Pharmacol.*1996;49(4):656-661.

328. Wilcox AJ, Baird DD, Weinberg CR. Time of implantation of the conceptus and loss of pregnancy. *N Engl J Med.* 1999;340(23):1796-1799.

329. Wong CC, Loewke KE, Bossert NL, et al. Non-invasive imaging of human embryos before embryonic genome activation predicts development to the blastocyst stage. *Nat Biotechnol.* 2010;28(10):1115-1121.

330. Woodward BJ, Montgomery SJ, Hartshorne GM, Campbell KH, Kennedy R. Spindle position assessment prior to ICSI does not benefit fertilization or early embryo quality.*Reprod Biomed Online.* 2008;16(2):232-238.

331. Wright G, Wiker S, Elsner C, et al. Observations on the morphology of pronuclei and nucleoli in human zygotes and implications for cryopreservation. *Hum Reprod.*1990;5(1):109-115.

332. Wright RW, Anderson GB, Cupps PT, Drost M. Blastocyst expansion and hatching of bovine ova cultured in vitro. *J Anim Sci.* 1976;43(1):170-174.

333. Xia P. Intracytoplasmic sperm injection: correlation of oocyte grade based on polar body, perivitelline space and cytoplasmic inclusions with fertilization rate and embryo quality. *Hum Reprod.* 1997;12(8):1750-1755.

334. Yang YJ, Cao YJ, Bo SM, Peng S, Liu WM, Duan EK. Leptin-directed embryo implantation: leptin regulates adhesion and outgrowth of mouse blastocysts and receptivity of endometrial epithelial cells. *Anim Reprod Sci.* 2006;92(1-2):155-167.

335. Zhang Y, Proenca R, Maffei M, Barone M, Leopold L, Friedman JM. Positional cloning of the mouse obese gene and its human homologue. *Nature.* 1994;372(6505):425-432.

336. Zhou W, Chu D, Sha W, Fu L, Li Y. Effects of granulocyte-macrophage colony-stimulating factor supplementation in culture medium on embryo quality and pregnancy outcome of women aged over 35 years. *J Assist Reprod Genet.* 2016;33(1):49-37.